Supporting Information

Engineering of phenylpyridine- and bipyridine-based covalent organic frameworks for the photocatalytic tandem aerobic oxidation/Povarov cyclization.

Maarten Debruyne,[a] Sander Borgmans,[b] Sambhu Radhakrishnan,[c] Eric Breynaert,[c] Henk Vrielinck,[d] Karen Leus,[e] Andreas Laemont,[f] Juul De Vos,[b] Kuber Singh Rawat,[b] Siebe Vanlommel,[b] Hannes Rijckaert,[f] Hadi Salemi,[a] Jonas Everaert,[a] Flore Vanden Bussche,[a,f] Dirk Poelman,[d] Rino Morent,[e] Nathalie De Geyter,[e] Pascal Van Der Voort,[f] Veronique Van Speybroeck,[b] Christian V. Stevens.*[a]

[a] Department of Green Chemistry and Technology, Ghent University. Coupure Links 653, 9000 Ghent, Belgium.

[b] Department of Applied Physics, Ghent University. Technologiepark 46, 9052, Zwijnaarde, Belgium.

[c] NMR/X-ray platform for Convergence Research (NMRCoRe) & Centre for Surface Chemistry and Catalysis: Characterisation and Application Team (COK-KAT), KU Leuven, Celestijnenlaan 200f - box 2461, 3001 Leuven, Belgium.

[d] Department of Solid State Sciences, Ghent University, Krijgslaan 281 (S1), 9000 Ghent, Belgium.

[e] Department of Applied Physics, Faculty of Engineering and Architecture, Ghent University, Sint-Pietersnieuwstraat 41 (B4), 9000 Ghent, Belgium.

[f] Department of Chemistry, Ghent University. Krijgslaan 281 (S3), 9000, Ghent, Belgium.

E-mail: Chris.Stevens@Ugent.be

Table of contents

S1 Linker synthesis

S1.1 Synthesis of 2,4,6-trimethoxybenzene-1,3,5-tricarbaldehyde **TpOMe**

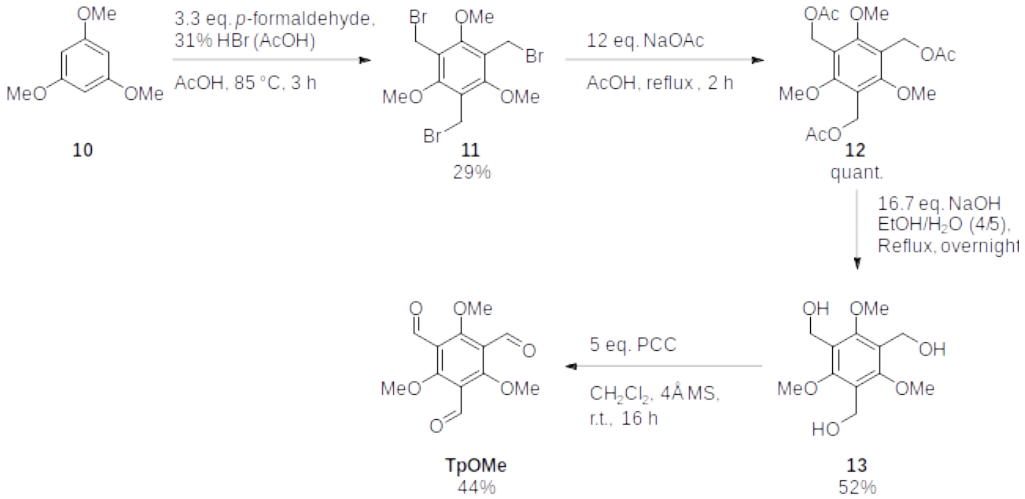

Scheme S1: Synthesis of **TpOMe**.

Step 1: Synthesis of 1,3,5-tris(bromomethyl)-2,4,6-trimethoxybenzene **11**

The procedure was adapted from literature.[1,2] 1,3,5-Trimethoxybenzene **10** (5,00 g, 29.7 mmol, 1 eq.) and paraformaldehyde (3.33 g, 110.9 mmol, 3.3 eq.) were added with 11 mL AcOH to a pressure tube and stirred at room temperature for one hour. Then 30 mL of 33% HBr in AcOH was slowly added and this was stirred at 85 °C for three hours. This was allowed to cool to room temperature and dichloromethane and water were added. The phases were separated, and the organic layer was washed three times with water. The organic layer was concentrated and purified using column chromatography (SiO_2, PE/EtOAc: 20/1), to give the product **11** as a white solid (3.87 g, 29%).

1,3,5-Tris(bromomethyl)-2,4,6-trimethoxybenzene 11

^{1}H-NMR (400 MHz, $CDCl_3$): δ 4.15 (9H, s, 3 x CH_3); 4.60 (6H, s, 3 x CH_2). **^{13}C-NMR** (100 MHz, $CDCl_3$): δ 22.6 (3 x CH_2); 62.8 (3 x CH_3); 123.4 (3 x $C_{arom,quat}$); 160.2 (3 x $C_{arom,quat}$). White solid, 29%. Spectral data matched literature.[2]

Step 2: Synthesis of 2,4,6-trimethoxybenzene-1,3,5-triyl)tris(methylene) triacetate **12**

The procedure for step 2 to 4 were based on a literature procedure.[3] 1,3,5-tris(bromomethyl)-2,4,6-trimethoxybenzene **11** (3.87 g, 8.7 mmol, 1 eq.) and NaOAc (8.5 g, 104 mmol, 12 eq.) were added to a round bottom flask containing 100 mL AcOH and refluxed for two hours until completion of the reaction (LC-MS). The reaction mixture was allowed to come to room temperature and 200 mL CH_2Cl_2 was added. This was then filtered, and the filtrate was concentrated under vacuum. To this crude solid EtOAc (100 mL) and aqueous $NaHCO_3$ (100 mL) were added. The phases were separated, and the organic phase was further extracted with aqueous $NaHCO_3$, H_2O and brine (100 mL each). The organic phase was concentrated to give the crude triacetate **12** as a white solid in quantitative yield.

(2,4,6-Trimethoxybenzene-1,3,5-triyl)tris(methylene) triacetate 12

^{1}H-NMR (400 MHz, $CDCl_3$): δ 2.08 (9H, s, 3 x CH_3C=O); 3.84 (9H, s, 3 x CH_3O); 5.17 (6H, s, 3 x CH_2). **^{13}C-NMR** (100 MHz, $CDCl_3$): δ 21.2 (3 x CH_3C=O); 56.9 (3 x CH_2O); 64.0 (3 x CH_3O); 120.0 (3 x $C_{arom,quat}$); 162.2 (3 x $C_{arom,quat}$); 170.9 (3 x C=O). White solid, quantitative.

Step 3: Synthesis of (2,4,6-trimethoxybenzene-1,3,5-triyl)trimethanol **13**

NaOH (5.78 g, 144.6 mmol, 16.7 eq.) was dissolved in 50 mL of water. The crude triacetate **12** from the previous step was dissolved in 40 mL of EtOH. The sodium hydroxide solution was added and refluxed overnight. After cooling to room temperature, the ethanol was removed via rotary evaporation and 1 N HCl was added until the pH was neutral. Brine (75 mL) was added and the solution was extracted five times with ethyl acetate (5 x 50 mL) furnishing the triol **13** as a white solid (1.167 g, 52%).

(2,4,6-Trimethoxybenzene-1,3,5-triyl)trimethanol 13

^{1}H-NMR (400 MHz, DMSO-d_6): δ 3.86 (9H, s, 3 x CH_3); 4.45 (6H, d, J = 4.1 Hz, 3 x CH_2); 4.76 (3H, t, J = 4.1 Hz, 3 x OH). **^{13}C-NMR** (100 MHz, DMSO-d_6): δ 52.9 (3 x CH_2O); 63.7 (3 x CH_3O); 124.3 and 159.1 (2 x 3 x $C_{arom,quat}$). White solid, 52%. Spectral data matches literature.[3]

Step 4: Synthesis of 2,4,6-trimethoxybenzene-1,3,5-tricarbaldehyde **TpOMe**

The triol **13** (608 mg, 4.5 mmol, 1 eq.) was dissolved in 30 mL dry CH_2Cl_2 under argon and powdered 4 Å molecular sieves were added. To this PCC (4.85 g, 22.5 mmol, 5 eq.) was added and the resulting suspension was stirred overnight. This was filtered over celite, the filter cake was rinsed with 2 x 100 mL CH_2Cl_2, and the filtrate was concentrated under vacuum and purified using column chromatography (SiO_2, PE/EtOAc: 3/2) resulting in **TpOMe** as a beige solid (150 mg, 44%).

2,4,6-Trimethoxybenzene-1,3,5-tricarbaldehyde TpOMe

^{1}H-NMR (400 MHz, $CDCl_3$): δ 4.03 (9H, s, 3 x CH_3); 10.35 (3H, s, 3 x CHO). **^{13}C-NMR** (100 MHz, $CDCl_3$): δ 65.7 (3 x CH_3); 120.3 (3 x $C_{arom,quat}$); 169.9 (3 x $C_{arom,quat}$); 187.2 (3 x C=O). **IR** (ATR, cm^{-1}): $\nu_{C=O}$ = 1680; ν_{max} = 2953, 2889, 2860, 1545, 1373, 1198, 1117, 866, 575. **MS** (ESI): m/z (%) 253 ([M + 1]$^+$, 100). Beige solid, 44%. Spectral data matches literature.[3]

S1.2 Synthesis of 1,3,5-triformylphloroglucinol **Tp**

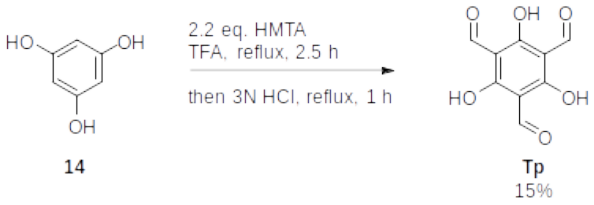

Scheme S2: Synthesis of **Tp**.

This procedure was taken from literature.[4] To a 500 mL flask containing hexamethylenetetramine (HMTA) (18.6 g, 133 mmol, 2.2 eq.) and phloroglucinol **14** (7.56 g, 60 mmol, 1 eq.) 120 mL of trifluoroacetic acid was added. A reflux condenser was attached to the flask, and it was heated in an oil bath at 100 °C for 2.5 hours under nitrogen atmosphere. Then 250 mL 3N HCl was slowly added to the reaction mixture and this reaction was kept in the oil bath at 100 °C for one hour. After cooling to room temperature, the reaction mixture was filtered and then extracted with dichloromethane (5 x 200 mL). The combined extracts were dried over $MgSO_4$, filtered and the solvent was removed by rotary evaporation yielding an orange sludge. This solid could further be purified by washing it with ethanol, yielding 1,3,5-triformylphloroglucinol **Tp** as a salmon colored powder (1.83 g, 15%).

1,3,5-Triformylphloroglucinol Tp

^{1}H-NMR (400 MHz, $CDCl_3$): δ 10.16 (3H, s, 3 x CHO); 14.12 (3H, s, 3 x OH). **^{13}C-NMR** (100 MHz, $CDCl_3$): δ 103.0 (3 x $C_{arom,quat}$); 173.7 (3 x $C_{arom,quat}$); 192.2 (3 x C=O). **IR** (ATR, cm^{-1}): $\nu_{C=O}$ = 1632; ν_{max} = 2886, 1584, 1427, 1240, 1153, 964, 820, 783, 604. **MS** (ESI): m/z (%) 209 ([M-1]$^-$, 100). Salmon colored powder, 15%. Spectral data matched literature.[4]

S1.3 Synthesis of 2,2'-bipyridine-5,5'-diamine **Bpy**

Bpy was synthesized according to literature procedures in three steps, starting from 2-bromo/chloro -5-amino-pyridine **15a/b**.

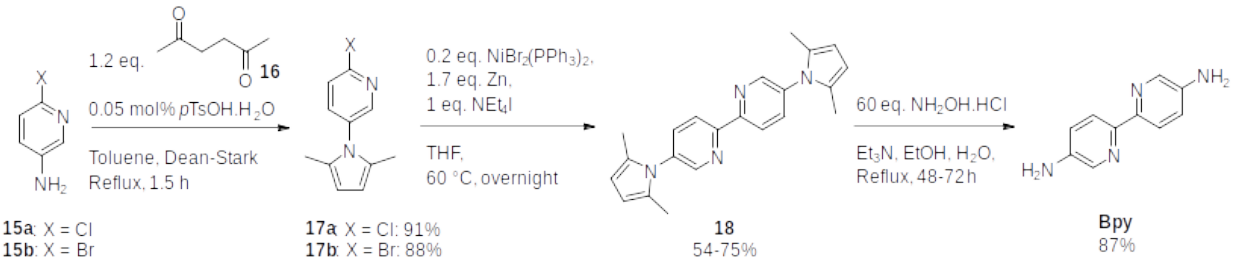

Scheme S3: Synthesis of **Bpy**.

Step 1: Synthesis of dimethylpyrrole protected amines **17a-b**

Based on literature procedure. [5] To a 100 mL flask was added 5-amino-2-bromopyridine **15b** (5.917 g, 29 mmol, 1 eq.), 50 mL toluene, 4.1 mL hexane-2,5-dione **16** (3.97 g, 34.8 mmol, 1.2 eq.) and *p*-toluenesulfonic acid monohydrate (276 mg, 1.5 mmol, 0.05 eq.). This mixture was heated in a Dean-Stark apparatus for 1.5 h until completion of the reaction (LC-MS). After cooling to room temperature the mixture was quenched with a saturated aqueous solution of $NaHCO_3$ (50 mL) and separated. The organic layer was washed with water (50 mL) and dried over $MgSO_4$. After removing the solvent by rotary evaporation the resultant crude product was purified by column chromatography (SiO_2, PE/EtOAc: 20/1) to yield to product **17b** as a pale pink solid (6.35 g, 88%). Using the same procedure the pyrrole protected chloropyridine **17a** was obtained as a yellow solid in 91% yield.

1-1-(2-Chloropyridine-5-yl)-2,5-dimethyl-1*H*-pyrrole 17a

^{1}H-NMR (400 MHz, $CDCl_3$): δ 2.04 (6H, s, 2 x CH_3); 5.94 (2H, s, 2 x CH_{arom}); 7.46 (1H, d, *J* = 8.3 Hz, CH_{arom}); 7.53 (1H, d x d, *J* = 8.3 x 2.6 Hz, CH_{arom}); 8.30 (1H, d, *J* = 2.6 Hz, CH_{arom}). **^{13}C-NMR** (100 MHz, $CDCl_3$): δ 13.1 (2 x CH_3); 107.2 (2 x CH_{arom}); 124.7 (CH_{arom}); 129.0 (2 x $C_{arom,quat}$); 134.7 ($C_{arom,quat}$); 138.3 (CH_{arom}); 149.1 (CH_{arom}); 150.5 (2 x $C_{arom,quat}$). Yellow solid, 91%. Spectral data matched literature.[6]

1-1-(2-Bromopyridine-5-yl)-2,5-dimethyl-1*H*-pyrrole 17b

^{1}H-NMR (400 MHz, $CDCl_3$): δ 2.04 (6H, s, 2 x CH_3); 5.94 (2H, s, 2 x CH_{arom}); 7.43 (1H, d x d, *J* = 8.3 x 2.1 Hz, CH_{arom}); 7.61 (1H, d, *J* = 8.3 Hz, CH_{arom}); 8.29 (1H, ~d, *J* = 2.1 Hz, CH_{arom}). **^{13}C-NMR** (100 MHz, $CDCl_3$): δ 13.1 (2 x CH_3); 107.3 (2 x CH_{arom}); 128.5 (CH_{arom}); 129.0 (2 x $C_{arom,quat}$); 135.2 ($C_{arom,quat}$); 138.1 (CH_{arom}); 140.9 ($C_{arom,quat}$); 149.6 (CH_{arom}). Pale pink solid, 88%. Spectral data matched literature.[7]

Step 2: Coupling to bipyridine **18**

This procedure was based on literature.[6,8] In a 250 mL two necked flask activated zinc powder (2.64 g, 40.4 mmol, 1.7 eq.), tetraethylammonium iodide (6.1 g, 23.7 mmol, 1 eq.) and $NiBr_2(PPh_3)_2$ (3.53 g, 4.8 mmol, 0.2 eq.) were suspended in 25 mL dry THF and stirred at 60 °C under argon for one hour.

Pyrrole protected bromopyridine **17b** (5.96 g, 23.7 mmol, 1 eq.) was dissolved in dry THF (60 mL) and slowly added to this mixture with an addition funnel and the reaction mixture was stirred overnight, after which it was allowed to cool down to room temperature. Then concentrated ammonia (25%, 100 mL), water (50 mL), and CH_2Cl_2 (100 mL) were added and this mixture was stirred for 15 min after which it was filtered over celite. The phases were separated and the aqueous phase was extracted twice with 100 mL of CH_2Cl_2. The combined organic phases were evaporated under reduced pressure and the crude product was purified by column chromatography (SiO_2, hexane/EtOAc/Et_3N: 10/1/0.05) as eluent to obtain the product **18** (2.23 g, 54%) as a light yellow solid.

Using the same procedure, but with the protected chloropyridine **17a** a yield of 75% was obtained. To eliminate the large amount of tailing due to the limited solubility of the product during the chromatograpy, it was found to be easier to first elute the triphenylphospine oxide with ~5-10 Column volumes of 9/1 PE/CH_2Cl_2, and then elute the product with 100% CH_2Cl_2.. The obtained product is slightly less pure, but can easily be cleaned up by stirring in boiling *i*PrOH (100 mL/gram of product), cooling in a freezer overnight and then filtering of the product.

5,5'-Bis(2,5-dimethyl-1*H*-pyrrol-1-yl)-2,2'-bipyridine 18

^{1}H-NMR (400 MHz, $CDCl_3$): δ 2.10 (12H, s, CH_3); 5.98 (4H, s, 4 x CH_{arom}); 7.72 (2H, d x d, *J* = 8.4 x 2.5 Hz, 2 x CH_{arom}); 8.57-8.60 (4H, m, 4 x CH_{arom}). **^{13}C-NMR** (100 MHz, $CDCl_3$): δ 13.2 (4 x CH_3); 107.0 (4 x CH_{arom}); 121.5 (2 x CH_{arom}); 129.1 (4 x $C_{arom,quat}$); 135.9 (2 x $C_{arom,quat}$); 136.5 (2 x CH_{arom}); 148.6 (2 x CH_{arom}); 154.5 (2 x $C_{arom,quat}$). Light yellow solid, 54-75%. Spectral data matched literature.[6]

Step 3: deprotection to 2,2'-bipyridine-5,5'-diamine **Bpy**

To a 100 mL flask were added: 5,5'-bis(2,5-dimethyl-1*H*-pyrrole)-2,2'-bipyridine **18** (2.23 g, 6.53 mmol, 1 eq.), hydroxylamine hydrochloride (13.61 g, 196 mol, 30 eq.), 20 mL H_2O, 50 mL absolute EtOH and 8 mL triethylamine. This mixture was refluxed for 24 hours after which another 30 eq. of hydroxylamine hydrochloride and 4 mL triethylamine were added and the reaction was continued for another 24 hours. If LC-MS analysis then indicated complete conversion of the starting material, the reaction was stopped, if not another 30 eq. of $NH_2OH.HCl$ and 8 mL of triethylamine were added and the reaction was stirred for another 24 h. Upon completion, the reaction was allowed to cool down to room temperature and then 30 mL of 3 N HCL was added followed by 100 mL of EtOH. The mixture was put in the freezer overnight and was filtered off, to obtain the hydrochloride salt of the product as an orange powder. This powder was dissolved in water and sodium hydroxide solution (3N) was added until the mixture was highly alkaline (pH 11). This was then extracted multiple times with dichloromethane, dried over $MgSO_4$, filtered and the solvent was removed under reduced pressure to obtain the product **Bpy** as a light yellow solid (1.06 g, 87%). It can also (more conveniently) be obtained in a similar yield by allowing the product to precipitate from the basic solution. The precipitate can then be filtered off and washed with water, followed by extensive drying under vacuum to remove residual water.

2,2'-Bipyridine-5,5'-diamine Bpy

^{1}H-NMR (400 MHz, DMSO-d_6): δ 5.32 (4H, s, 2 x NH_2); 6.95 (2H, d x d, *J* = 8.5 x 2.6 Hz, 2 x CH_{arom}); 7.86 (2H, d, J = 8.5 Hz, 2 x CH_{arom}); 7.91 (2H, d, *J* = 2.5 Hz, 2 x CH_{arom}). **^{13}C-NMR** (100 MHz, DMSO-d_6): δ 119.1 (2 x CH_{arom}); 120.6 (2 x CH_{arom}); 135.0 (2 x CH_{arom}); 143.8 ($C_{arom,quat}$); 144.8 ($C_{arom,quat}$). **IR** (ATR, cm^{-1}): ν_{max} = 3308, 3198, 1626, 1593, 1562, 1470, 1408, 1281, 841, 503. **MS** (ESI): *m/z* (%) 395 ($[2M + 23]^+$, 20); 187 ($[M + H]^+$, 100). Yellow solid, 87%. Spectral data matched literature.[6]

S1.4 Synthesis of 6-(4-aminophenyl)pyridin-3-amine **Ppy**

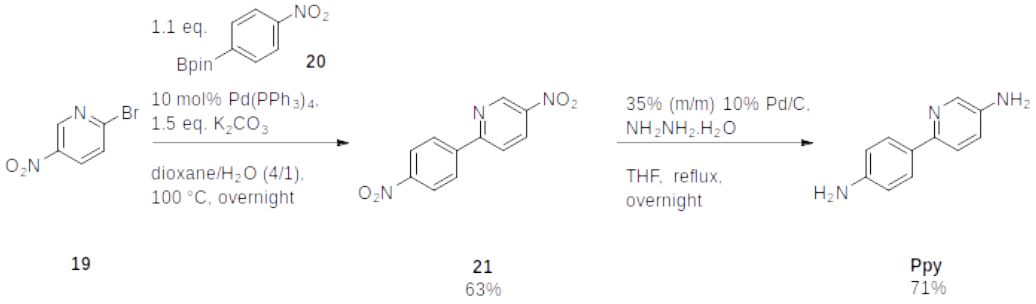

Scheme S4: Synthesis of **Ppy**.

Step 1: Synthesis of 5-nitro-2-(4-nitrophenyl)pyridine **21**

2-Bromo-5-nitropyridine **19** (1.02 g, 5 mmol, 1 eq.), 4,4,5,5-tetramethyl-2-(4-nitrophenyl)-1,3,2-dioxaborolane **20** (1.37 g, 5.5 mmol, 1.1 eq.) and potassium carbonate (1.10 g, 7.5 mmol, 1.5 eq.) were added to a two necked flask equipped with a reflux condenser together with 80 mL dioxane and 20 mL water. Nitrogen was bubbled through this mixture for 30 min. Then $Pd(PPh_3)_4$ (0.58 g, 0.5 mmol, 0.1 eq.) was added. The reaction mixture was refluxed overnight, filtered and rinsed thoroughly with EtOAc. Water was added and the layers were separated. The water layer was further extracted with EtOAc (2x). The combined organic layers were concentrated and purified using column chromatography (C18, gradient CH_3CN/H_2O: 40/60 - 100/0) furnishing the product **21** as a light yellow solid (776 mg, 63%).

5-Nitro-2-(4-nitrophenyl)pyridine 21

^{1}H-NMR (400 MHz, DMSO-d_6): δ 8.39-8.49 (5H, m, 5 x CH_{arom}); 8.75 (1H, d x d, *J* = 8.8 x 2.5 Hz, CH_{arom}); 9.51 (1H, d, *J* = 2.5 Hz, CH_{arom}). **^{13}C-NMR** (100 MHz, DMSO-d_6): δ 122.0 (CH_{arom}); 124.2 (2 x CH_{arom}); 128.9 (2 x CH_{arom}); 133.1 (CH_{arom}); 142.3 ($C_{arom,quat}$); 143.9 ($C_{arom,quat}$); 145.1 (CH_{arom}); 148.7 ($C_{arom,quat}$); 158.6 ($C_{arom,quat}$). Light yellow solid, 63%. Spectral data matched literature.[9]

Step 2: Synthesis of 6-(4-aminophenyl)pyridin-3-amine **Ppy**

5-Nitro-2-(4-nitrophenyl)pyridine **21** (776 mg, 3.2 mmol, 1 eq.) was dissolved in 100 mL THF in a 250 mL round bottom flask equipped with a reflux condenser and put under a flow of nitrogen. 270 mg 10% Pd/C and then 4.6 mL 80% $NH_2NH_2.H_2O$ were added and the resulting mixture was refluxed overnight. The catalyst was filtered of and the filtrate was concentrated under vacuum with a rotavapor in a fume hood. The product was purified using column chromatography (C18, gradient CH_3CN/H_2O: 10/90 - 40/60) and this furnished the product **Ppy** as a yellow to brown solid (426 mg, 71%).

6-(4-Aminophenyl)pyridin-3-amine Ppy

^{1}H-NMR (400 MHz, DMSO-d_6): δ 5.11 (2H, s, NH_2); 5.16 (2H, s, NH_2); 6.55-6.58 (2H, m, 2 x CH_{arom}); 6.92 (1H, d x d, *J* = 8.5 x 2.7 Hz, CH_{arom}); 7.41 (1H, d, *J* = 8.5 Hz, CH_{arom}); 7.57-7.60 (2H, m, 2 x CH_{arom}); 7.92 (1H, d, *J* = 2.7 Hz, CH_{arom}). **^{13}C-NMR** (100 MHz, DMSO-d_6): δ 113.8 (2 x CH_{arom}); 118.7 (CH_{arom}); 121.4 (CH_{arom}); 126.0 (2 x CH_{arom}); 127.0 ($C_{arom,quat}$); 135.1 (CH_{arom}); 142.6 ($C_{arom,quat}$); 144.9 ($C_{arom,quat}$); 148.1 ($C_{arom,quat}$). **IR** (ATR, cm^{-1}): ν_{max} = 3443, 3318, 3192, 1605, 1477, 1281, 1242, 826, 465, 449. **MS** (ESI): *m/z* (%) 186 ($[M + 1]^+$, 100). Yellow to brown solid, 71%. Spectral data matched literature.[9]

S2 Characterization of COFs

S2.1 Pore size distributions

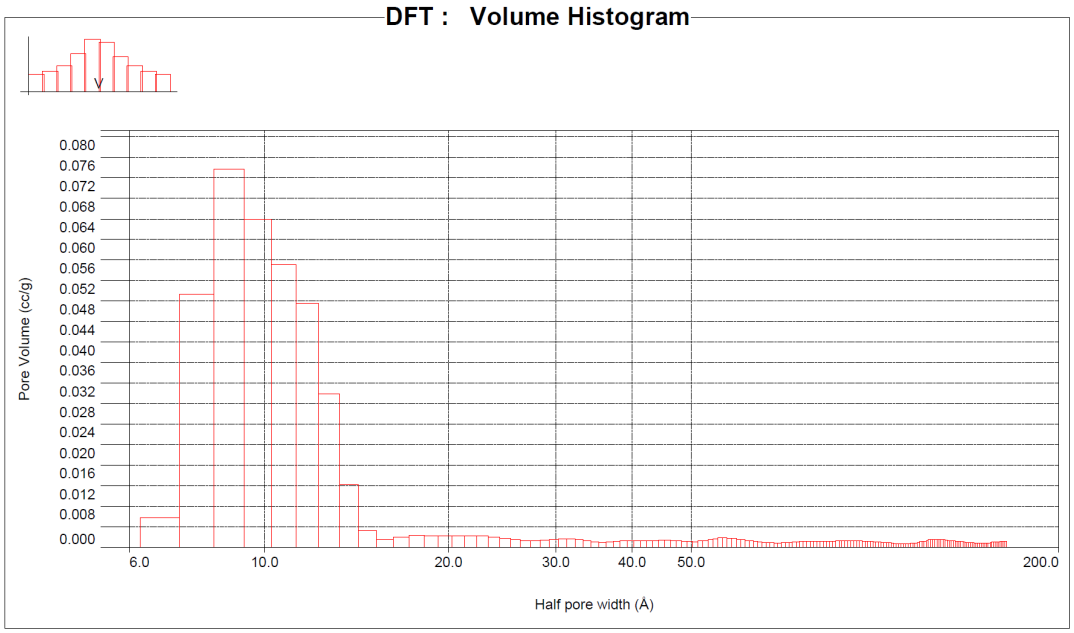

Figure S1: Pore size distribution of **TpBpyCOF**, calculated half pore width: 8.928 Å.

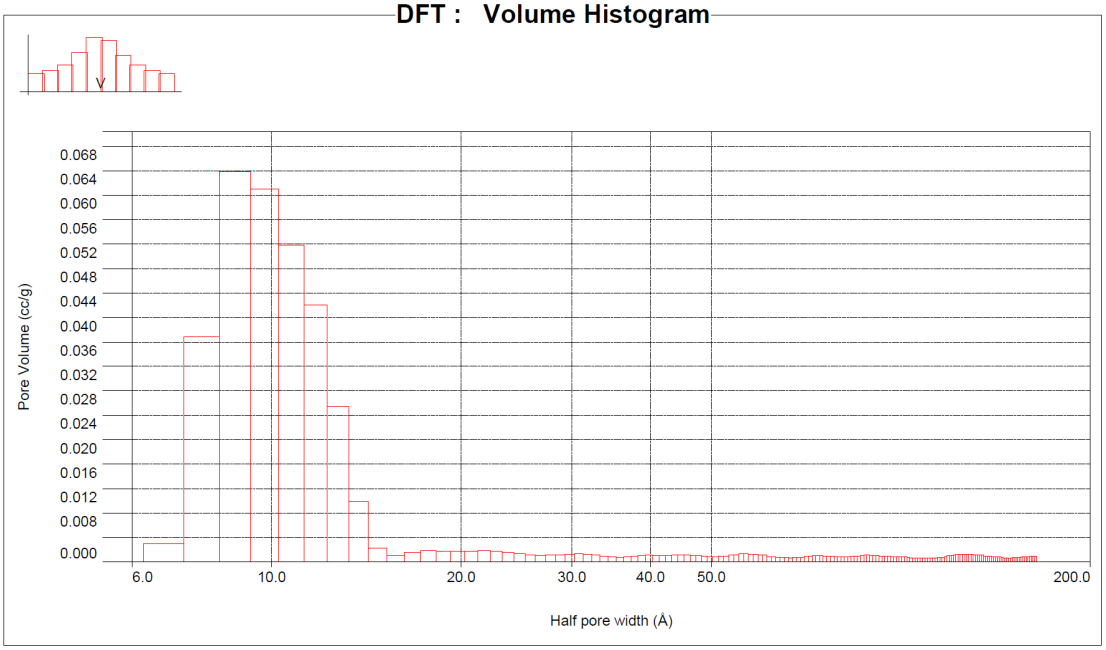

Figure S2: Pore size distribution of **TpPpyCOF**, calculated half pore width: 9.240 Å.

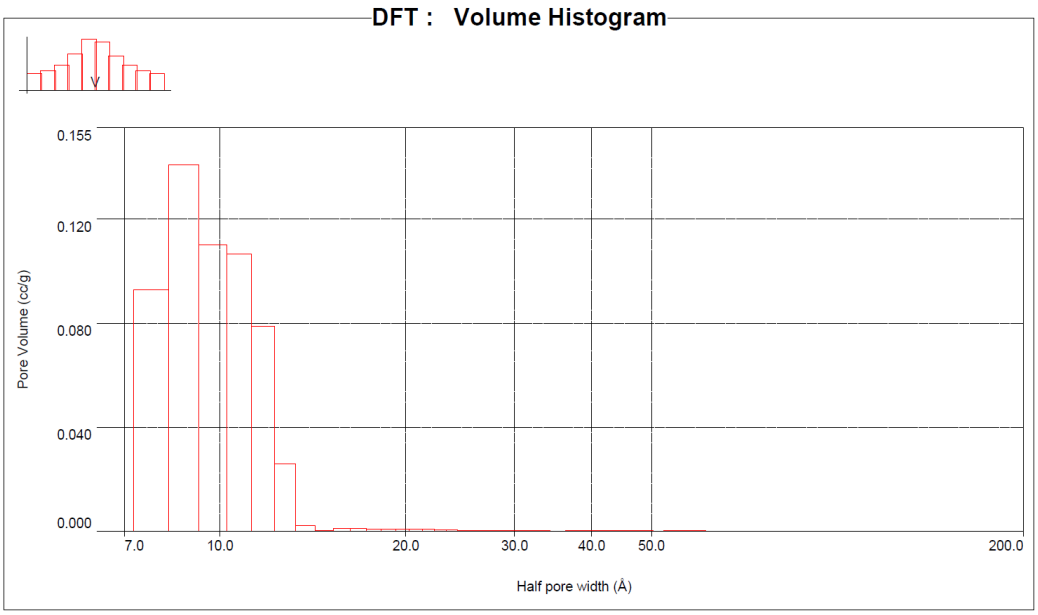

Figure S3: Pore size distribution of **'TpOMeBpyCOF'**, calculated half pore width: 8.626 Å.

S2.2 FTIR spectra

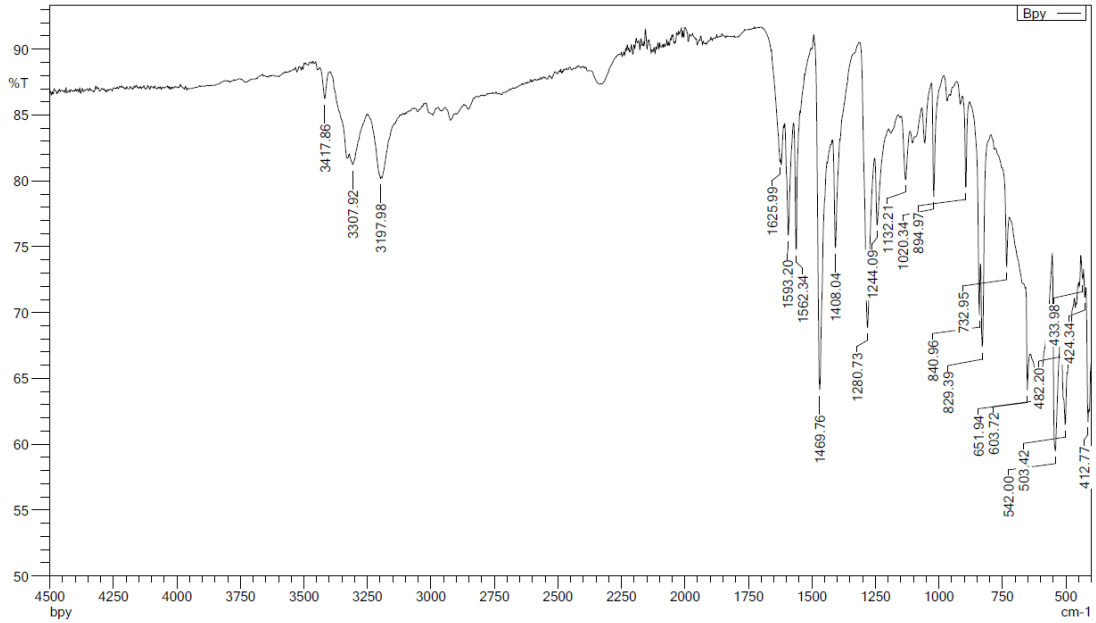

Figure S4: FTIR spectrum of **Bpy**.

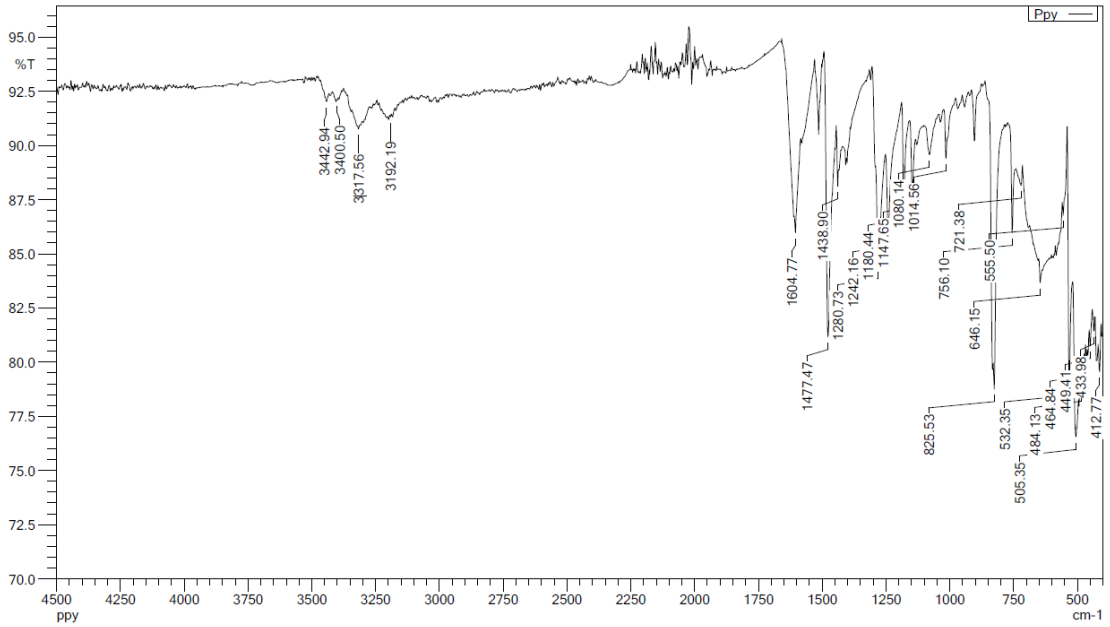

Figure S5: FTIR spectrum of **Ppy**.

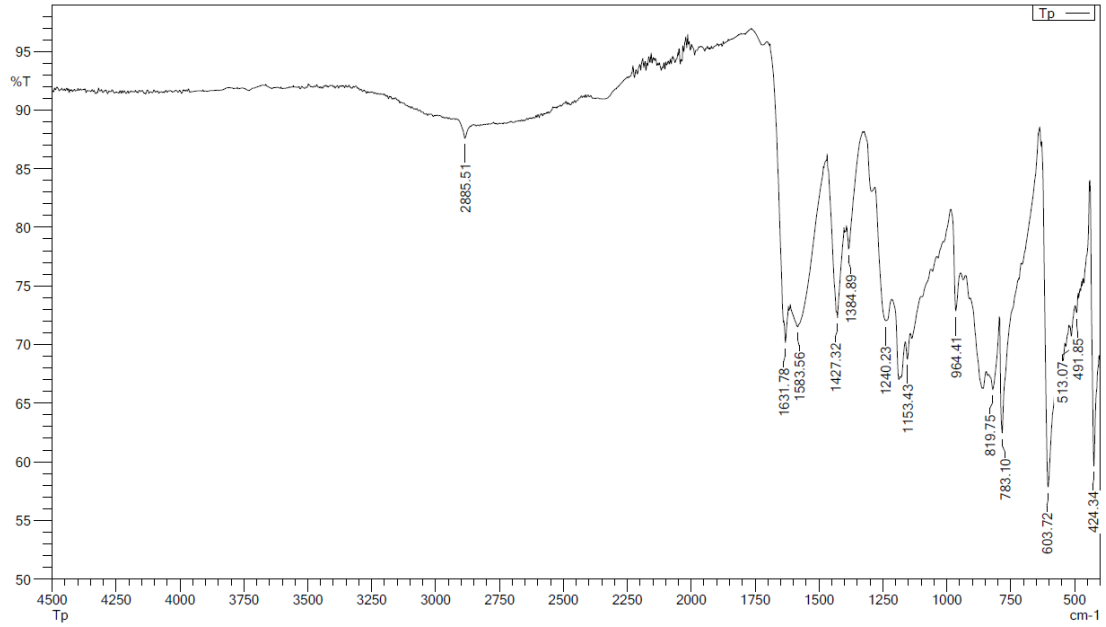

Figure S6: FTIR spectrum of **Tp**.

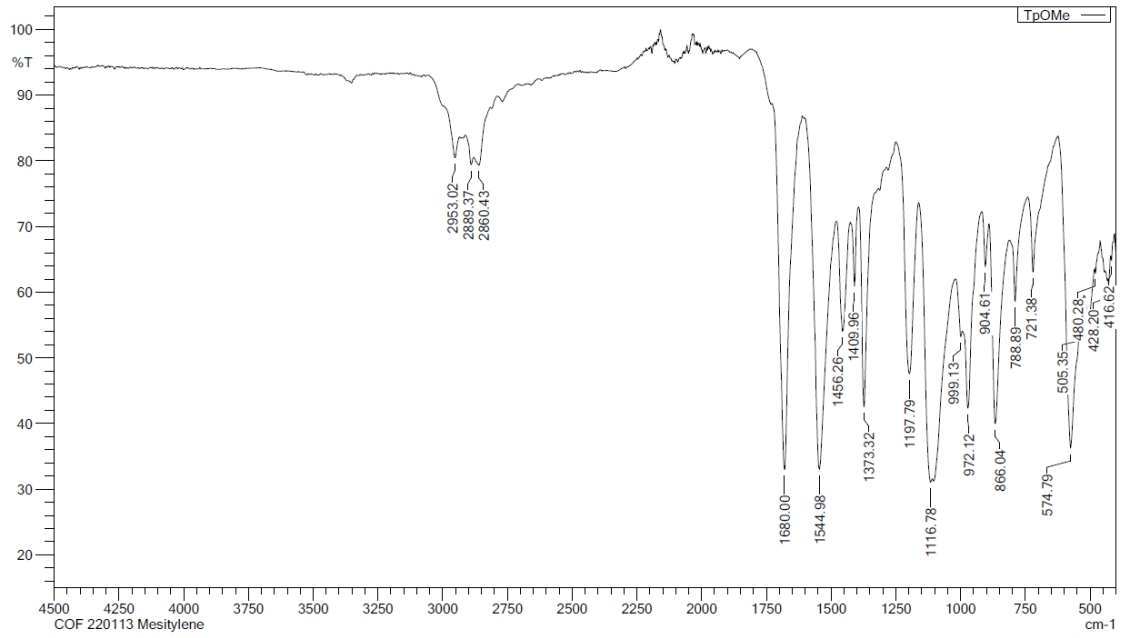

Figure S7: FTIR spectrum of **TpOMe**.

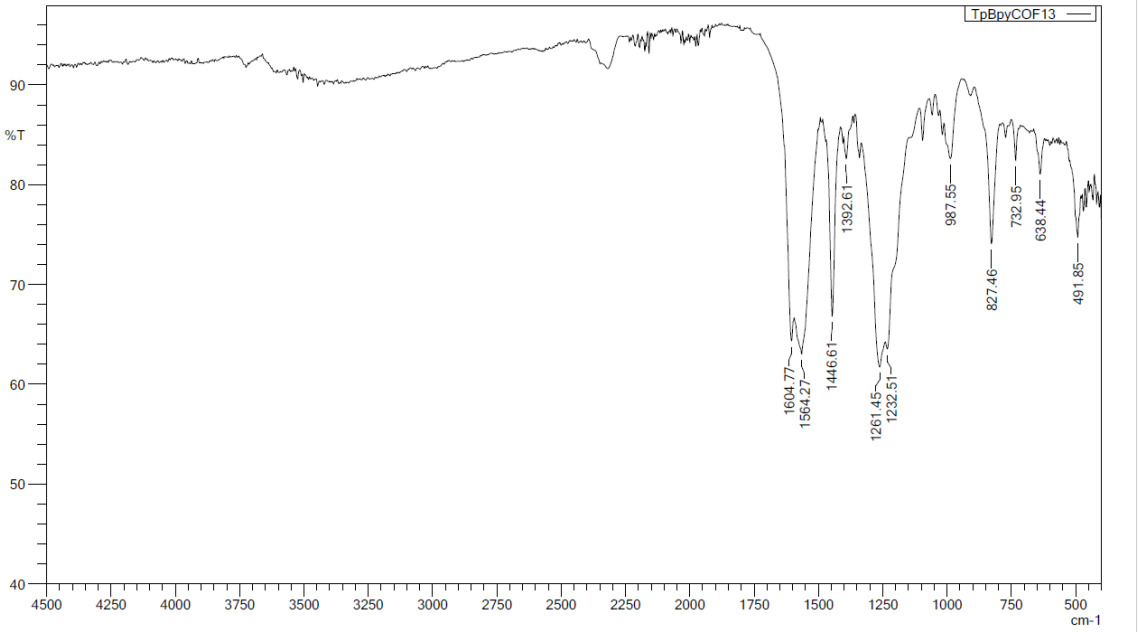

Figure S8: FTIR spectrum of **TpBpyCOF**.

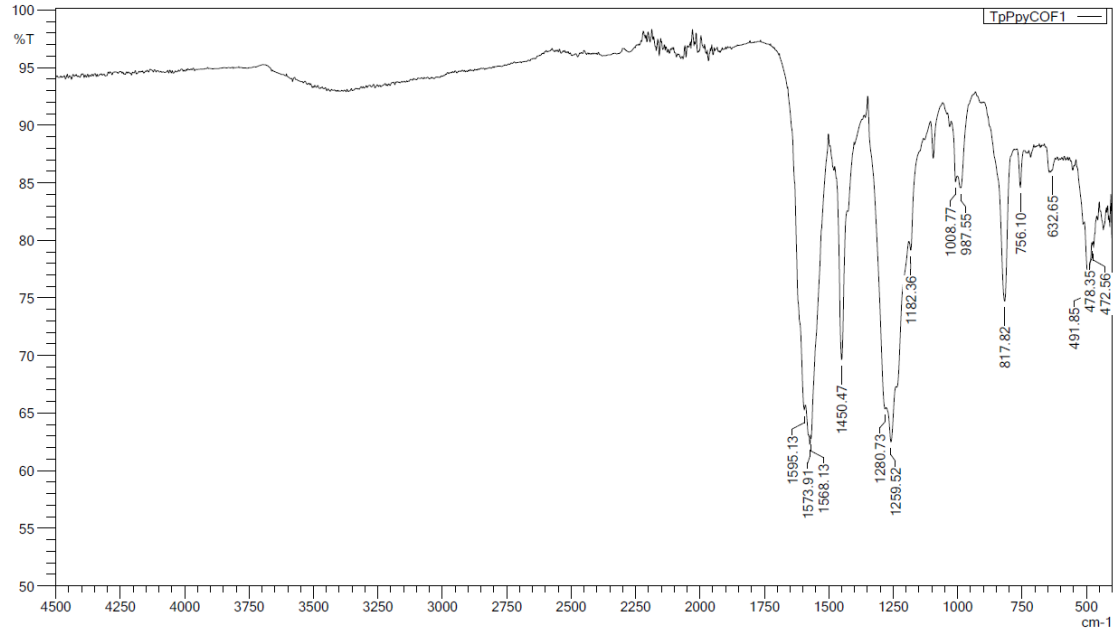

Figure S9: FTIR spectrum of **TpPpyCOF**.

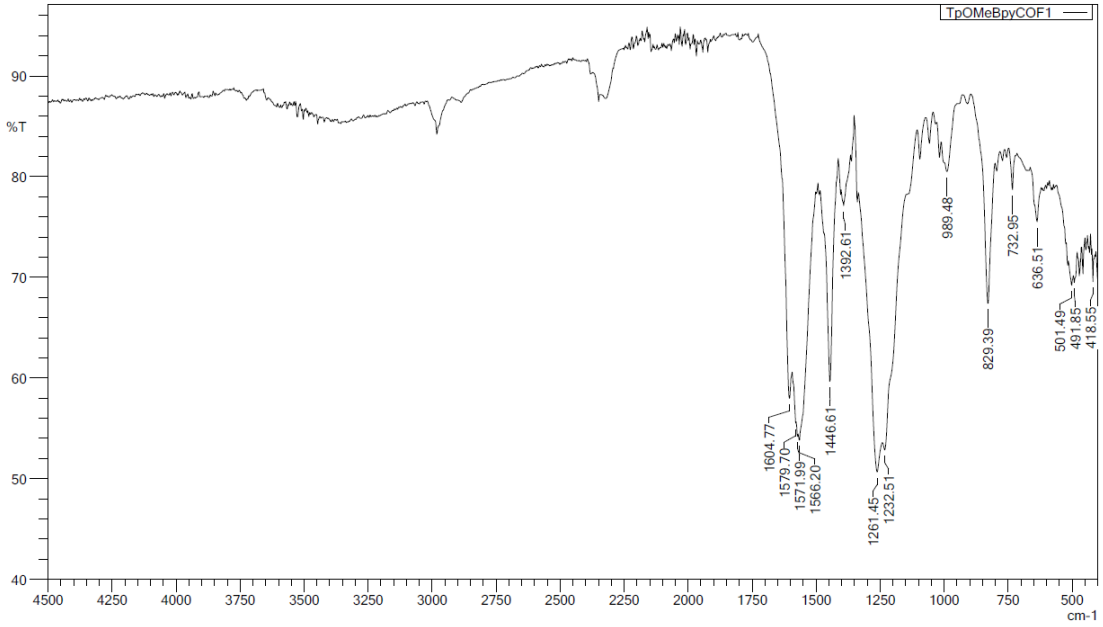

Figure S10: FTIR spectrum of **'TpOMeBpyCOF'**.

S2.3 BF-TEM

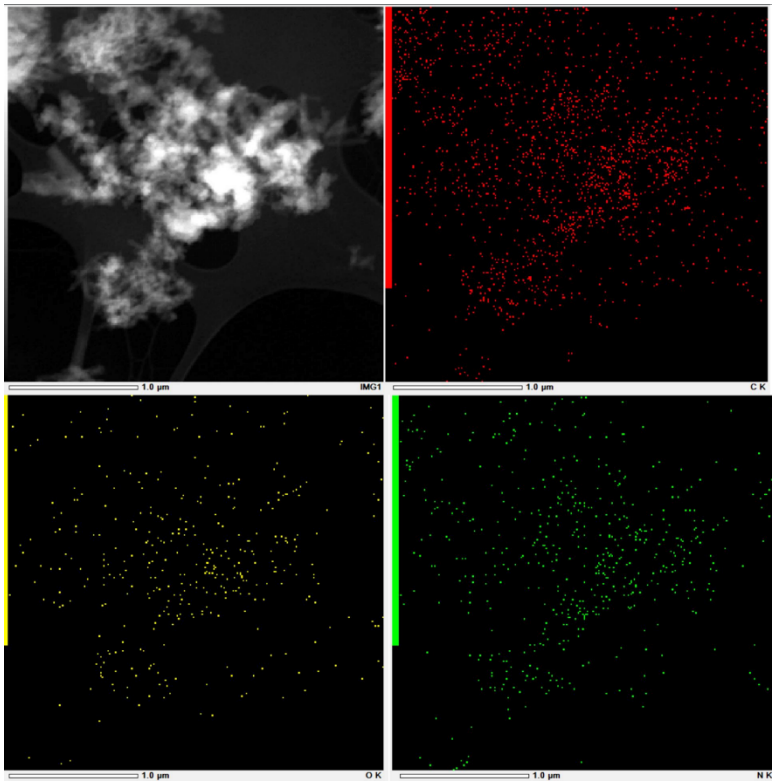

Figure S11: BF-TEM image of **TpBpyCOF** with corresponding EDX elemental map of carbon (red), oxygen (yellow) and nitrogen (green).

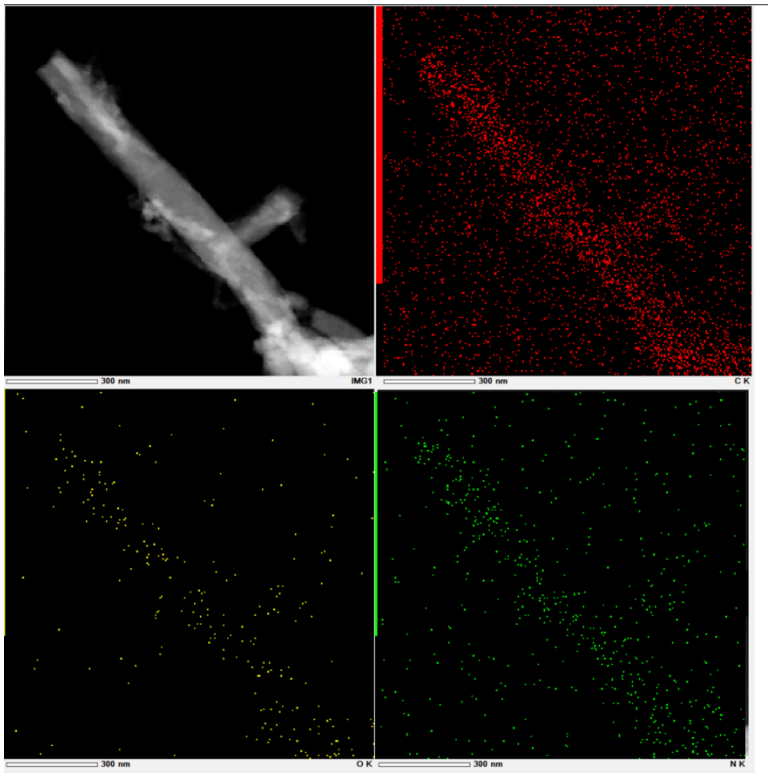

Figure S12: BF-TEM image of **TpPpyCOF** with corresponding EDX elemental map of carbon (red), oxygen (yellow) and nitrogen (green).

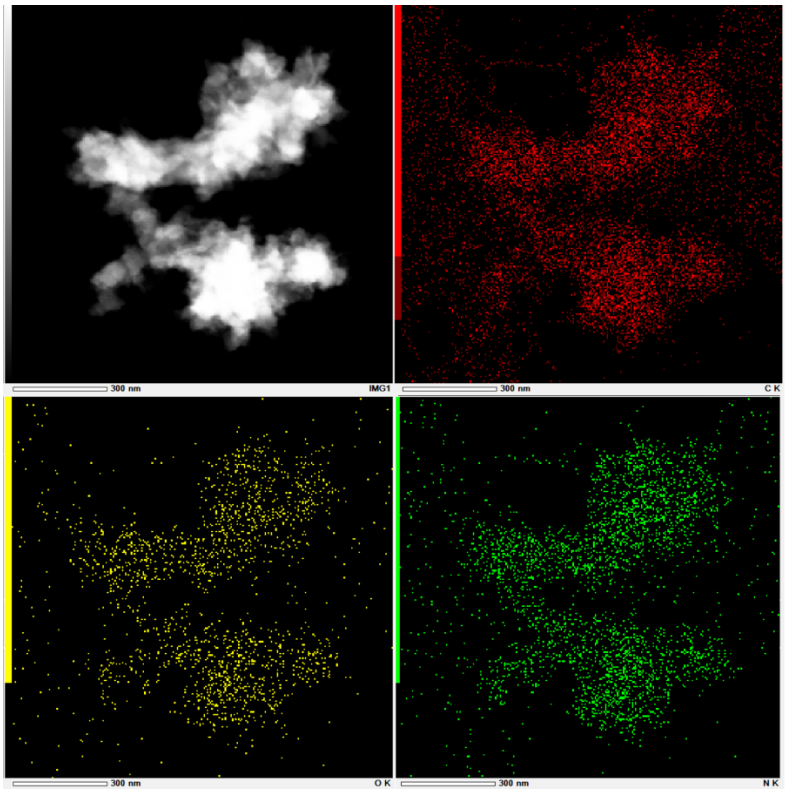

Figure S13: BF-TEM image of **'TpOMeBpyCOF'** with corresponding EDX elemental map of carbon (red), oxygen (yellow) and nitrogen (green).

S2.4 XPS spectra

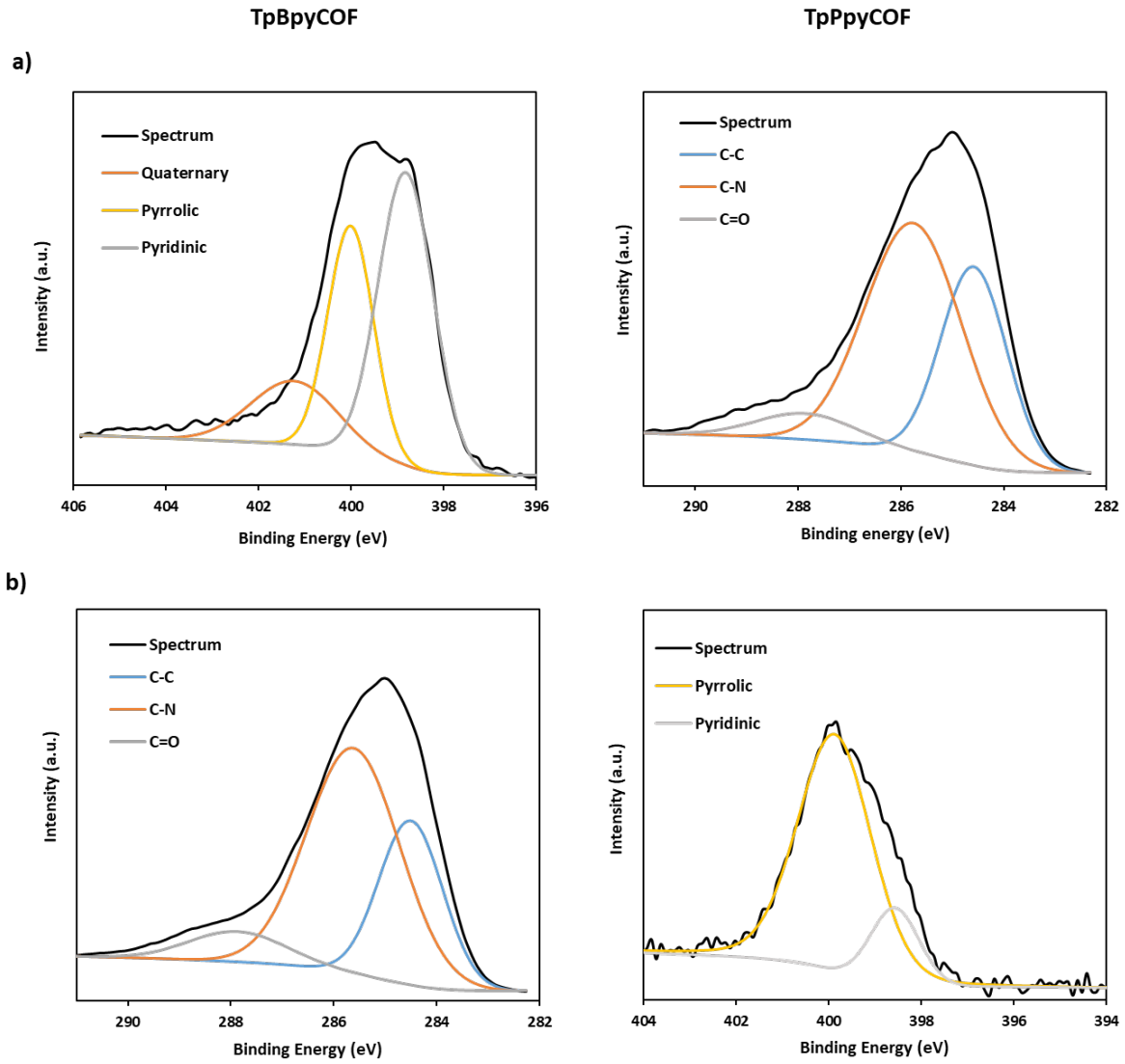

Figure S14: (a) C 1s XPS spectra and (b) N 1s XPS spectra of **TpBpyCOF** and **TpPpyCOF**.

S2.5 NMR

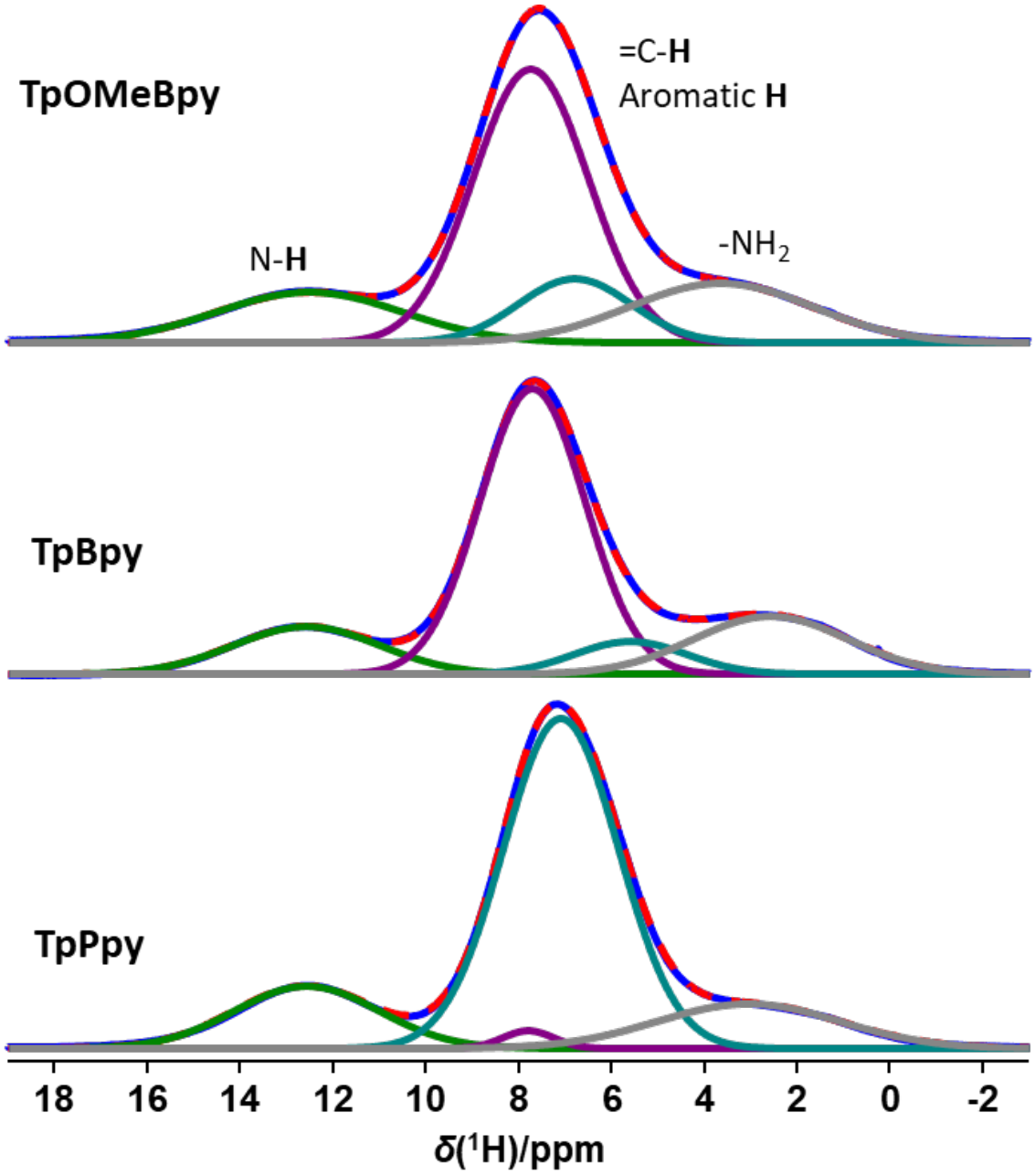

Figure S15: ^{1}H direct-excitation spectra of **TpPpyCOF**, **TpBPyCOF**, and **'TpOMeBpyCOF'** recorded at 295 K at 18.8 T. The expected methoxy resonance was absent in the case of **'TpOMeBpyCOF'**, indicating demethylation of this material.

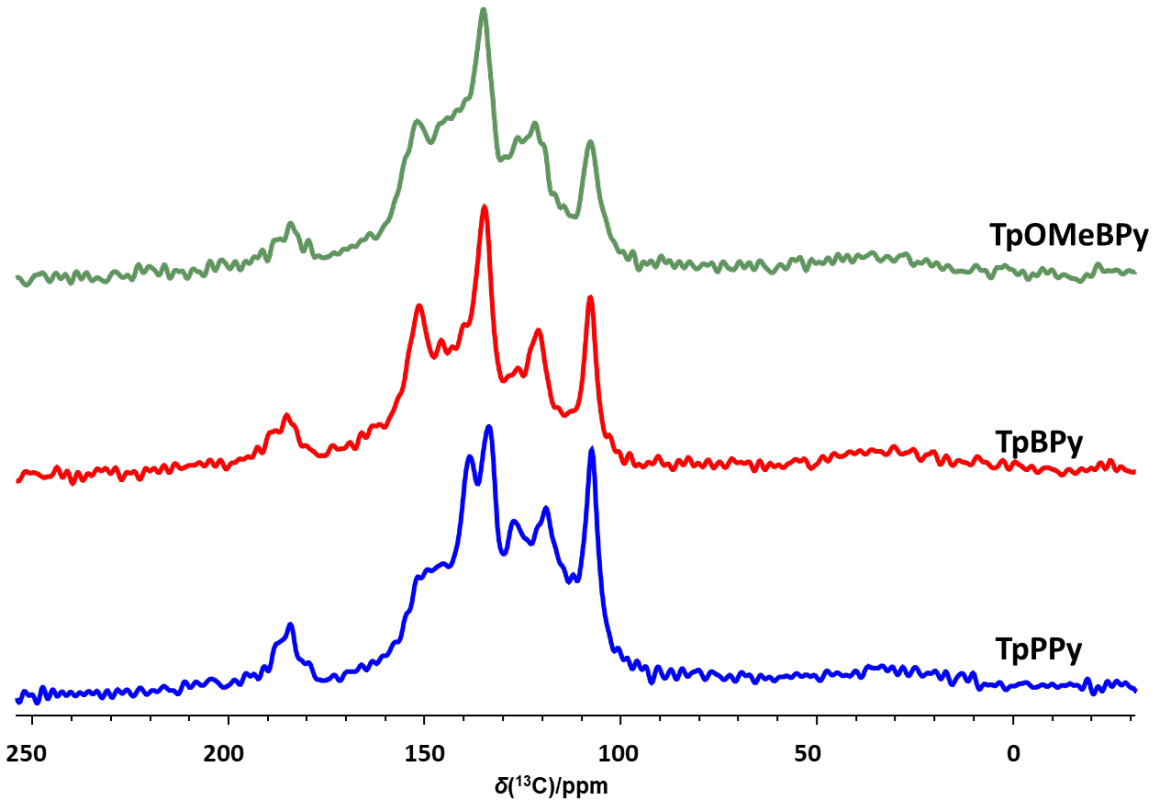

Figure S16: ^{1}H-^{13}C CPMAS spectra of **TpPpyCOF**, **TpBPyCOF**, and **'TpOMeBpyCOF'** recorded at 295 K at 18.8 T. The methoxy resonance was absent in the case of **'TpOMeBpyCOF'**, indicating demethylation of this material.

S2.6 Cyclic voltammetry curves

The procedure to obtain the CB energy levels of the COFs was adapted from a literature method.[10] Mechanical grinding was used to exfoliate the COFs to dropcast them on the FTO substrate, in order to obtain the working electrode.

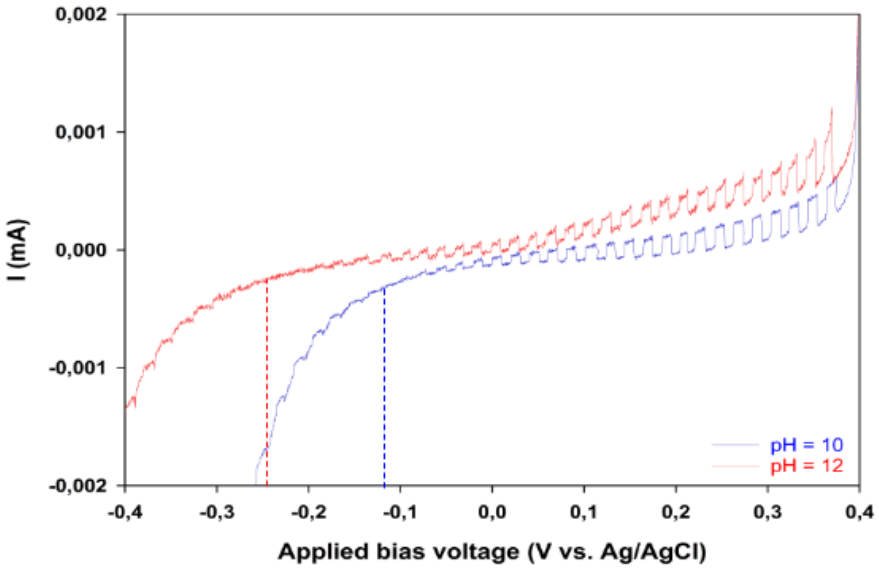

Figure S17: Linear sweep voltammetry of **TpBpyCOF** under chopped illumination in electrolytes at pH 10 or 12. The umklappotential is marked by the red and blue lines.

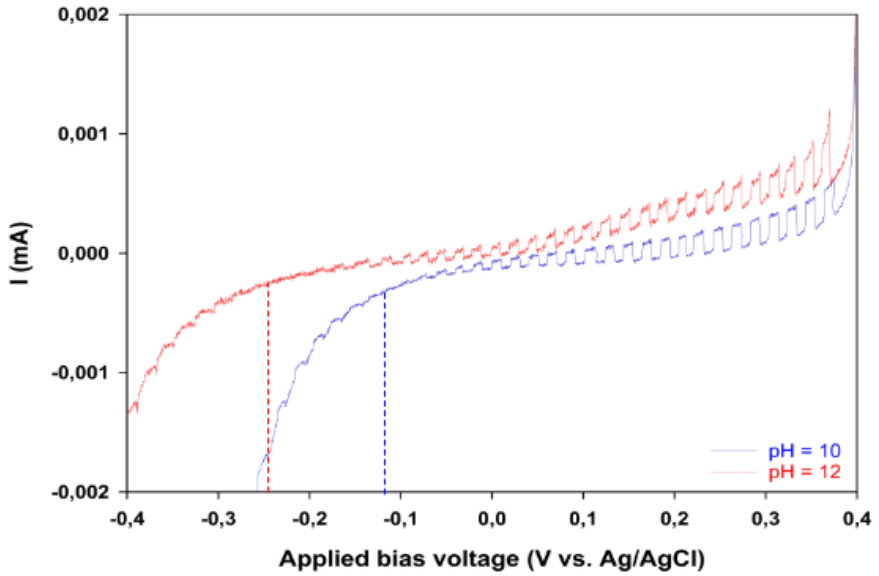

Figure S18: Linear sweep voltammetry of **TpPpyCOF** under chopped illumination in electrolytes at pH 10 or 12. The umklappotential is marked by the red and blue dotted lines.

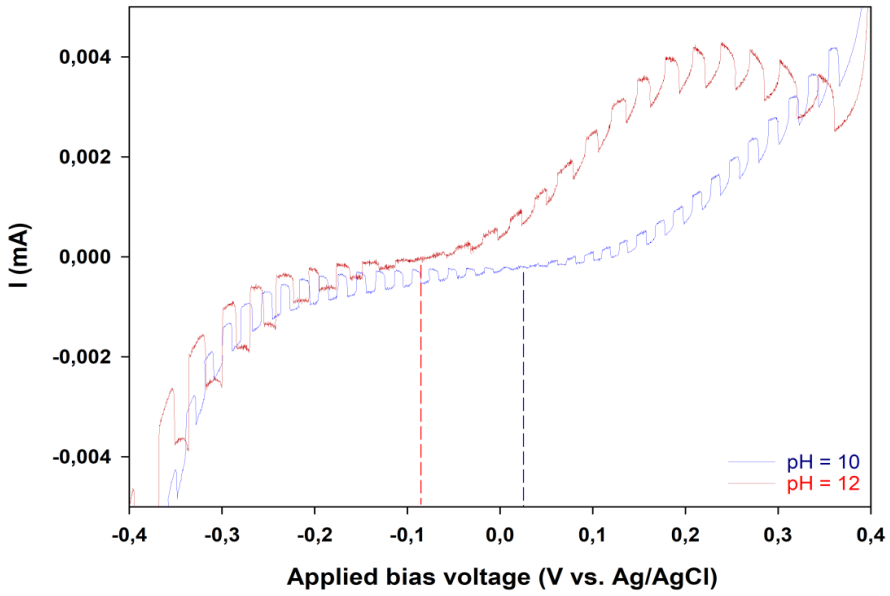

Figure S19: Linear sweep voltammetry of **'TpOMeBpyCOF'** under chopped illumination in electrolytes at pH 10 or 12. The umklappotential is marked by the red and blue dotted lines.

S2.7 Synthesis and characterization of 'TpOMeBpyCOF'

S2.7.1 Synthesis procedure

'TpOMeBpyCOF' was synthesized by charging an Agilent GC vial (size: 22.75 mm x 75 mm; 20 mm cap) with **TpOMe** (76 mg, 0.3 mmol, 1 eq.) and **Bpy** (83.7 mg, 0.45 mmol, 1.5 eq.). Dimethylacetamide (DMAc, 4.5 mL) and *o*-dichlorobenzene (*o*DCB, 1.5 mL) were added via the sides of the vial, to flush the remaining solids from the walls. Then 0.6 mL of 6.0 M aqueous acetic acid was added and the vial was capped. This mixture was then sonicated for 10 minutes, flash frozen at 77 K in liquid N_2 and degassed by three freeze-pump-thaw cycles, after which the vial was put under argon. After warming to room temperature the vial was placed in an oven pre-heated at 120 °C. The resulting red powder was collected via filtration and washed sequentially with copious DMAc-DMF-H_2O-acetone-ethanol-THF. Further purification was done by Soxhlet extraction with methanol for 72 hours. Finally, the material was dried under vacuum overnight giving '**TpOMeBpyCOF'** as a dark red powder (115 mg).

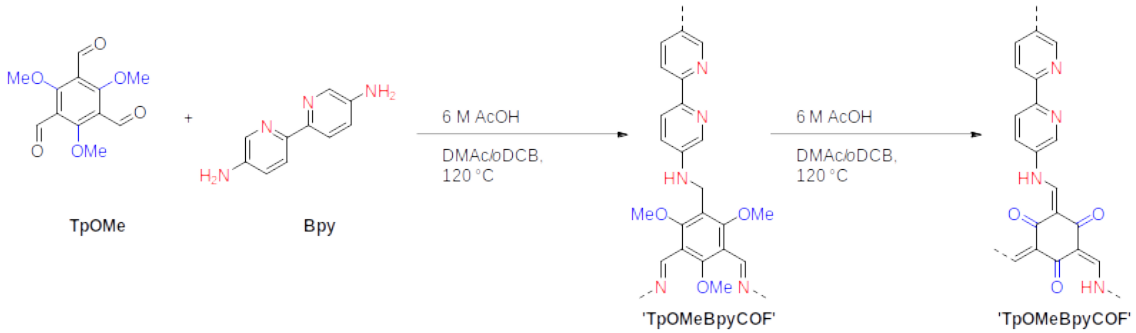

Scheme S5: Schematic representation of the synthesis of **'TpOMeBpyCOF'**.

S2.7.2 Characterization

The synthesis of **TpOMeBpyCOF** has already been described in literature via a mechanochemical reaction, and the resulting material certainly contained methyl groups, as indicated by its carbon NMR spectra.[3] In our case the material was made via solvothermal synthesis and the resulting material was clearly a COF, as it has distinct diffraction peaks and a crystalline structure according to TEM as well. However, the IR and NMR spectra matches with that of **TpBpyCOF**, and no methoxy groups or imine carbons are visible on NMR (Figures S15-16). This material is therefore designated as **'TpOMeBpyCOF'** as it is not truly a **TpOMe** containing COF. We hypothesize that during the synthesis demethylation takes place, to give a material like **TpBpyCOF**. Compared with **TpBpyCOF** synthesized by condensing **Tp** with **Bpy** this material has a much larger surface area and different morphology, optical properties and catalytic activity as well (Table S1).

Table S1: Comparison between **TpBpyCOF** and **'TpOMeBpyCOF'**

Technique	Result
XRD	Very similar
IR	Almost identical
NMR	Almost identical
Surface area	Larger for **'TpOMeBpyCOF'** (1322 vs 879 m^2/g)
Morphology (visual)	Fluffy dark red powder, **TpBpyCOF** is a dense red powder
SEM	**'TpOMeBpyCOF'** has a more flower like, branched morphology, while **TpBpyCOF** forms large aggregates
Band gap	Lower for **'TpOMeBpyCOF'** (1.95 vs 2.10 eV)
EPR signal	Much lower than for **TpBpyCOF**
Catalytic activity	Lower for **'TpOMeBpyCOF'** (24% vs 38% using $BF_3{\cdot}OEt_2$ 50% vs 61% using $Sc(OTf)_3$)

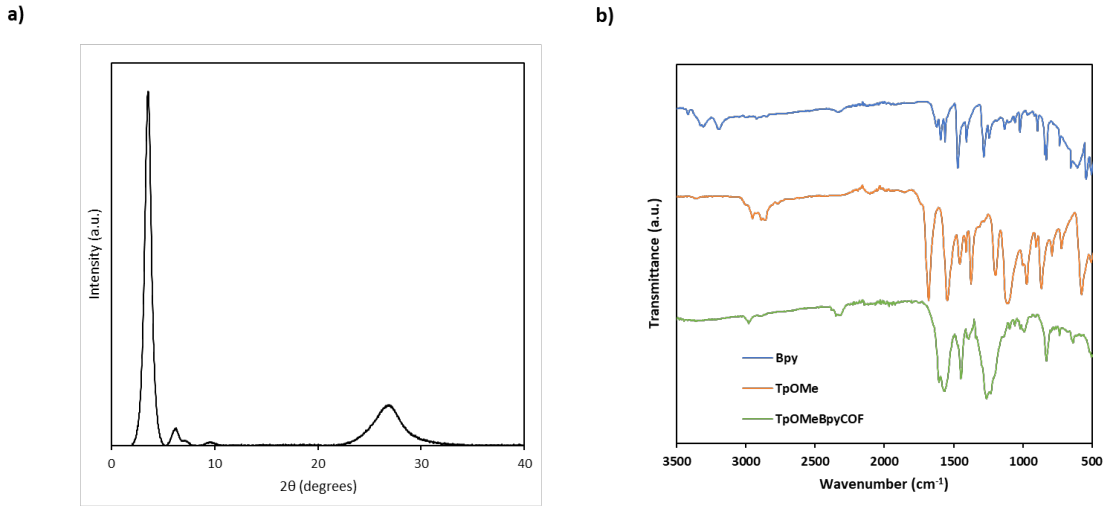

Figure S20: (a) XRD spectrum of **'TpOMeBpyCOF'**; (b) IR spectra of **Bpy**, **TpOMe** and **'TpOMeBpyCOF'**.

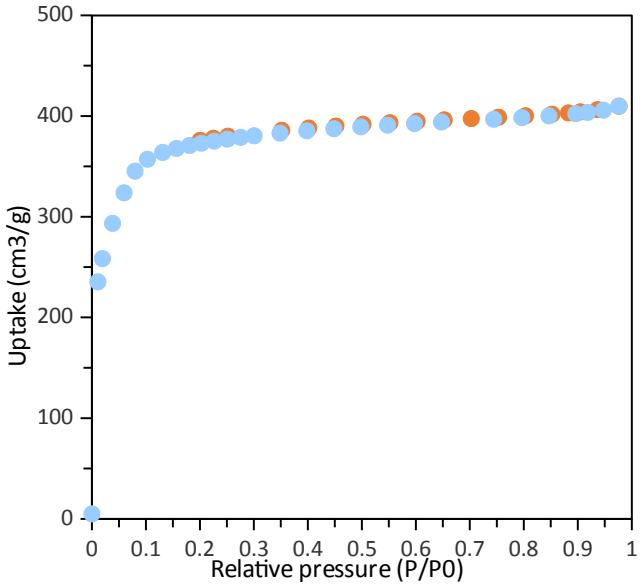

Figure S21: Nitrogen adsorption/desorption isotherms at 77K of **'TpOMeBpyCOF'**.

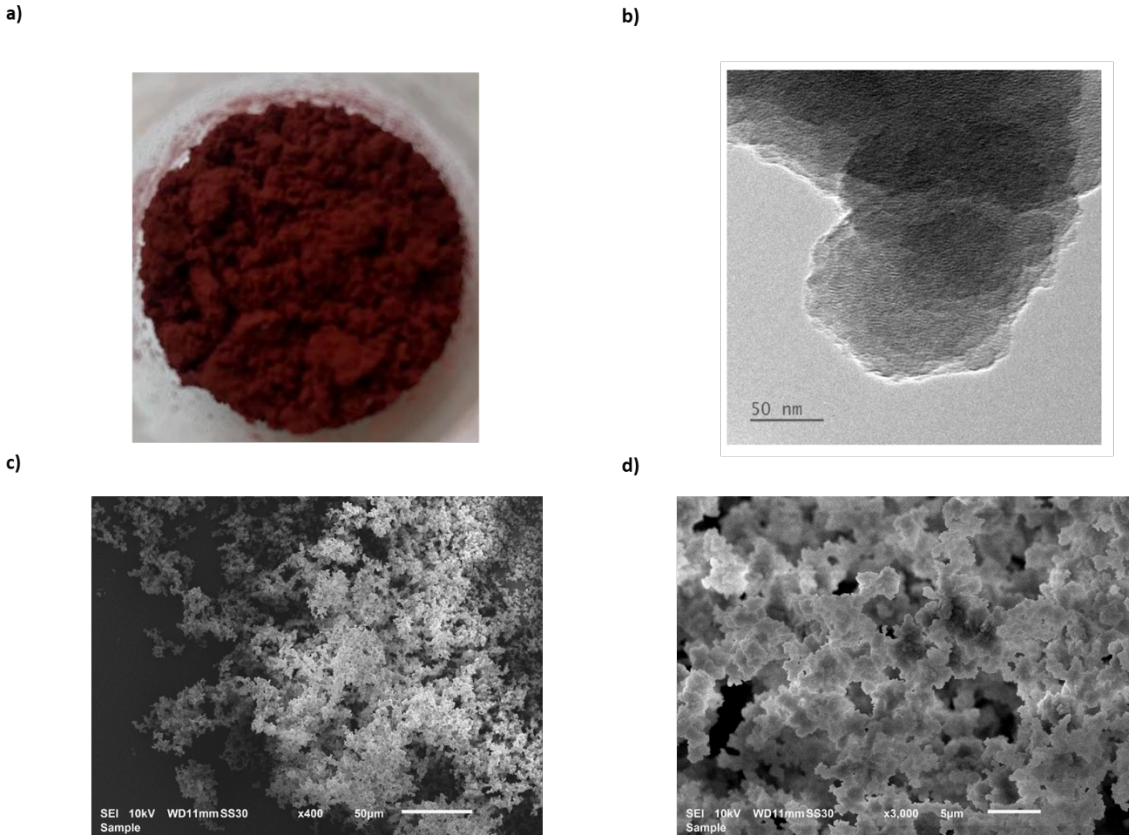

Figure S22: (a) Picture; (b) TEM image; (c) and (d) SEM images with x400 and x3000 magnification of **'TpOMeBpyCOF'**.

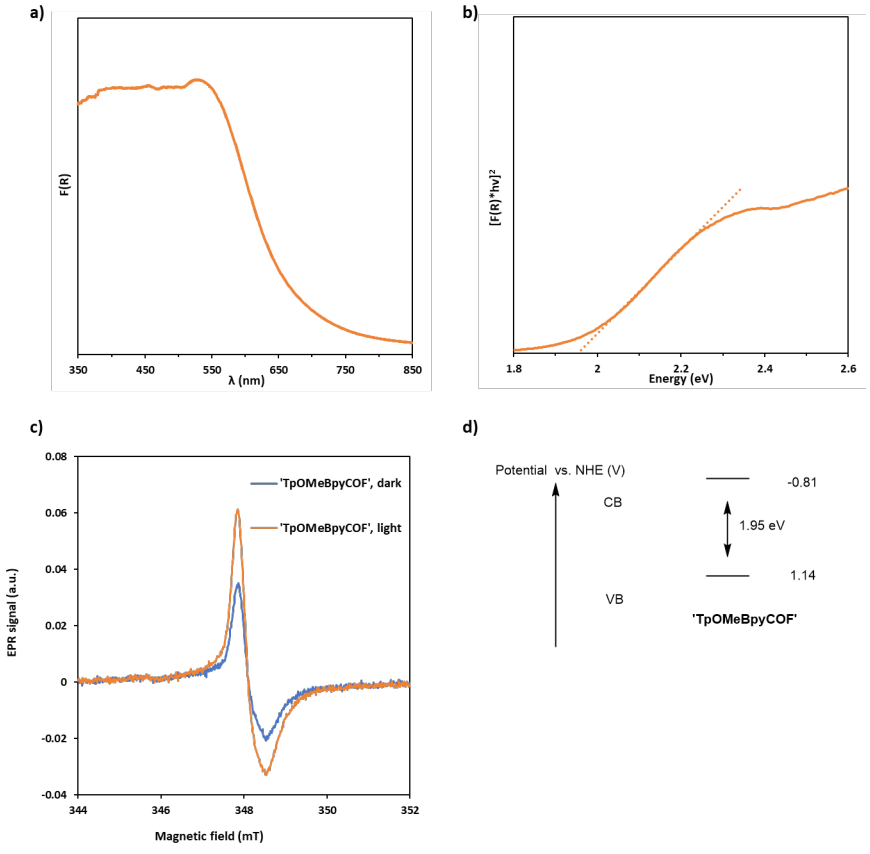

Figure S23: (a) Kubelka-Munk absorption spectrum; (b) Tauc plot; (e) EPR spectra and (d) Band structure of **'TpOMeBpyCOF'**

S3 Computational modelling

S3.1 Construction of system-specific force fields

S3.1.1 Cluster force fields

A system specific force field is derived for each of the materials from the cluster force fields of the underlying building blocks.[11–19] The cluster models are terminated properly as such that they mimic the periodic structure. The used cluster models and their termination are visualized in Figure S24. The Bpy and Ppy linkers are combined with the Tp building block, forming an amine linkage. The Tp cluster is terminated with a phenyl ring, linked by an amine linkage. It is assumed that the nitrogen atoms in the Bpy and Ppy do not influence the resulting covalent and electrostatic parameters of these clusters significantly.

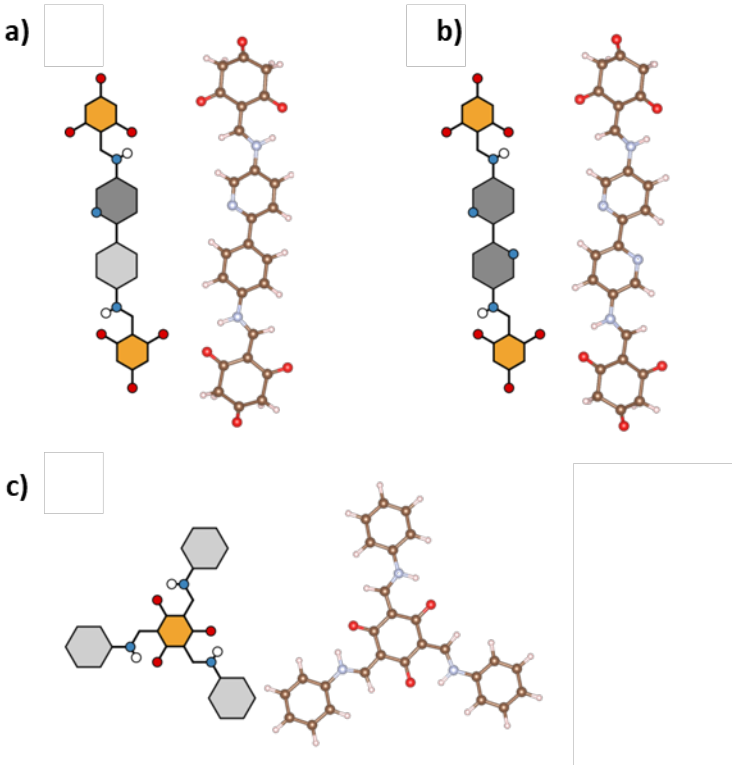

Figure S24: Atomic and abstract visualization of the cluster models that are used to derive the cluster force fields. a) Ppy with a Tp termination (Ppy_amine), b) Bpy with a Tp termination (Bpy_amine), c) Tp with an amine linkage (Tp_amine). The color code that was used: (white) hydrogen, (brown) carbon, (blue) nitrogen, (red) oxygen.

After an optimization, the *ab initio* hessian of each cluster is derived with Gaussian16[20] using the B3LYP exchange-correlation functional[21–23] extended with Grimme D3 dispersion corrections[24] and the 6-311++G(d,p) Pople basis set.[25] For the optimization, the default convergence criteria were adopted and the NoSymm keyword is used. The YQC self-consistent field procedure was followed for both optimization and hessian calculations.

Subsequently, the partial charges are derived from the electron density distribution with the MBIS partitioning scheme,[26] as implemented in HORTON,[27] and adopted by QuickFF[28,29] to determine the electrostatic force field parameters, using Gaussian charge distributions[30] and bond charge increments.[31] Finally, QuickFF[28,29] fits the covalent parameters as such that the force field derived hessian reproduces the *ab initio* hessian as accurately as possible. Besides the covalent and electrostatic interactions, the force field also comprises Van der Waals interactions, as dispersion corrections are included in the *ab initio* calculations. These are described by a Buckingham potential using the fully transferable MM3 parameters.[32]

S3.1.2 Validation

Once the cluster force fields are derived, their capability in reproducing both the *ab initio* relaxed structure and the *ab initio* frequencies is examined. The clusters are first optimized using yaff,[33] after which a normal mode analysis (NMA)[34] is performed with TAMkin[35] to derive the vibrational frequencies. These force field derived frequencies are compared with the earlier derived *ab initio* frequencies in Figure S25. In Figure S26, the internal coordinates (bonds, bends, dihedral angles and out-of-plane distances) from the force field and *ab initio* relaxed structures are compared. For both the frequency and geometry comparison, the mean deviation (MD) and root mean square deviation (RMSD) have been indicated.

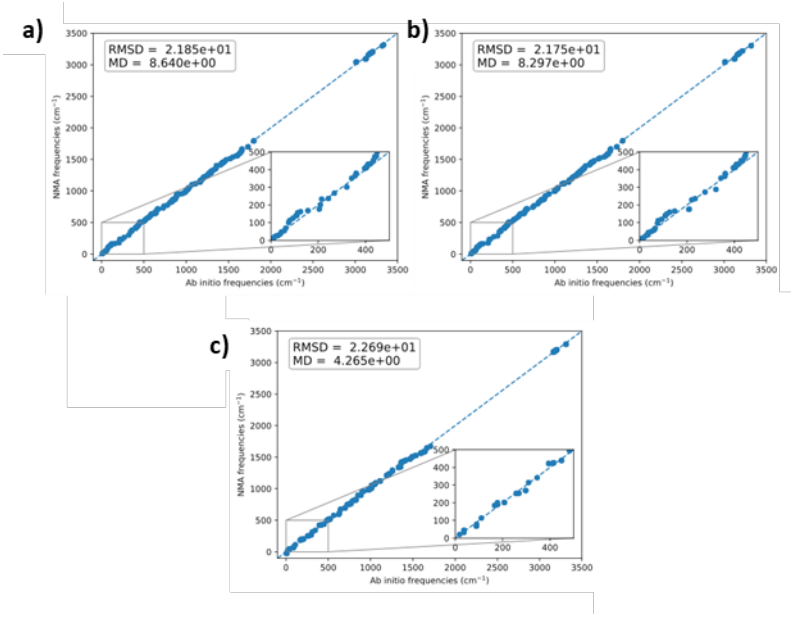

Figure S25 Comparison of the *ab initio* (AI) and force field (FF) derived vibrational frequencies, with an inset of the low frequencies. The dashed lines correspond to perfect agreement. Both the mean deviation (MD) and root mean square deviation (RMSD) are reported. Alphabetical labels correspond to the cluster models in Figure S24: a) Ppy with a Tp termination (Ppy_amine), b) Bpy with a Tp termination (Bpy_amine), c) Tp with an amine linkage (Tp_amine).

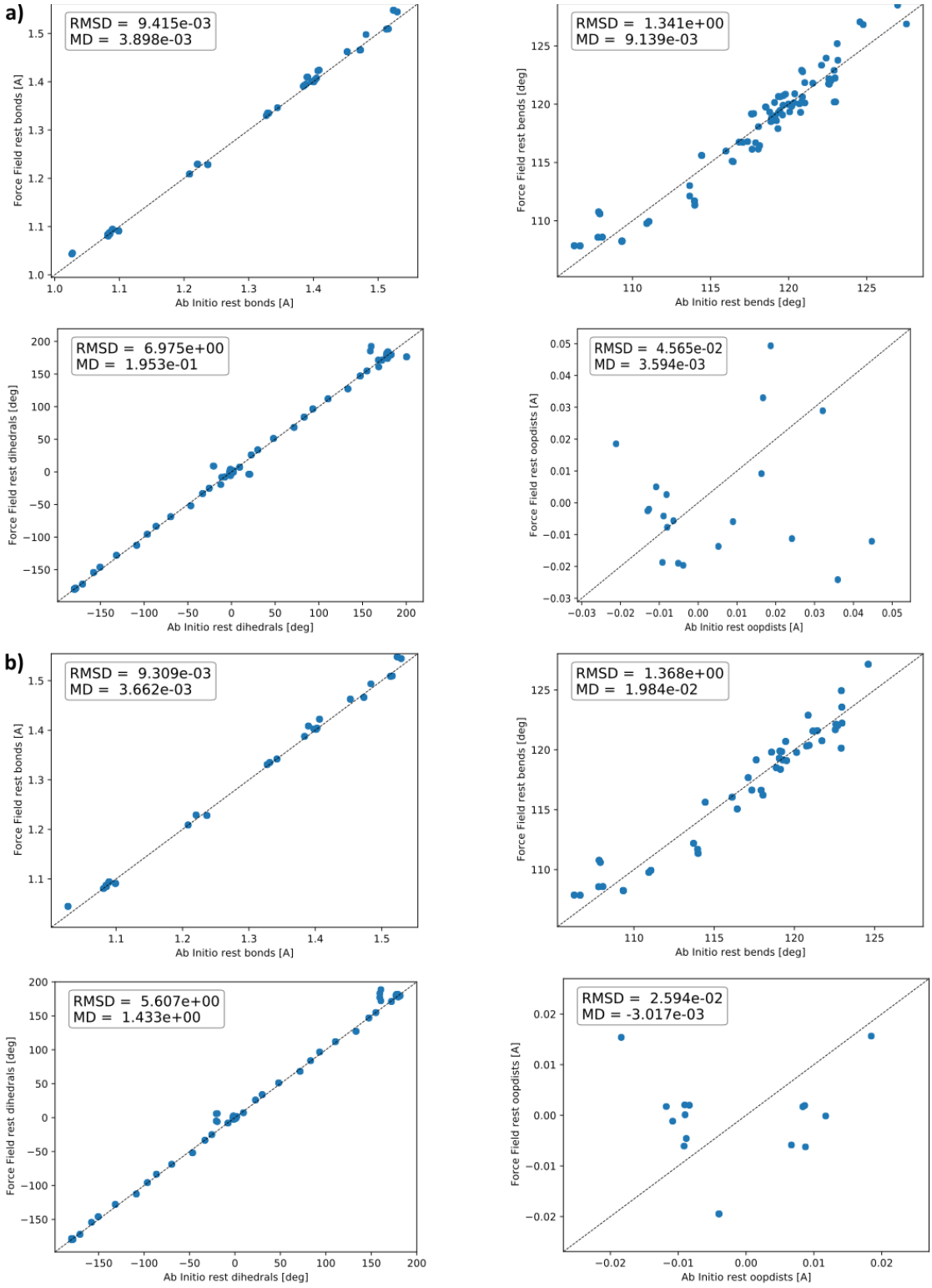
a)
RMSD = 9.415e-03
MD = 3.898e-03
Force Field rest bonds [A]
Ab Initio rest bonds [A]
RMSD = 1.341e+00
MD = 9.139e-03
Force Field rest bends [deg]
Ab Initio rest bends [deg]
RMSD = 6.975e+00
MD = 1.953e-01
Force Field rest dihedrals [deg]
Ab Initio rest dihedrals [deg]
RMSD = 4.565e-02
MD = 3.594e-03
Force Field rest oopdists [A]
Ab Initio rest oopdists [A]
b)
RMSD = 9.309e-03
MD = 3.662e-03
Force Field rest bonds [A]
Ab Initio rest bonds [A]
RMSD = 1.368e+00
MD = 1.984e-02
Force Field rest bends [deg]
Ab Initio rest bends [deg]
RMSD = 5.607e+00
MD = 1.433e+00
Force Field rest dihedrals [deg]
Ab Initio rest dihedrals [deg]
RMSD = 2.594e-02
MD = -3.017e-03
Force Field rest oopdists [A]
Ab Initio rest oopdists [A]

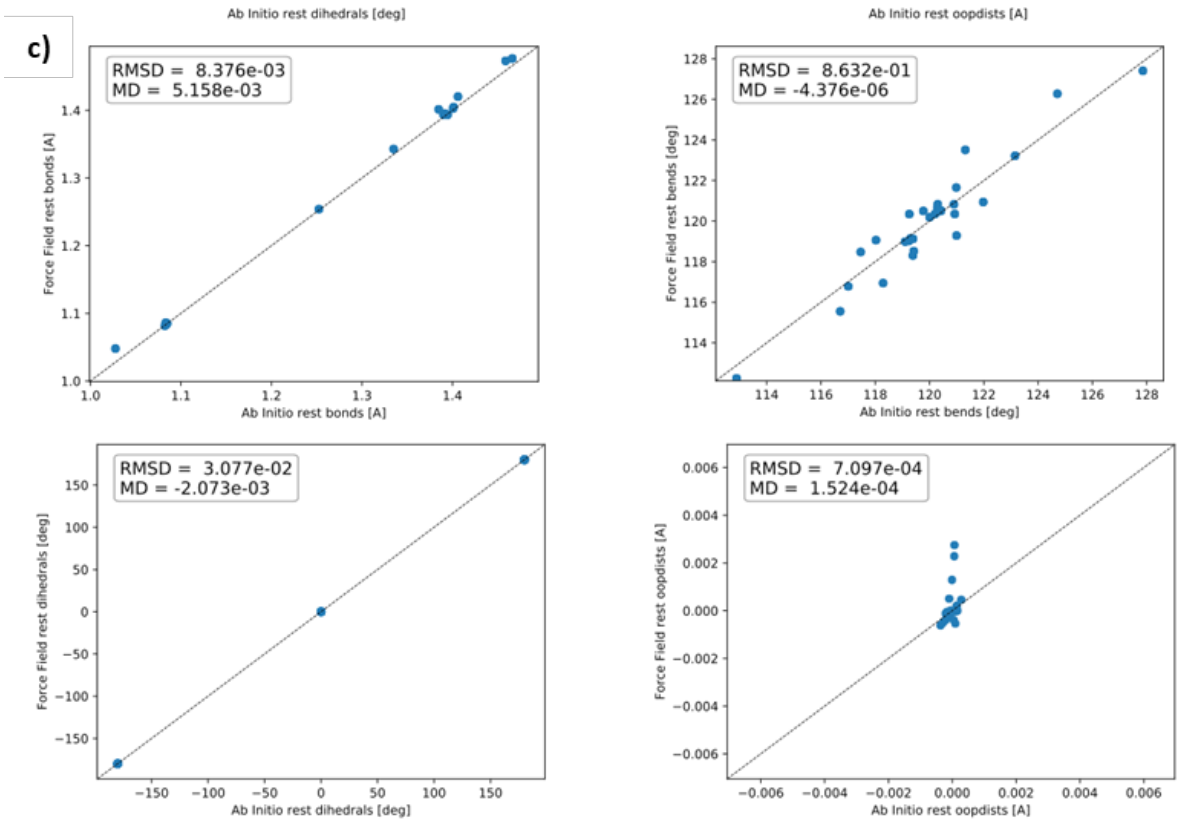

Figure S26: Comparison of the *ab initio* (AI) and force field (FF) derived relaxed internal coordinates. The dashed lines correspond to perfect agreement. Both the mean deviation (MD) and root mean square deviation (RMSD) are reported. Alphabetical labels correspond to the cluster models in Figure S24: a) Ppy with a Tp termination (Ppy_amine), b) Bpy with a Tp termination (Bpy_amine), c) Tp with an amine linkage (Tp_amine). For each cluster, the bonds, bends, dihedral angles, and out-of-plane distances are visualized from top left to bottom right respectively.

S3.1.3 Additional dihedral terms

When considering the deviations in the dihedral angles after optimizing the optimal *ab initio* geometry with the force field, it is clear that the clusters force field needs to be adapted to better account for the rotational barrier of the imine/amine linkage and the phenyl/pyridine rotations. This is facilitated by *ab initio* rotational scans, such that the relevant force field terms can be replaced by more accurate sixth order polynomials. As evidenced by Figures S27-S31, it is clear that the new force field significantly improves the reproduction of this rotational barrier.

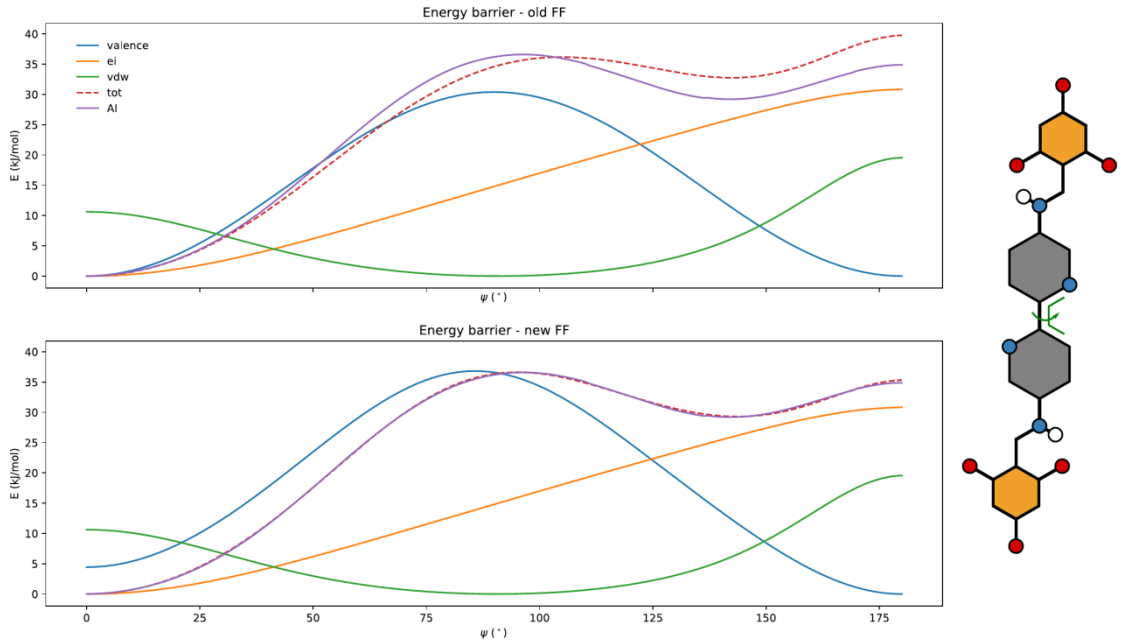

Figure S27: Force field contributions of the old and newly fitted force field for the rotational barrier of the bipyridine unit, with an amine linkage (Bpy_amine), compared to the corresponding *ab initio* barrier. The total (tot) contribution is equal to the sum of the covalent contributions (valence), the electrostatic interactions (ei), and the dispersion interactions (vdw).

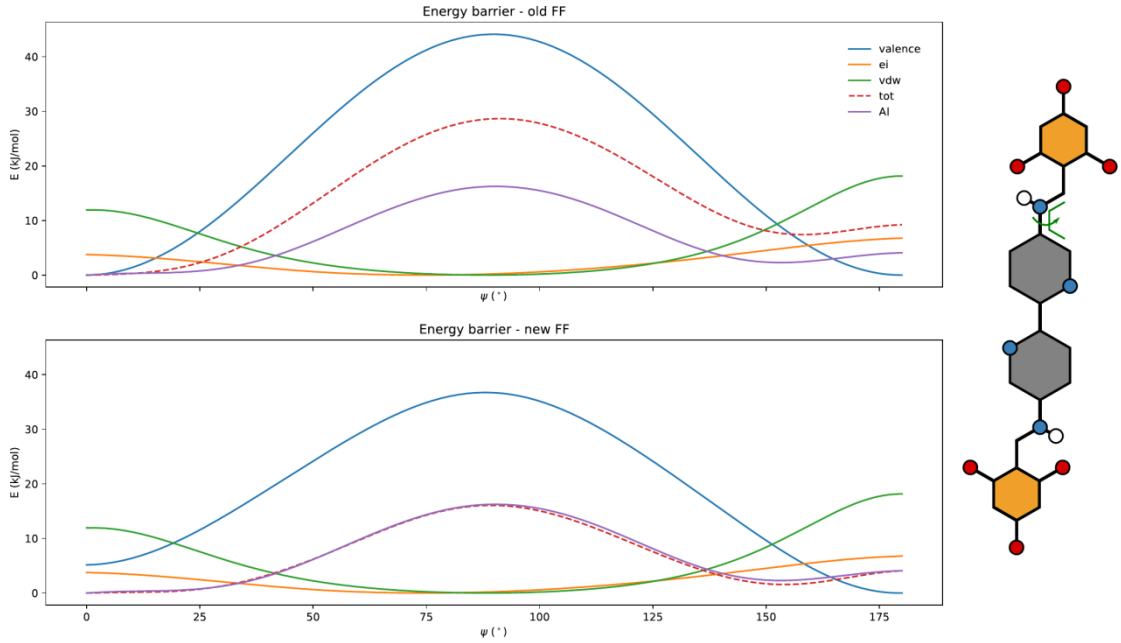

Figure S28: Force field contributions of the old and newly fitted force field for the rotational barrier of the amine linkage, linked to the bipyridine unit (Bpy_amine), compared to the corresponding *ab initio* barrier. The total (tot) contribution is equal to the sum of the covalent contributions (valence), the electrostatic interactions (ei), and the dispersion interactions (vdw).

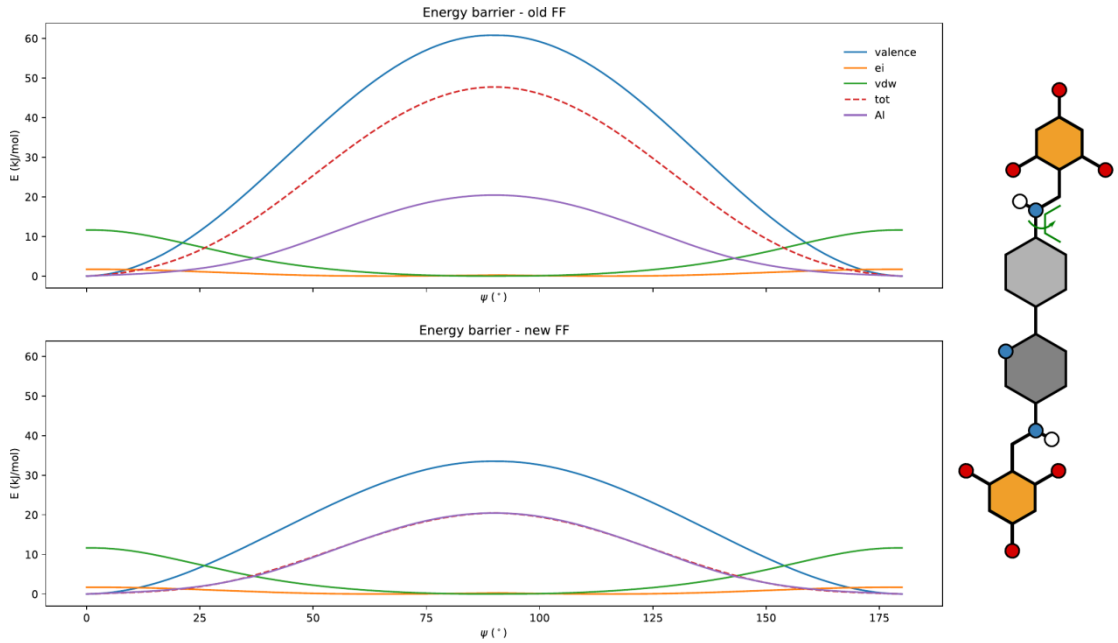

Figure S29: Force field contributions of the old and newly fitted force field for the rotational barrier of the amine linkage, linked to the phenylpyridine unit (Ppy_amine), compared to the corresponding *ab initio* barrier. The total (tot) contribution is equal to the sum of the covalent contributions (valence), the electrostatic interactions (ei), and the dispersion interactions (vdw).

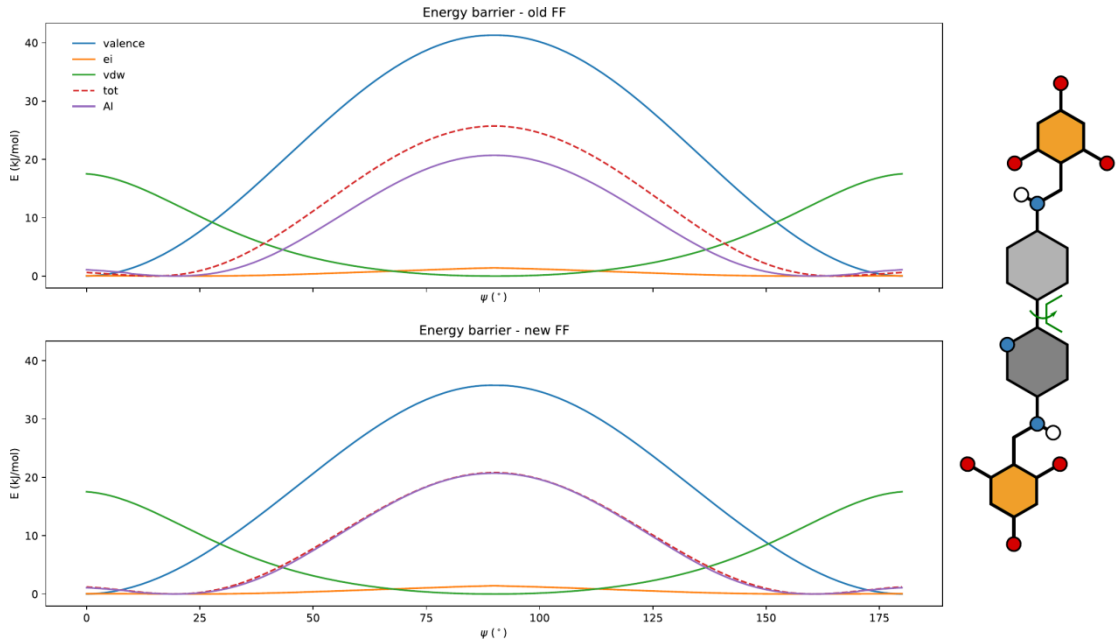

Figure S30: Force field contributions of the old and newly fitted force field for the rotational barrier of the phenylpyridine unit, with an amine linkage (Ppy_amine), compared to the corresponding *ab initio* barrier. The total (tot) contribution is equal to the sum of the covalent contributions (valence), the electrostatic interactions (ei), and the dispersion interactions (vdw).

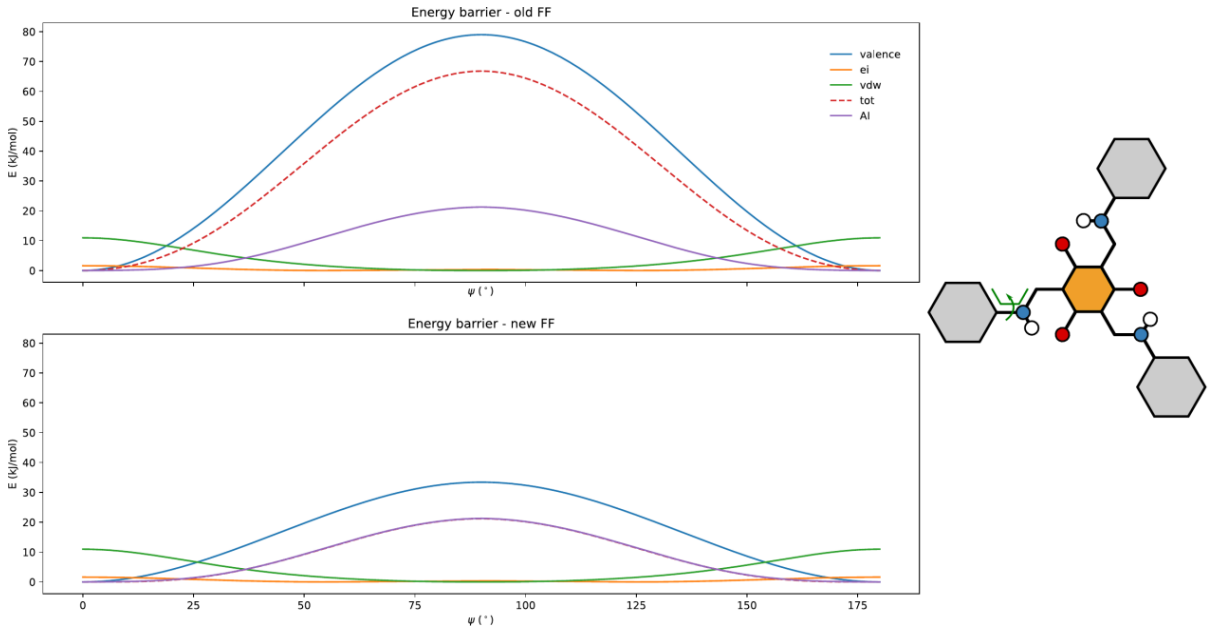

Figure S31: Force field contributions of the old and newly fitted force field for the rotational barrier of the amine linkage, with respect to the Tp unit (Tp_amine), compared to the corresponding *ab initio* barrier. The total (tot) contribution is equal to the sum of the covalent contributions (valence), the electrostatic interactions (ei), and the dispersion interactions (vdw).

S3.1.4 Combining cluster force field into periodic force fields

Following our earlier established procedure,[18,19] accurate, system-specific periodic force fields can be generated from the cluster force field of their underlying building blocks, on the condition that their framework environment is properly mimicked in the cluster termination. This cluster approximation has the smallest impact on the covalent terms that are embedded fully in the cluster. Therefore, these terms are directly adopted from the cluster force field. On the other hand, overlap terms that span two building blocks are described most accurately in the force field of the building block with the majority of the atoms. The parameters of these overlap terms are defined by a weighted average over the respective terms in both constituent cluster force fields.

Similarly, the bond charge increments of bonds between atoms that are assigned to different building blocks is formed by an average of the bond charge increments in the two respective clusters. Charge neutrality is guaranteed as bond charge increments are used. The Van der Waals interactions can be adopted directly as the parameters of the Buckingham potential are derived from atomic parameters.

S3.2 Structural models

The initial structural models are generated *in silico* with our in-house structure assembly software, which is based on a top-down approach.[36] This requires a predefined topology, which is in this work always the honeycomb **hcb** lattice, and a set of building blocks that can be placed on its nodes. TpBpy and TpPpy are generated using a combination of clusters d and b and clusters d and a, respectively (see Figure S24), similar to their synthesis procedure. For each cluster, an appropriate set of points of extension is defined as the points where the building block can link with other building blocks. The points of extension are here always chosen in the center of the C-N amine bond. The termination of the clusters, *i.e.* all atoms beyond the points of extension, are omitted in the building procedure.

After careful selection of the building blocks and the topology, the topological nodes are decorated in a three-step procedure. Initially, the unit cell of the topology is isotropically rescaled to accommodate the building blocks. Secondly, the configurations of each building block are selected for which the points of extension are nicely oriented towards the neighboring topological nodes. The symmetry of the atomic representation of the building blocks can be lower than the symmetry of the points of extension. In these cases, multiple configurations that result in the same alignment within the topology, have a different atomic representation. In the final step, one configuration for each building block is chosen from the remaining ones based on an energetical descriptor that defines the energy penalty introduced by inserting the building blocks in this configuration. Once all topological nodes are decorated with the appropriate building blocks, a two-layer structure is obtained by taking a 1,1,2-supercell with a sub-optimal interlayer distance of 10 Å. The initial models are realized by relaxing these structures with the periodic force fields as derived in Section S3.1.

Within the materials discussed in the main text, several asymmetric moieties are present, which might give rise to variations in the powder X-ray diffraction (PXRD) pattern depending on their relative orientations. Moreover, as the emergent behavior of 2D COFs is typically dependent on the behavior of subsequent layers, variations in these orientations of subsequent layers is also taken into account. Although molecular dynamics (MD) simulations are performed to sample the relevant parts of the potential energy surface (PES), the stacking of the layers might inhibit variations in the orientations of these moieties to occur, such that they have to be modelled explicitely.

Here, we explicitly take the orientation of the following units into account:

- Imine/amine linkage
- Bipyridine/phenylpyridine linker

Within one layer their orientation can be either parallel or antiparallel, whereas between subsequent layers their orientation can be either symmetric or antisymmetric. Moreover, the relative sequence of the phenyl ring and pyridine ring in phenylpyridine can be switched between subsequent rings, which will be denoted as either aligned or alternating. These variations are all abstractly visualized in Figure S32 for clarity.

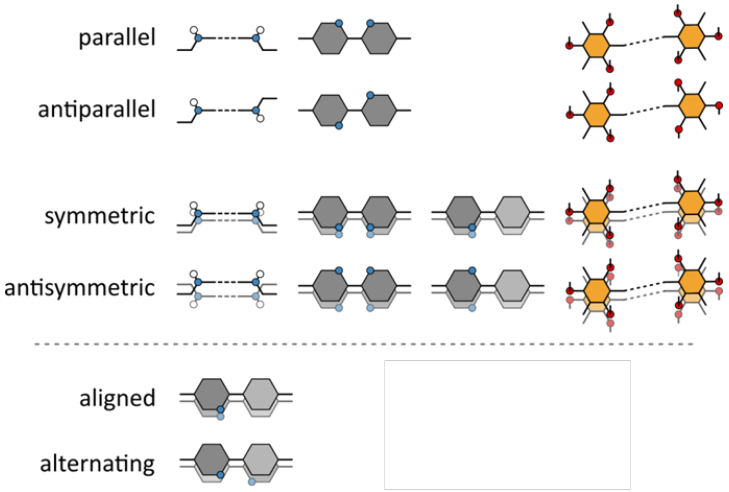

Figure S32: Abstract illustration of the terminology for the different structural models. (Top) General labels which are applicable to most building units. As the imine and amine linkage behave identically (terminology wise) only the amine examples are provided. The parallel/antiparallel label is based on the single layer orientation, whereas the symmetric/antisymmetric label is based on the two layer orientation. (Bottom) The aligned/alternating label is a specific label for the phenylpyridine moiety to account for the relative position of the pyridine ring.

S3.3 PXRD generation

As in our previous work,[37] all structural models were first optimized for a static approach to the PXRD pattern, sampling the PES at zero Kelvin. However, in general, this is a poor approximation for reproducing the experimental reference pattern when dealing with 2D COFs with dynamically shearing layers. Instead, simulating at the elevated pressures and temperatures that occur during the experimental measurement, results in small dynamic fluctuations of the reflection planes that mimic the peak broadening effects that occur during the inherently time-averaged diffraction measurement. As such, by averaging the PXRDs calculated at 50 uniformly distributed snapshots throughout the MD simulation, a much better agreement is obtained. In accordance with our previously reported workflow[37] a metric comparison was performed to identify the optimal models, as illustrated in Figures S33-S34. The corresponding PXRD patterns are provided as additional supplementary files.

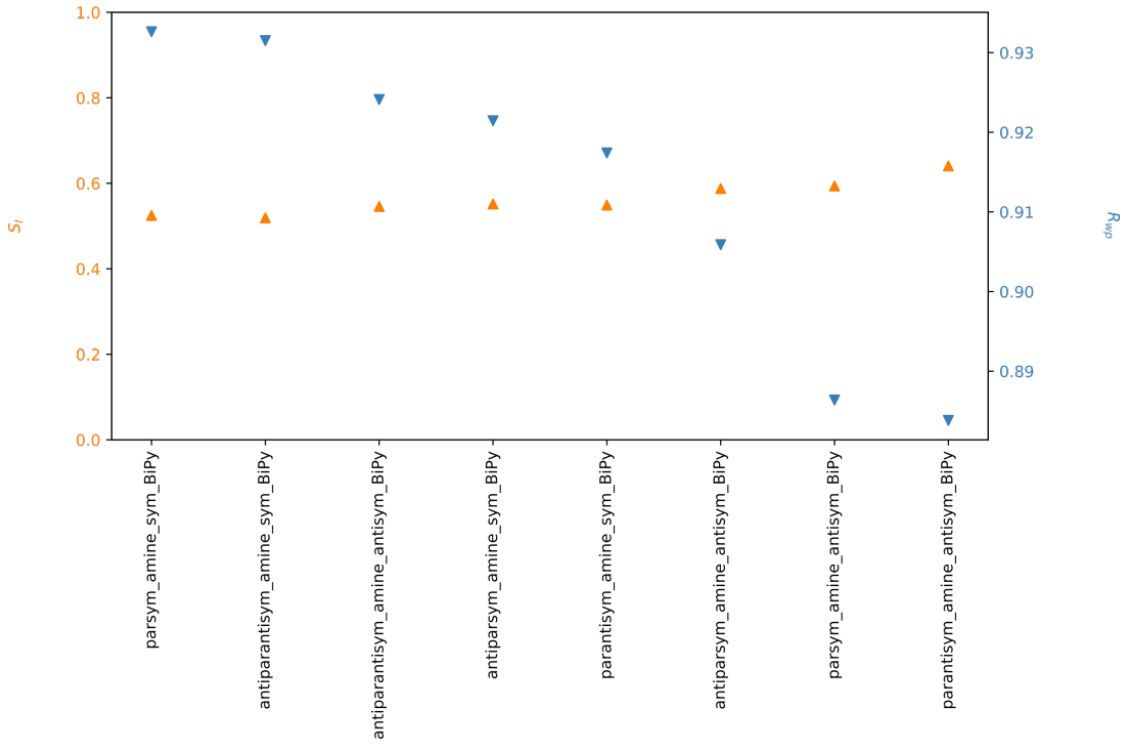

Figure S33: Metric ranking for **TpBpy** to identify the optimal model, based on the MD averaged PXRD pattern.

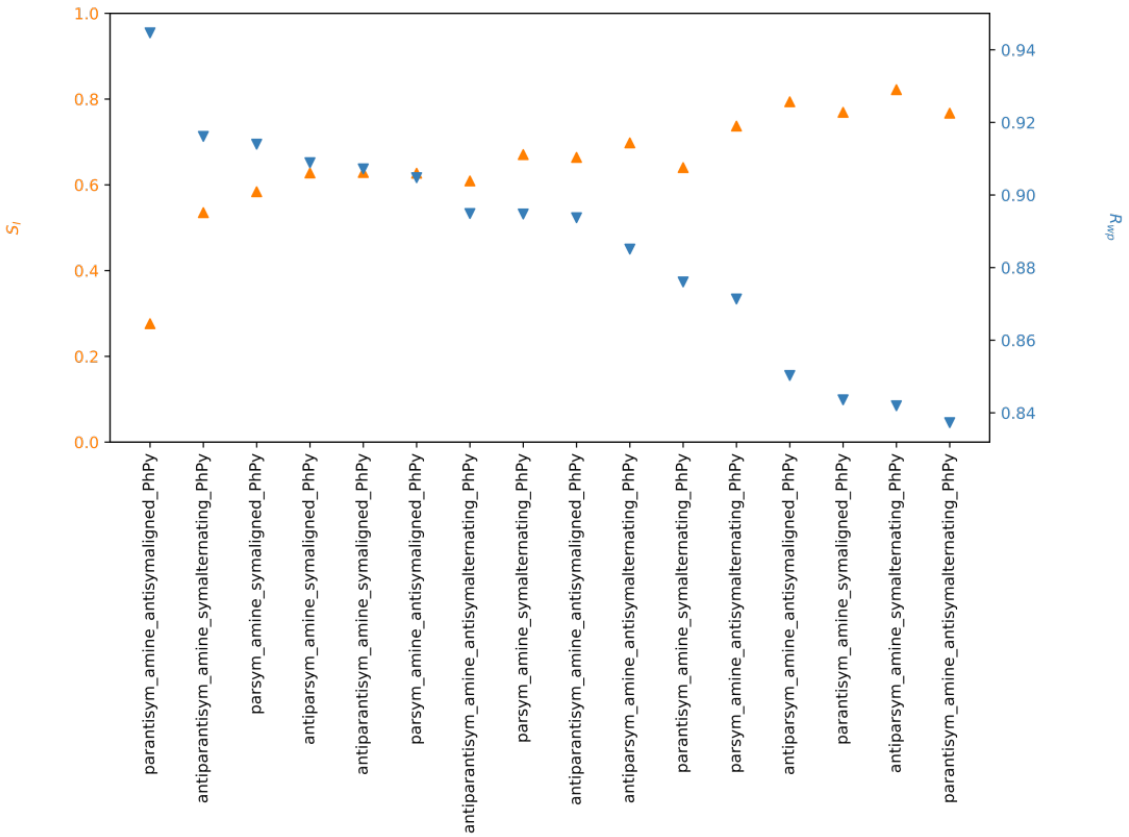

Figure S34: Metric ranking for **TpPpy** to identify the optimal model, based on the MD averaged PXRD pattern.

S3.4 Computational details: Structural modelling

The PXRD patterns were calculated using the pyobjcryst python package, which is a wrapper for the ObjCryst++ Object-Oriented Crystallographic Library.[38] The program settings were chosen in accordance with the experimental settings, taking 1.54056 Å as the scattering wavelength for Cu K_α. A pseudo-Voigt peak shape was employed, with equal parts of a Gaussian and a Lorentzian peak shape function, and a full width at half maximum of 0.14°.

The interactions in our molecular systems were evaluated with the aforementioned system-specific force fields (Section S3.1), using the Yaff[33] package (v1.6.0) interfaced with LAMMPS[39] (stable_3Mar2020) to efficiently calculate the long range interactions. The long-range electrostatic interactions were calculated through Ewald summations, with a real space cut-off r_{cut} of 12 Å, a scaling factor α of 0.267 $Å^{-1}$, a reciprocal space cut-off k_{max} of 0.4 $Å^{-1}$, and tail corrections. For the van der Waals interactions a real space cut-off of 15 Å was used. Both cut-offs were smoothed by a truncation model.

The geometric optimizations were performed using the following criteria: *gpos_rms*=*grvecs_rms*=1e-8 and *dpos_rms*=*drvecs_rms*=1e-6. The subsequent molecular dynamics simulations were performed in the (N,P,$\boldsymbol{\sigma_a}$ = $\boldsymbol{0}$,T) ensemble,[40] integrated through a velocity verlet integration scheme with a timestep of 0.5 fs. The temperature was controlled by a thermostat at 300 K, employing the Nosé-Hoover chain thermostat[41–43] with three beads and a relaxation time of 0.1 ps, whereas the pressure was controlled at 1 bar, using the Martyna-Tuckerman-Tobias-Klein barostat[44,45] with a relaxation time of 1 ps. To account for sufficient layer dynamics throughout the simulations, supercells were constructed, starting from the single two layer unit cell from the geometric optimization, and periodically extending them to a ten layer unit cell for the molecular dynamics simulation.

S3.5 Computational details: Simulation of bandgaps and density of states

Density functional theory (DFT) calculations were carried out using a projector augmented wave (PAW)[46] with the Vienna ab initio simulation package (VASP).[47–49] The electron exchange-correlational functional was considered via the generalized gradient approximation with the Perdew-Burke-Ernzerhof (PBE)[50] functional with Grimme's D3 corrections with Becke-Johnson damping.[51,52] The Brillouin zone was sampled using $1 \times 1 \times 4$ Γ-centered grids. A kinetic energy cutoff at 600 eV was considered to describe the electronic wave function. All the structures were optimized until the convergence criteria of energy becomes less than 1×10^{-5} eV. The hybrid functional (HSE06) was used for the better estimation of the electronic band gap.[53]

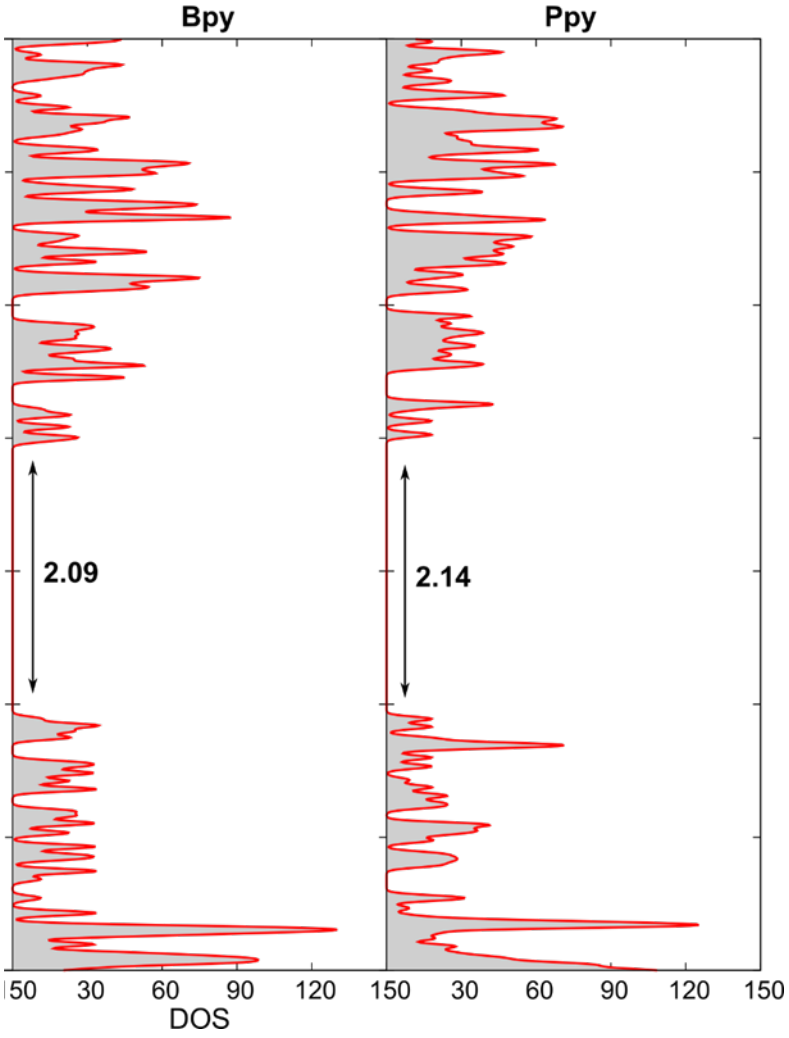

Figure S35: Band structure and density of states of **TpBpyCOF** and **TpPpyCOF**.

S3.6 Computational details: assignment of the NMR spectra

The building blocks of the COFs under investigation are shown in Figure 36 and are labeled (a) Tp node, (b) TpOMe node, (c) Ppy linker and (d) Bpy linker. We give each carbon atom in these building blocks an index and let it represent a group of carbon atoms that are in the same framework position across all nodes and linkers. We then calculate the NMR response of all of the carbon atoms.

We have taken the available force field parameters for the building blocks and used them to perform a geometry optimization on a unit cell of two layers of COF material to obtain a decent starting structure for each of the three proposed COFs. Next, the models were doubled in size to obtain supercells of 4 layers of COF and were optimized at the DFT level within the PAW formalism implemented in VASP (PBE functional with Grimme D3 dispersion correction and BJ damping, plane wave cutoff of 500 eV). The final structures were used to calculate chemical shieldings with GIPAW [54] through VASP.[47–49] The linear relation between the chemical shielding and chemical shift $\delta = a\sigma + b$ was fitted by minimizing the MSE fitting error between a theoretical spectrum consisting of summed gaussian NMR lineshapes and the experimental ^{13}C NMR spectrum. The resulting chemical shifts for each model are then used to compare to the experimental spectrum. We have also calculated average chemical shifts per atom class of each building block and for each of these atom classes plotted this average and a boxplot representing the spread of the chemical shifts within each class (see Figures S37-39).

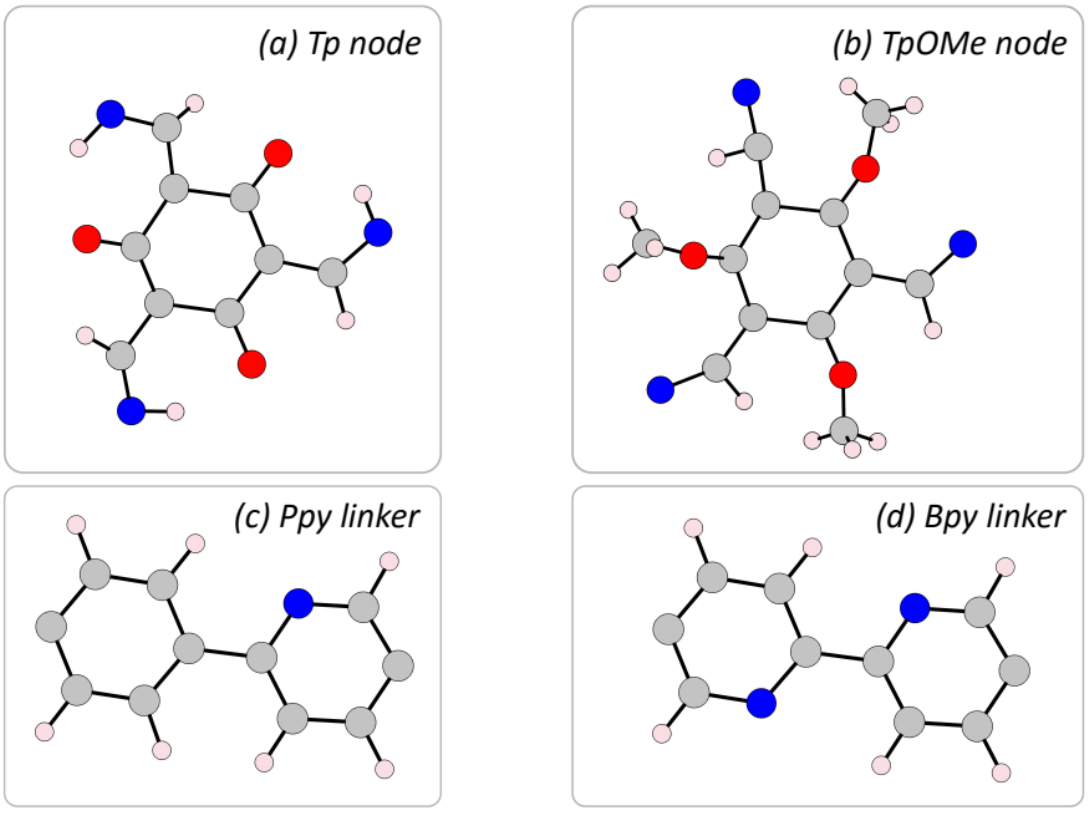

Figure S36: Illustration of four building blocks: a) Tp Node, b) TpOMe node, c) Ppy linker and d) Bpy linker that were used to construct the COFs under investigation. Atoms are coloured according to the following convention: red = O, gray = C, blue = N, pink = H.

The spectra of **TpPpyCOF** and **TpBpyCOF** spectra are perfectly consistent with the theoretical chemical shifts. The agreement between the theoretical average resonances (indicated with ♦ in the

plots) and the peak locations of the experimental spectrum seems slightly better for the **TpBpyCOF** than for the **TpPpyCOF**. Limited disagreement in the location of some resonances is to be expected: as these are static models, there is no motional averaging of chemical shifts. The carbon atoms labelled 12, 16, 13 and 15 in the **TpPpyCOF** are in reality more mobile than the carbon atoms at the same places in **TpBpyCOF**, but the static model cannot capture this mobility. This inhibited mobility in **TpBpyCOF** can e.g. be due to the extra stabilizing effect of the hydrogen atom at the carbon label 12 hydrogen bonding to the additional nitrogen in **Bpy**. Overall, we expect the **Bpy** linker to be less mobile than the **Ppy** linker, which can explain why the agreement with this static model is better for **TpBpyCOF**. Moreover, for both **TpPpyCOF** and **TpBpyCOF** there are some peaks that can be directly attributed to specific carbon sites and some peaks are generated by multiple carbon sites with overlapping chemical shifts.

The situation is different for **'TpOMeBpyCOF'**. The calculated chemical shifts for an imine linked, methoxy containing COF do not agree with the experimental spectrum. For the **'TpOMeBpyCOF'** model system, the methoxy groups (labelled 10, 11, 12) show a resonance well separated from the rest of the spectrum, near 60 ppm. This resonance is not present in the experimental sample. Additionally, the location of the other carbon atoms bound to the oxygen atom (labels 1, 2, 3) show a chemical shift that is lower than the resonance that is found in the spectrum. We are therefore forced to conclude that in the sample that was measured, the methoxy groups are not present on the framework and as such, this sample is not a **TpOMeBpyCOF**, and was accordingly renamed **'TpOMeBpyCOF'**.

Furthermore, there are two reasons to believe that not an imine but rather an enamine group is present in the node for **'TpOMeBpyCOF'** sample. First, the resonance in the experimental spectrum just above 100 ppm is inconsistent with an imine group in the node: this resonance agrees with the resonances in the experimental spectra of the **TpPpyCOF** and **TpBpyCOF**, where they originate from the atoms (4, 5, 6). The locations of the theoretical resonances of the atoms 4, 5 and 6 of **TpPpyCOF** and **TpBpyCOF** agree with the peak in the unknown sample spectrum just above 100 ppm. Additionally, the location of the theoretical resonances 7, 8 and 9 in the **'TpOMeBpyCOF'** does not agree with the unknown sample: given the fact that these and additionally the 13 and 14 atoms are more or less the same, a stronger peak should be visible in the experimental spectrum just above 150 ppm. The location of the theoretical resonances 7, 8 and 9 of **TpPpyCOF** and **TpBpyCOF** models would be consistent with the unknown spectrum, if it contained enamine linkages.

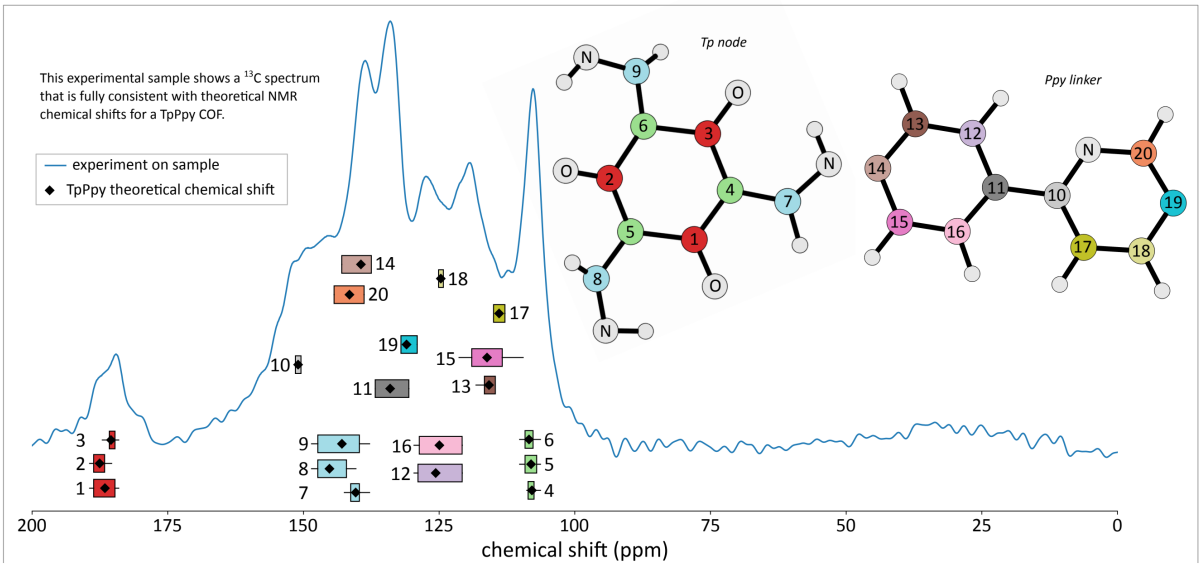

Figure S37: Assignment of the different ^{13}C resonances in the ^{1}H-^{13}C CPMAS spectrum (blue) of **TpPpyCOF** to the different ^{13}C moieties via modelling.

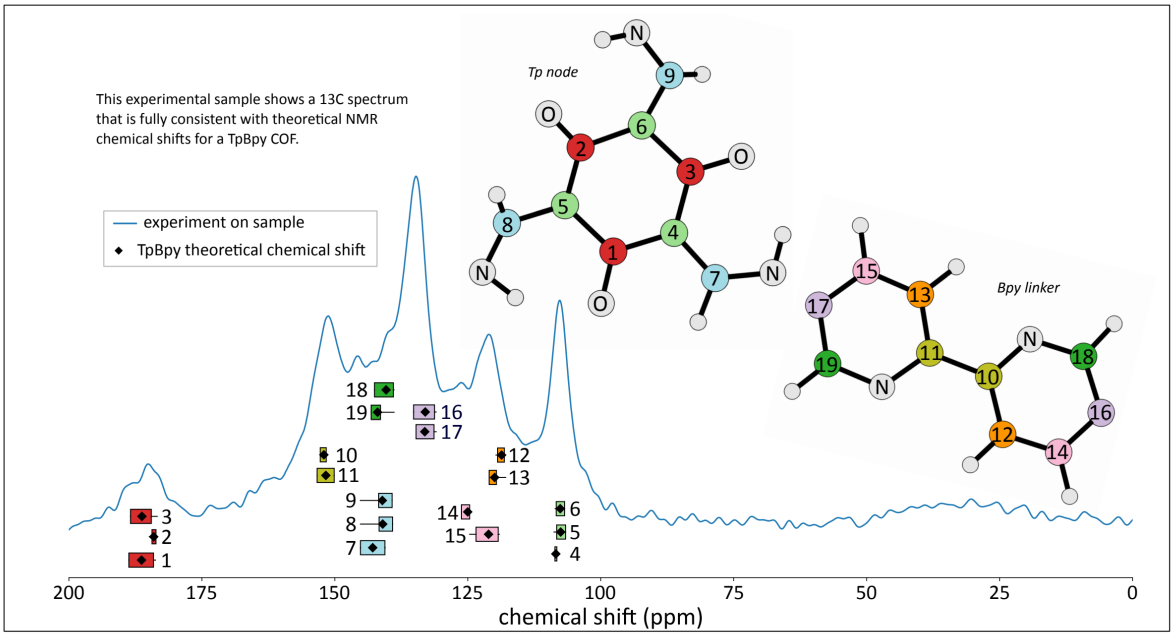

Figure S38: Assignment of the different ^{13}C resonances in the ^{1}H-^{13}C CPMAS spectrum (blue) of **TpBpyCOF** to the different ^{13}C moieties via modelling.

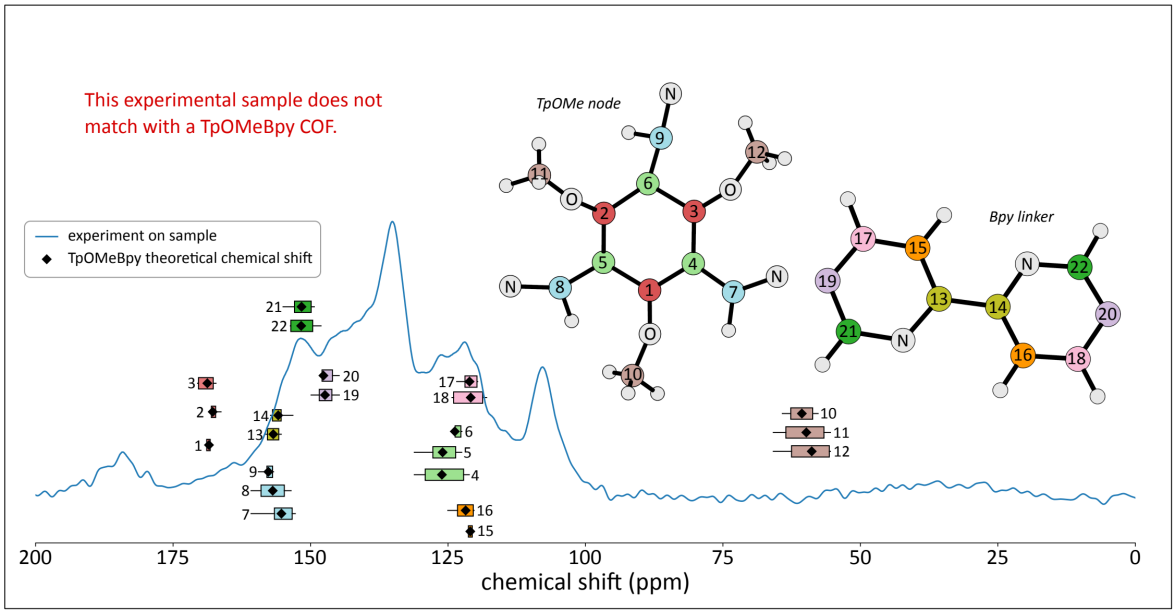

Figure S39: Attempted assignment of the different ^{13}C resonances in the ^{1}H-^{13}C CPMAS spectrum (blue) of **TpOMeBpyCOF** to the different ^{13}C moieties via modelling. As no methoxy or imine carbons are present, demethylation and isomerization has taken place. The resulting spectra matches well with that of **TpBpyCOF**.

S3.7 Computational details: Simulation of pore size distributions

As an additional validation of the structural models, the pore size distributions (PSDs) were calculated for each of the structural models with Zeo++[55,56] and dynamically averaged over the MD trajectory as for the diffraction patterns. The PSDs for the optimal structural models, determined by the PXRD comparison analysis, were subsequently compared to the experimentally determined PSDs from Section S2.1 As illustrated in Figures S40-41, the agreement is limited, where the calculated PSDs contain only a single, relatively narrow peak, corresponding to the singular channel shape in the structural models. While the channel shape varies slightly over time during the MD simulation, due to its stacking, the models lack any mesoporous features which are clearly present in the experimental PSD. The effective peak location of the calculated PSD does agree to the first peak in the experimental PSD, due to the specific pore shape, where the effective diameter is controlled by the specific stacking of the layers.

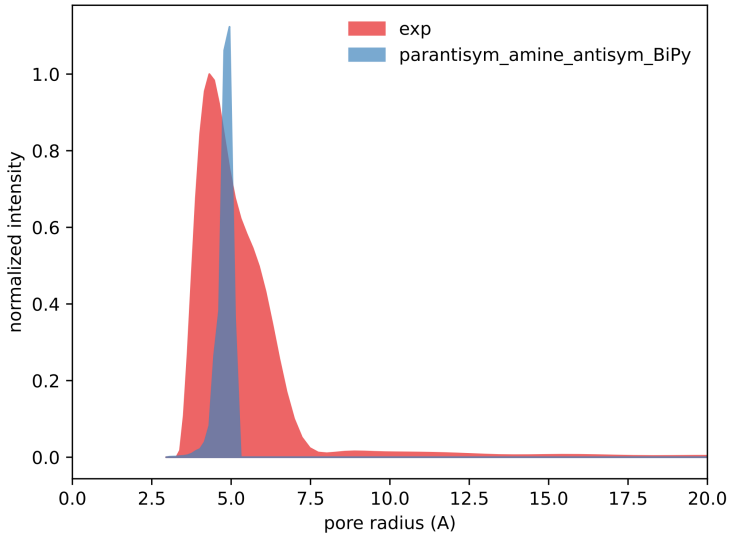

Figure S40: Experimental and simulated pore size distribution of **TpBpyCOF**, calculated half pore width: 8.928 Å. Note that the experimental PSD is derived from MD (QSDFT) calculations using ASiQwin, using the experimental N_2 sorption data.

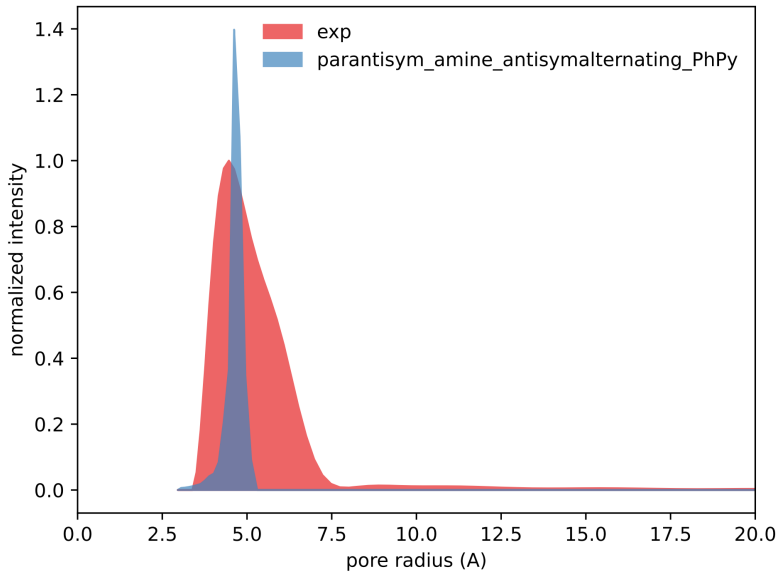

Figure S41: Pore size distribution of **TpPpyCOF**, calculated half pore width: 9.240 Å. Note that the experimental PSD is derived from MD (QSDFT) calculations using ASiQwin, using the experimental N_2 sorption data.

S4 Synthesis of substrates

S4.1 Synthesis of (*E*)-3-(naphthalen-2-yl)prop-2-en-1-ol **25b**

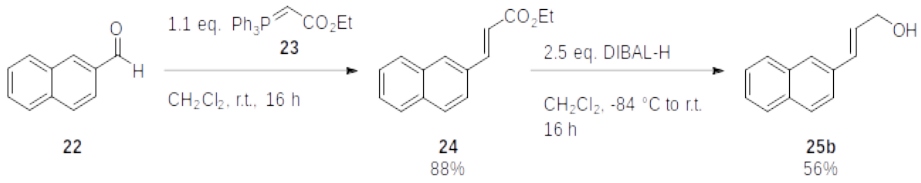

Scheme S6: Synthesis of (*E*)-3-(naphthalen-2-yl)prop-2-en-1-ol **25b**.

The synthesis was adapted from a literature procedure.[57] 2-Naphthaldehyde **22** (2.34 g, 15 mmol, 1 eq.) was added to a flame dried flask, under argon, containing 30 mL dry CH_2Cl_2. To this ethyl (triphenylphosphoranylidene)acetate **23** (5.75 g, 16.5 mmol, 1.1 eq.) was added and the mixture was stirred overnight at room temperature. The solvent was then removed, and 150 mL of PE/EtOAc (10/1) was added. This was then filtered to remove triphenylphosphine oxide and the solvent was removed to give ethyl (*E*)-3-(naphthalen-2-yl)acrylate **24** as a white solid (2.99 g, 88%) which was used without further purification.

Ethyl (*E*)-3-(naphthalen-2-yl)acrylate **24** (2.625 g, 11.6 mmol, 1 eq.) was dissolved in 100 mL dry CH_2Cl_2, under argon and 29 mL 1N DIBAL-H in toluene (29 mmol, 2.5 eq.) was added dropwise at -84 °C. This mixture was allowed to come to room temperature and stirred overnight. To quench the reaction the flask was put in an ice bath and 150 mL 1N HCl was slowly (!) added and stirred for 15 minutes. The phases were separated and the aqueous phase was further extracted with 2 x 100 mL CH_2Cl_2. The combined organic phases were washed with $NaHCO_3$, dried over $MgSO_4$ and evaporated. The crude was purified using column chromatography (SiO_2, PE/EtOAc: 1/7) furnishing (*E*)-3-(naphthalen-2-yl)prop-2-en-1-ol **25b** as a white solid (1.20 g, 56%).

(*E*)-3-(Naphthalen-2-yl)prop-2-en-1-ol 25b

^{1}H-NMR (400 MHz, $CDCl_3$): δ 1.52 (1H, t, *J* = 5.8 Hz, OH); 4.39 (2H, d x d x d, *J* = 5.8 x 5.8 x 1.3 Hz, CH_2); 6.50 (1H, d_{AB} x t, *J* = 15.9 x 5.8 Hz, $CH_2C\underline{H}$=CH); 6.79 (1H, br d_{AB}, *J* = 15.9 Hz, CH_2CH=C<u>H</u>); 7.42-7.49 (2H, m, 2 x CH_{arom}); 7.61 (1H, d x d, *J* = 8.6 x 1.7, CH_{arom}); 7.40-7.82 (4H, m, 4 x CH_{arom}). **^{13}C-NMR** (100 MHz, $CDCl_3$): 64.0 (CH_2); 123.7, 126.1, 126.4, 126.6, 127.8, 128.1 and 128.4 (7 x CH_{arom}); 129.0 ($CH_2\underline{C}$H=CH); 131.4 (CH_2CH=<u>C</u>H); 133.2, 133.7 and 134.2 (3 x $C_{arom,quat}$). **IR** (ATR, cm^{-1}): ν_{OH} = 3302; ν_{max} = 1090, 1007, 962, 905, 862, 826, 812, 739, 517. **MS** (ESI): *m/z* (%) 167 [$C_{13}H_{11}^{+}$, 100]. White solid, 56%. Spectral data matched literature.[58]

S4.2 Synthesis of *N*-aryl glycine esters **1a-k**

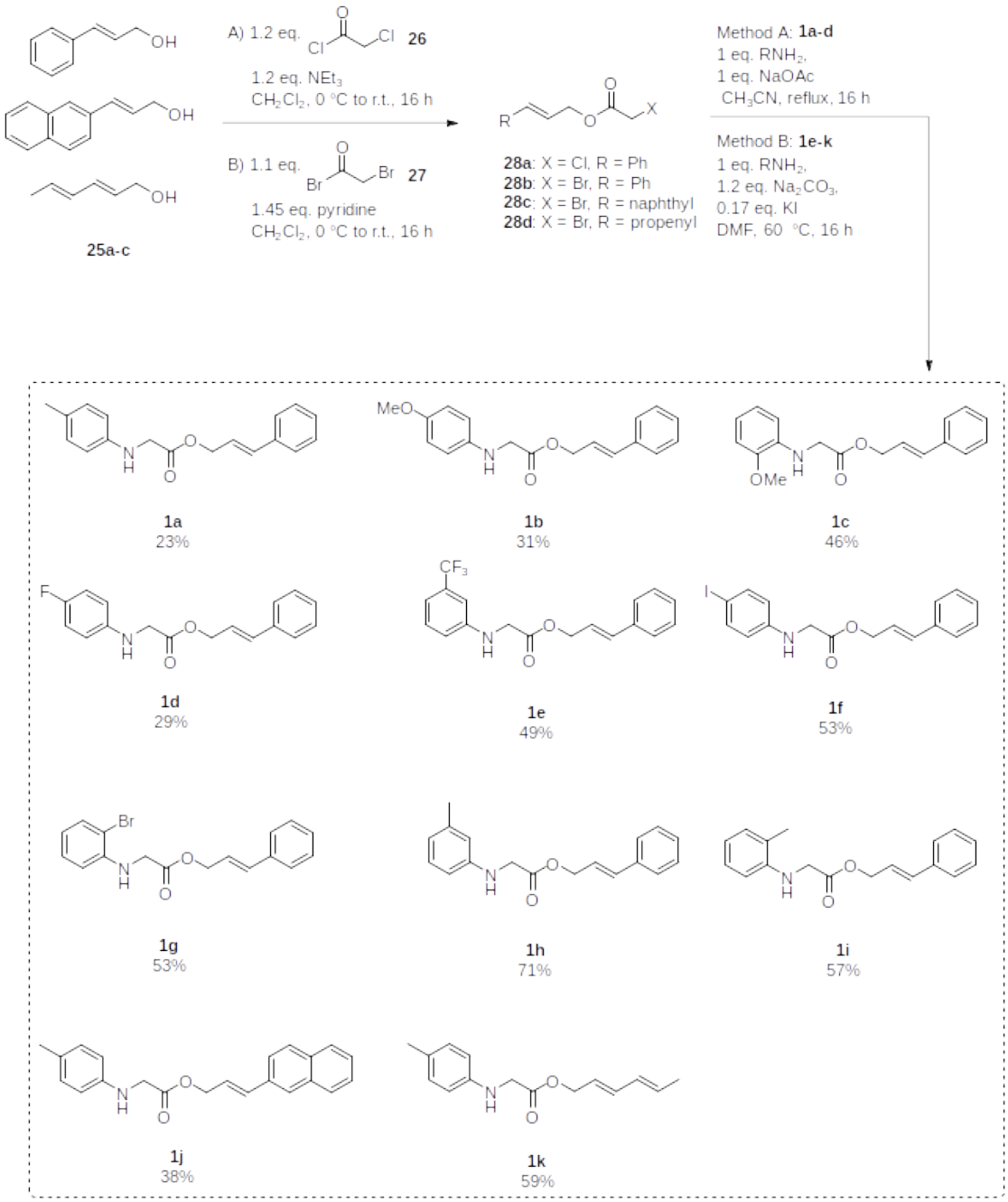

Scheme S7: Synthesis of *N*-aryl glycine esters **1a-k**.

For the synthesis of the cinnamyl 2-(phenylamino)acetates two different procedures based on literature were followed. For compounds **1a-d** procedure 1[59] was followed, however it was found that this required long reaction times and didn't allow for full conversion of starting materials in the case of more electron poor anilines. Therefore procedure 2[60] was followed for the synthesis of the other substrates **1e**-**1k**.

Procedure 1[59]

The synthesis of cinnamyl *p*-tolylglycinate **1a** is described as a representative example for the synthesis of compounds **1a-d**.

Step 1

To a flame dried flask equipped with a pressure equalized addition funnel, under nitrogen, 1.3 mL cinnamyl alcohol **25a** (1.34 g, 10 mmol, 1 eq.) was added together with 1.7 mL triethylamine (1.21 g, 12 mmol, 1.2 eq.) and 20 mL dry CH_2Cl_2. To this reaction mixture 0.96 mL chloroacetyl chloride **26** (1.36 g, 12 mmol, 1.2 eq.) in 10 mL CH_2Cl_2 was slowly added in five minutes, at 0 °C. After addition the mixture was allowed to come to room temperature, after which it was stirred overnight. The mixture was then filtered, 30 mL water was added to the filtrate and the two phases were separated. The aqueous phase was further extracted twice with 30 mL of CH_2Cl_2. The combined organic phases were dried over $MgSO_4$, filtered and concentrated under vacuum. This crude cinnamyl 2-chloroacetate **28a** was taken to the next step without additional purification.

Step 2

The crude cinnamyl 2-chloroacetate **28a** was dissolved in 5 mL CH_3CN. *p*-Toluidine (1.07 g, 10 mmol, 1 eq.) and NaOAc (0.82 g, 10 mmol, 1 eq.) were added. This mixture was refluxed overnight, filtered and purified using column chromatography (SiO_2, PE/EtOAc: 20/1) followed by recrystallisation in EtOH furnishing cinnamyl *p*-tolylglycinate **1a** as a yellow solid (0.66 g, 23%). For compounds **1b-d** the reaction was refluxed for 48 h to ensure full conversion and the crudes were purified using column chromatography (C18, gradient H_2O/CH_3CN: 50/50 - 0/100).

Procedure 2[60]

The synthesis of cinnamyl (4-iodophenyl)glycinate **1f** is described as a representative example for compounds **1e-k**.

Step 1

To a flame dried flask equipped with a pressure equalized addition funnel, under nitrogen, 3.2 mL cinnamyl alcohol **25a** (3.35 g, 25 mmol, 1 eq.) was dissolved in 50 mL dry CH_2Cl_2 and 2.9 mL pyridine (2.85 g, 36 mmol, 1.45 eq.) was added. To this reaction mixture 2.4 mL bromo acetylbromide **27** (5.55 g, 27.5 mmol, 1.1 eq.) in 15 mL dry CH_2Cl_2 was slowly added in 5 minutes, at 0 °C. The mixture was then allowed to come to room temperature, after which it was stirred overnight. Water (50 mL) was added and the two phases were separated. The aqueous phase was further extracted twice with 50 mL CH_2Cl_2. The combined organic phases were dried over $MgSO_4$, filtered and concentrated under vacuum resulting in the crude cinnamyl 2-bromoacetate **28b** (5.17 g, 81%) which was used without additional purification.

Step 2

Cinnamyl 2-bromoacetate **28b** (740 mg, 2.9 mmol, 1 eq.), Na_2CO_3 (369 mg, 3.5 mmol, 1.2 eq.), 4-iodoaniline (635 mg, 2.9 mmol, 1 eq.) and potassium iodide (86 mg, 0.5 mmol , 0.17 eq.) were added to a flask containing 15 mL DMF. The resulting suspension was stirred at 60 °C until consumption of starting material (LC-MS). Upon completion of the reaction 100 mL of water was added and the mixture was extracted with EtOAc (3 x 100 mL), dried over $MgSO_4$ and the solvent removed in vacuo. The product was purified using column chromatography (SiO_2, PE/EtOAc: 10/1) resulting in cinnamyl (4-iodophenyl)glycinate **1f** as a yellow powder (602 mg, 53%).

For the 2-haloacetates **28a-d** the spectral data is derived from the crude mixture.

Cinnamyl 2-chloroacetate 28a

^{1}H-NMR (400 MHz, $CDCl_3$): δ 4.11 (2H, s, CH_2Cl); 4.85 (2H, d, *J* = 6.6 Hz, CH_2O); 6.29 (1H, d x t, *J* = 15.7 x 6.6 Hz, $CH_2C\underline{H}$=CH); 6.70 (1H, br d, *J* = 15.7 Hz, CH_2CH=C$\underline{H}$); 7.28-7.41 (5H, m, 5 x CH_{arom}). **^{13}C-NMR** (100 MHz, $CDCl_3$): δ 41.0 (CH_2Cl); 66.9 (CH_2O); 122.1, 126.9, 128.5, 128.8, 135.6 (5x CH_{arom} and $CH_2\underline{C}H$=$\underline{C}$H); 136.0 ($C_{arom,quat}$); 167.3 (C=O).

Cinnamyl 2-bromoacetate 28b

^{1}H-NMR (400 MHz, $CDCl_3$): δ 3.88 (2H, s, CH_2Br); 4.83 (2H, d, *J* = 6.4 Hz, CH_2O); 6.29 (1H, d x t, *J* = 15.9 x 6.4 Hz, $CH_2C\underline{H}$=CH); 6.70 (1H, br d, *J* = 15.9 Hz, CH_2CH=C$\underline{H}$); 7.27-7.41 (5H, m, 5 x CH_{arom}).**^{13}C-NMR** (100 MHz, $CDCl_3$): δ 25.9 (CH_2Br); 66.9 (CH_2O); 122.2 ($CH_2\underline{C}H$=CH); 126.8 (2 x CH_{arom}); 128.5 (CH_{arom}); 128.8 (2 x CH_{arom}); 135.4 (CH_2CH=$\underline{C}$H); 136.1 ($C_{arom,quat}$); 167.2 (C=O).

(*E*)-3-(Naphthalen-2-yl)allyl 2-bromoacetate 28c

^{1}H-NMR (400 MHz, $CDCl_3$): 3.90 (2H, s, CH_2Br); 4.89 (2H, d x d, *J* = 6.6 x 1.2 Hz, CH_2O); 6.37-6.45 (1H, m, $CH_2C\underline{H}$=CH); 6.86 (1H, br d, *J* = 15.9 Hz, CH2CH=C$\underline{H}$); 7.44-7.48 (2H, m, 2 x CH_{arom}); 7.58-7.61 (1H, m, CH_{arom}); 7.72-7.82 (4H, m, 4 x CH_{arom}).

(2*E*,4*E*)-Hexa-2,4-dien-1-yl 2-bromoacetate 28d

^{1}H-NMR (400 MHz, $CDCl_3$): δ 1.77 (3H, d, *J* = 6.7 Hz, CH_3); 3.84 (2H, s CH_2Br); 4.67 (2H, d, *J* = 6.7 Hz, CH_2O); 5.58-5.65 (1H, m, C$\underline{H}$=CH-CH=CHCH_3); 5.74 -5.84 (1H, m, CH=CH-CH=C$\underline{H}CH_3$); 6.02-6.09 (1H, m, CH=CH-C$\underline{H}$=$CHCH_3$); 6.26-6.35 (1H, m, CH=C$\underline{H}$-CH=$CHCH_3$).

Cinnamyl *p*-tolylglycinate 1a

^{1}H-NMR (400 MHz, $CDCl_3$): δ 2.24 (3H, s, CH_3); 3.95 (2H, d, *J* = 5.6 Hz, NCH_2); 4.16 (1H, br s, NH); 4.83 (2H, d, *J* = 6.5 Hz, OCH_2); 6.28 (1H, d_{AB} x t, *J* = 15.7 x 6.5 Hz, $CH_2C\underline{H}$=CH); 6.56 (2H, d, *J* = 7.7 Hz, 2 x C$\underline{H}_{arom}$); 6.65 (1H, br d_{AB}, *J* = 15.7 Hz, CH_2CH=C$\underline{H}$); 7.01 (2H, d, *J* = 7.7 Hz, 2 x CH_{arom}); 7.29-7.39 (5H, m, 5 x CH_{arom}). **^{13}C-NMR** (100 MHz, $CDCl_3$): δ 20.5 (CH_3); 46.4 (NCH_2); 65.9 (OCH_2); 113.4 (2 x CH_{arom}); 122.6 ($CH_2\underline{C}H$=CH); 126.8 (2 x CH_{arom}); 127.7 ($C_{arom,quat}$); 128.4 (CH_{arom}); 128.8 (2 x CH_{arom}); 130.0 (2 x CH_{arom}); 134.9 (CH_2CH=$\underline{C}$H); 136.1 ($C_{arom,quat}$); 144.9 ($C_{arom,quat}$); 171.3 (C=O). **IR** (ATR, cm^{-1}): ν_{NH} = 3395; $\nu_{C=O}$ = 1728; ν_{max} = 1526, 1196, 1184, 972, 953, 802, 691, 507. **MS** (ESI): *m/z* (%) 282 ($[M + 1]^+$, 100). Light yellow solid, 23%. Spectral data matched literature.[61]

Cinnamyl (4-methoxyphenyl)glycinate 1b

^{1}H-NMR (400 MHz, $CDCl_3$): δ 3.74 (3H, s, CH_3); 3.93 (2H, s, NCH_2); 4.03 (1H, br s, NH); 4.83 (2H, d, *J* = 6.4 Hz, OCH_2); 6.27 (1H, d_{AB} x t, *J* = 15.8 x 6.4 Hz, $CH_2C\underline{H}$=CH); 6.60 (2H, d_{AB}, *J* = 8.3 Hz, 2 x C$\underline{H}_{arom}$); 6.65 (1H, br d_{AB}, *J* = 15.8 Hz, CH_2CH=C$\underline{H}$); 6.79 (2H, d_{AB}, *J* = 8.3 Hz, 2 x C$\underline{H}_{arom}$); 7.29-7.39 (5H, m, 5 x CH_{arom}). **^{13}C-NMR** (100 MHz, DMSO-d_6): 45.5 (NCH_2); 55.3 (OCH_3); 64.4 (OCH_2); 113.2 (2 x CH_{arom}); 114.5 (2 x CH_{arom}); 123.7 ($CH_2C\underline{H}$=CH); 126.4 (2 x CH_{arom}); 128.0 (CH_{arom}); 128.6 (2 x CH_{arom}); 132.8 (CH_2CH=C$\underline{H}$); 136.0 ($C_{arom,quat}$); 142.2 ($C_{arom,quat}$); 151.1 ($C_{arom,quat}$); 171.4 (C=O). **IR** (ATR, cm^{-1}): ν_{NH} = 3387; $\nu_{C=O}$ = 1726; ν_{max} = 1514, 1190, 970, 935, 820, 745, 692, 503. **MS** (ESI): *m/z* (%) 298 ($[M + 1]^+$, 100). Brown solid, 31%. Spectral data matched literature.[61*]

[*]In $CDCl_3$ ^{13}C-NMR did not match the literature, in DMSO however the expected signals were obtained.

Cinnamyl (2-methoxyphenyl)glycinate 1c

^{1}H-NMR (400 MHz, $CDCl_3$): δ 3.87 (3H, s, CH_3); 3.99 (2H, s, NCH_2); 4.84 (3H, d, *J* = 6.4 Hz, OCH_2 and NH); 6.29 (1H, d_{AB} x t, *J* = 16.0 x 6.4 Hz, $CH_2C\underline{H}$=CH); 6.51 (1H, d, *J* = 7.8 Hz, CH_{arom}); 6.66 (1H, br d_{AB}, *J* = 16.0 Hz, CH_2CH=C$\underline{H}$); 6.70-6.88 (3H, m, 3 x CH_{arom}); 7.29-7.39 (5H, m, 5 x CH_{arom}). **^{13}C-NMR** (100 MHz, $CDCl_3$): δ 45.9 (NCH_2); 55.6 (OCH_3); 65.9 (OCH_2); 109.8, 110.2, 117.7 and 121.3 (4 x CH_{arom}); 122.8 ($CH_2\underline{C}$H=CH); 126.8 (2 x CH_{arom}); 128.3 (CH_{arom}); 128.8 (2 x CH_{arom}); 134.9 (CH_2CH=$\underline{C}$H); 136.2, 137.2 and 147.3 (3 x $C_{arom,quat}$); 171.1 (C=O). **IR** (ATR, cm^{-1}): ν_{NH} = 3420; $\nu_{C=O}$ = 1734; ν_{max} = 1600, 1510, 1190, 1177, 1026, 964, 736, 692. **MS** (ESI): *m/z* (%) 298 ($[M + 1]^+$, 100). Brown solid, 46%.

Cinnamyl (4-fluorophenyl)glycinate 1d

^{1}H-NMR (400 MHz, $CDCl_3$): δ 3.93 (2H, s, NCH_2); 4.18 (1H, br s, NH); 4.84 (2H, d, *J* = 6.5 Hz, OCH_2); 6.28 (1H, d_{AB} x t, *J* = 15.8 x 6.5 Hz, $CH_2C\underline{H}$=CH); 6.55-6.58 (2H, m , 2 x CH_{arom}); 6.67 (1H, br d_{AB}, *J* = 15.8 Hz, CH_2CH=C$\underline{H}$); 6.91 (2H, t, *J* = 8.5 Hz, 2 x C$\underline{H}_{arom}$); 7.28-7.39 (5H, m, 5 x CH_{arom}). **^{19}F-NMR** (376 MHz, $CDCl_3$): δ -127.03 (1F, m). **^{13}C-NMR** (100 MHz, $CDCl_3$): δ 46.7 (NCH_2); 66.0 (OCH_2); 114.1 (d, *J* = 7.6 Hz, 2 x CH_{arom}); 116.0 (d, *J* = 22.4 Hz, 2 x CH_{arom}); 122.5 ($CH_2\underline{C}$H=CH); 126.8 (2 x CH_{arom}); 128.4 (CH_{arom}); 128.8 (2 x CH_{arom}); 135.1 (CH_2CH=$\underline{C}$H); 136.1 ($C_{arom,quat}$), 143.5 (d, *J* = 1.1 Hz, $C_{arom,quat,\ 1}$), 156.5 (d, *J* = 235.9 Hz, $C_{arom,quat}$), 171.1 (C=O). **IR** (ATR, cm^{-1}): ν_{NH} = 3387; $\nu_{C=O}$ = 1724; ν_{max} = 1512, 1190, 1140, 972, 818, 752, 692, 503. **MS** (ESI): *m/z* (%) 117 ($[C_9H_9]^+$, 100); 286 ($[M + 1]^+$, 30). Brown solid, 29%. Spectral data matched literature.[62]

Cinnamyl (3-(trifluoromethyl)phenyl)glycinate 1e

^{1}H-NMR (400 MHz, $CDCl_3$): δ 3.98 (2H, d, *J* = 5.4 Hz, NCH_2); 4.51 (1H, br s, NH); 4.86 (2H, d, *J* = 6.5 Hz, OCH_2); 6.29 (1H, d_{AB} x t, *J* = 15.8 x 6.5 Hz, $CH_2C\underline{H}$=CH); 6.68 (1H, br d_{AB}, *J* = 15.8 Hz, CH_2CH=C$\underline{H}$); 6.75-6.81 (2H, m, 2 x CH_{arom}); 6.99 (1H, d, *J* = 7.6 Hz, CH_{arom}); 7.28-7.40 (6H, m, 6 x CH_{arom}). **^{19}F-NMR** (376 MHz, $CDCl_3$): δ -62.87 (3F, s). **^{13}C-NMR** (100 MHz, $CDCl_3$): δ 45.7 (NCH_2); 66.2 (OCH_2); 109.3 (q, *J* = 3.9 Hz, CH_{arom}); 114.8 (q, *J* = 3.9 Hz, CH_{arom}); 116.1 (~d, *J* = 0.9 Hz, CH_{arom}); 122.3 ($CH_2\underline{C}$H=CH); 124.4 (q, *J* = 272.8 Hz, CF_3); 126.8 (2 x CH_{arom}); 128.5 (CH_{arom}); 128.8 (2 x CH_{arom}); 129.9 (CH_{arom}); 131.8 (q, *J* = 31.8 Hz, $C_{arom,quat}$); 135.3 (CH_2CH=$\underline{C}$H); 136.1 ($C_{arom,quat}$); 147.2 ($C_{arom,quat}$); 170.6 (C=O). **IR** (ATR, cm^{-1}): ν_{NH} = 3391; $\nu_{C=O}$ = 1722; ν_{max} = 1614, 1522, 1364, 1171, 1113, 1069, 787, 698. **MS** (ESI): *m/z* (%) 117 ($[C_9H_9]^+$, 100); 336 ($[M + 1]^+$, 20). White-yellow crystals, 49%.

Cinnamyl (4-iodophenyl)glycinate 1f

^{1}H-NMR (400 MHz, $CDCl_3$): δ 3.92 (2H, d, *J* = 5.6 Hz, NCH_2); 4.33 (1H, br t, *J* = 5.3 Hz, NH); 4.84 (2H, d x d, *J* = 6.5 x 1.0 Hz, OCH_2); 6.27 (1H, d_{AB} x t, *J* = 15.9 x 6.5 Hz, $CH_2C\underline{H}$=CH); 6.39-6.42 (2H, m , 2 x C$\underline{H}_{arom}$); 6.66 (1H, br d_{AB}, *J* = 15.9 Hz, CH_2CH=C$\underline{H}$); 7.28-7.46 (7H, m, 7 x CH_{arom}). **^{13}C-NMR** (100 MHz, $CDCl_3$): δ 45.8 (NCH_2); 66.1 (OCH_2); 79.3 ($C_{arom,quat}$); 115.3 (2 x CH_{arom}); 122.4 ($CH_2\underline{C}$H=CH); 126.8 (2 x CH_{arom}); 128.4 (CH_{arom}); 128.8 (2 x CH_{arom}); 135.2 (CH_2CH=$\underline{C}$H); 136.1 ($C_{arom,quat}$), 138.1 (CH_{arom}), 146.7 ($C_{arom,quat}$), 170.7 (C=O). **IR** (ATR, cm^{-1}): ν_{NH} = 3391; $\nu_{C=O}$ = 1726; ν_{max} = 1589, 1508, 1443, 1381, 1202, 1180, 968, 689. **MS** (ESI): *m/z* (%) 267 ($[M - I + 1]^+$, 100). Yellow powder, 53%.

Cinnamyl (2-bromophenyl)glycinate 1g

^{1}H-NMR (400 MHz, $CDCl_3$): δ 4.01 (2H, d, *J* = 5.4 Hz, NCH_2); 4.86 (2H, d x d, *J* = 6.5 x 1.2 Hz, OCH_2); 4.99 (1H, t, *J* = 5.4 Hz, NH); 6.29 (1H, d_{AB} x t, *J* = 15.9 x 6.5 Hz, $CH_2C\underline{H}$=CH); 6.53 (1H, d x d, *J* = 8.1 x 1.3 Hz, $C\underline{H}_{arom}$); 6.63 (1H, t x d, *J* = 7.8 x 1.4 Hz, CH_{arom}); 6.68 (1H, br d_{AB}, *J* = 15.9 Hz, CH_2CH=$C\underline{H}$); 7.16-7.20 (1H , m, CH_{arom}); 7.27-7.40 (5H, m, 5 x CH_{arom}); 7.45 (1H, d x d, *J* = 7.8 x 1.4 Hz, CH_{arom}). **^{13}C-NMR** (100 MHz, $CDCl_3$): δ 45.9 (NCH_2); 66.1 (OCH_2); 110.2 ($C_{arom,quat}$); 111.5 (CH_{arom}); 118.9 (CH_{arom}); 122.5 ($CH_2\underline{C}H$=CH); 126.8 (2 x CH_{arom}); 128.4 (CH_{arom}); 128.7 (CH_{arom}); 128.8 (2 x CH_{arom}); 132.8 (CH_{arom}); 135.1 (CH_2CH=$\underline{C}H$); 136.1 ($C_{arom,quat}$); 144.1 ($C_{arom,quat}$); 170.4 (C=O). **IR** (ATR, cm^{-1}): ν_{NH} = 3397; $\nu_{C=O}$ = 1738; ν_{max} = 1595, 1508, 1443, 1196, 1018, 961, 739, 661. **MS** (ESI): *m/z* (%) 117 ($[C_9H_9]^+$, 100); 346 ($[M + 1]^+$, 15); 348 ($[M + 1]^+$, 15). Colorless oil, 53 %.

Cinnamyl m-tolylglycinate 1h

^{1}H-NMR (400 MHz, $CDCl_3$): δ 2.28 (3H, s, CH_3); 3.96 (2H, d, *J* = 5.4 Hz, NCH_2); 4.23 (1H, br s, NH); 4.84 (2H, d, *J* = 6.4 Hz, OCH_2); 6.28 (1H, d_{AB} x t, *J* = 15.9 x 6.4 Hz, $CH_2C\underline{H}$=CH); 6.43-6.45 (2H, m , 2 x $C\underline{H}_{arom}$); 6.59 (1H, d , *J* = 7.4 Hz, $C\underline{H}_{arom}$); 6.67 (1H, br d_{AB}, *J* = 15.9 Hz, CH_2CH=$C\underline{H}$); 7.09 (1H, t, *J* = 7.6 Hz, $C\underline{H}_{arom}$); 7.29-7.40 (5H, m, 5 x CH_{arom}). **^{13}C-NMR** (100 MHz, $CDCl_3$): δ 21.7 (CH_3); 46.1 (NCH_2); 65.9 (OCH_2); 110.3, 114.0 and 119.4 (3 x CH_{arom}); 122.6 ($CH_2\underline{C}H$=CH); 126.8 (2 x CH_{arom}); 128.4 (CH_{arom}); 128.8 (2 x CH_{arom}); 135.0 (CH_2CH=$\underline{C}H$); 136.2, 139.3 and 147.2 (3 x $C_{arom,quat}$); 171.2 (C=O). **IR** (ATR, cm^{-1}): ν_{NH} = 3387; $\nu_{C=O}$ = 1730; ν_{max} = 1587, 1493, 1447, 1348, 1331, 1204, 964, 987. **MS** (ESI): *m/z* (%) 282 ($[M + 1]^+$, 100). White to yellow crystals, 71%.

Cinnamyl o-tolylglycinate 1i

^{1}H-NMR (400 MHz, $CDCl_3$): δ 2.22 (3H, s, CH_3); 4.01 (2H, d, *J* = 5.2 Hz, NCH_2); 4.2 (1H, br t, *J* = 5.2 Hz, NH); 4.86 (2H, d, *J* = 6.5 Hz, OCH_2); 6.30 (1H, d_{AB} x t, *J* = 15.8 x 6.5 Hz, $CH_2C\underline{H}$=CH); 6.50 (1H, d, *J* = 8.0 Hz, CH_{arom}); 6.66-6.73 (2H, m, CH_2CH=$C\underline{H}$ and CH_{arom}); 7.08-7.15 (2H, m, 2 x CH_{arom}); 7.28-7.40 (5H, m, 5 x CH_{arom}). **^{13}C-NMR** (100 MHz, $CDCl_3$): δ 17.5 (CH_3); 46.1 (NCH_2); 66.0 (OCH_2); 110.1 (CH_{arom}), 118.0 (CH_{arom}); 122.6 ($CH_2\underline{C}H$=CH); 122.7 ($C_{arom,quat}$); 126.8, 127.3, 128.4, 128.8 and 130.4 (7 x CH_{arom}); 135.0 (CH_2CH=$\underline{C}H$); 136.1 ($C_{arom,quat}$); 145.1 ($C_{arom,quat}$); 171.3 (C=O). **IR** (ATR, cm^{-1}): ν_{NH} = 3421; $\nu_{C=O}$ = 1736; ν_{max} = 1607, 1587, 1514, 1193, 1150, 962, 743, 691. **MS** (ESI): *m/z* (%) 282 ($[M + 1]^+$, 100). Light yellow oil, 57%. Spectral data matched literature.[62]

(*E*)-3-(Naphthalen-2-yl)allyl p-tolylglycinate 1j

^{1}H-NMR (400 MHz, $CDCl_3$): δ 2.24 (3H, s, CH_3); 3.97 (2H, d, *J* = 5.6 Hz, CH_2N); 4.17 (1H, br s, NH); 4.89 (2H, d x d, *J* = 6.5 x 1.1 Hz, CH_2O); 6.40 (1H, d x t, 15.9 x 6.5 Hz, $CH_2C\underline{H}$=CH); 6.56-6.59 (2H, m, 2 x CH_{arom}); 6.82 (1H, br d, *J* = 15.9 Hz, CH_2CH=$C\underline{H}$); 7.00-7.03 (2H, m, 2 x CH_{arom}); 7.44-7.50 (2H, m, 2 x CH_{arom}); 7.58 (1H, d x d, *J* = 8.6 x 1.6 Hz, CH_{arom}); 7.74-7.82 (4H, m, 4 x CH_{arom}). **^{13}C-NMR** (100 MHz, $CDCl_3$): δ 20.6 (CH_3); 46.5 (CH_2N); 65.9 (CH_2O); 113.4 (2 x CH_{arom}); 123.0 ($CH_2\underline{C}H$=CH); 123.6, 126.3, 126.5 and 127.1 (4 x CH_{arom}); 127.75 ($C_{arom,quat}$); 127.84 (CH_{arom}); 128.2 (CH_{arom}); 128.5 (CH_{arom}); 130.0 (2 x CH_{arom}); 133.4 ($C_{arom,quat}$); 133.6 (CH_{arom}); 135.0 (CH_2CH=$\underline{C}H$); 144.9 ($C_{arom,quat}$); 171.3 (C=O). **IR** (ATR, cm^{-1}): ν_{NH} = 3397; $\nu_{C=O}$ = 1724; ν_{max} = 1520, 1358, 1200, 1180, 1138, 806, 739, 476. **MS** (ESI): *m/z* (%) 167 ($[C_{13}H_{11}]^+$, 100); 332 ($[M + 1]^+$, 5); 354 ($[M + 23]^+$, 5). Beige solid, 38%.

(*E*)-Penta-2,4-dien-1-yl p-tolylglycinate 1k

^{1}H-NMR (400 MHz, $CDCl_3$): δ 1.77 (3H, d, *J* = 6.7 Hz, $C\underline{H}_3CH=CH$); 2.24 (3H, s, $CH_3C_{arom,quat}$); 3.90 (2H, s, NCH_2); 4.13 (1H, br s, NH); 4.67 (2H, d, *J* = 6.7 Hz, CH_2O); 5.59-5.66 (1H, m, $C\underline{H}$=CH-CH=$CHCH_3$); 5.72-5.81 (1H, m, CH=CH-CH=$C\underline{H}CH_3$); 6.02-6.09 (1H, m, CH=CH-$C\underline{H}$=$CHCH_3$); 6.23-6.29 (1H, m, CH=$C\underline{H}$-CH=$CHCH_3$); 6.52-6.57 (2H, m, 2 x CH_{arom}); 7.00-7.01 (m, 2H, 2 x CH_{arom}). **^{13}C-NMR** (100 MHz, $CDCl_3$): δ 18.3 ($\underline{C}H_3CH=CH$); 20.5 ($\underline{C}H_3C_{arom,quat}$); 46.4 ($CH_2N$); 65.8 ($CH_2O$); 113.4 (2 x CH_{arom}); 123.1 ($\underline{C}H$=CH-CH=$CHCH_3$); 127.6 ($C_{arom,quat}$); 130.0 (2 x CH_{arom}); 130.4 (CH=CH-$\underline{C}H$=$CHCH_3$); 131.9 (CH=CH-CH=$\underline{C}HCH_3$); 135.7 (CH=$\underline{C}H$-CH=$CHCH_3$); 144.9 ($C_{arom,quat}$); 171.3 (C=O). **IR** (ATR, cm^{-1}): ν_{NH} = 3383; $\nu_{C=O}$ = 1728; ν_{max} = 1618, 1522, 1352, 1204, 1182, 988, 802, 505. **MS** (ESI): *m/z* (%) 246 ($[M + 1]^+$, 100). Red crystals, 59%. Spectral data matched literature.[61]

S4.3 Synthesis of *N*-aryl glycine amides **1l-m**

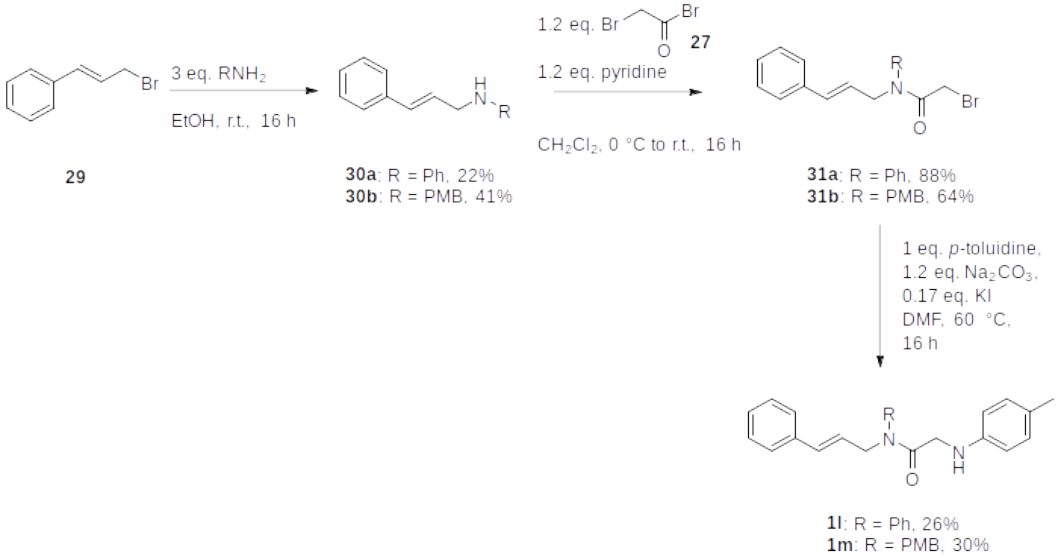

Scheme S8: Synthesis of *N*-aryl glycine amides **1l-m**.

Step 1: Synthesis of cinnamyl amines **30a-b**.

The synthesis of *N*-cinnamylaniline **30a** is described as a representative example for compounds **30a-b**.

Aniline (2.79 g, 30 mmol, 3 eq.) was added to a flask containing 30 mL EtOH. Cinnamyl bromide **29** (1.98 g, 10 mmol, 1 eq.), dissolved in 15 mL EtOH, was added dropwise to this flask at 0 °C. After stirring at room temperature for 16 hours, 30 mL 1N NaOH and 150 mL water were added and the mixture was extracted using ethyl acetate (3 x 100 mL). The organic phases were concentrated under vacuum and purified using column chromatography (SiO_2, PE/EtOAc: 99/1) giving the product as yellow oil (464 mg, 22%).

***N*-Cinnamylaniline 30a**

^{1}H-NMR (400 MHz, $CDCl_3$): δ 3.84 (1H, br s, NH); 3.94 (2H, d, *J* = 5.1 Hz, CH_2); 6.33 (1H, d_{AB} x t, *J* = 15.7 x 5.1 Hz, $CH_2C\underline{H}$=CH); 6.61-6.74 (4H, m, CH_2CH=CH and 3 x CH_{arom}); 7.17-7.38 (7H, m, 7 x CH_{arom}). **^{13}C-NMR** (100 MHz, $CDCl_3$): δ 46.4 (CH_2); 113.2 (2 x CH_{arom}); 117.8 (CH_{arom}); 126.5 (2 x CH_{arom}); 127.2 ($CH_2\underline{C}H$=CH); 127.7 (CH_{arom}); 128.7 (2 x CH_{arom}); 129.4 (2 x CH_{arom}); 131.7 ($CH_2CH=\underline{C}H$); 137.0 ($C_{arom,quat}$); 148.2 ($C_{arom,quat}$). Yellow oil, 22%. Spectral data matched literature.[63]

(*E*)-*N*-(4-Methoxybenzyl)-3-phenylprop-2-en-1-amine 30b

^{1}H-NMR (400 MHz, $CDCl_3$): δ 3.43 (2H, d x d, *J* = 6.3 x 1.4 Hz, $C\underline{H}_2CH=CH$); 3.78 (2H, s, $CH_2C_{arom,quat}$); 3.80 (3H, s, CH_3); 6.32 (1H, d_{AB} x t, *J* = 15.9 x 6.3 Hz, $CH_2C\underline{H}=CH$); 6.54 (1H, br d_{AB}, *J* = 15.9 Hz, $CH_2CH=C\underline{H}$); 6.86-6.89 (2H, m, 2 x CH_{arom}); 7.20-7.32 (5H, m, 5 x CH_{arom}); 7.36-7.38 (2H, m, 2 x CH_{arom}). **^{13}C-NMR** (100 MHz, $CDCl_3$): δ 51.3 ($\underline{C}H_2CH=CH$); 52.9 ($\underline{C}H_2C_{arom,quat}$); 55.4 ($CH_3$); 114.0 (2 x CH_{arom}); 126.4 (2 x CH_{arom}); 127.5 (CH_{arom}); 128.7 (2 x CH_{arom} and $CH_2\underline{C}H=CH$); 129.5 (2 x CH_{arom}); 131.5 ($CH_2CH=\underline{C}H$); 132.6 ($C_{arom,quat}$); 137.3 ($C_{arom,quat}$); 158.8 ($C_{arom,quat}$). Yellow oil, 41%. Spectral data matched literature.[64]

Step 2: Synthesis of 2-bromophenylacetamides **31a-b**

The synthesis of 2-bromo-*N*-cinnamyl-*N*-phenylacetamide **31a** is described as an example for compounds **31a-b**.

N-cinnamylaniline **30a** (464 mg, 2.20 mmol, 1 eq.) was dissolved in 15 mL dry CH_2Cl_2 in a flame dried flask under nitrogen and NEt_3 (267 mg, 2.64 mmol, 1.2 eq.) was added. To this reaction mixture bromo acetylbromide **27** (533 mg, 2.64 mmol, 1.2 eq.) in 5 mL dry CH_2Cl_2 was slowly added in 5 minutes, at 0 °C. The mixture was then allowed to come to room temperature, after which it was stirred overnight. Water (25 mL) was added and the two phases were separated. The aqueous phase was further extracted twice with 25 mL CH_2Cl_2. The combined organic phases were dried over $MgSO_4$, filtered and purified using column chromatography (SiO_2, PE/EtOAc: 10/1) yielding the title product as a light yellow oil (635 mg, 88%).

2-Bromo-*N*-cinnamyl-*N*-phenylacetamide 31a

^{1}H-NMR (400 MHz, $CDCl_3$): δ 3.67 (2H, s, CH_2Br); 4.46 (2H, d, *J* = 6.7 Hz, CH_2N); 6.26 (1H, d_{AB} x t, *J* = 15.8 x 6.7 Hz, $CH_2C\underline{H}=CH$); 6.40 (1H, br d_{Ab}, *J* = 15.8 Hz, $CH_2CH=C\underline{H}$); 7.21-7.45 (10H, m, 10 x CH_{arom}). **^{13}C-NMR** (100 MHz, $CDCl_3$): δ 27.4 (CH_2Br); 52.6 (CH_2N); 123.4 ($CH_2C\underline{H}=CH$); 126.6 (2 x CH_{arom}); 128.0 (CH_{arom}); 128.3 (2 x CH_{arom}); 128.7 (2 x CH_{arom}); 128.9 (CH_{arom}); 130.0 (2 x CH_{arom}); 134.2 ($CH_2CH=\underline{C}H$); 136.6 ($C_{arom,quat}$); 141.5 ($C_{arom,quat}$); 166.3 (C=O). Yellow oil, 88%.

2-Bromo-*N*-cinnamyl-*N*-(4-methoxybenzyl)acetamide 31b

Found as a mixture of 2 rotamers (60/40 in $CDCl_3$).

^{1}H-NMR (400 MHz, $CDCl_3$): δ 3.80 and 3.82 (3H, 2 x s, OCH_3); 3.91 and 3.94 (2H, 2 x s, CH_2Br); 4.07 and 4.15 (2H, 2 x d, *J* = 5.5 x 1.4 Hz and 6.5 x 0.7 Hz, $C\underline{H}_2CH=CH$); 4.57 and 4.61 (2H, 2 x s, NCH_2PMP); 6.08-6.18 (1H, m, $CH_2C\underline{H}=CH$); 6.42-6.48 (1H, m, $CH_2CH=C\underline{H}$); 6.86-6.92 (2H, m, 2 x CH_{arom}); 7.14-7.16 (2H, m, 2 x CH_{arom}); 7.24-7.36 (5H, m, 5 x CH_{arom}). **^{13}C-NMR** (100 MHz, $CDCl_3$): δ 26.5 and 26.6 (CH_2Br); 47.8 ($C\underline{H}_2CH=CH_{rotameric}$); 48.2 ($NCH_2PMP_{rotameric}$); 49.4 ($C\underline{H}_2CH=CH_{rotameric}$); 50.7 ($NCH_2PMP_{rotameric}$); 55.4 and 55.5 ($OCH_3$); 114.3 and 114.6 (2 x CH_{arom}); 123.6 and 123.8 ($CH_2\underline{C}H=CH$); 126.6 (2 x CH_{arom}); 127.90, 127.96, 127.99, 128.3, 128.7, 128.9 and 129.7 (2 x (2 x CH_{arom}), CH_{arom} and $C_{arom,quat}$); 132.6 and 133.6 ($CH_2CH=\underline{C}H$); 136.0 and 136.6 ($C_{arom,quat}$); 159.3 and 159.5 ($C_{arom,quat}$); 167.15 and 167.27 (C=O). Yellow oil, 64%

Step 3: Synthesis of *N*-aryl glycine amides **1l-m**

The synthesis of *N*-cinnamyl-*N*-phenyl-2-(*p*-tolylamino)acetamide **1l** is described as an example for the synthesis of compounds **1l-m**.

2-Bromo-*N*-cinnamyl-*N*-phenylacetamide **31a** (635 mg, 1.93 mmol, 1 eq.), Na_2CO_3 (245 mg, 2.31 mmol, 1.2 eq.), *p*-toluidine (206 mg, 1.93 mmol, 1 eq.) and potassium iodide (58 mg, 0.39 mmol, 0.2 eq.) were added to a flask containing 20 mL DMF. The resulting suspension was stirred at 60 °C for 16 h. Upon completion of the reaction 100 mL of water was added and the mixture was extracted with EtOAc (3 x 100 mL), dried over $MgSO_4$ and the solvent removed in vacuo. The product was purified using column chromatography (SiO_2, PE/EtOAc: 92/8) resulting in *N*-cinnamyl-*N*-phenyl-2-(*p*-tolylamino)acetamide **1l** as a yellow solid (176 mg, 26%).

***N*-Cinnamyl-*N*-phenyl-2-(*p*-tolylamino)acetamide 1l**

^{1}H-NMR (400 MHz, $CDCl_3$): δ 2.18 (3H, s, CH_3); 3.54 (2H, s, CH_2N); 4.46 (2H, d x d, *J* = 6.6 x 0.5 Hz, C$\underline{H}_2$CH=CH); 4.59 (1H, br s, NH); 6.24 (1H, d_{AB} x t, *J* = 15.8 x 6.6 Hz, $CH_2C\underline{H}$=CH); 6.35-6.40 (3H, m, CH_2CH=CH and 2 x CH_{arom}); 6.93 (2H, d, *J* = 8.2 Hz, 2 x CH_{arom}); 7.18-7.31 (7H, m, 7 x CH_{arom}); 7.39-7.44 (3H, m, 3 x CH_{arom}). **^{13}C-NMR** (100 MHz, $CDCl_3$): δ 20.4 (CH_3); 46.7 (CH_2N); 52.1 ($\underline{C}H_2$CH=CH); 113.2 (CH_{arom}); 123.8 ($CH_2C\underline{H}$=CH); 126.5 (2 x CH_{arom}); 126.8 ($C_{arom,quat}$); 127.8 (CH_{arom}); 128.3 (2 x CH_{arom}); 128.6 (2 x CH_{arom}); 128.7 (CH_{arom}); 129.7 (2 x CH_{arom}); 130.0 (2 x CH_{arom}); 133.8 ($CH_2CH=\underline{C}H$); 136.6 ($C_{arom,quat}$); 140.8 ($C_{arom,quat}$); 145.2 ($C_{arom,quat}$); 169.4 (C=O). **IR** (ATR, cm^{-1}): ν_{NH} = 3375; ν_{CO} = 1657; ν_{max} = 1493, 1393, 1393, 1244, 966, 802, 700, 687. **MS** (ESI): *m/z* (%) 357 ($[M + 1]^+$, 100); 713 ($[2M + 1]^+$, 5); 735 $[2M + 23]^+$, 10). Yellow solid, 26%.

***N*-Cinnamyl-*N*-(4-methoxybenzyl)-2-(*p*-tolylamino)acetamide 1m**

Found as a mixture of 2 rotamers (52/48 in $CDCl_3$).

^{1}H-NMR (400 MHz, $CDCl_3$): δ 2.22 (3H, s, $CH_3C_{arom,quat}$); 3.77 and 3.78 (3H, 2 x s, OCH_3); 3.94-3.97 (4H, m, NHC$\underline{H}_2$ and C$\underline{H}_2$CH=$CH_{rotameric}$); 4.19 (2H, d, *J* = 6.5 Hz, C$\underline{H}_2$CH=$CH_{rotameric}$); 4.46 and 4.63 (2H, 2 x s, NC$\underline{H}_2$PMP); 6.04 and 6.14 (1H, 2 x d x t, *J* = 15.9 x 5.5 Hz and 15.8 x 6.6 Hz, $CH_2C\underline{H}$=CH); 6.46-6.58 (3H, m, 2 x CH_{arom} and $CH_2CH=C\underline{H}$); 6.84-6.89 (2H, m, 2 x CH_{arom}); 6.96-6.99 (2H, m, 2 x CH_{arom}); 7.10-7.13 (1H, m, CH_{arom}); 7.19-7.33 (5H, m, 5 x CH_{arom}). **^{13}C-NMR** (100 MHz, $CDCl_3$): δ 20.5 ($\underline{C}H_3C_{arom,quat}$); 45.8 and 45.9 (NH$\underline{C}H_2$CO); 47.6 and 47.7 (N$\underline{C}H_2$CH=CH); 48.2 and 48.7 ($CH_2$PMP); 55.3 and 55.4 ($OCH_3$); 113.3 (2 x CH_{arom}); 114.1 and 114.5 (2 x CH_{arom}); 123.4 and 124.0 ($NHCH_2\underline{C}H$=CH); 126.49 and 126.51 (2 x CH_{arom}); 126.8, 127.7, 127.87, 127.91, 128.2, 128.6, 128.8, 129.1, 129.8 (2 x $C_{arom,quat}$, 3 x (2 x CH_{arom}) and CH_{arom}); 132.6 and 133.6 ($CH_2CH=\underline{C}H$); 136.0 and 136.5 ($C_{arom,quat}$); 145.2 and 145.3 ($C_{arom,quat}$); 159.2 and 159.4 ($C_{arom,quat}$); 169.5 and 169.6 (C=O). **IR** (ATR, cm^{-1}): ν_{NH} = 3401; ν_{CO} = 1641; ν_{max} = 1611, 1510, 1252, 1161, 1030, 818, 739, 692. **MS** (ESI): *m/z* (%) 401 ($[M + 1]^+$, 100). Yellow solid, 30%.

S4.4 Synthesis of substrates for the α-oxidation

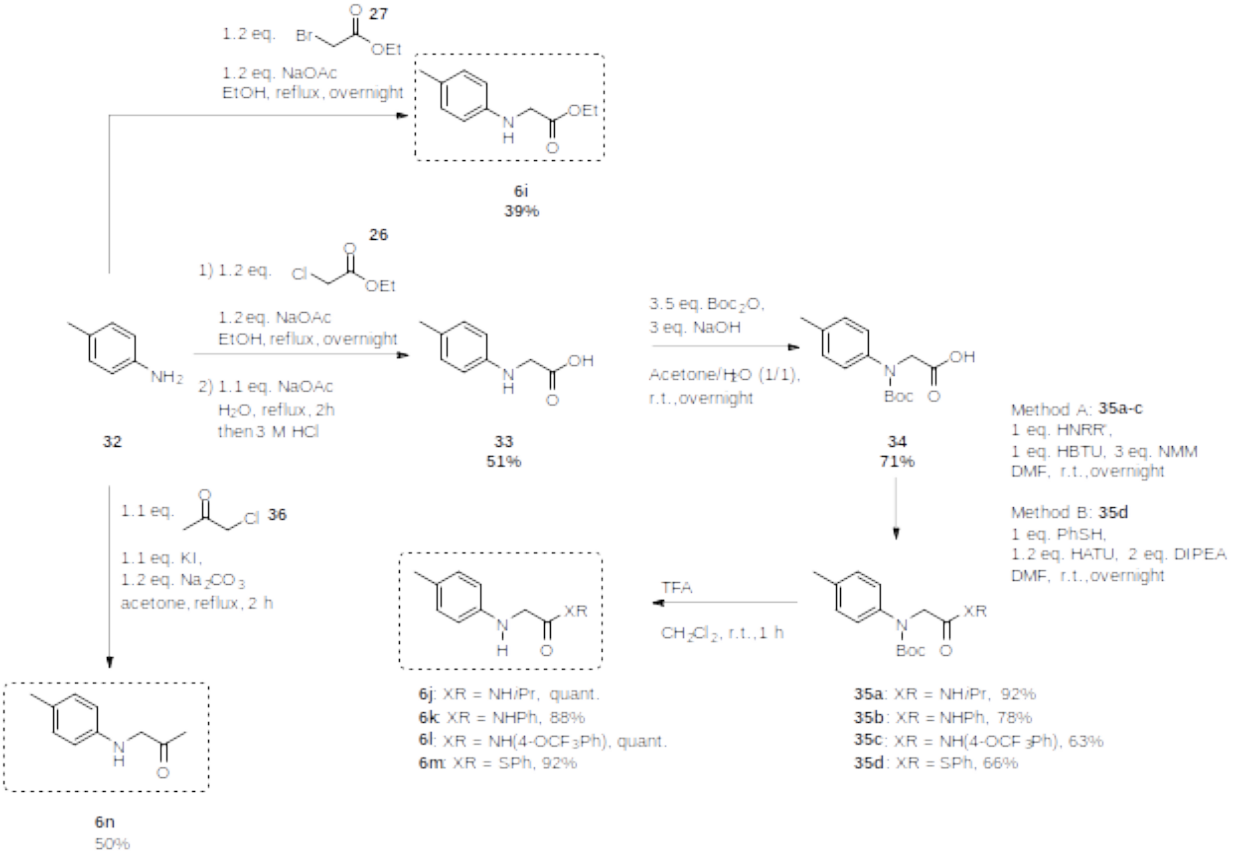

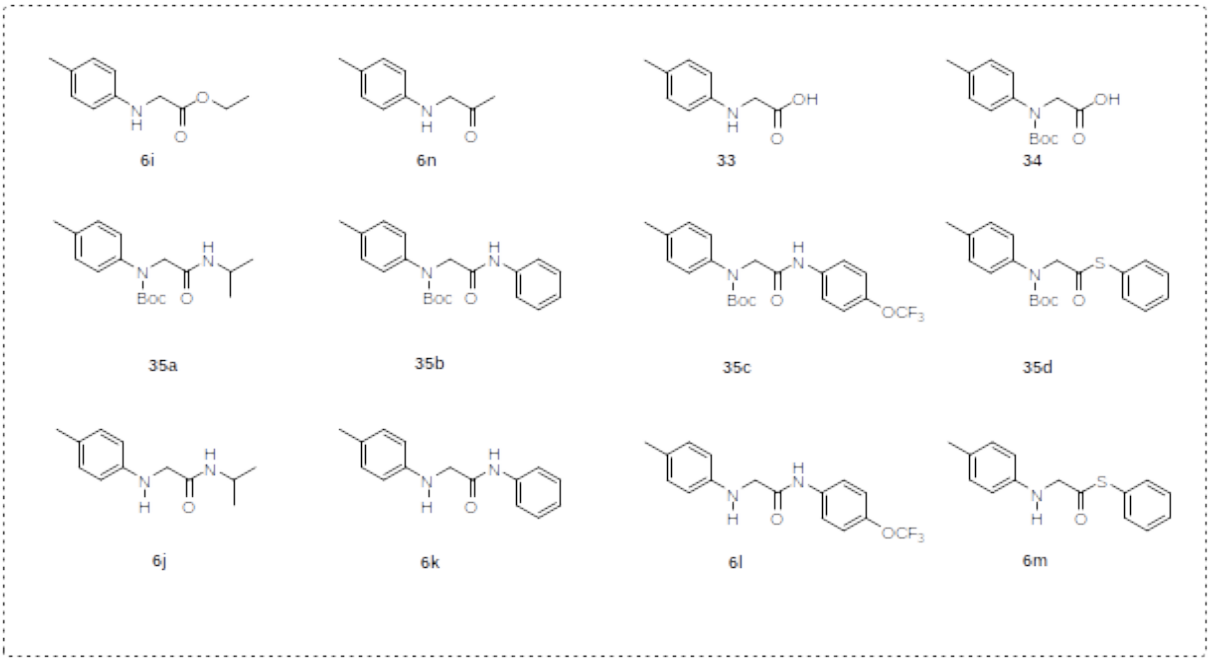

Scheme S9: Synthesis of compounds substrates **6i-m** for the α-oxidation.

S4.4.1 Synthesis of Ethyl *p*-tolylglycinate **6i**

Ethyl *p*-tolylglycinate **6i** was synthesized according to literature.[65] *p*-Toluidine **32** (2.14 g, 20 mmol, 1 eq.) and sodium acetate (3.28 g, 40 mmol, 2 eq.) were brought in a flask containing 50 mL EtOH. To this mixture was added 2.44 mL ethyl bromoacetate **27** (3.67 g, 22 mmol, 1.1 eq.) and this was refluxed overnight. The reaction was allowed to cool down to room temperature and water was added. The resulting precipitate was filtered off and purified via recrystallisation from EtOH/H_2O to give the title compound as grey needles (1.543 g, 39%).

Ethyl *p*-tolylglycinate 6i

^{1}H-NMR (400 MHz, $CDCl_3$): δ 1.29 (3H, t, *J* = 7.1 Hz, $C\underline{H}_3CH_2$); 2.24 (3H, s, $CH_3C_{arom,quat}$); 3.88 (2H, d, *J* = 5.60 Hz, CH_2N); 4.15 (1H, br s, NH); 4.23 (2H, q, *J* = 7.1 Hz, $CH_3C\underline{H}_2$); 6.54 (2H, d, *J* = 7.8 Hz, 2 x CH_{arom}); 7.01 (2H, d, *J* = 7.8 Hz, 2 x CH_{arom}). **^{13}C-NMR** (100 MHz, $CDCl_3$): δ 14.3 ($\underline{C}H_3CH_2$); 20.5 ($\underline{C}H_3C_{arom,quat}$); 46.4 ($CH_2N$); 61.4 ($CH_2O$); 113.3 (2 x CH_{arom}); 127.6 ($C_{arom,quat}$); 130.0 (2 x CH_{arom}); 144.9 ($C_{arom,quat}$); 171.5 (C=O). **IR** (ATR, cm^{-1}): ν_{NH} = 3379; ν_{CO} = 1724; ν_{max} = 2978, 2905, 1516, 1508, 1449, 1364, 1339, 806. **MS** (ESI): *m/z* (%) 194 ($[M + 1]^+$, 100). Grey needles, 39%. Spectral data matched literature.[66]

S4.4.2 Synthesis of 1-(*p*-tolylamino)propan-2-one **6n**

1-(p-tolylamino)propan-2-one **6n** was synthetized according to literature.[67] *p*-Toluidine **32** (1.071 g, 10 mmol, 1 eq.), K_2CO_3 (1.66 g, 12 mmol, 1.2 eq.) and KI (1.83 g, 11 mmol, 1 eq.) were added to a 50 mL flask containing 20 mL acetone. To this mixture 0.91 ml chloroacetone (1.018 g, 11 mmol, 1.1 eq.) was added, at room temperature, and the mixture was then refluxed overnight under a nitrogen atmosphere. This was evaporated, CH_2Cl_2 was added and the solution was washed twice with $NaHCO_3$ (aq. sat.). The crude mixture was purified via column chromatography (SiO_2, EtOAc/PE: 20/80) to give the title compound as yellow-orange crystals (0.824 g, 50%).

1-(*p*-Tolylamino)propan-2-one 6n

^{1}H-NMR (400 MHz, $CDCl_3$): δ 2.24 (3H, s, CH_3); 2.25 (3H, s, CH_3); 3.99 (2H, s, CH_2); 4.43 (1H, br s, NH); 6.51-6.54 (2H, m, 2 x CH_{arom}); 7.00-7.02 (2H, m, 2 x CH_{arom}). **^{13}C-NMR** (100 MHz, $CDCl_3$): δ 20.5 ($\underline{C}H_3C_{arom,quat}$); 27.5 ($CH_3CO$); 54.8 ($CH_2$); 113.1 (2 x CH_{arom}); 127.2 ($C_{arom,quat}$); 130.0 (2 x CH_{arom}); 144.8 ($C_{arom,quat}$); 204.5 (C=O). **IR** (ATR, cm^{-1}): ν_{NH} = 3379; $\nu_{C=O}$ = 1724; ν_{max} = 2978, 2905, 2860, 1516, 1508, 1449, 1364, 806. **MS** (ESI): *m/z* (%) 164 ($[M + 1]^+$, 100) Yellow crystals, 50%. Spectral data matched literature.[67]

S4.4.3 Synthesis of 2-((4-methylphenyl)amino)acetic acid **33**

2-((4-methylphenyl)amino)acetic acid **33** was synthesized according to a literature procedure. [68] *p*-Toluidine **32** (16.1 g, 150 mmol, 1 eq.), 19.2 mL ethyl chloroacetate (22.1 g, 180 mmol, 1.2 eq.) and sodium acetate (14.8 g, 180 mmol, 1.2 eq.) were added to a flask containing 50 mL EtOH and the resulting mixture was refluxed overnight. The mixture was then poured on ice, filtered and dried. The filter cake was added to a flask together with 75 mL H_2O and NaOH (6.6 g, 165 mmol, 1.1 eq.) and this was refluxed for 30 minutes. The mixture was allowed to come to room temperature and the pH was adjusted by slow addition of 3N HCl until it was about 2. The resulting precipitate was filtered and washed with water. The crude was purified by recrystallisation from EtOH/water giving the title compound **33** as a brown solid (12.56 g, 51%).

2-((4-Methylphenyl)amino)acetic acid 33

^{1}H-NMR (400 MHz, $CDCl_3$): δ 2.25 (3H, s, CH_3); 3.94 (2H, s, CH_2); 6.57 (2H, d, *J* = 8.3 Hz, 2 x CH_{arom}); 7.02 (2H, d, *J* = 8.3 Hz, 2 x CH_{arom}). **^{13}C-NMR** (100 MHz, $CDCl_3$): δ 20.6 (CH_3); 46.5 (CH_2); 113.7 (2 x CH_{arom}); 128.5 ($C_{arom,quat}$); 129.9 (2 x CH_{arom}); 144.4 ($C_{arom,quat}$); 174.9 (C=O). **IR** (ATR, cm^{-1}): ν_{max} = 3347, 1653, 1510, 1381, 1310, 812, 712, 644, 565, 453. **MS** (ESI): *m/z* (%) 166 ($[M + 1]^+$, 100). Brown solid, 51%. Spectral data matched literature.[68]

S4.4.4 Synthesis of glycine derivatives **6j-m**

Step 1: Synthesis of *N*-(*tert*-butoxycarbonyl)-*N*-(*p*-tolyl)glycine **34**

2-((4-methylphenyl)amino)acetic acid **33** (4.29 g, 25.9 mmol, 1 eq.) was dissolved in 50 mL acetone/H_2O (1/1) and sodium hydroxide (4.66 g, 116.6 mmol, 4.5 eq.) was added. Boc_2O (16.98 g, 77.8 mmol, 3 eq.) dissolved in 15 mL acetone was added to the 2-((4-methylphenyl)amino)acetic acid solution. The reaction was stirred at room temperature overnight. The acetone was then removed via rotary evaporation and the mixture was extracted with diethyl ether (25 mL). The water layer was acidified using 3N HCl until the pH was about 3 and then extracted three times with CH_2Cl_2 (3 x 50 mL). After evaporation the crude was further purified using column chromatography (C18, gradient CH_3CN/H_2O: 10/100 - 100/0) furnishing compound **34** as a yellow oil/off white solid (4.91 g, 71%).

***N*-(*Tert*-butoxycarbonyl)-*N*-(*p*-tolyl)glycine 34**

^{1}H-NMR (400 MHz, $CDCl_3$): δ 1.43 (9H, br s, $(CH_3)_3CO$); 2.33 (3H, s, $CH_3C_{arom,quat}$); 4.31 (2H, s, CH_2); 7.11-7.15 (4H, m, 4 x CH_{arom}). **^{13}C-NMR** (100 MHz, $CDCl_3$): δ 21.1 ($\underline{C}H_3C_{arom,quat}$); 28.3 ($(\underline{C}H_3)_3CO$); 52.3 ($CH_2N$); 81.4 ($(CH_3)_3\underline{C}O$); 126.4 ($C_{arom,quat}$); 129.6 (2 x CH_{arom}); 136.4 (2 x CH_{arom}); 140.1 ($C_{arom,quat}$); 154.8* (NC=O); 175.5* (C(O)OH). **IR** (ATR, cm^{-1}): $\nu_{C=O}$ = 1705; ν_{max} = 2980, 1512, 1366, 1246, 1233, 1152, 1046, 870, 764. **MS** (ESI): *m/z* (%) 166 ($[M - C_4H_8 - CO_2 + 1]^+$, 75); 210 ($[M - C_4H_8 + 1]^+$, 100); 553 ($[2 x M + 23]^+$, 5); 834 ($[3 x M + 39]^+$, 10). Yellow oil/off white solid, 71%.
*peak broadening

Step 2: Synthesis of Boc protected compounds **35a-d**

The synthesis of *tert*-butyl (2-(isopropylamino)-2-oxoethyl)(*p*-tolyl)carbamate **35a** is described as a representative example for the synthesis of amides **35a-c**.

N-(*Tert*-butoxycarbonyl)-*N*-(*p*-tolyl)glycine **34** (805 mg, 3.03 mmol, 1 eq.), HBTU (1.150 g, 3.03 mmol, 1 eq.) and 1 mL NMM (919 mg, 9.09 mmol, 3 eq.) were added to a flask containing 15 mL dry DMF under argon. The flask was stirred for 10 minutes at room temperature and then 260 µL isopropylamine (179 mg, 3.03 mmol, 1 eq.) was added. This was stirred at room temperature overnight, then water (100 mL) and EtOAc (100 mL) were added and the layers were separated. The organic layer was further washed with brine (2 x 100 mL), evaporated and purified using column chromatography (C18, gradient CH_3CN/H_2O: 30/100 - 100/0)* to furnish the title compound as a white solid (855 mg, 92%).
*For **35b**: C18, CH_3CN/H_2O: 50/50. For **35c**: C18, gradient CH_3CN/H_2O: 60/100 - 100/0.

For the synthesis of compound **35d** the following procedure was used. *N*-(*Tert*-butoxycarbonyl)-*N*-(*p*-tolyl)glycine **34** (505 mg, 1.9 mmol, 1 eq.), HATU (868 mg, 2.3 mmol, 1.2 eq.) and 662 µL DIPEA (491 mg, 3.8 mmol, 2 eq) were stirred in 10 mL dry DMF under argon for 10 minutes. To this 194 µl thiophenol (209 mg, 1.9 mmol, 1 eq.) was added and the mixture was stirred at room temperature overnight. Water (100 mL) and ethyl acetate (100 mL) were added and the organic layer was further washed with brine (2 x 100 mL). The organic layer was evaporated and purified via column

chromatography (C18, gradient CH_3CN/H_2O: 60/100 - 100/0) to give the title compound **35d** as a colorless oil (445 mg, 66%).

***Tert*-butyl (2-(isopropylamino)-2-oxoethyl)(*p*-tolyl)carbamate 35a**

^{1}H-NMR (400 MHz, $CDCl_3$): 1.15 (6H, d, *J* = 6.6 Hz, $(C\underline{H}_3)_2CH$); 1.45 (9H, s, $(C\underline{H}_3)_3CO$); 2.31 (3H, s, $CH_3C_{arom,quat}$); 4.06-4.13 (1H, m, $(CH_3)_2C\underline{H}$); 4.15 (2H, s, CH_2); 6.02 (1H, br s, NH); 7.12 (4H, s, 4 x CH_{arom}). **^{13}C-NMR** (100 MHz, $CDCl_3$): δ 21.0 ($\underline{C}H_3C_{arom,quat}$); 22.9 ($(\underline{C}H_3)_2CH$); 28.3 ($(\underline{C}H_3)_3CO$); 41.5 ($(CH_3)_2\underline{C}H$); 54.8 ($CH_2$); 81.6 ($(CH_3)_3\underline{C}$); 125.6 (2 x CH_{arom}); 129.6 (2 x CH_{arom}); 136.1 ($C_{arom,quat}$); 140.1 ($C_{arom,quat}$); 154.9 (NC(O)O); 168.6 (NC=O). **IR** (ATR, cm^{-1}): ν_{NH} = 3348; $\nu_{C=O}$ = 1678; ν_{max} = 2976, 2934, 1678, 1516, 1381, 1366, 1223, 1175. **MS** (ESI): *m/z* (%) 207 ($[M - C_4H_8 - CO_2 + 1]^+$, 80); 251 ($[M - C_4H_8 + 1]^+$, 100); 307 ($[M + 1]^+$, 20); 635 ($[2 x M + 23]^+$, 10). White solid, 92%.

***Tert*-butyl (2-oxo-2-(phenylamino)ethyl)(*p*-tolyl)carbamate 35b**

^{1}H-NMR (400 MHz, $CDCl_3$): δ 1.46 (9H, s, $(CH_3)_3CO$); 2.33 (3H, s, $CH_3C_{arom,quat}$); 4.32 (2H, s, CH_2); 7.10-7.18 (5H, m, 5 x CH_{arom}); 7.33 (2H, t, *J* = 7.9 Hz, 2 x CH_{arom}); 7.52 (2H, d, *J* = 7.9 Hz, 2 x CH_{arom}); 8.28 (1H, br s, NH). **^{13}C-NMR** (100 MHz, $CDCl_3$): δ 21.1 ($\underline{C}H_3C_{arom,quat}$); 28.4 ($(\underline{C}H_3)_3CO$); 55.8 ($CH_2$); 82.0 ($(CH_3)_3\underline{C}O$); 119.9 (2 x CH_{arom}); 124.5 (CH_{arom}); 125.9 (2 x CH_{arom}); 129.2 (2 x CH_{arom}); 129.8 (2 x CH_{arom}); 136.5 ($C_{arom,quat}$); 137.8 ($C_{arom,quat}$); 140.0 ($C_{arom,quat}$); 155.5 (NC(O)O); 167.9 (HNC=O). **IR** (ATR, cm^{-1}): ν_{NH} = 3285; $\nu_{C=O}$ = 1692 and 1672; ν_{max} = 2970, 1516, 1429, 1385, 1152, 826, 519. **MS** (ESI): *m/z* (%) 241 ($[M - C_4H_8 - CO_2 + 1]^+$, 100); 285 ($[M - C_4H_8 + 1]^+$, 40); 703 ($[2 x M + 23]^+$, 10). White solid, 78%.

***Tert*-butyl (2-oxo-2-((4-(trifluoromethoxy)phenyl)amino)ethyl)(p-tolyl)carbamate 35c**

^{1}H-NMR (400 MHz, $CDCl_3$): δ 1.45 (9H, s, $(CH_3)_3CO$); 2.33 (3H, s, $CH_3C_{arom,quat}$); 4.32 (2H, s, CH_2); 7.12-7.18 (6H, m, 6 x CH_{arom}); 7.54 (2H, d, *J* = 9.0 Hz, 2 x CH_{arom}); 8.51 (1H, br s, NH). **^{19}F-NMR** (376 MHz, $CDCl_3$): -58.1 (CF_3) **^{13}C-NMR** (100 MHz, $CDCl_3$): δ 21.1 ($\underline{C}H_3C_{arom,quat}$); 28.4 ($(\underline{C}H_3)_3CO$); 55.8 ($CH_2$); 82.1 ($(CH_3)_3\underline{C}O$); 119.3 ($CF_3$);* 121.0 (2 x CH_{arom}); 121.9 (2 x CH_{arom}); 125.9 (2 x CH_{arom}); 129.8 (2 x CH_{arom}); 136.5 ($C_{arom,quat}$); 136.7 ($C_{arom,quat}$); 139.9 ($C_{arom,quat}$); 145.4 ($C_{arom,quat}$); 155.7 (NC(O)O); 168.1 (HNC=O). **IR** (ATR, cm^{-1}): ν_{NH} = 3292; $\nu_{C=O}$ = 1697 and 1672; ν_{max} = 1541, 1508, 1248, 1221, 1200, 1150, 826. **MS** (ESI): *m/z* (%) 325 ($[M - C_4H_{8+} - CO_2 + 1]^+$, 100); 369 ($[M - C_4H_8 + 1]^+$, 45); 447 ($[M + 23]^+$, 5); 871 ($[2 x M + 23]^+$, 10). White solid, 63%.

*rest of CF_3 quartet not visible

***S*-Phenyl 2-((*tert*-butoxycarbonyl)(*p*-tolyl)amino)ethanethioate 35d**

^{1}H-NMR (400 MHz, $CDCl_3$): δ 1.48 (9H, br s, $(CH_3)_3CO$); 2.34 (3H, s, $CH_3C_{arom,quat}$); 4.52 (2H, s, CH_2); 7.14-7.16 (2H, m, 2 x CH_{arom}); 7.23-7.26 (2H, m, 2 x CH_{arom}); 7.42 (5H, s, 5 x CH_{arom}). **^{13}C-NMR** (100 MHz, $CDCl_3$): δ 21.0 ($\underline{C}H_3C_{arom,quat}$); 28.2 ($(\underline{C}H_3)_3CO$); 60.0 ($CH_2$); 81.4 ($(CH_3)_3\underline{C}O$); 126.3 (2 x CH_{arom}); 126.9 (CH_{arom}); 129.3, 129.4 and 129.5 (5 x CH_{arom}); 134.7 (2 x CH_{arom}); 136.2 ($C_{arom,quat}$); 139.3 ($C_{arom,quat}$); 154.3 (NC=O); 195.7 (SC=O). **IR** (ATR, cm^{-1}): $\nu_{C=O}$ = 1697; ν_{max} = 2976, 1514, 1366, 1225, 1150, 1016, 745, 729, 583. **MS** (ESI): *m/z* (%) 258 ($[M - C_4H_8 - CO_2 + 1]^+$, 100); 737 ($[2 x M + 23]^+$, 5). Colorless oil, 66%.

Step 3: Synthesis of Boc deprotected compounds **6j-m**

The synthesis of compound **6j** is described as a representative example for the synthesis of compounds **6j-m**.

Tert-butyl (2-(isopropylamino)-2-oxoethyl)(*p*-tolyl)carbamate **35a** (855 mg, 2.8 mmol, 1 eq.) was dissolved in 7.5 mL dry CH_2Cl_2 under nitrogen and 2.5 mL TFA was added. This was stirred at room temperature for one hour until completion (LC-MS). The reaction mixture was evaporated and the residue was redissolved in CH_2Cl_2 and washed with saturated $NaHCO_3$ solution. The water phase was further extracted with CH_2Cl_2, the combined organic layers were washed with brine, dried over $MgSO_4$, filtered and evaporated to give the product as a colorless oil (577 mg, quant.).

***N*-Isopropyl-2-(*p*-tolylamino)acetamide 6j**

^{1}H-NMR (400 MHz, $CDCl_3$): δ 1.12 (6H, d, *J* = 6.6 Hz, $(C\underline{H}_3)_2CH$); 2.25 (3H, s, $CH_3C_{arom,quat}$); 3.72 (2H, s, CH_2); 4.06-4.19 (2H, m, $C\underline{H}(CH_3)_2$ and $N\underline{H}CH_2$); 6.53 (2H, d, *J* = 8.3 Hz, 2 x CH_{arom}); 6.57 (1H, br s, NHCO); 7.02 (2H, d, *J* = 8.3 Hz, 2 x CH_{arom}). **^{13}C-NMR** (100 MHz, $CDCl_3$): δ 20.5 ($\underline{C}H_3C_{arom,quat}$); 22.8 ($(\underline{C}H_3)_2CH$); 41.2 ($(CH_3)_2\underline{C}H$); 49.7 ($CH_2$); 113.5 (2 x CH_{arom}); 128.6 ($C_{arom,quat}$); 130.0 (2 x CH_{arom}); 145.2 ($C_{arom,quat}$); 169.9 (C=O). **IR** (ATR, cm^{-1}): ν_{NH} = 3337; $\nu_{C=O}$ = 1649; ν_{max} = 2972, 1616, 1516, 1312, 1258, 1171, 806, 513. **MS** (ESI): *m/z* 207 ($[M + 1]^+$, 100). Colorless oil, quant.

***N*-Phenyl-2-(*p*-tolylamino)acetamide 6k**

^{1}H-NMR (400 MHz, $CDCl_3$): δ 2.26 (3H, s, CH_3); 3.88 (2H, s, CH_2); 6.62 (2H, d, *J* = 8.2 Hz, 2 x CH_{arom}); 7.05 (2H, d, *J* = 8.2 Hz, 2 x CH_{arom}); 7.11 (1H, t, *J* = 7.7 Hz, CH_{arom}); 7.31 (2H, d x d, *J* = 7.8 x 7.7 Hz, 2 x CH_{arom}); 7.53 (2H, d, *J* = 7.8 Hz, 2 x CH_{arom}); 8.64 (1H, br s, NH). **^{13}C-NMR** (100 MHz, $CDCl_3$): δ 20.5 (CH_3); 50.4 (CH_2); 113.8 (2 x CH_{arom}); 120.0 (2 x CH_{arom}); 124.6 (CH_{arom}); 129.1 (2 x CH_{arom}); 129.3 ($C_{arom,quat}$); 130.2 (2 x CH_{arom}); 137.4 ($C_{arom,quat}$); 144.8 ($C_{arom,quat}$); 169.2 (C=O). **IR** (ATR, cm^{-1}): ν_{NH} = 3410 and 3314; $\nu_{C=O}$ = 1655; ν_{max} = 1620, 1599, 1508, 1441, 1315, 1258, 806. **MS** (ESI): *m/z* 241 ($[M + 1]^+$, 100). Light brown solid, 88%.

2-(*p*-Tolylamino)-*N*-(4-(trifluoromethoxy)phenyl)acetamide 6l

^{1}H-NMR (400 MHz, $CDCl_3$): δ 2.27 (3H, s, CH_3); 3.89 (2H, s, CH_2); 6.59-6.63 (2H, m, 2 x CH_{arom}); 7.05 (2H, d, *J* = 8.3 Hz, 2 x CH_{arom}); 7.16 (2H, d, *J* = 8.3 Hz, 2 x CH_{arom}); 7.54-7.58 (2H, m, 2 x CH_{arom}); 8.72 (1H, br s, NH). **^{19}F-NMR** (376 MHz, $CDCl_3$): -58.14 (CF_3). **^{13}C-NMR** (100 MHz, $CDCl_3$): δ 20.5 (CH_3); 50.4 (CH_2); 113.8 (2 x CH_{arom}); 119.3 (CF_3);* 121.1 (2 x CH_{arom}); 121.9 (2 x CH_{arom}); 129.5 ($C_{arom,quat}$); 130.3 (2 x CH_{arom}); 136.1 ($C_{arom,quat}$); 144.7 ($C_{arom,quat}$); 145.6 ($C_{arom,quat}$); 169.3 (C=O). **IR** (ATR, cm^{-1}): ν_{NH} = 3379; $\nu_{C=O}$ = 1697; ν_{max} = 1614, 1508, 1171, 1155, 1130, 1109, 816, 532. **MS** (ESI): *m/z* 325 ($[M + 1]^+$, 100). White solid, quant.

*rest of CF_3 quartet not visible

***S*-Phenyl 2-(*p*-tolylamino)ethanethioate 6m**

^{1}H-NMR (400 MHz, $CDCl_3$): δ 2.28 (3H, s, CH_3); 4.13 (2H, s, CH_2); 4.30 (1H, br s, NH); 6.60 (2H, d, *J* = 8.1 Hz, 2 x CH_{arom}); 7.06 (2H, d, *J* = 8.1 Hz, 2 x CH_{arom}); 7.41 (5H, s, 5 x CH_{arom}). **^{13}C-NMR** (100 MHz, $CDCl_3$): δ 20.6 (CH_3); 54.7 (CH_2); 113.2 (2 x CH_{arom}); 127.6 ($C_{arom,quat}$); 128.2 ($C_{arom,quat}$); 129.3 (2 x CH_{arom}); 129.5 (CH_{arom}); 130.0 (2 x CH_{arom}); 134.7 (2 x CH_{arom}); 144.4 ($C_{arom,quat}$); 199.7 (C=O). **IR** (ATR, cm^{-1}): ν_{NH} = 3418; $\nu_{C=O}$ = 1692; ν_{max} = 2920, 1520, 1304, 1263, 1057, 806, 756, 579. **MS** (ESI): *m/z* 258 ($[M + 1]^+$, 100). White crystals, 92%.

S4.4.5 Synthesis of ethyl cyclohexylglycinate **6n**

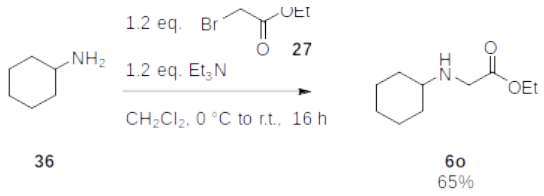

Scheme S10: Synthesis of ethyl cyclohexylglycinate **6n**

Ethyl cyclohexylglycinate was synthesized according to a modified literature procedure.[69] Cyclohexylamine **36** (0.99 g, 10 mmol, 1eq.) and triethylamine (1.21 g, 12 mmol, 1.2 eq.) were added to a flame dried flask containing 25 mL dry CH_2Cl_2 under nitrogen. Ethyl bromoacetate **27** (2.00 g, 12 mmol, 1.2 eq.) in 10 mL CH_2Cl_2 was added dropwise at 0 °C. This mixture was stirred at room temperature for 16 h and then water was added (50 mL) and the layers separated. The water layer was further extracted with CH_2Cl_2 (2 x 50 mL) and the combined organic fractions were concentrated under vacuum. The pure product **6o** was obtained by column chromatography (SiO_2, PE/EtOAc: 66/33) as a brown oil (1.20 g, 65%).

Ethyl cyclohexylglycinate 6o

^{1}H-NMR (400 MHz, $CDCl_3$): δ 1.04-1.29 (8H, m, $OCH_2C\underline{H}_3$ and $NHCHC(\underline{H})HC(\underline{H})HC(\underline{H})H$); 1.58-1.63 (2H, m, NH and $NHCHCH_2CH_2C(H)\underline{H}$); 1.71-1.76 (2H, m, $NHCHCH_2C(H)\underline{H}CH_2$); 1.83-1.87 (2H, m, $NHCHC(H)\underline{H}CH_2CH_2$); 2.40 (1H, t x t, *J* = 15.5 x 3.8 Hz, $NHC\underline{H}CH_2CH_2CH_2$), 3.42 (2H, $NHC\underline{H}_2CO$); 4.19 (2H, t, *J* = 7.1 Hz, $OC\underline{H}_2CH_3$) **^{13}C-NMR** (100 MHz, $CDCl_3$): δ 14.4 ($\underline{C}H_3CH_2O$); 25.0 ($NHCHCH_2\underline{C}H_2CH_2$); 26.2 ($NHCHCH_2CH_2\underline{C}H_2$); 33.5 ($NHCH\underline{C}H_2CH_2CH_2$); 48.5 ($NH\underline{C}H_2CO$); 56.6 ($NH\underline{C}HCH_2CH_2CH_2$); 60.9 ($CH_3\underline{C}H_2O$); 173.1 (C=O). **IR** (ATR, cm^{-1}): $\nu_{C=O}$ = 1736; ν_{max} = 2926, 2853, 1449, 1373, 1182, 1152, 1024, 891, 692. **MS** (ESI): *m/z* 186 ($[M + 1]^+$, 100). Brown oil, 65%. Spectral data matched literature.[69]

S5 Photocatalysis

S5.1 Background information

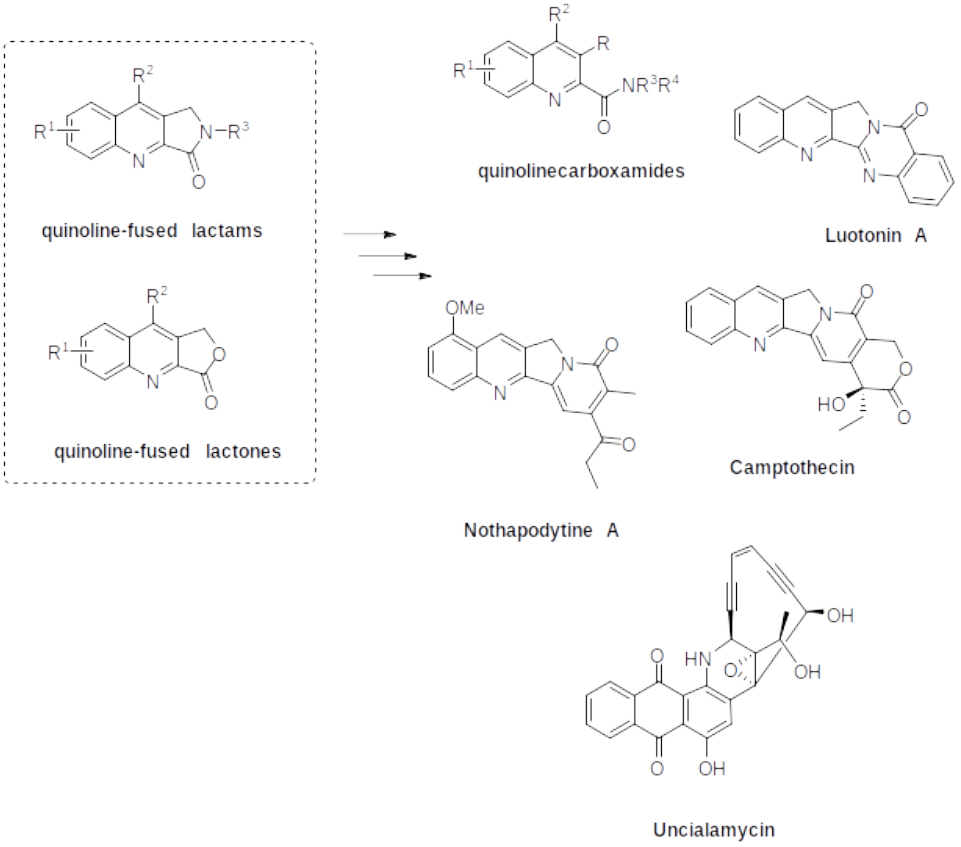

Figure S42: Utility of quinoline-fused lactams and lactones.

S5.2 Screening and control experiments

To a small glass test tube were added the photocatalyst, Lewis acid and cinnamyl *p*-tolylglycinate* **1a** (28 mg, 0.1 mmol, 1 eq.)* after which 1 mL solvent was added. This was stirred under air and irradiation from a 26 W CFL (~10 cm distance) for 24 h. The reaction mixture was filtered over filter paper and the filter was rinsed thoroughly with acetone. The filtrate was evaporated under vacuum and the internal standard, 1,3,5-trimethoxybenzene (17 mg, 0.1 mmol, 1 eq.)* or mesitylene (12 mg, 0.1 mmol, 1 eq.)* was added. The NMR yield was determined by integration of the aromatic signals of the internal standard (3H) and the CH_2 of the lactone at δ = 5.36 ppm (^{1}H-NMR, $CDCl_3$).

*To make the yield determination using NMR more precise these quantities were weighed exactly using a Mettler Toledo ME204/M Analytical balance.

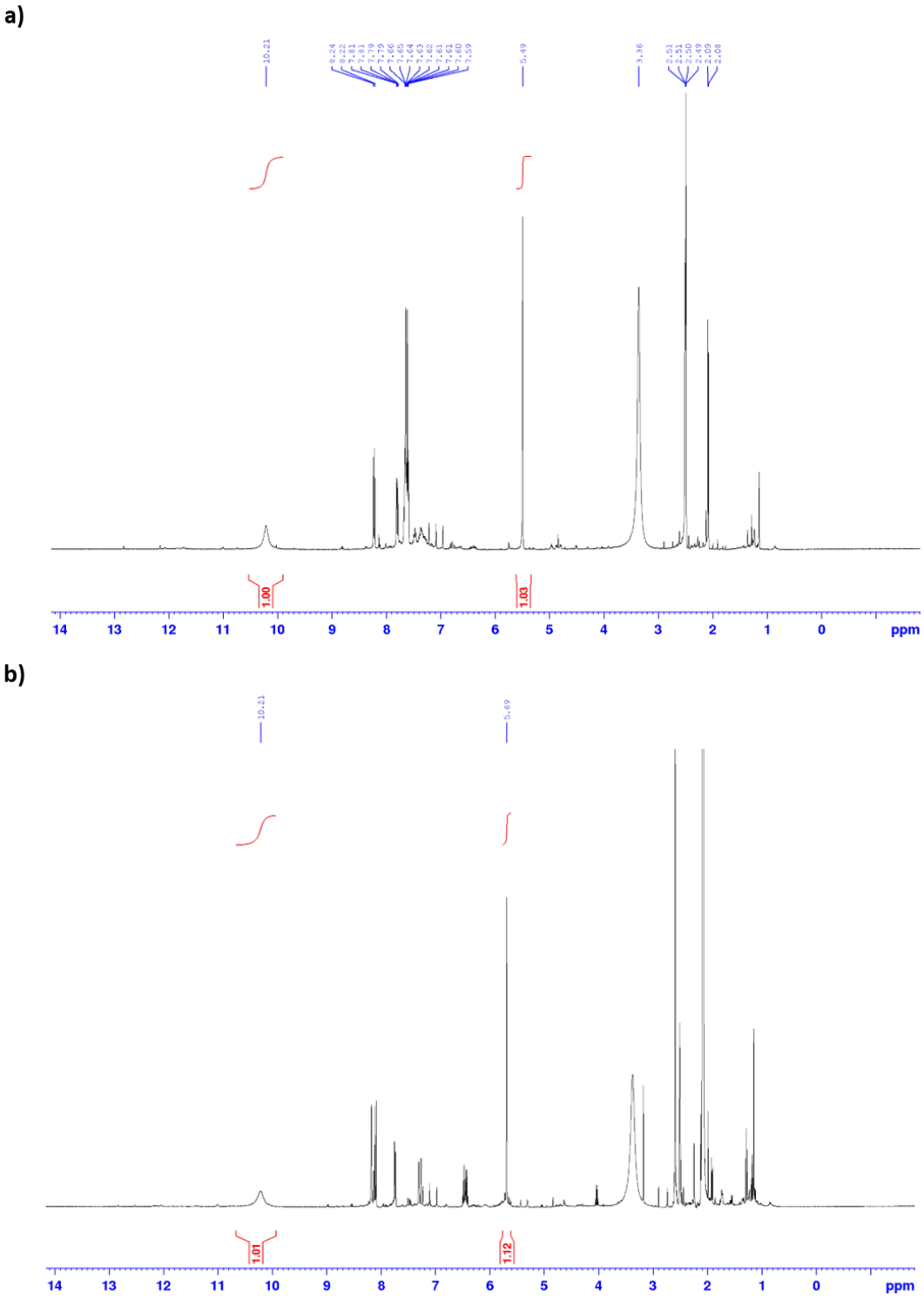

Figure S43: Detection of hydrogen peroxide in the crude reaction mixtures of compound (a) **4a** and (b) **4k** in DMSO-d_6, H_2O_2 is visible at 10.20 ppm.[29] The ratio of H_2O_2 to the product, given that both signals account for 2H, is about 1/1.

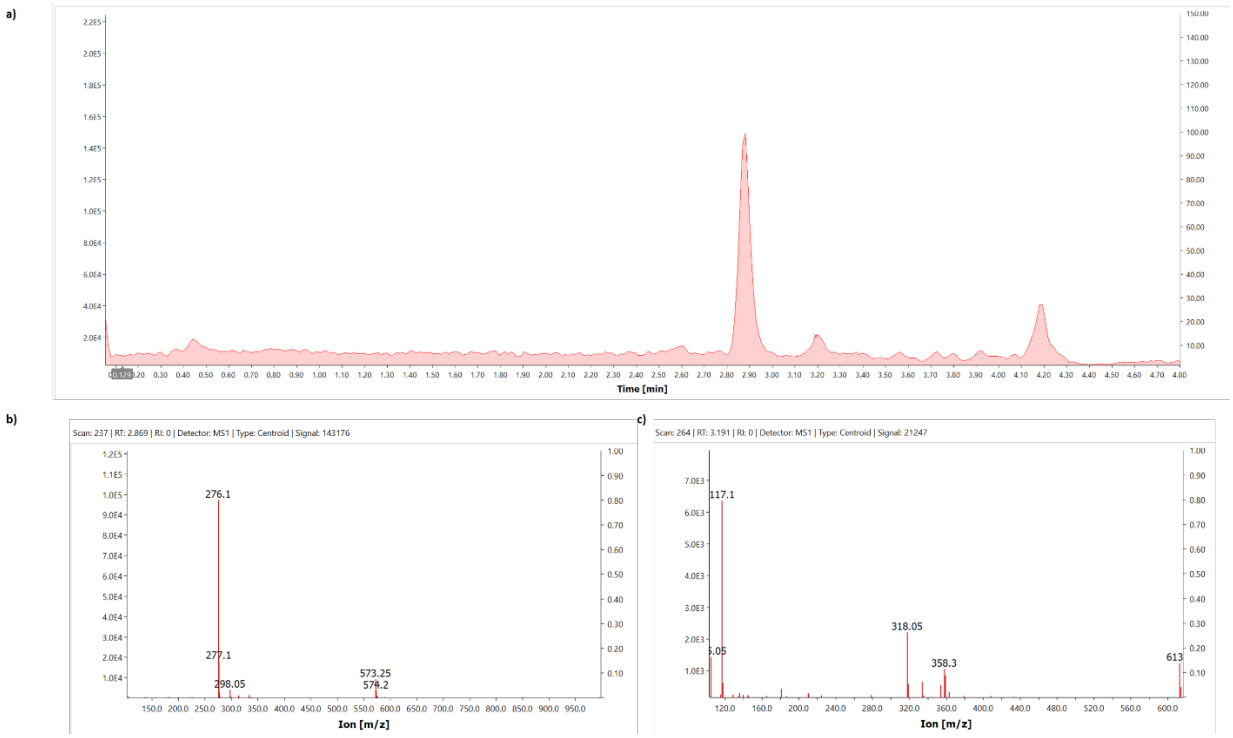

Figure S44: Crude LC-MS of **4a** after 24 hours. The large peak (t_r = 2.9 min.) corresponds to the product (MS spectrum in (b): M+1). The smaller peak around 3.2 min. corresponds to the α-oxidized product **7a** (MS spectrum in (c): M+23) which was detectable as a minor side product. The peak around 4.2 min. stems from the column itself.

S5.3 Testing of Lewis acid coordination on the COF.

TpBpyCOF (20 mg) and $ScOTf_3$ (10 mg, 0.02 mmol, 0.1 eq.) were stirred in 2 mL CH_3CN, under air and irradiated with a 26 W CFL (~10 cm distance) for 24 h. The reaction mixture was filtered over a membrane filter and washed thoroughly with acetone and acetonitrile. The filter cake was then dried, scraped off and added to another test tube. (*E*)-Penta-2,4-dien-1-yl *p*-tolylglycinate **1k** (49 mg, 0.2 mmol, 1 eq.) and 2 mL CH_3CN were then added to this test tube, which was stirred under air and irradiated with a 26 W CFL (~10 cm distance) for 24 h. The filtrate was then evaporated and the internal standard, mesitylene (24 mg, 0.2 mmol, 1 eq.) was added to determine the yield. For condition B, the reaction was performed as usual, *i.e.* by adding $ScOTf_3$ together with the COF and the substrate. In condition C the Lewis acid was omitted.

Table S2: Complexation of $Sc(OTf)_3$ on **TpBpyCOF**

Conditions	Yield (%)
A	52% **4k**
B	46% **4k**
C	38% **7h**

S5.4 Tandem aerobic oxidation/Povarov reaction of *N*-aryl glycine derivatives

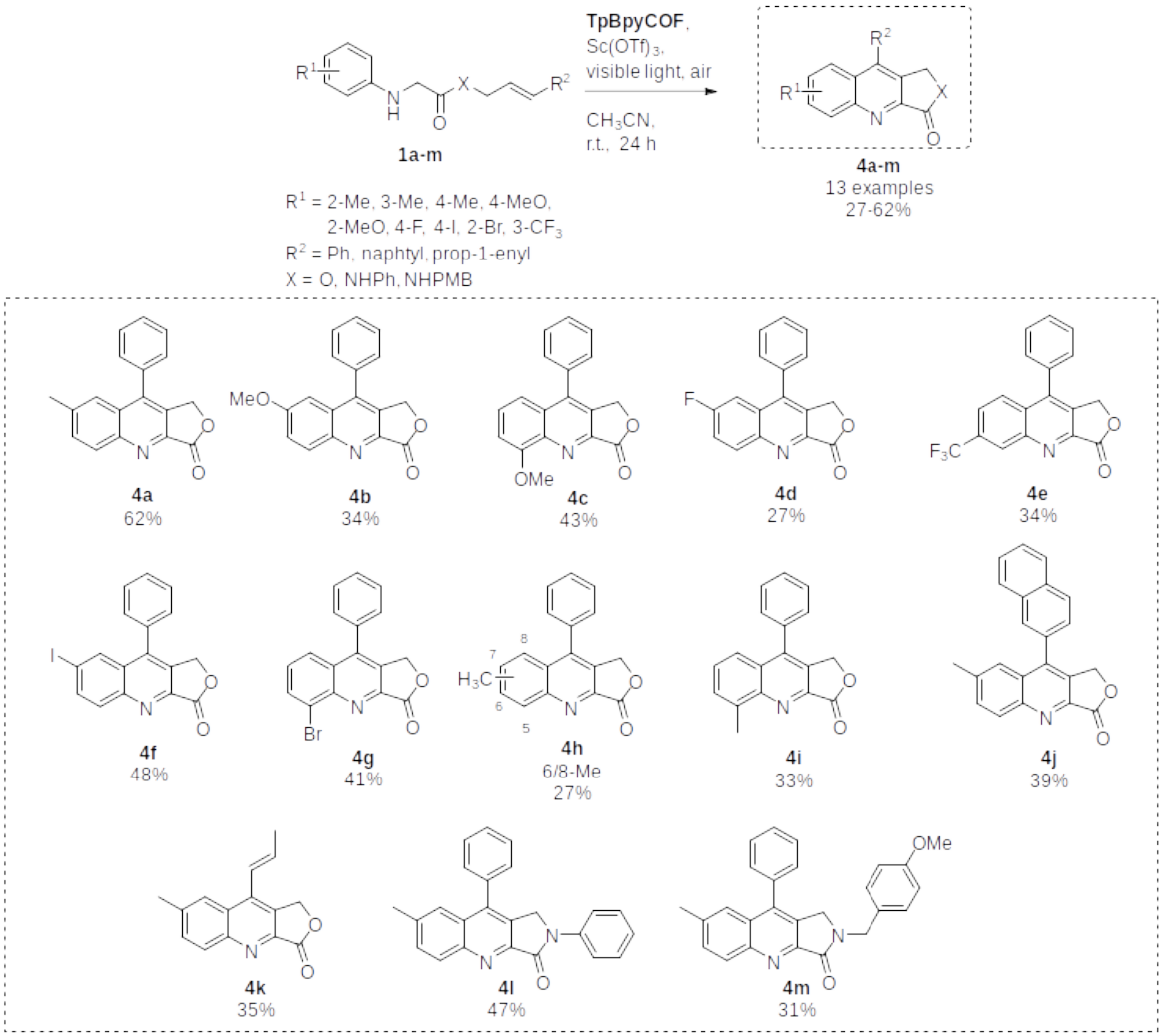

Scheme S11: Substrate scope of the photocatalytic tandem oxidation/Povarov reaction catalyzed by **TpBpyCOF**.

7-Methyl-9-phenylfuro[3,4-*b*]quinolin-3(1*H*)-one 4a

^{1}H-NMR (400 MHz, $CDCl_3$): δ 2.51 (3H, s, CH_3); 5.36 (2H, s, OCH_2); 7.43-7.45 (2H, m, 2 x CH_{arom}); 7.55-7.64 (4H, m, 4 x CH_{arom}); 7.67 (1H, d x d, *J* = 8.7 x 1.8 Hz, CH_{arom}); 8.31 (1H, d, *J* = 8.7 Hz, CH_{arom}). **^{13}C-NMR** (100 MHz, $CDCl_3$): δ 22.3 (CH_3); 67.9 (CH_2); 124.4 (CH_{arom}); 128.1 ($C_{arom,quat}$); 129.0 (2 x CH_{arom}); 129.4 (2 x CH_{arom}); 129.5 (CH_{arom}); 131.2 (CH_{arom}); 132.6 ($C_{arom,quat}$); 133.3 (CH_{arom}); 133.9, 140.1, 143.0, 143.5 and 149.6 (5 x $C_{arom,quat}$); 169.0 (C=O). **IR** (ATR, cm^{-1}): $\nu_{C=O}$ = 1776; ν_{max} = 2922, 1371, 1132, 1057, 826, 725, 700, 538, 453. **MS** (ESI): *m/z* (%) 276 ([M + 1]$^+$, 100). White solid, 62%. Spectral data matched literature.[61]

7-Methoxy-9-phenylfuro[3,4-*b*]quinolin-3(1*H*)-one 4b

^{1}H-NMR (400 MHz, $CDCl_3$): δ 3.81 (3H, s, CH_3); 5.34 (2H, s, CH_2); 7.10 (1H, d, *J* = 2.8 Hz, CH_{arom}); 7.44-7.46 (2H, m, 2 x CH_{arom}); 7.51 (1H, d x d, *J* = 9.3 x 2.8 Hz, CH_{arom}); 7.55-7.63 (3H, m, 3 x CH_{arom}); 8.33 (1H, d, *J* = 9.3 Hz, CH_{arom}).**^{13}C-NMR** (100 MHz, $CDCl_3$): δ 55.6 (CH_3); 67.7 (CH_2); 102.9 (CH_{arom}); 123.9 (CH_{arom}); 128.6 (2 x CH_{arom}); 129.4 (CH_{arom} and 1 x (2 x CH_{arom})); 129.6 ($C_{arom,quat}$), 132.9 (CH_{arom}), 133.1, 133.9, 141.7, 141.9, 147.1 and 160.2 (6 x $C_{arom,quat}$); 169.0 (C=O). **IR** (ATR, cm^{-1}): $\nu_{C=O}$ = 1775; ν_{max} = 1620, 1582, 1371, 1242, 1225, 1126, 1018, 837, 745. **MS** (ESI): *m/z* (%) ([M + 1]$^+$, 292). Beige solid, 34%. Spectral data matched literature.[70]

5-Methoxy-9-phenylfuro[3,4-*b*]quinolin-3(1*H*)-one 4c

^{1}H-NMR (400 MHz, $CDCl_3$): δ 4.14 (3H, s, CH_3); 5.37 (2H, s, CH_2); 7.17 (1H, d, *J* = 7.8 Hz, CH_{arom}); 7.42-7.44 (3H, m, 3 x CH_{arom}); 7.56-7.62 (4H, m, 4 x CH_{arom}). **^{13}C-NMR** (100 MHz, $CDCl_3$): δ 56.4 (CH_3); 67.7 (CH_2); 108.5 (CH_{arom}); 117.3 (CH_{arom}); 129.0 (2 x CH_{arom}); 129.3 ($C_{arom,quat}$); 129.4 (2 x CH_{arom}); 129.6 (CH_{arom}); 129.9 (CH_{arom}); 133.3, 134.0, 143.1, 143.2, 143.8 and 156.9 (6 x $C_{arom,quat}$); 168.4 (C=O). **IR** (ATR, cm^{-1}): $\nu_{C=O}$ = 1773; ν_{max} = 1510, 1400, 1368, 1256, 1136, 1049, 1007, 743, 706. **MS** (ESI): *m/z* (%) 292 ([M + 1]$^+$, 100). **HRMS** (ESI): calcd. for $C_{18}H_{14}NO_3^+$: 292.0968 [M + H]$^+$, found: 292.0960. White solid, 43%.

7-Fluoro-9-phenylfuro[3,4-*b*]quinolin-3(1*H*)-one 4d

^{1}H-NMR (400 MHz, $CDCl_3$): δ 5.40 (2H, s, CH_2); 7.42-7.45 (2H, m, 2 x CH_{arom}); 7.50 (1H, d x d, *J* = 9.8 x 2.7 Hz, CH_{arom}); 7.59-7.65 (4H, m, 4 x CH_{arom}); 8.44 (1H, d x d, *J* = 9.3 x 5.6 Hz, CH_{arom}). **^{19}F-NMR** (376 MHz, $CDCl_3$): -107.1 (1F, m). **^{13}C-NMR** (100 MHz, $CDCl_3$): δ 67.9 (CH_2); 109.3 (d, *J* = 23.7 Hz, CH_{arom}); 121.6 (d, *J* = 26.4 Hz, CH_{arom}); 128.8 (2 x CH_{arom}); 129.3 (d, *J* = 10.1 Hz, $C_{arom,quat}$); 129.7 (2 x CH_{arom}); 130.0 (CH_{arom}); 133.1 ($C_{arom,quat}$); 133.2 ($C_{arom,quat}$); 134.2 (d, *J* = 9.6 Hz, CH_{arom}); 143.5 (d, *J* = 6.3 Hz, $C_{arom,quat}$); 144.1 (d, *J* = 2.9 Hz, $C_{arom,quat}$); 148.0 ($C_{arom,quat}$); 162.5 (d, *J* = 253.2 Hz, $C_{arom,quat}$); 168.6 (C=O). **IR** (ATR, cm^{-1}): $\nu_{C=O}$ = 1773; ν_{max} = 1508, 1495, 1456, 1229, 1200, 1134, 1051, 1009, 737. **MS** (ESI): *m/z* (%) 280 ([M + 1]$^+$, 100). Beige solid, 27%. Spectral data matched literature.[70]

9-Phenyl-6-(trifluoromethyl)furo[3,4-*b*]quinolin-3(1*H*)-one 4e

Crude contained a mixture of regio-isomers (6/8-CF_3: 87/13). Only 9-phenyl-6-(trifluoromethyl)furo[3,4-*b*]quinolin-3(1*H*)-one could be isolated and characterized after reversed phase chromatography.

^{1}H-NMR (400 MHz, $CDCl_3$): δ 5.44 (2H, s, OCH_2); 7.44-7.46 (2H, m, 2 x CH_{arom}); 7.62-7.66 (3H, m, 3 x CH_{arom}); 7.82 (1H, d x d, *J* = 8.9 x 1.8, CH_{arom}); 8.06 (1H, d, *J* = 8.9 Hz, CH_{arom}); 8.75 (1H, s, CH_{arom}). **^{13}C-NMR** (100 MHz, $CDCl_3$): δ 67.9 (CH_2), 122.3* (CF_3), 125.0 (q, *J* = 3.0 Hz, CH_{arom}), 127.4 (CH_{arom}); 128.9 (2 x CH_{arom}); 129.3 (q, *J* = 4.4 Hz, CH_{arom}); 129.4 ($C_{arom,quat}$); 129.7 (2 x CH_{arom}); 130.2 (CH_{arom}); 132.7 (q, *J* = 33.2 Hz); 132.9, 134.0, 144.5, 146.0, 149.9 (5 x $C_{arom,quat}$); 168.0 (C=O). **IR** (ATR, cm^{-1}): $\nu_{C=O}$ = 1771; ν_{max} =

1335, 1317, 1296, 1125, 1107, 1065, 903, 700, 681. **MS** (ESI): *m/z* (%) 330 ([M + 1]$^+$, 100). **HRMS** (ESI): calcd. for $C_{18}H_{11}F_3NO_2^+$: 330.0736 [M + H]$^+$, found: 330,0732. White solid, 34%.
*Rest of CF_3 quartet not visible

7-Iodo-9-phenylfuro[3,4-*b*]quinolin-3(1*H*)-one 4f

^{1}H-NMR (400 MHz, $CDCl_3$): δ 5.39 (2H, s, CH_2O); 7.42-7.44 (2H, m, 2 x CH_{arom}); 7.60-7.64 (3H, m, 3 x CH_{arom}); 8.07 (1H, d_{AB}, *J* = 9.0 x 1.6 Hz, CH_{arom}); 8.12 (1H, d_{AB}, *J* = 9.0 Hz, CH_{arom}); 8.26 (1H, *J* = 1.6 Hz, CH_{arom}). **^{13}C-NMR** (100 MHz, $CDCl_3$): δ 67.9 (CH_2); 96.6 ($C_{arom,quat}$); 128.9 (2 x CH_{arom}); 129.3 ($C_{arom,quat}$); 129.7 (2 x CH_{arom}); 130.0 (CH_{arom}); 132.8 (CH_{arom}); 133.0 ($C_{arom,quat}$); 133.1 ($C_{arom,quat}$); 134.7 (CH_{arom}); 139.8 (CH_{arom}); 142.9, 144.8 and 149.6 (3 x $C_{arom,quat}$); 168.4 (C=O). **IR** (ATR, cm^{-1}): $\nu_{C=O}$ = 1773; ν_{max} = 2930, 1574, 1485, 1369, 1132, 1007, 831, 708, 534. **MS** (ESI): *m/z* (%) 388 ([M + 1]$^+$, 100). **HRMS** (ESI): calcd. for $C_{17}H_{11}INO_2^+$: 387.9829 [M + H]$^+$, found: 387.9817. White solid, 48%.

5-Bromo-9-phenylfuro[3,4-*b*]quinolin-3(1*H*)-one 4g

^{1}H-NMR (400 MHz, $CDCl_3$): δ 5.39 (2H, s, CH_2); 7.42-7.45 (2H, m, 2 x CH_{arom}); 7.49 (1H, d x d, *J* = 8.5 x 7.4, 1H); 7.59-7.62 (3H, m, 3 x CH_{arom}); 7.87 (1H, d x d, *J* = 8.5 x 1.2 Hz, CH_{arom}); 8.20 (1H, d x d, *J* = 7.4 x 1.2 Hz, CH_{arom}). **^{13}C-NMR** (100 MHz, $CDCl_3$): δ 67.7 (CH_2); 125.8 (CH_{arom}); 127.2 ($C_{arom,quat}$); 129.0 (2 x CH_{arom}); 129.47 ($C_{arom,quat}$); 129.54 (2 x CH_{arom}); 129.6 (CH_{arom}); 129.9 (CH_{arom}); 133.3 ($C_{arom,quat}$); 133.4 ($C_{arom,quat}$); 134.7 (CH_{arom}); 144.9, 145.1 and 148.0 (3 x $C_{arom,quat}$); 168.1 (C=O). **IR** (ATR, cm^{-1}): $\nu_{C=O}$ = 1782; ν_{max} = 1485, 1454, 1121, 1047, 1007, 768, 760, 712, 700, 629. **MS** (ESI): *m/z* (%) 343 ([M + 1]$^+$, 20); 342 ([M + 1]$^+$, 98); 341 ([M + 1]$^+$, 20); 340 ([M + 1]$^+$, 100). **HRMS** (ESI): calcd. for $C_{17}H_{11}BrNO_2^+$: 339.9968 [M + H]$^+$, found: 339.9955. White solid, 41%.

8- and 6-Methyl-9-phenylfuro[3,4-*b*]quinolin-3(1*H*)-one 4h

Spectral data derived from the mixture of the two regio-isomers (6/8-Me: 64/36).

^{1}H-NMR (400 MHz, $CDCl_3$): δ 2.10 (3H, s, CH_3); 2.62 (3H, s, CH_3); 5.16 (2H, s, OCH_2); 5.38 (2H, s, OCH_2); 7.31-7.34 (2H, m, 2 x 1 x CH_{arom}); 7.43-7.62 (5H, m, 2 x 5 x CH_{arom}); 7.73 (1H, d x d, *J* = 8.3 x 7.2 Hz, CH_{arom}); 7.80 (1H, d, *J* = 8.7 Hz, CH_{arom}); 8.22 (1H, s, CH_{arom}); 8.34 (1H, d, *J* = 8.3 Hz, CH_{arom}). **^{13}C-NMR** (100 MHz, $CDCl_3$): 21.9 (CH_3); 24.6 (CH_3); 67.9 (CH_2); 68.1 (CH_2); 125.5 (CH_{arom}); 126.2 ($C_{arom,quat}$); 127.2 ($C_{arom,quat}$); 128.0 (CH_{arom}); 129.0 (2 x CH_{arom}); 129.07 (2 x CH_{arom}); 129.12 (CH_{arom}); 129.4 (2 x CH_{arom}); 129.6 (2 x CH_{arom}); 130.3 (CH_{arom}); 130.4 (CH_{arom}); 130.7 (CH_{arom}); 131.9 ($C_{arom,quat}$); 132.0 (CH_{arom}); 132.7 (CH_{arom}); 133.9 ($C_{arom,quat}$); 134.4 ($C_{arom,quat}$); 136.1 ($C_{arom,quat}$); 137.8 ($C_{arom,quat}$); 141.5 ($C_{arom,quat}$); 143.4 ($C_{arom,quat}$); 144.35 ($C_{arom,quat}$); 144.44 ($C_{arom,quat}$); 151.2 ($C_{arom,quat}$); 152.2 ($C_{arom,quat}$); 168.9 (C=O); 169.0 (C=O). **IR** (ATR, cm^{-1}): $\nu_{C=O}$ = 1777; ν_{max} = 2926, 1585, 1445, 1371, 1236, 1173, 1125, 1007, 704. **MS** (ESI): *m/z* (%) 276 ([M + 1]$^+$, 100). **HRMS** (ESI): calcd. for $C_{18}H_{14}NO_2^+$: 276.1019 [M + H]$^+$, found: 276.1011. Colorless oil, 27%.

5-Methyl-9-phenylfuro[3,4-*b*]quinolin-3(1*H*)-one 4i

^{1}H-NMR (400 MHz, $CDCl_3$): δ 2.97 (3H, s, CH_3); 5.37 (2H, s, OCH_2); 7.41-7.44 (2H, m, 2 x CH_{arom}); 7.52-7.60 (4H, m, 4 x CH_{arom}); 7.69-7.74 (2H, m, 2 x CH_{arom}). **^{13}C-NMR** (100 MHz, $CDCl_3$): δ 18.8 (CH_3); 67.8 (CH_2); 123.8 (CH_{arom}); 128.1 ($C_{arom,quat}$); 129.0 (2 x CH_{arom}); 129.3 (CH_{arom}); 129.4 (2 x CH_{arom}); 129.5 (CH_{arom}); 130.8 (CH_{arom}); 132.3, 134.2, 139.9, 143.2, 144.0 and 150.1 (6 x $C_{arom,quat}$); 169.2 (C=O). **IR** (ATR, cm^{-1}): $\nu_{C=O}$ = 1767; ν_{max} = 1393, 1273, 1236, 1207, 1194, 1136, 1003, 841, 770. **MS** (ESI): *m/z* (%) 276 ([M + 1]$^+$, 100). White solid, 33%. Spectral data matched literature.[62]

7-Methyl-9-(naphthalen-2-yl)furo[3,4-*b*]quinolin-3(1*H*)-one 4j

^{1}H-NMR (400 MHz, $CDCl_3$): δ 2.48 (3H, s, CH_3); 5.33-5.44 (2H, m, OCH_2); 7.53 (1H, d x d, *J* = 8.4 x 1.5 Hz, CH_{arom}); 7.62-7.70 (4H, m, 4 x CH_{arom}); 7.93-8.01 (2H, m, CH_{arom}); 8.09 (1H, d, *J* = 8.4 Hz, CH_{arom}); 8.34 (1H, d, *J* = 8.6 Hz, CH_{arom}). **^{13}C-NMR** (100 MHz, $CDCl_3$): δ 22.2 (CH_3); 68.0 (OCH_2); 124.5, 126.2, 127.3, 127.5 and 128.1 (5 x CH_{arom}); 128.2 ($C_{arom,quat}$); 128.4, 128.5, 129.3 and 131.2 (4 x CH_{arom}); 131.3 ($C_{arom,quat}$); 132.9 ($C_{arom,quat}$); 133.3 (CH_{arom}); 133.4, 133.5, 140.2, 143.0, 143.5 and 149.5 (6 x $C_{arom,quat}$); 169.0 (C=O). **IR** (ATR, cm^{-1}): $\nu_{C=O}$ = 1771; ν_{max} = 2930, 1574, 1449, 1371, 1132, 1057, 1049, 1001, 827. **MS** (ESI): *m/z* (%) 326 ([M + 1]$^+$, 100). **HRMS** (ESI): calcd. for $C_{22}H_{16}NO_2^+$: 326.1176 [M + H]$^+$, found: 326.1169. Light yellow solid, 39%.

(*E*)-7-Methyl-9-(prop-1-en-1-yl)furo[3,4-*b*]quinolin-3(1*H*)-one 4k

^{1}H-NMR (400 MHz, $CDCl_3$): δ 2.14 (3H, d x d, *J* = 6.6 x 1.7 Hz, $C\underline{H}_3CH{=}CH$); 2.62 (3H, s, $CH_3C_{arom,quat}$); 5.55 (2H, s, CH_2); 6.28 (1H, d x q, *J* = 16.1 x 6.6 Hz, $CH_3C\underline{H}{=}CH$); 7.06 (1H, d x q, *J* = 16.1 x 1.7 Hz, $CH_3CH{=}C\underline{H}$); 7.66 (1H, d x d, *J* = 8.7 x 1.8 Hz, CH_{arom}); 7.96 (1H, s, CH_{arom}); 8.25 (1H, d, *J* = 8.7 Hz, CH_{arom}). **^{13}C-NMR** (100 MHz, $CDCl_3$): δ 19.9 (CH_3); 22.4 (CH_3); 68.6 (OCH_2); 122.9 (CH_{arom}); 124.1 ($\underline{C}H{=}CHCH_3$); 127.2 ($C_{arom,quat}$); 130.9 ($C_{arom,quat}$); 131.4 (CH_{arom}); 133.0 (CH_{arom}); 137.1 ($CH{=}CHCH_3$); 138.3, 139.7, 143.5 and 149.2 (4 x $C_{arom,quat}$); 169.1 (C=O). **IR** (ATR, cm^{-1}): $\nu_{C=O}$ = 1778; ν_{max} = 3056, 2914, 1574, 1503, 1443, 1140, 1080, 959, 843. **MS** (ESI): *m/z* (%) 240 ([M + 1]$^+$, 100). White solid, 35%. Spectral data matched literature.[61]

7-Methyl-2,9-diphenyl-1,2-dihydro-3*H*-pyrrolo[3,4-*b*]quinolin-3-one 4l

^{1}H-NMR (400 MHz, $CDCl_3$): δ 2.48 (3H, s, CH_3); 4.80 (2H, s, CH_2); 7.19 (1H, t x t, *J* = 7.5 x 1.1 Hz, CH_{arom}); 7.39-7.43 (2H, m, CH_{arom}); 7.46-7.50 (2H, m, 2 x CH_{arom}); 7.55 (1H, s, CH_{arom}); 7.59-7.66 (4H, m, 4 x CH_{arom}); 7.87-7.79 (2H, m, 2 x CH_{arom}); 8.34 (1H, d, *J* = 8.7 Hz, CH_{arom}). **^{13}C-NMR** (100 MHz, $CDCl_3$): δ 22.2 (CH_3); 48.3 (CH_2); 119.8 (2 x CH_{arom}); 124.5 (CH_{arom}); 125.3 (CH_{arom}); 127.7 ($C_{arom,quat}$); 128.0 ($C_{arom,quat}$); 129.16 (2 x CH_{arom}); 129.20 (CH_{arom}); 129.32 (2 x CH_{arom}); 129.34 (2 x CH_{arom}); 131.0 (CH_{arom}); 132.5 (CH_{arom}); 134.7, 138.8, 139.4, 142.8, 148.7 and 150.0 (6 x $C_{arom,quat}$); 165.6 (C=O). **IR** (ATR, cm^{-1}): $\nu_{C=O}$ = 1709; ν_{max} = 1597, 1493, 1385, 1300, 1267, 1173, 824, 754, 704. **MS** (ESI): *m/z* (%) 351 ([M + 1]$^+$, 100). Off white solid, 47%. Spectral data matched literature.[60]

2-(4-Methoxybenzyl)-7-methyl-9-phenyl-1,2-dihydro-3*H*-pyrrolo[3,4-*b*]quinolin-3-one 4m

^{1}H-NMR (400 MHz, $CDCl_3$): δ 2.46 (3H, s, $CH_3C_{arom,quat}$); 3.77 (3H, s, CH_3O); 4.18 (2H, s, $NCH_2C_{quinoline}$); 4.82 (2H, s, NCH_2PMP); 6.82-6.84 (2H, m , 2 x CH_{arom}); 7.23-7.25 (2H, m, 2 x CH_{arom}); 7.35-7.37 (m, 2H, 2 x CH_{arom}); 7.49-7.57 (4H, m, 4 x CH_{arom}); 7.62 (1H, d x d, *J* = 8.7 x 1.9 Hz, CH_{arom}); 8.32 (1H, d, *J* = 8.7 Hz, CH_{arom}). **^{13}C-NMR** (100 MHz, $CDCl_3$): δ 22.1 ($\underline{C}H_3C_{arom,quat}$); 44.6 and 46.8 ($NCH_2$PMP and $NCH_2C_{quinoline}$); 55.4 (CH_3O); 114.3 (2 x CH_{arom}); 124.4 (CH_{arom}); 127.6 ($C_{arom,quat}$); 128.5 ($C_{arom,quat}$); 128.6 ($C_{arom,quat}$); 129.0 (CH_{arom}); 129.10 (2 x CH_{arom}); 129.11 (2 x CH_{arom}); 129.8 (2 x CH_{arom}); 130.8 (CH_{arom}); 132.3 (CH_{arom}); 134.7 ($C_{arom,quat}$); 138.4 ($C_{arom,quat}$); 142.7 ($C_{arom,quat}$); 148.3 ($C_{arom,quat}$); 150.1 ($C_{arom,quat}$); 159.4 ($C_{arom,quat}$); 166.5 (C=O). **IR** (ATR, cm^{-1}): $\nu_{C=O}$ = 1692; ν_{max} = 1512, 1242, 1175, 1032, 908, 827, 729, 702, 546. **MS** (ESI): *m/z* (%) 395 ([M + 1]$^+$, 100); 789 ([2M + 1]$^+$, 45); 811 ([2M + 23]$^+$, 10). **HRMS** (ESI): calcd. for $C_{26}H_{23}N_2O_2^+$: 395.1754 [M + H]$^+$, found: 395.1735. Light pink solid, 31%.

S5.5 α-Oxidation of *N*-aryl glycine derivatives.

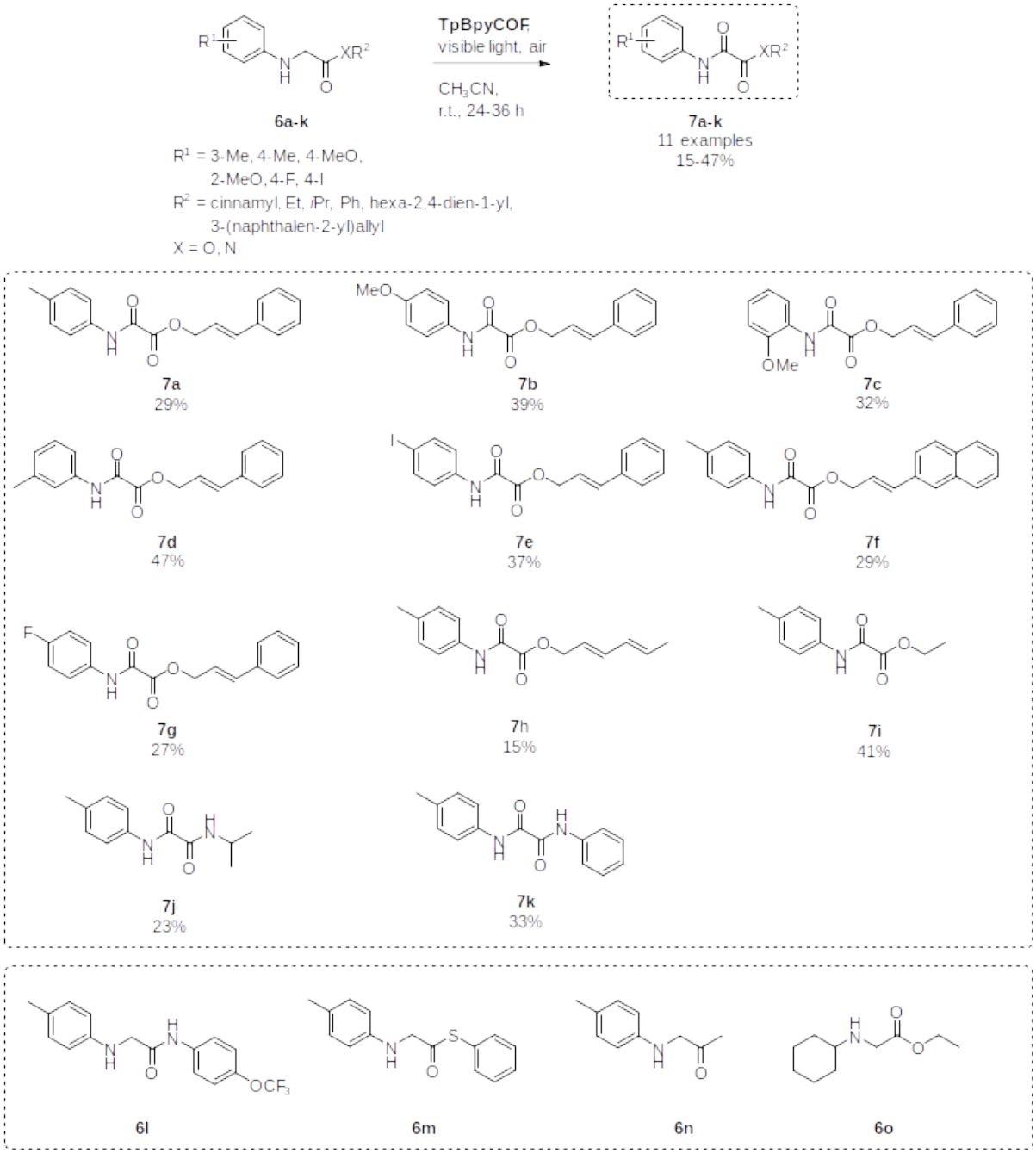

Scheme S12: Oxidation of substrates **6** catalyzed by **TpBpyCOF**.

Cinnamyl 2-oxo-2-(*p*-tolylamino)acetate 7a

^{1}H-NMR (400 MHz, $CDCl_3$): δ 2.34 (3H, s, CH_3); 4.99 (2H, d x d, *J* = 6.7 x 1.1 Hz, CH_2); 6.36 (1H, d x t, *J* = 15.9 x 6.7 Hz, $CH_2C\underline{H}$=CH); 6.77 (1H, br d, *J* = 15.9 Hz, CH_2CH=C$\underline{H}$); 7.18 (2H, d, *J* = 8.4 Hz, 2 x CH_{arom}); 7.28-7.36 (3H, m, 3 x CH_{arom}); 7.40-7.42 (2H, m, 2 x CH_{arom}); 7.52 (2H, d, *J* = 8.4 Hz, 2 x CH_{arom}); 8.81 (1H, br s, NH). **^{13}C-NMR** (100 MHz, $CDCl_3$): δ 21.1 (CH_3); 68.1 (CH_2); 120.0 (2 x CH_{arom}); 121.4 ($CH_2\underline{C}$H=CH); 126.9, 128.6, 128.8 and 129.9 (7 x CH_{arom}); 133.9, 135.5 and 135.9 (3 x $C_{arom,quat}$); 136.4 (CH_2CH=$\underline{C}$H); 153.7 (NC=O); 161.0 (OC=O). **IR** (ATR, cm^{-1}): ν_{NH} = 3300; $\nu_{C=O}$ = 1732 and 1695; ν_{max} = 1595, 1526, 1513, 1271, 1161, 964, 941. **MS** (ESI): *m/z* (%) 117 ($[C_9H_9]^+$, 100); 613 ($[2M + 23]^+$, 10). Red oil, 29%.

Cinnamyl 2-((4-methoxyphenyl)amino)-2-oxoacetate 7b

^{1}H-NMR (400 MHz, $CDCl_3$): δ 3.81 (3H, s, CH_3); 5.00 (2H, d x d, *J* = 6.7 x 1.0 Hz, CH_2); 6.36 (1H, d x t, *J* = 15.9 x 6.7 Hz, $CH_2C\underline{H}$=CH); 6.77 (1H, br d, *J* = 15.9 Hz, CH_2CH=C$\underline{H}$); 6.89-6.92 (2H, m, 2 x CH_{arom}); 7.28-7.35 (3H, m, 3 x CH_{arom}); 7.55-7.57 (2H, m, 2 x CH_{arom}); 8.78 (1H, br s, NH). **^{13}C-NMR** (100 MHz, $CDCl_3$): δ 55.6 (CH_3); 68.1 (CH_2); 114.5 (2 x CH_{arom}); 121.4 ($CH_2\underline{C}$H=CH); 121.6 (2 x CH_{arom}); 126.8 (2 x CH_{arom}); 126.9 (CH_{arom}); 128.6 (2 x CH_{arom}); 128.8 ($C_{arom,quat}$); 129.6 ($C_{arom,quat}$); 135.9 ($C_{arom,quat}$); 136.4 (CH_2CH=C$\underline{H}$); 153.6 (NC=O); 157.4 ($C_{arom,quat}$); 161.2 (OC=O). **IR** (ATR, cm^{-1}): ν_{NH} = 3345; $\nu_{C=O}$ = 1722 and 1695; ν_{max} = 1541, 1508, 1279, 1171, 941, 692, 515. **MS** (ESI): *m/z* (%) 117 ($[C_9H_9]^+$, 100); 334 ($[M + 23]^+$, 5); 645 ($[2M + 23]^+$, 15). Yellow solid, 39%.

Cinnamyl 2-((2-methoxyphenyl)amino)-2-oxoacetate 7c

^{1}H-NMR (400 MHz, $CDCl_3$): δ 3.92 (3H, s, CH_3); 5.00 (2H, d x d, *J* = 6.7 x 1.1 Hz, CH_2); 6.37 (1H, d x t, *J* = 15.9 x 6.7 Hz, $CH_2C\underline{H}$=CH); 6.78 (1H, br d, *J* = 15.9 Hz, CH_2CH=C$\underline{H}$); 6.91 (1H, d x d, *J* = 8.0 x 1.0 Hz, CH_{arom}); 7.00 (1H, d x d x d, *J* = 7.9 x 7.8 x 1.0 Hz, CH_{arom}); 7.13 (1H, d x d x d, *J* = 8.0 x 7.8 x 1.5 Hz); 7.28-7.35 (3H, m, 3 x CH_{arom}); 7.40-7.42 (2H, m, 2 x CH_{arom}); 8.41 (1H, d x d, *J* = 7.9 x 1.5 Hz, CH_{arom}); 9.51 (1H, br s, NH). **^{13}C-NMR** (100 MHz, $CDCl_3$): δ 55.9 (CH_3); 68.0 (CH_2); 110.3 (CH_{arom}); 120.1 (CH_{arom}); 121.2 (CH_{arom}); 121.5 ($CH_2C\underline{H}$=CH); 125.4 (CH_{arom}); 126.2 ($C_{arom,quat}$); 126.9 (2 x CH_{arom}); 128.5 (CH_{arom}); 128.8 (2 x CH_{arom}); 135.9 ($C_{arom,quat}$); 136.3 (CH_2CH=C$\underline{H}$); 148.6 ($C_{arom,quat}$); 153.7 (NC=O); 160.8 (OC=O). **IR** (ATR, cm^{-1}): ν_{NH} = 3383; $\nu_{C=O}$ = 1705; ν_{max} = 1601, 1528, 1279, 1250, 1159, 1113, 745, 691. **MS** (ESI): *m/z* (%) 117 ($[C_9H_9]^+$, 100); 645 ($[2M + 23]^+$, 10). Brown oil, 32%.

Cinnamyl 2-oxo-2-(*m*-tolylamino)acetate 7d

^{1}H-NMR (400 MHz, $CDCl_3$): δ 2.37 (3H, s, CH_3); 5.00 (2H, d x d, *J* = 6.7 x 1.0 Hz, CH_2); 6.36 (1H, d x t, *J* = 15.8 x 6.7 Hz, $CH_2C\underline{H}$=CH); 6.77 (1H, br d, *J* = 15.8 Hz, CH_2CH=C$\underline{H}$); 7.01 (2H, d, J = 7.6 Hz, 2 x CH_{arom}); 7.24-7.36 (4H, m, 4 x CH_{arom}); 7.40-7.46 (4H, m, 4 x CH_{arom}); 8.81 (1H, br s, NH). **^{13}C-NMR** (100 MHz, $CDCl_3$): δ 21.6 (CH_3); 68.2 (CH_2); 117.1 (CH_{arom}); 120.6 (CH_{arom}); 121.3 ($CH_2\underline{C}$H=CH); 126.5 (CH_{arom}); 126.9 (2 x CH_{arom}); 128.6 (CH_{arom}); 128.8 (2 x CH_{arom}); 129.2 (CH_{arom}); 135.9 ($C_{arom,quat}$); 136.3 ($C_{arom,quat}$); 136.4 (CH_2CH=$\underline{C}$H); 139.4 ($C_{arom,quat}$); 153.8 (NC=O); 161.0 (OC=O). **IR** (ATR, cm^{-1}): ν_{NH} = 3329; $\nu_{C=O}$ = 1726 and 1697; ν_{max} = 1551, 1491, 1275, 1190, 1158, 789, 689. **MS** (ESI): *m/z* (%) 117 ($[C_9H_9]^+$, 100); 613 ($[2M + 23]^+$, 10). Brown oil, 47%.

Cinnamyl 2-((4-iodophenyl)amino)-2-oxoacetate 7e

^{1}H-NMR (400 MHz, $CDCl_3$): δ 4.99 (2H, d x d, *J* = 6.8 x 0.9 Hz, CH_2); 6.35 (1H, d x t, *J* = 15.8 x 6.8 Hz, $CH_2C\underline{H}$=CH); 6.77 (1H, br d, *J* = 15.8 Hz, CH_2CH=C$\underline{H}$); 7.27-7.44 (7H, m, 7 x CH_{arom}); 7.66-7.70 (2H, m, 2 x CH_{arom}); 8.56 (1H, br s, NH). **^{13}C-NMR** (100 MHz, $CDCl_3$): δ 68.3 (CH_2); 89.3 ($C_{arom,quat}$); 121.1 ($CH_2\underline{C}$H=CH); 121.7 (2 x CH_{arom}); 126.9 (2 x CH_{arom}); 128.7 (CH_{arom}); 128.8 (2 x CH_{arom}); 135.8 ($C_{arom,quat}$); 136.2 ($C_{arom,quat}$); 136.7 (CH_2CH=$\underline{C}$H); 138.4 (2 x CH_{arom}); 153.9 (NC=O); 160.7 (OC=O). **IR** (ATR, cm^{-1}): ν_{NH} = 3398; $\nu_{C=O}$ = 1738 and 1688; ν_{max} = 1565, 1483, 1271, 1173, 945, 818, 683. **MS** (ESI): *m/z* (%) 117 ($[C_9H_9]^+$, 100); 430 ($[M + 23]^+$, 10); 837 ($[2M + 23]^+$, 15). Brown oil, 37%.

(*E*)-3-(Naphthalen-2-yl)allyl 2-oxo-2-(*p*-tolylamino)acetate 7f

^{1}H-NMR (400 MHz, $CDCl_3$): δ 2.34 (3H, s, CH_3); 5.05 (2H, d, *J* = 6.7, CH_2); 6.49 (1H, d x t, 15.8 x 6.7 Hz, $CH_2C\underline{H}$=CH); 6.93 (1H, br d, *J* = 15.8 Hz, CH_2CH=C$\underline{H}$); 7.18 (2H, d, *J* = 8.4 Hz, 2 x CH_{arom}); 7.46-7.48 (2H, m, 2 x CH_{arom}); 7.53 (2H, d, *J* = 8.4 Hz, 2 x CH_{arom}); 7.61 (1H, d x d, *J* = 8.6 x 1.5 Hz, CH_{arom}); 7.78-7.83 (4H, m, 4 x CH_{arom}); 8.81 (1H, br s, NH). **^{13}C-NMR** (100 MHz, $CDCl_3$): δ 21.1 (CH_3); 68.2 (CH_2O); 120.0 (2 x CH_{arom}); 121.7 ($CH_2\underline{C}$H=CH); 123.6, 126.5, 126.6, 127.5, 127.9, 128.3, and 128.6 (7 x CH_{arom}); 129.9 (2 x CH_{arom}); 133.4, 133.5, 133.6, 133.9 and 135.5 (5 x $C_{arom,quat}$); 136.5 (CH_2CH=$\underline{C}$H); 153.7 (NC=O); 161.1 (C=O). **IR** (ATR, cm^{-1}): ν_{NH} = 3273; $\nu_{C=O}$ = 1730 and 1690; ν_{max} = 2982, 1597, 1531, 1514, 1275, 1165, 816. **MS** (ESI): *m/z* (%) 167 ($[C_{13}H_{11}]^+$, 100); 713 ($[2M + 23]^+$, 20). Off white solid, 29%

Cinnamyl 2-((4-fluorophenyl)amino)-2-oxoacetate 7g

^{1}H-NMR (400 MHz, $CDCl_3$): δ 5.00 (2H, d x d, *J* = 6.7 x 0.9 Hz, CH_2); 6.36 (1H, d x t, *J* = 15.8 x 6.7 Hz, $CH_2C\underline{H}$=CH); 6.77 (1H, br d, *J* = 15.8 Hz, CH_2CH=C$\underline{H}$); 7.04-7.10 (2H, m, 2 x CH_{arom}); 7.27-7.42 (5H, m, 5 x CH_{arom}); 7.60-7.64 (2H, m, 2 x CH_{arom}); 8.86 (1H, br s, NH). **^{19}F-NMR** (376 MHz, $CDCl_3$): -115.88 (1F, m). **^{13}C-NMR** (100 MHz, $CDCl_3$): δ 68.3 (CH_2); 116.2 (d, *J* = 22.7 Hz, 2 x CH_{arom}); 121.2 ($CH_2\underline{C}$H=CH); 121.8 (d, *J* = 8.1 Hz, 2 x CH_{arom}); 126.9 (2 x CH_{arom}); 128.7 (CH_{arom}); 128.8 (2 x CH_{arom}); 132.5 (d, *J* = 2.7 Hz, $C_{arom,quat}$); 135.8 (CH_2CH=$\underline{C}$H); 136.6 ($C_{arom,quat}$); 153.8 (NC=O); 160.2 (d, *J* = 245.4 Hz, $C_{arom,quat}$); 160.9 (OC=O). **IR** (ATR, cm^{-1}): ν_{NH} = 3362; $\nu_{C=O}$ = 1705 and 1694; ν_{max} = 1551, 1508, 1279, 1171, 837, 692, 503. **MS** (ESI): *m/z* (%) 117 ($[C_9H_9]^+$, 100); 322 ($[M + 23]^+$, 15); 621 ($[2M + 23]^+$, 15). Brown solid, 27%.

(2*E*,4*E*)-Hexa-2,4-dien-1-yl 2-oxo-2-(*p*-tolylamino)acetate 7h

^{1}H-NMR (400 MHz, $CDCl_3$): δ 1.78 (2H, d, *J* = 6.5 Hz, $C\underline{H}_3CH$=CH); 2.33 (3H, s, $CH_3C_{arom,quat}$); 4.83 (2H, d, *J* = 7.1 Hz, CH_2); 5.70 (1H, d x t, J = 14.5 x 7.2 Hz, C$\underline{H}$=CH-CH=CHCH$_3$); 5.77-5.85 (1H, m, CH=CH-CH=C$\underline{H}$CH$_3$); 6.03-6.10 (1H, m, CH=CH-C$\underline{H}$=CHCH$_3$); 6.32-6.39 (1H, m, CH=C$\underline{H}$-CH=CHCH$_3$); 7.17 (2H, d, *J* = 8.3 Hz, 2 x CH_{arom}); 7.51 (m, 2H, *J* = 8.3 Hz, 2 x CH_{arom}). **^{13}C-NMR** (100 MHz, $CDCl_3$): δ 18.3 ($\underline{C}H_3CH$=CH); 21.1 ($\underline{C}H_3C_{arom,quat}$); 68.2 ($CH_2O$); 119.9 (2 x CH_{arom}); 121.8 ($\underline{C}$H=CH-CH=CHCH$_3$); 129.9 (2 x CH_{arom}); 130.3 (CH=CH-$\underline{C}$H=CHCH$_3$); 132.7 (CH=CH-CH=$\underline{C}$HCH$_3$); 134.0 ($C_{arom,quat}$); 135.5 ($C_{arom,quat}$); 137.1 (CH=$\underline{C}$H-CH=CHCH$_3$); 153.8 (NC=O); 161.0 (OC=O). **IR** (ATR, cm^{-1}): ν_{NH} = 3362; $\nu_{C=O}$ = 1703 and 1690; ν_{max} = 1526, 1279, 1165, 989, 937, 820, 696. **MS** (ESI): *m/z* (%) 81 ($[C_6H_9]^+$, 100); 541 ($[2M + 23]^+$, 15). Brown to orange solid, 15%.

Ethyl 2-oxo-2-(*p*-tolylamino)acetate 7i

^{1}H-NMR (400 MHz, $CDCl_3$): δ 1.42 (3H, t, *J* = 7.1 Hz, $C\underline{H}_3CH_2$); 2.33 (3H, s, $CH_3C_{arom,quat}$); 4.41 (2H, q, *J* = 7.1 Hz, $CH_3C\underline{H}_2$); 7.17 (2H, d, *J* = 8.4 Hz, 2 x CH_{arom}); 7.52 (2H, d, *J* = 8.4 Hz, 2 x CH_{arom}); 8.83 (1H, br s, NH). **^{13}C-NMR** (100 MHz, $CDCl_3$): δ 14.1 ($\underline{C}H_3CH_2$); 21.1 ($\underline{C}H_3C_{arom,quat}$); 63.8 ($CH_3\underline{C}H_2$); 119.9 (2 x CH_{arom}); 129.8 (2 x CH_{arom}); 134.0 ($C_{arom,quat}$); 135.4 ($C_{arom,quat}$); 153.9 (NC=O); 161.2 (OC=O). **IR** (ATR, cm^{-1}): ν_{NH} = 3337; $\nu_{C=O}$ = 1703 and 1697; ν_{max} = 2980, 1551, 1491, 1275, 1190, 1157, 691, 496. **MS** (ESI): *m/z* (%) 208 ($[M + 1]^+$, 100). Yellow solid, 41%. Spectral data matched literature.[71]

N^1-Isopropyl-N^2-(*p*-tolyl)oxalamide 7j

^{1}H-NMR (400 MHz, $CDCl_3$): δ 1.25 (6H, d, *J* = 6.6 Hz, $(C\underline{H}_3)_2CH$); 2.34 (3H, s, $CH_3C_{arom,quat}$); 4.04-4.16 (1H, m, $C\underline{H}(CH_3)_2$); 7.17 (2H, d, *J* = 8.3 Hz, 2 x CH_{arom}); 7.41 (1H, br s, $NHC_{arom,quat}$); 7.51 (2H, d, *J* = 8.3 Hz, 2 x CH_{arom}); 9.23 (1H, br s, $N\underline{H}CH(CH_3)_2$). **^{13}C-NMR** (100 MHz, $CDCl_3$): δ 21.1 ($\underline{C}H_3C_{arom,quat}$); 22.5 ($(\underline{C}H_3)_2CH$); 42.5 ($(CH_3)_2\underline{C}H$); 119.9 (2 x CH_{arom}); 129.9 (2 x CH_{arom}); 134.1 ($C_{arom,quat}$); 135.2 ($C_{arom,quat}$); 157.6 (C=O); 159.2 (C=O). **IR** (ATR, cm^{-1}): ν_{NH} = 3339; $\nu_{C=O}$ = 1655; ν_{max} = 2974, 1518, 1504, 1406, 812, 747, 729, 511. **MS** (ESI): *m/z* (%) 221 ($[M + 1]^+$, 40). Off white solid, 41%. Spectral data matched literature.[72]

N^1-Phenyl-N^2-(*p*-tolyl)oxalamide 7k

^{1}H-NMR (400 MHz, $CDCl_3$): δ 2.36 (3H, s, CH_3); 7.19-7.23 (3H, m, 3 x CH_{arom}); 7.38-7.42 (2H, m, 2 x CH_{arom}); 7.56 (2H, d, *J* = 8.4 Hz, 2 x CH_{arom}); 7.66-7.69 (2H, m, 2 x CH_{arom}); 9.31 (1H, br s, NH); 9.37 (1H, br s, NH).**^{13}C-NMR** (100 MHz, $CDCl_3$): δ 21.1 (CH_3); 119.99 (2 x CH_{arom}); 120.00 (2 x CH_{arom}); 125.7 (CH_{arom}); 129.4 (2 x CH_{arom}); 129.9 (2 x CH_{arom}); 133.9 ($C_{arom,quat}$); 135.5 ($C_{arom,quat}$); 136.4 ($C_{arom,quat}$); 157.5 (C=O); 157.8 (C=O). **IR** (ATR, cm^{-1}): ν_{NH} = 3306; $\nu_{C=O}$ = 1665; ν_{max} = 2972, 2922, 1593, 1516, 1501, 1443, 727, 689. **MS** (ESI): *m/z* (%) 255 ($[M + 1]^+$, 35). Beige solid, 33%.

***S*-Phenyl 2-oxo-2-(*p*-tolylamino)ethanethioate 7m**

^{1}H-NMR (400 MHz, $CDCl_3$): δ 2.35 (3H, s, CH_3); 7.19 (2H, d, *J* = 8.3 Hz, 2 x CH_{arom}); 7.48 (5H, s, 5 x CH_{arom}); 7.53 (2H, d, *J* = 8.3 Hz, 2 x CH_{arom}); 8.48 (1H, br s, NH). **^{13}C-NMR** (100 MHz, $CDCl_3$): δ 21.1 (CH_3); 120.1 (2 x CH_{arom}); 126.7 ($C_{arom,quat}$); 129.2 ($C_{arom,quat}$); 129.7 (2 x CH_{arom}); 130.0 (2 x CH_{arom}); 130.1 (CH_{arom}); 134.5 (2 x CH_{arom}); 135.7 ($C_{arom,quat}$); 156.2 (NC=O); 190.9 (SC=O). **IR** (ATR, cm^{-1}): ν_{NH} = 3348; $\nu_{C=O}$ = 1688 and 1678; ν_{max} = 2920, 1526, 1225, 999, 806, 687, 453. **MS** (ESI): *m/z* (%) 272 ($[M + 1]^+$, 100). White solid, 22%, purity ~90%.

358N 2-Oxo-*N*-(p-tolyl)propenamide 7n

^{1}H-NMR (400 MHz, $CDCl_3$): δ 2.34 (3H, s, $CH_3C_{arom,quat}$); 2.56 (3H, s, CH_3CO); 7.17 (2H, d, *J* = 8.3 Hz, 2 x CH_{arom}); 7.52 (2H, d, *J* = 8.3 Hz, 2 x CH_{arom}); 8.66 (1H, br s, NH). **^{13}C-NMR** (100 MHz, $CDCl_3$): δ 21.1 ($\underline{C}H_3C_{arom,quat}$); 24.2 ($\underline{C}H_3CO$); 119.8 (2 x CH_{arom}); 129.9 (2 x CH_{arom}); 133.9 ($C_{arom,quat}$); 135.2 ($C_{arom,quat}$); 157.6 (NC=O); 197.6 (CH_3C=O). **IR** (ATR, cm^{-1}): ν_{NH} = 3333; $\nu_{C=O}$ = 1682; ν_{max} = 2922, 1533, 1508, 1256, 1136, 816, 691, 604. **MS** (ESI): *m/z* (%) 178 ($[M + 1]^+$, 70). Off white solid, 6%. Spectral data matched literature.[73]

S5.6 Recycling experiments

To a small glass test tube were added: 20 mg **TpBpyCOF**, $ScOTf_3$ (10 mg, 0.02 mmol, 0.1 eq.), 0.2 mmol of cinnamyl *p*-tolylglycinate **1a** and 2 mL CH_3CN. This was stirred under air and irradiation from a 26 W CFL (~10 cm distance) for 24 h. The reaction mixture was filtered over a membrane filter and washed with copious amounts of acetone. The filtrate was then evaporated and the internal standard, 1,3,5-trimethoxybenzene (33.6 mg, 0.2 mmol, 1 eq.) was added. The-NMR yield was determined by integration of the aromatic signals of the internal standard (3H) and the CH_2 of the lactone at δ = 5.36 ppm (^{1}H-NMR, $CDCl_3$). The filter cake was dried, scraped off, and used for the next cycle.

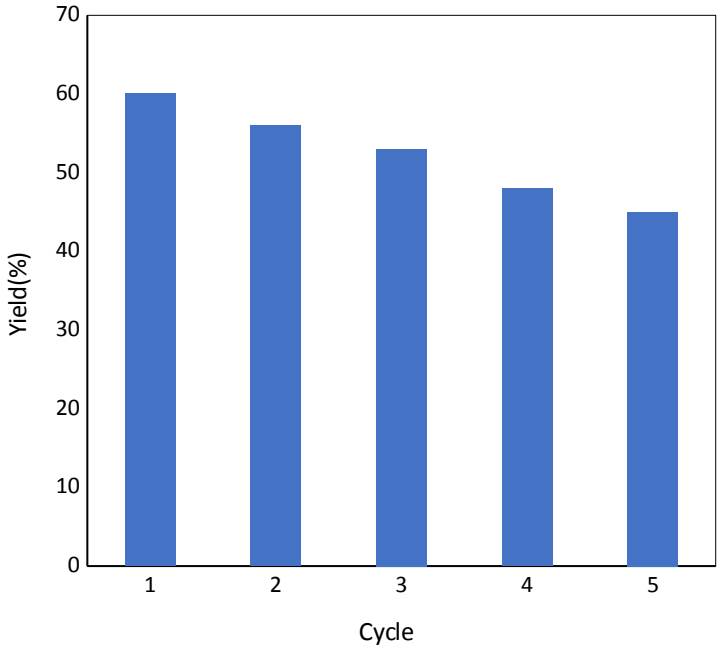

Figure S45: Yields of the recycling experiments.

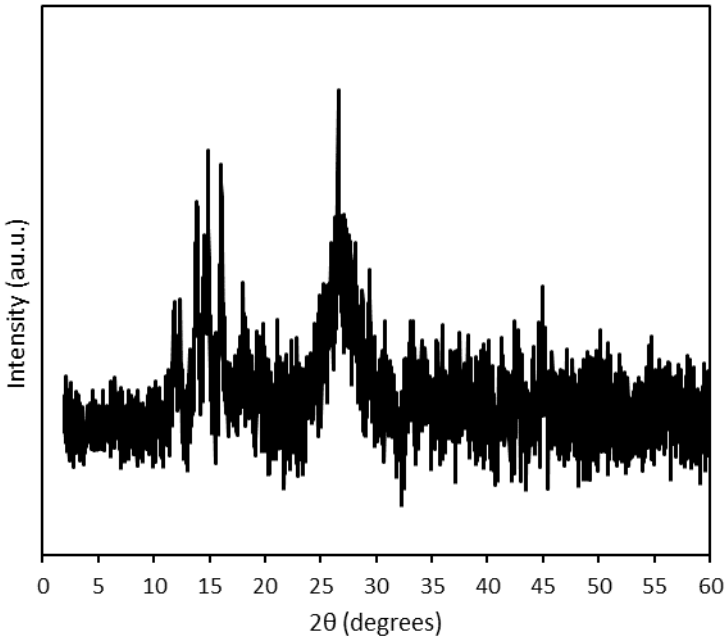

Figure S46: PXRD of **TpBpyCOF** after five runs.

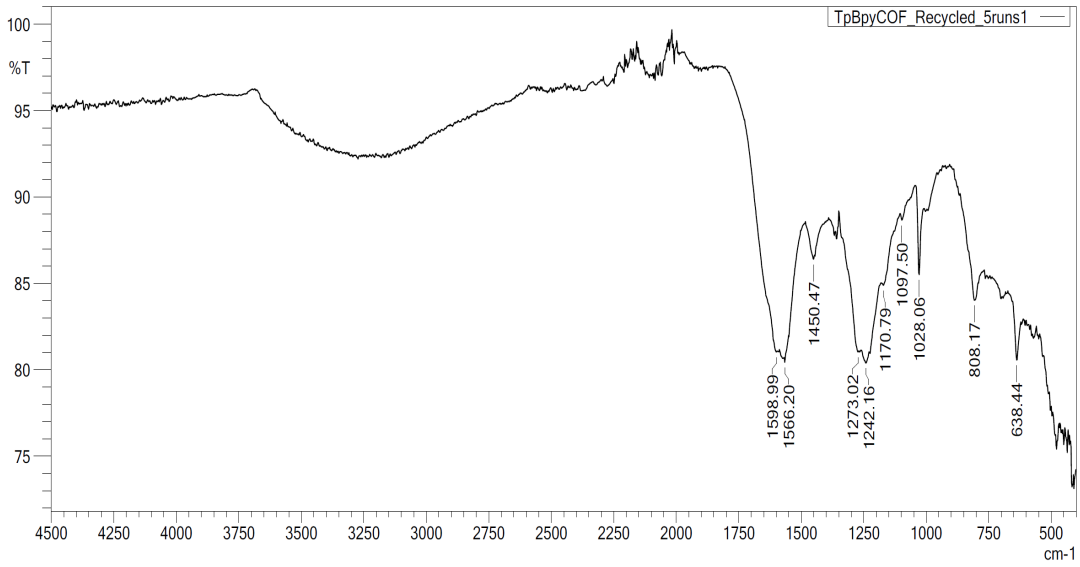

Figure S47: FTIR of **TpBpyCOF** after five runs.

S6 Spectra

S6.1 Building blocks

1,3,5-tris(bromomethyl)-2,4,6-trimethoxybenzene 11

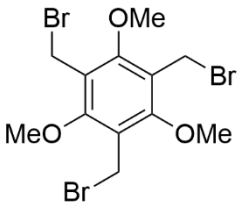

^{1}H NMR (400 MHz, $CDCl_3$)

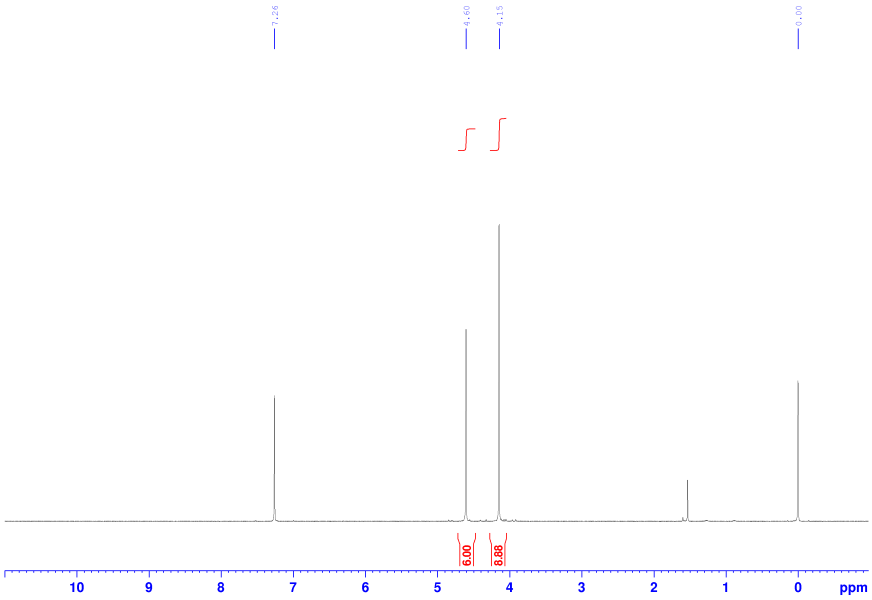

^{13}C NMR (100.6 MHz, $CDCl_3$)

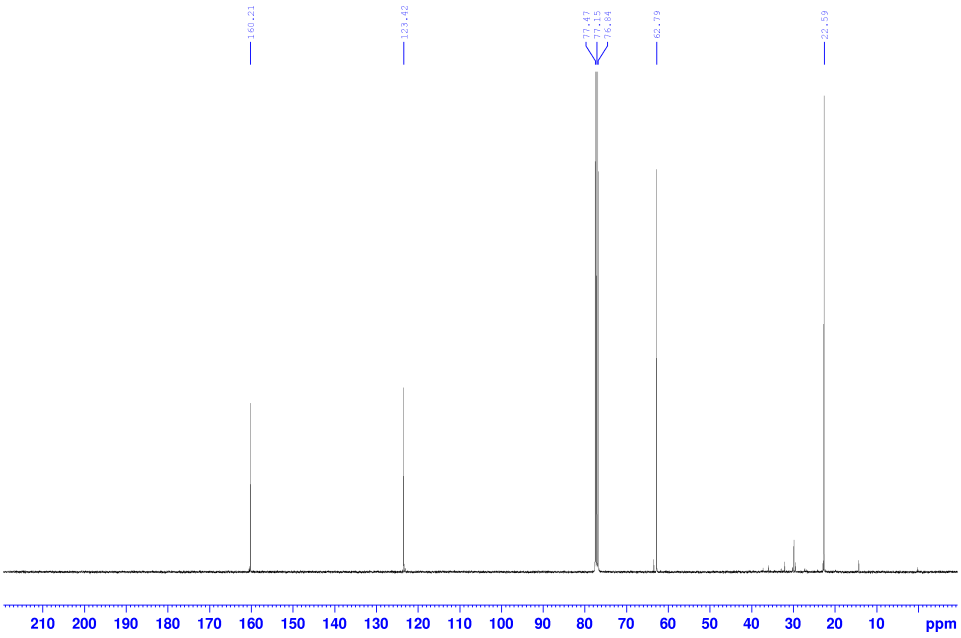

(2,4,6-trimethoxybenzene-1,3,5-triyl)tris(methylene) triacetate 12

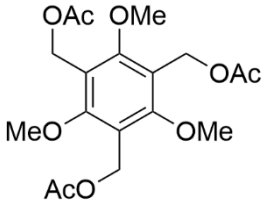

^{1}H NMR (400 MHz, $CDCl_3$)

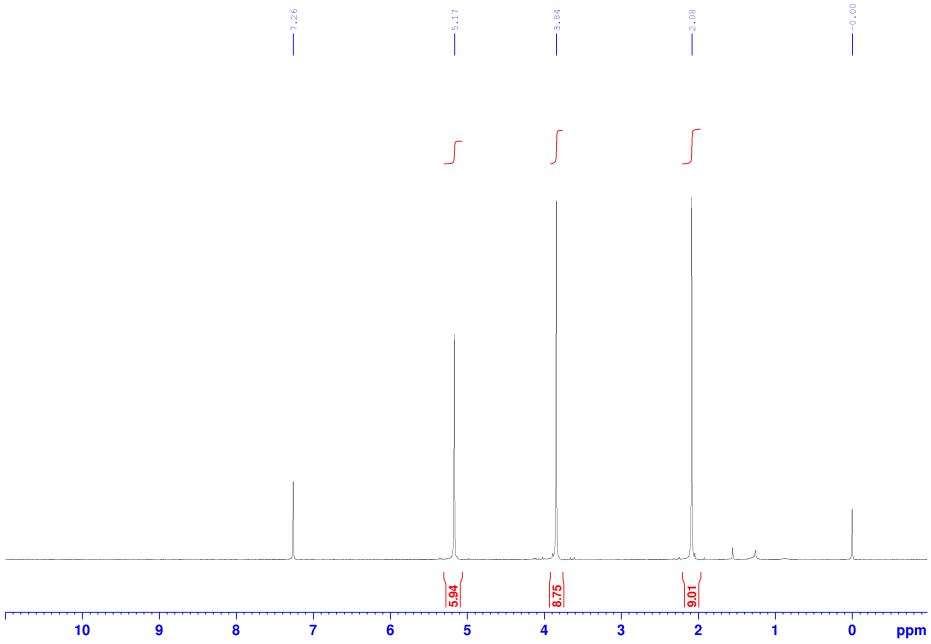

^{13}C NMR (100.6 MHz, $CDCl_3$)

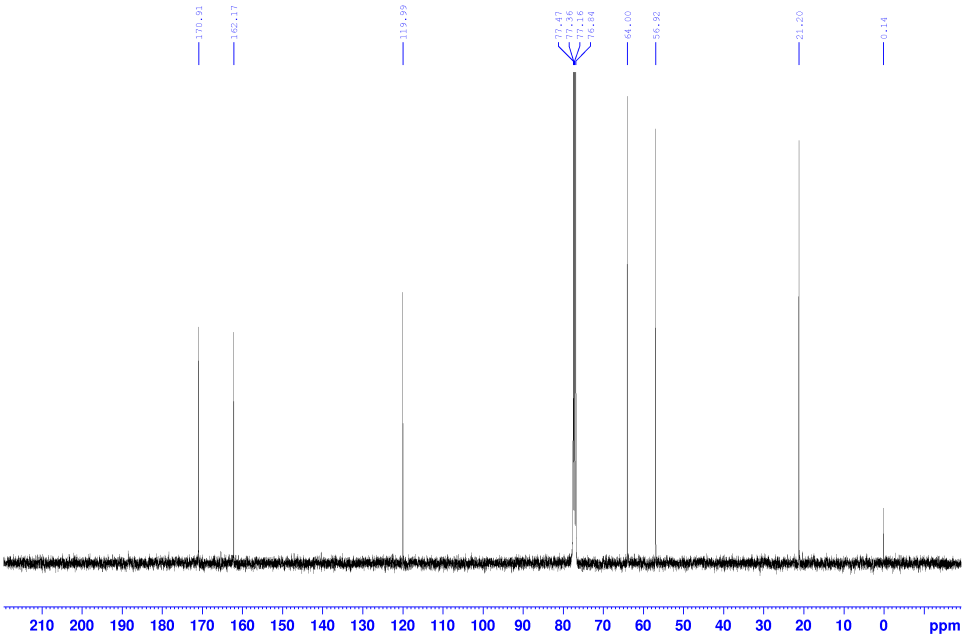

(2,4,6-trimethoxybenzene-1,3,5-triyl)trimethanol 13

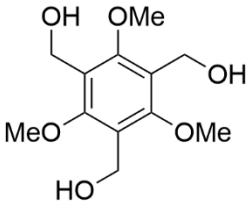

^{1}H NMR (400 MHz, DMSO-d_6)

^{13}C NMR (100.6 MHz, DMSO-d_6)

2,4,6-trimethoxybenzene-1,3,5-tricarbaldehyde TpOMe

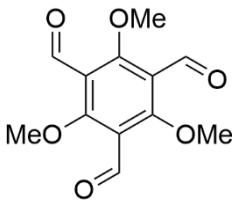

^{1}H NMR (400 MHz, $CDCl_3$)

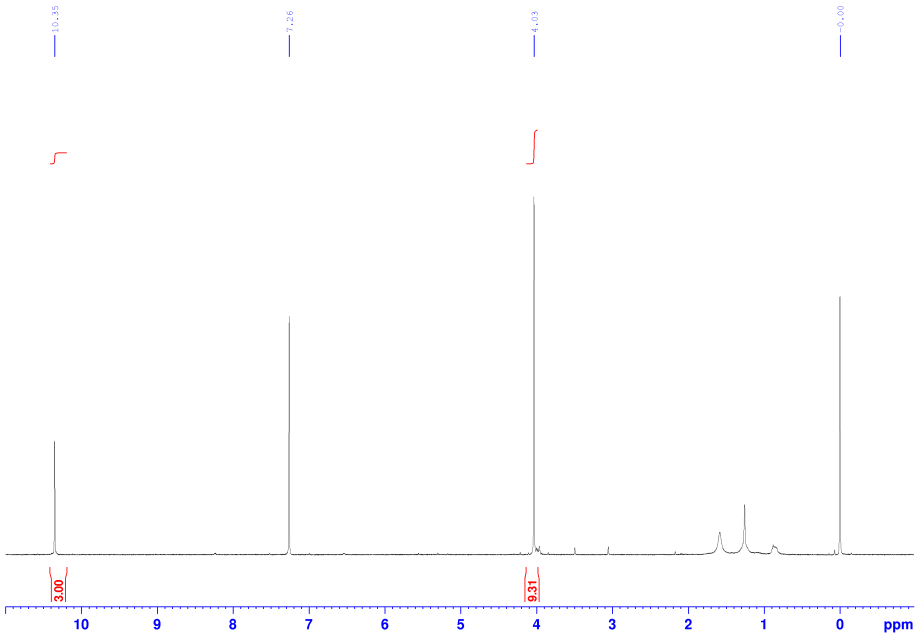

^{13}C NMR (100.6 MHz, $CDCl_3$)

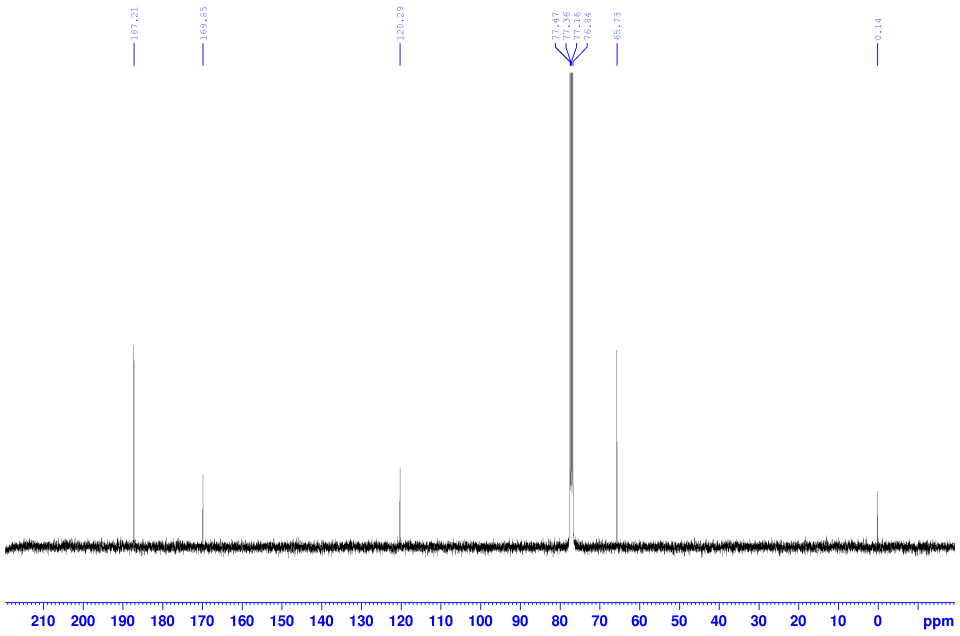

1,3,5-triformylphloroglucinol Tp

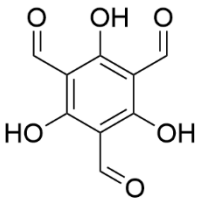

^{1}H NMR (400 MHz, $CDCl_3$)

^{13}C NMR (100.6 MHz, $CDCl_3$)

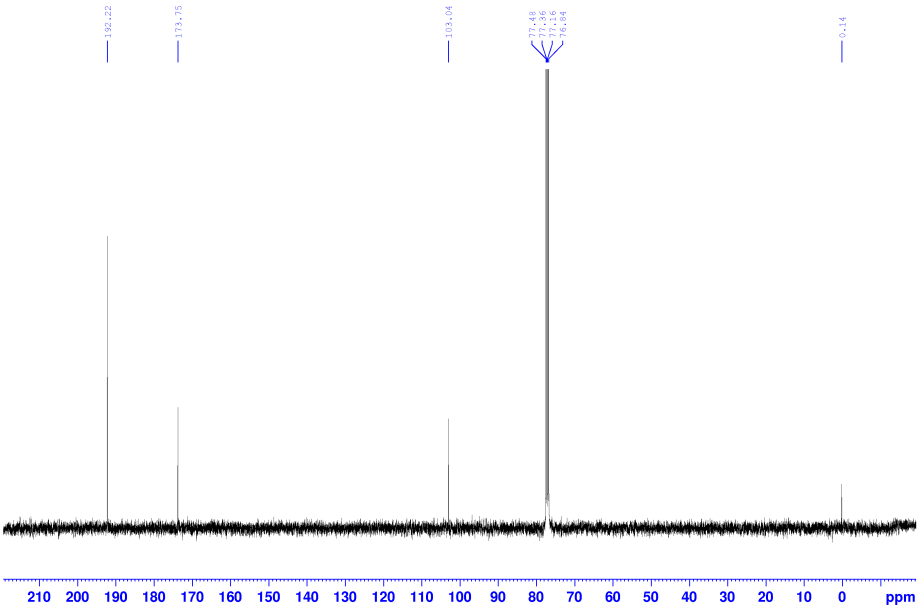

1-1-(2-chloropyridine-5-yl)-2, 5-dimethyl-1H-pyrrole 17a

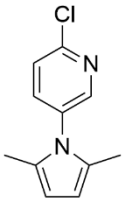

^{1}H NMR (400 MHz, $CDCl_3$)

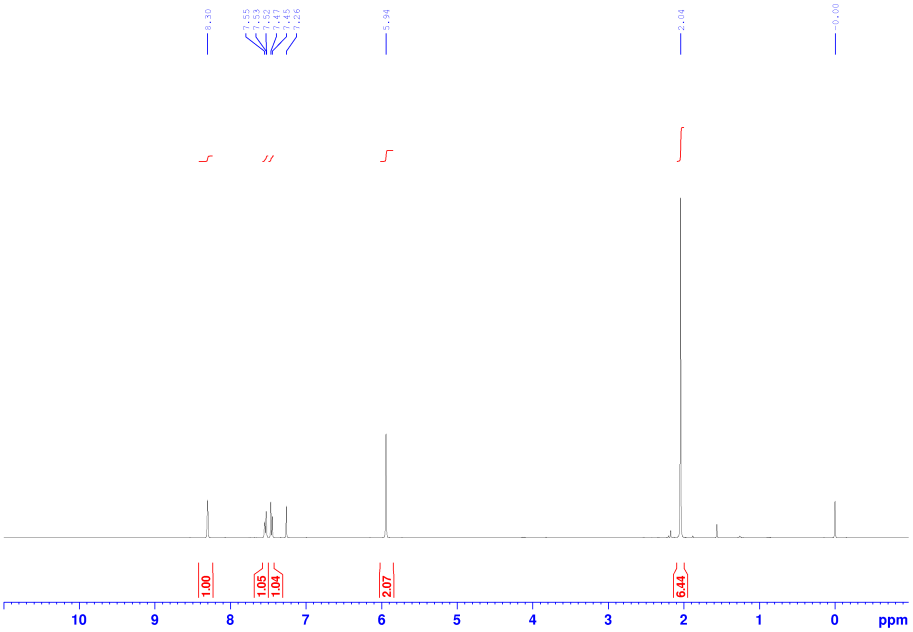

^{13}C NMR (100.6 MHz, $CDCl_3$)

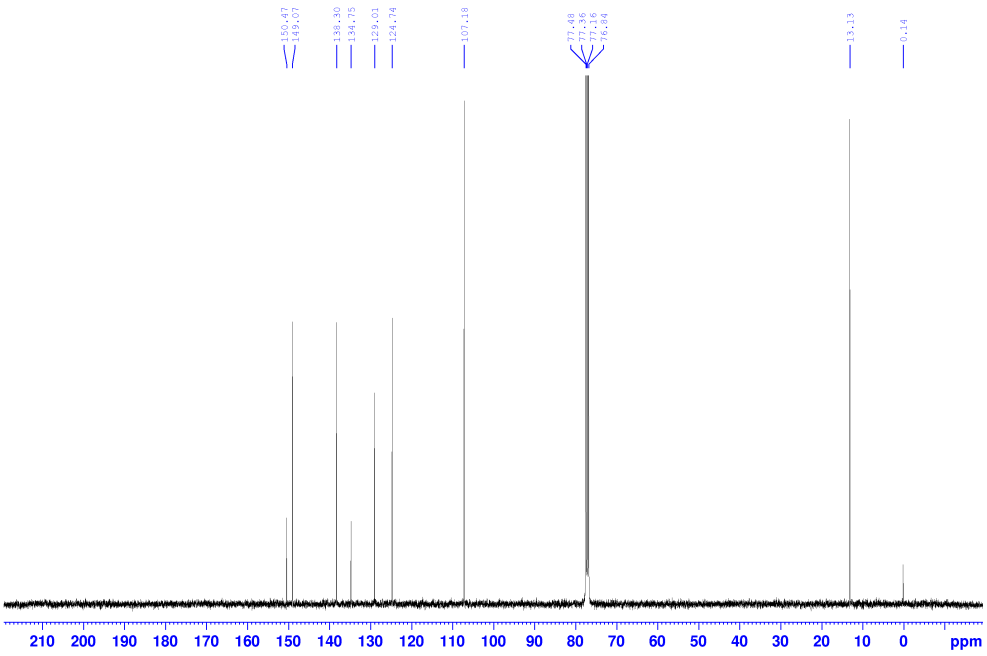

1-1-(2-Bromopyridine-5-yl)-2, 5-dimethyl-1H-pyrrole 17b

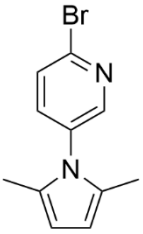

^{1}H NMR (400 MHz, $CDCl_3$)

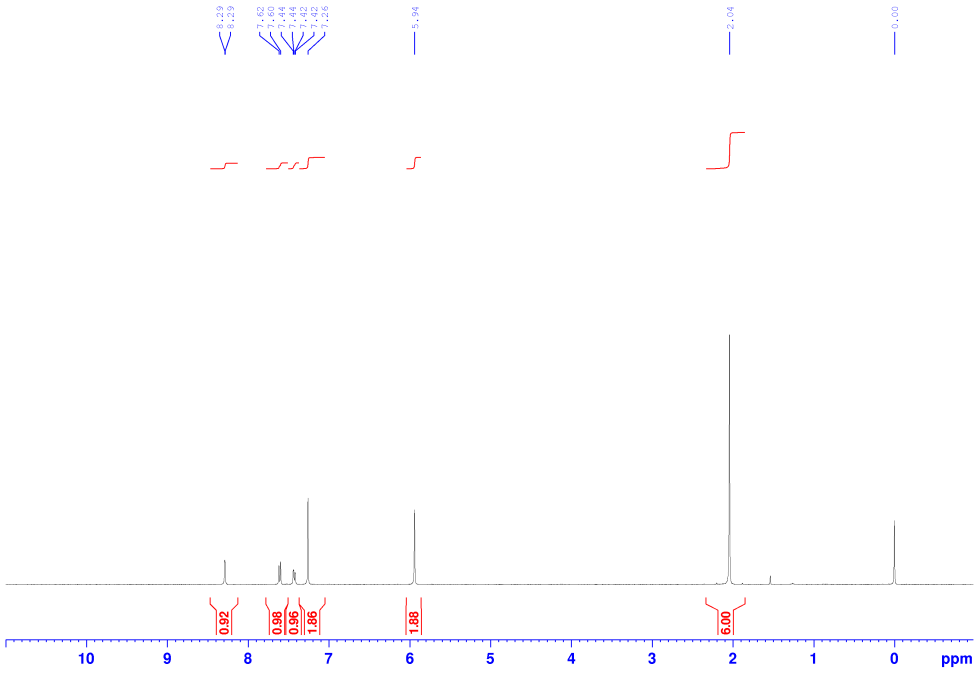

^{13}C NMR (100.6 MHz, $CDCl_3$)

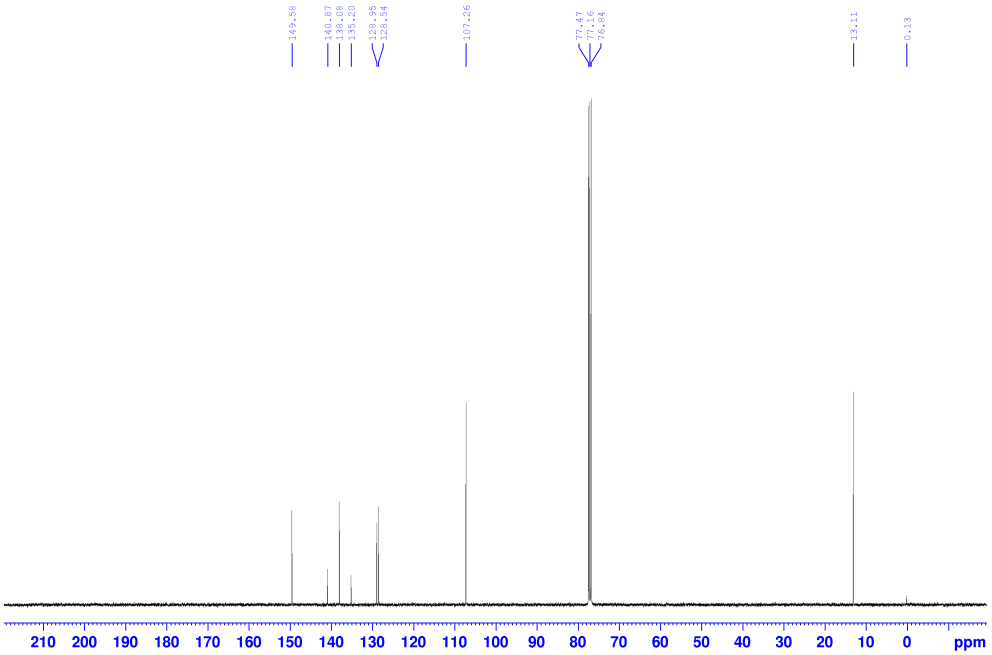

5,5'-bis(2,5-dimethyl-1*H*-pyrrol-1-yl)-2,2'-bipyridine 18

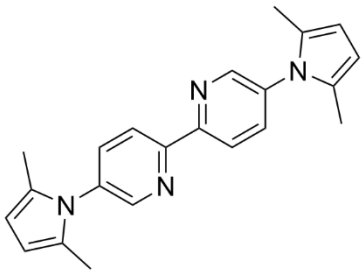

^{1}H NMR (400 MHz, $CDCl_3$)

^{13}C NMR (100.6 MHz, $CDCl_3$)

2,2'-bipyridine-5,5'-diamine Bpy

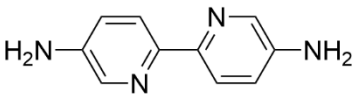

^{1}H NMR (400 MHz, DMSO-d_6)

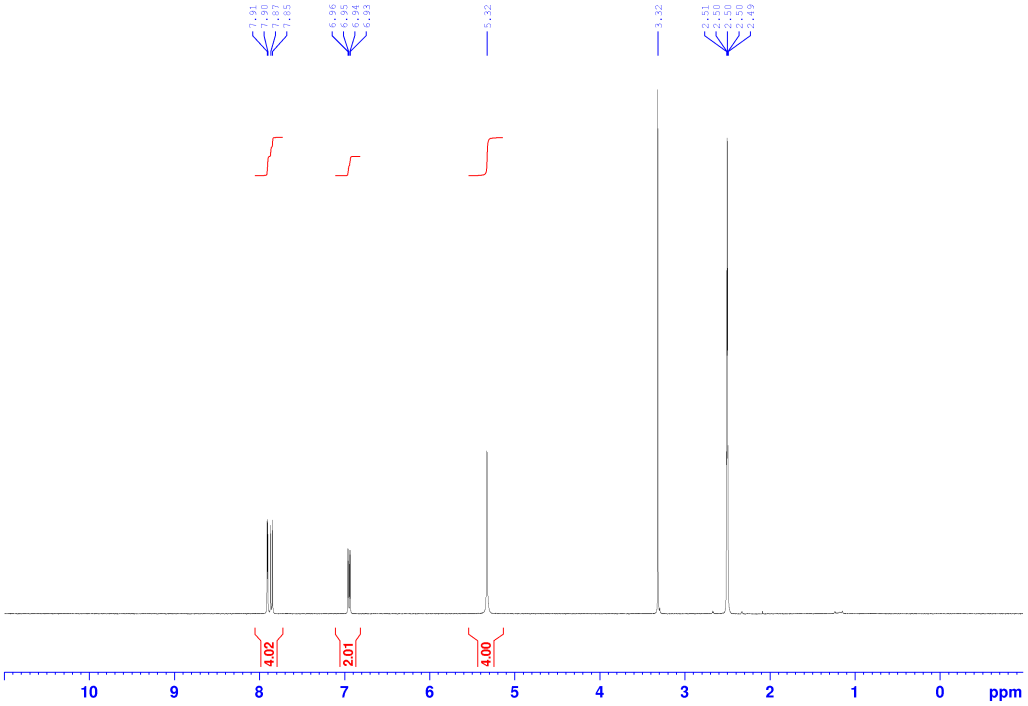

^{13}C NMR (100.6 MHz, DMSO-d_6)

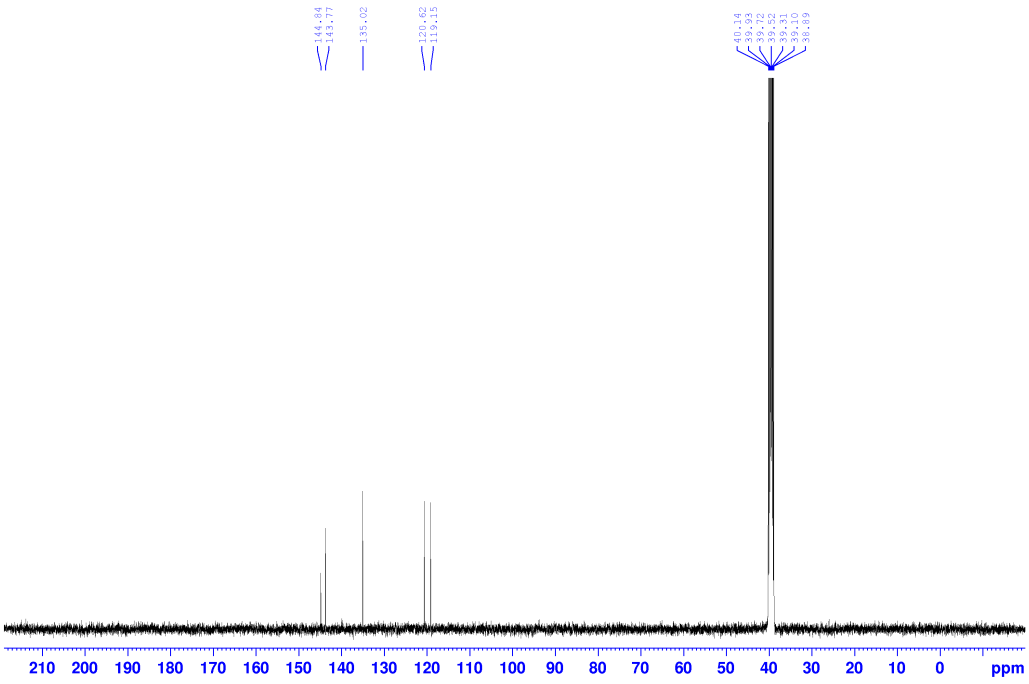

5-Nitro-2-(4-nitrophenyl)pyridine 21

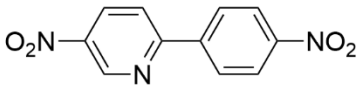

^{1}H NMR (400 MHz, DMSO-d_6)

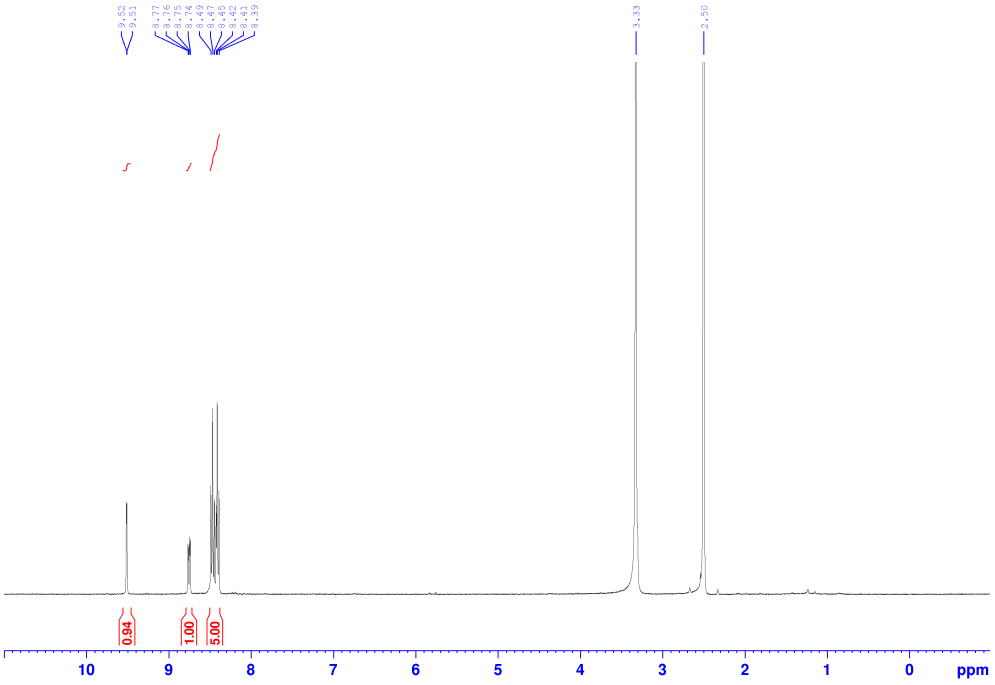

^{13}C NMR (100.6 MHz, DMSO-d_6)

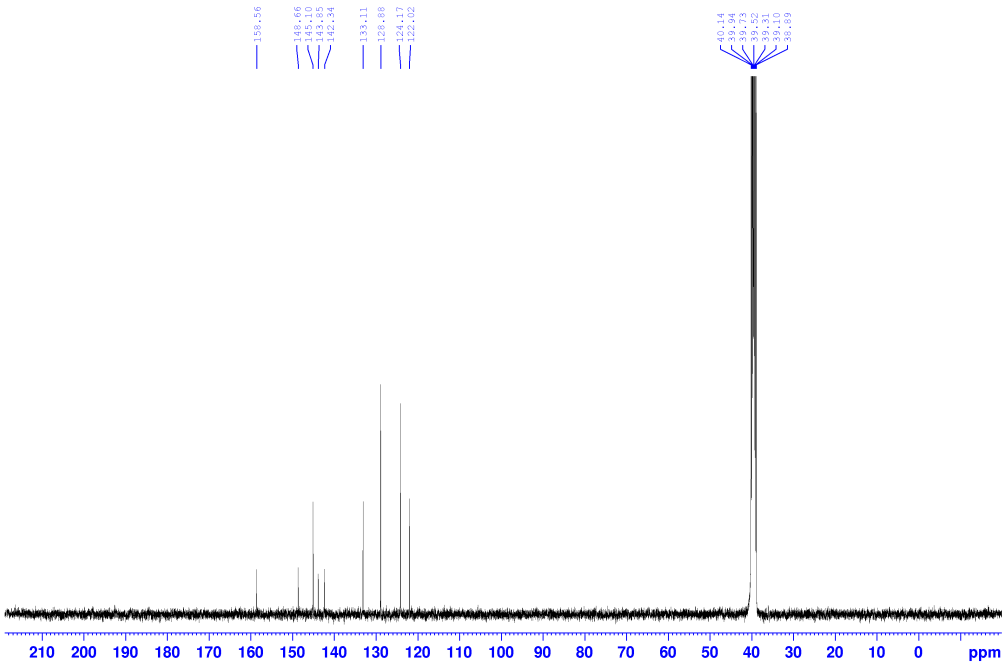

6-(4-aminophenyl)pyridin-3-amine Ppy

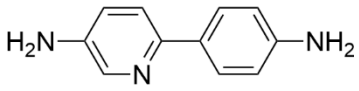

^{1}H NMR (400 MHz, DMSO-d_6)

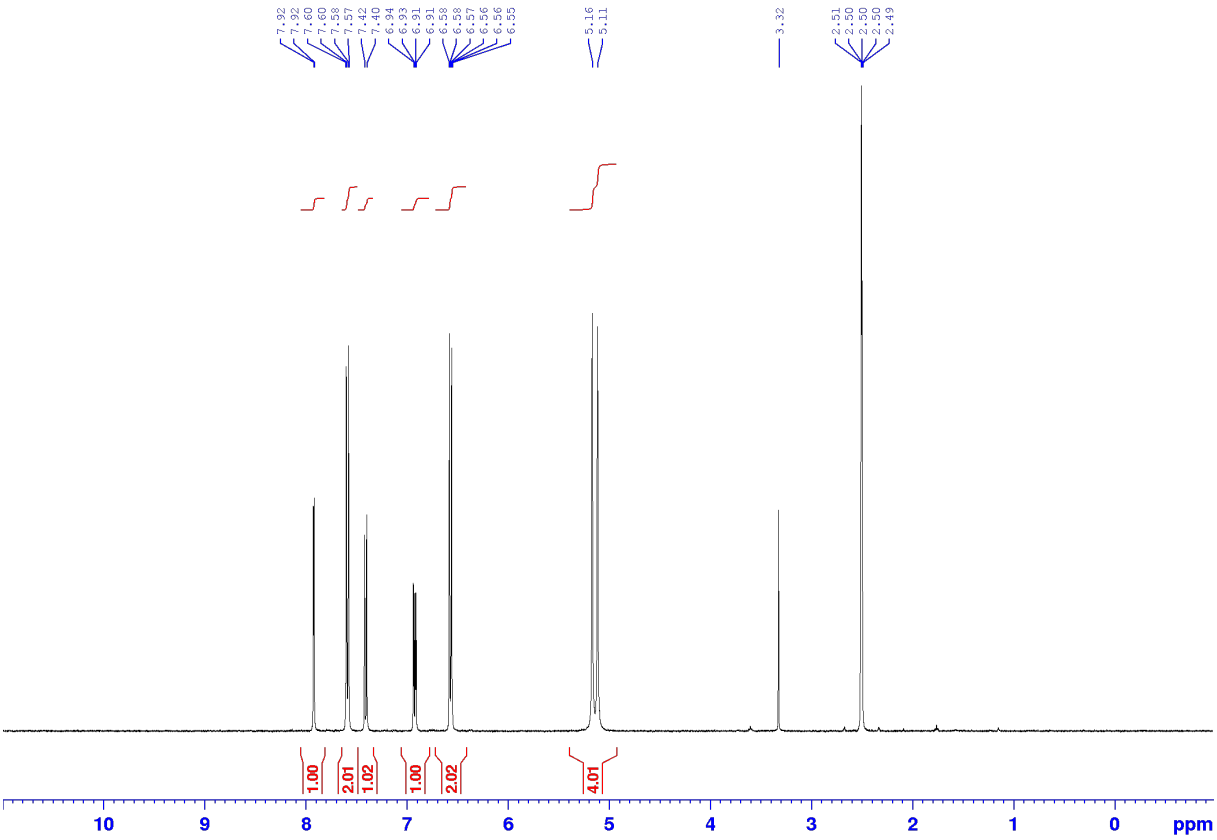

^{13}C NMR (100.6 MHz, DMSO-d_6)

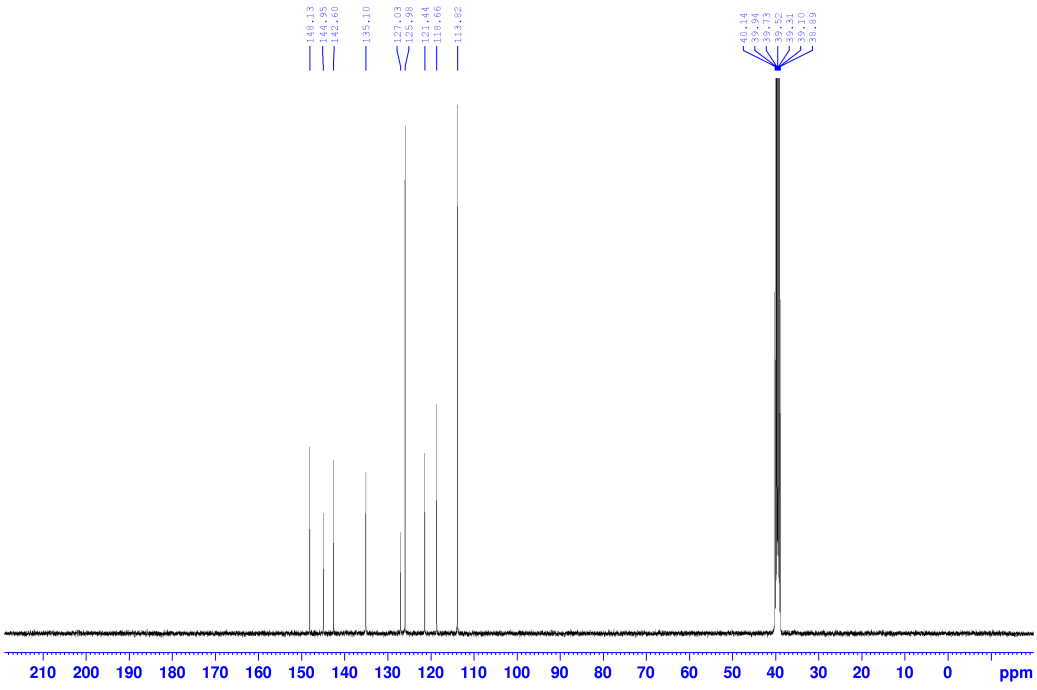

S6.2 Substrates

(*E*)-3-(naphthalen-2-yl)prop-2-en-1-ol 25b

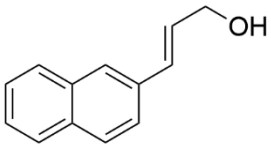

^{1}H NMR (400 MHz, $CDCl_3$)

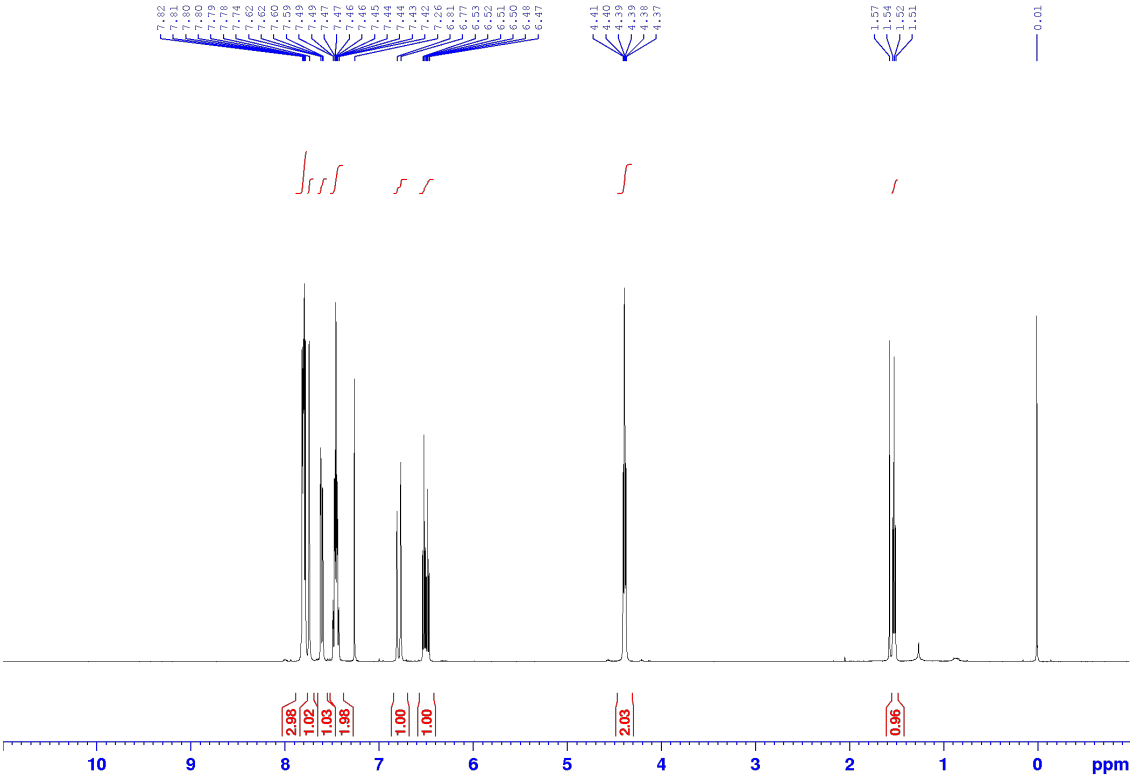

^{13}C NMR (100.6 MHz, $CDCl_3$)

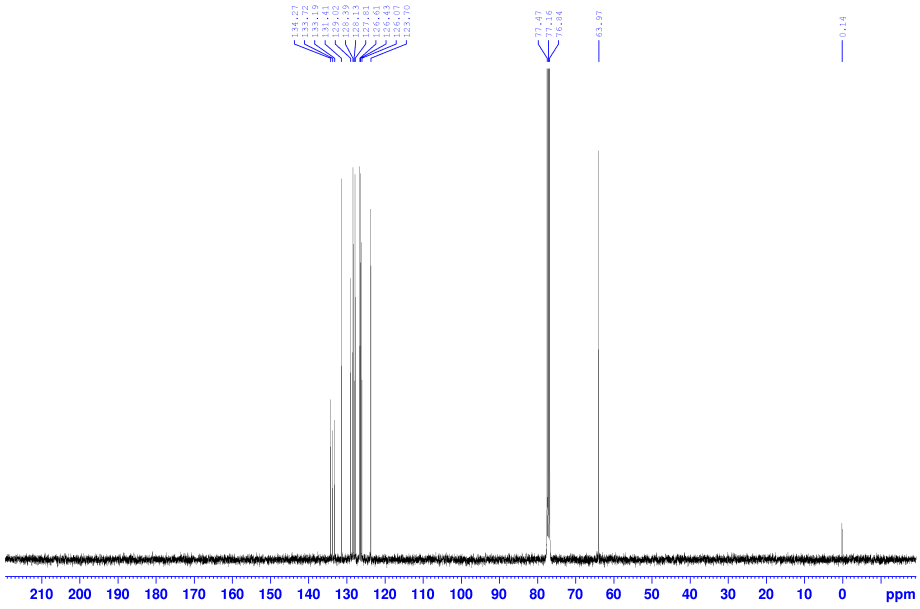

Cinnamyl 2-chloroacetate (crude) 28a

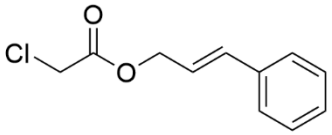

^{1}H NMR (400 MHz, $CDCl_3$)

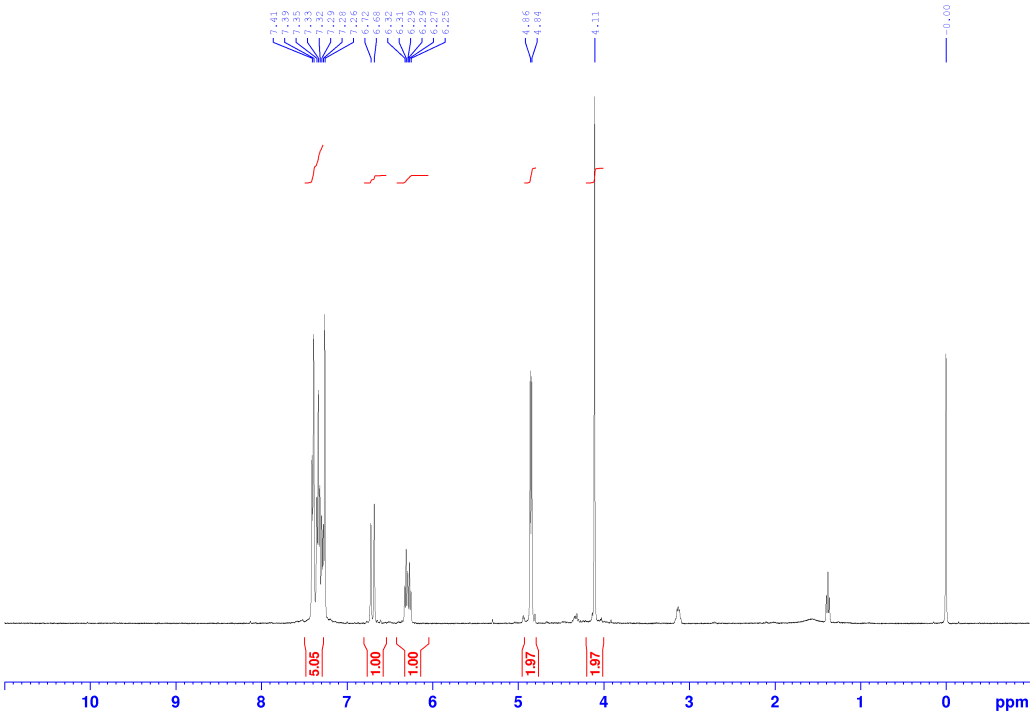

^{13}C NMR (100.6 MHz, $CDCl_3$)

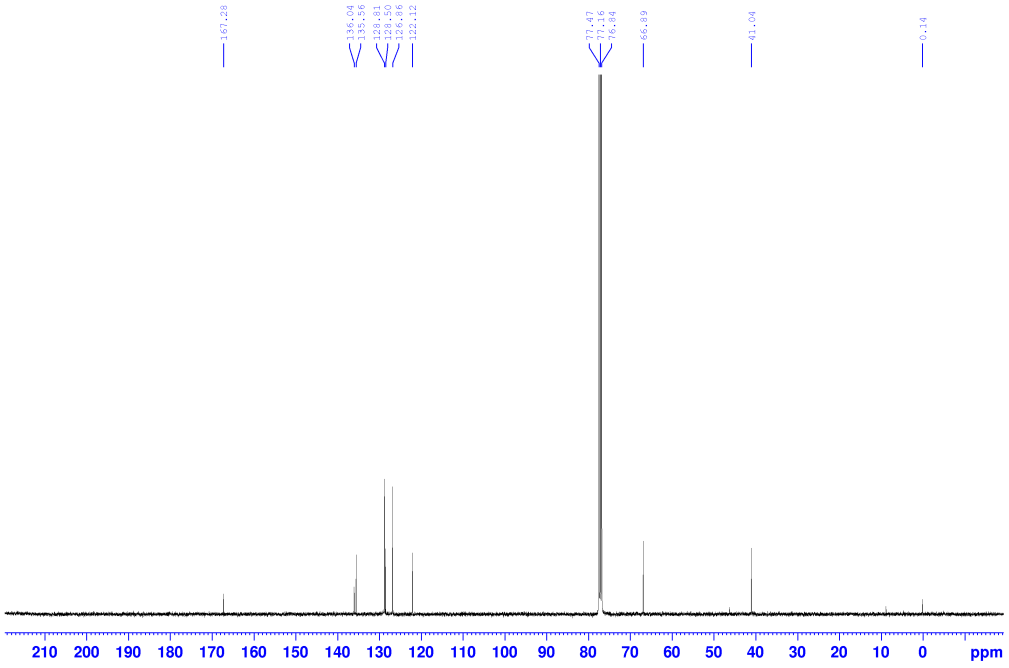
167.28
136.04
135.56
128.81
128.50
126.86
122.12
77.47
77.16
76.84
66.89
41.04
0.14
210 200 190 180 170 160 150 140 130 120 110 100 90 80 70 60 50 40 30 20 10 0 ppm

Cinnamyl 2-bromoacetate (crude) 28b

^{1}H NMR (400 MHz, $CDCl_3$)

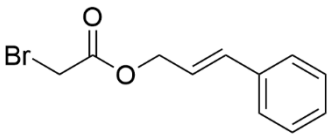

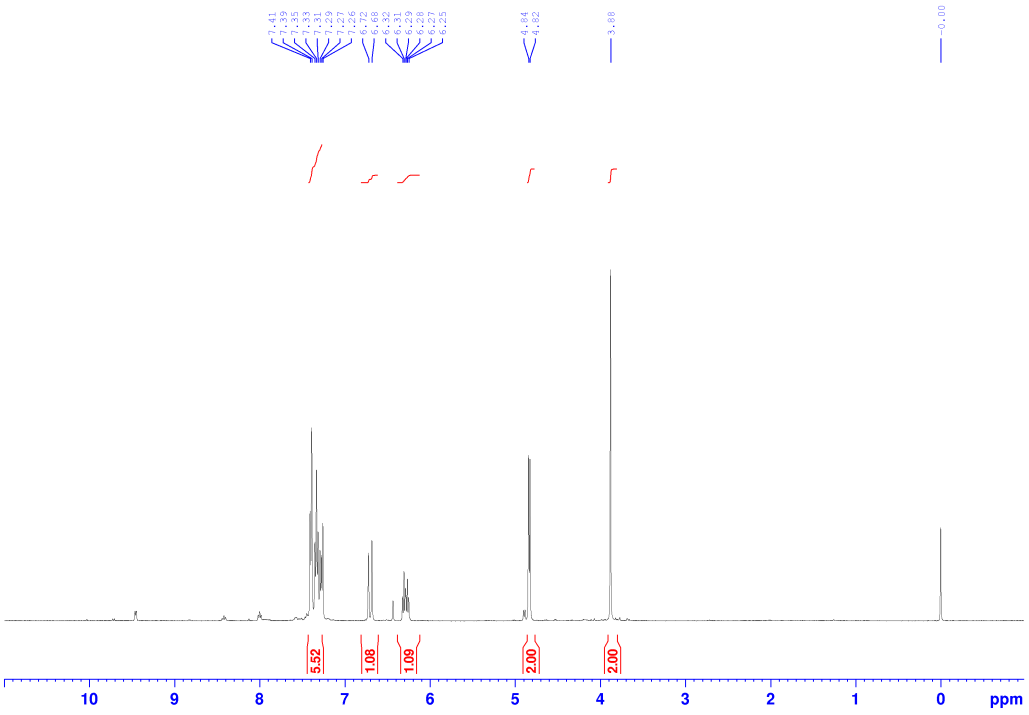

^{13}C NMR (100.6 MHz, $CDCl_3$)

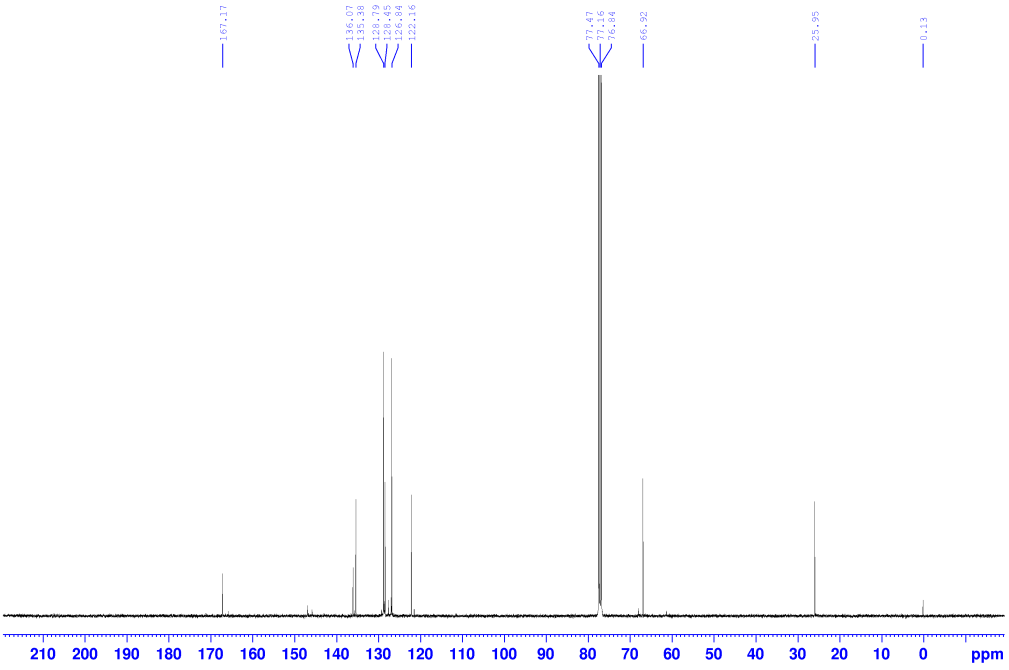
167.17
136.07
135.38
128.79
128.45
126.84
122.16
77.47
77.16
76.84
66.92
25.95
0.13
210 200 190 180 170 160 150 140 130 120 110 100 90 80 70 60 50 40 30 20 10 0 ppm

(*E*)-3-(Naphthalen-2-yl)allyl 2-bromoacetate (crude) 28c

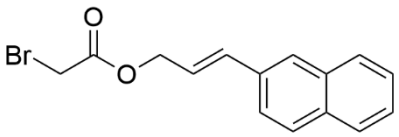

^{1}H NMR (400 MHz, $CDCl_3$)

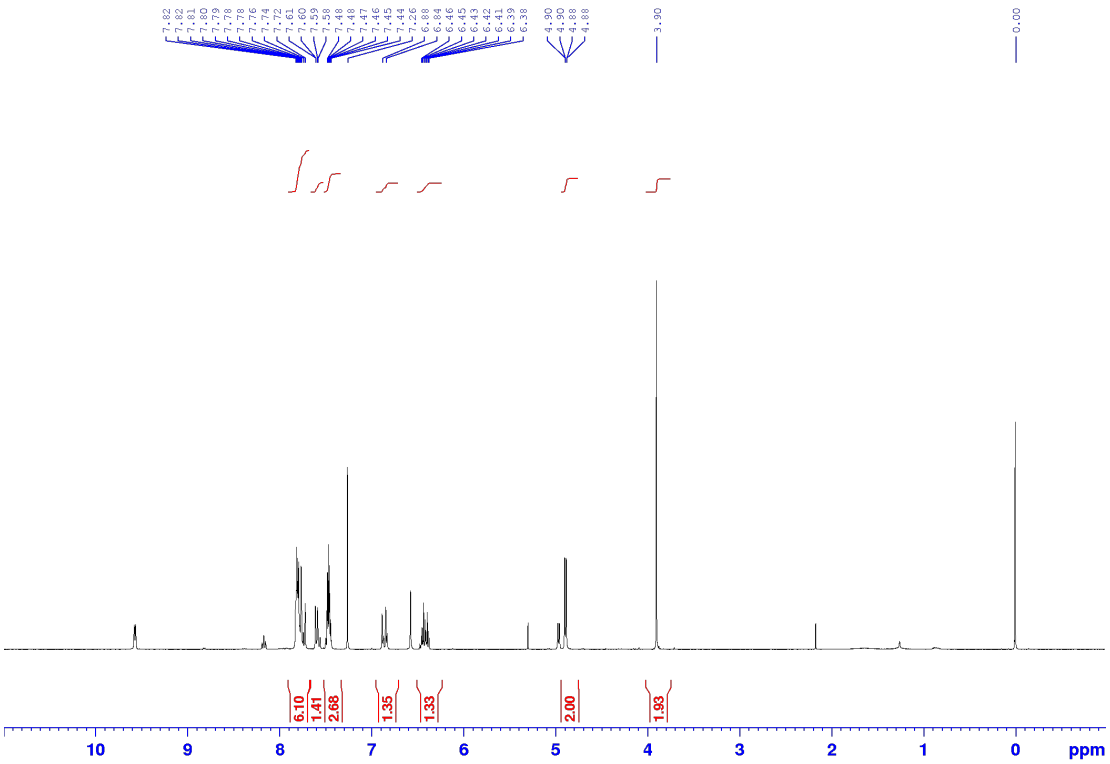

(2*E*,4*E*)-Hexa-2,4-dien-1-yl 2-bromoacetate (crude) 28d

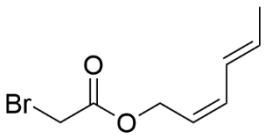

^{1}H NMR (400 MHz, $CDCl_3$)

Cinnamyl *p*-tolylglycinate 1a

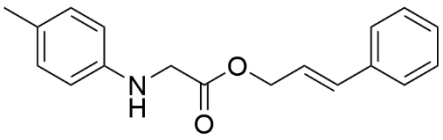

^{1}H NMR (400 MHz, $CDCl_3$)

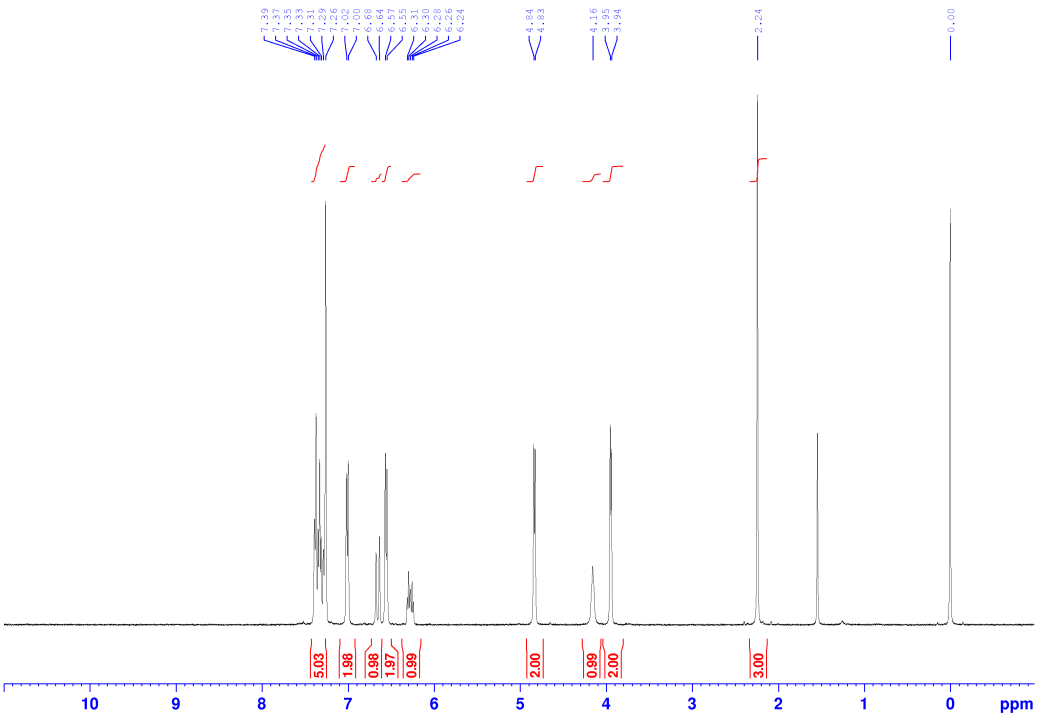

^{13}C NMR (100.6 MHz, $CDCl_3$)

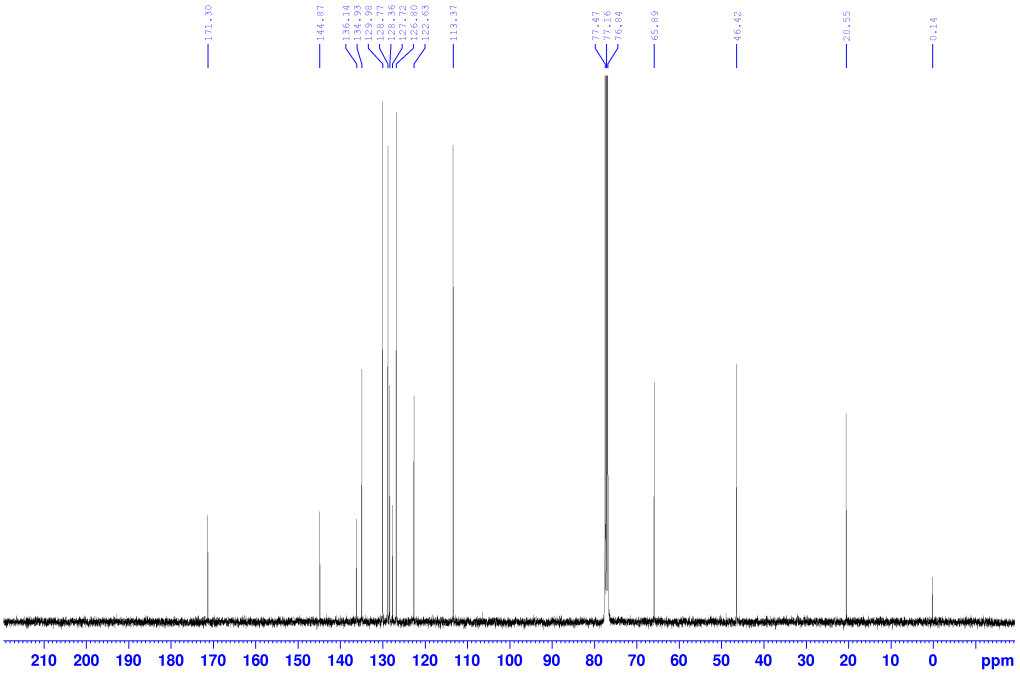

Cinnamyl (4-methoxyphenyl)glycinate 1b

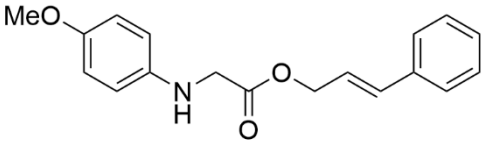

^{1}H NMR (400 MHz, $CDCl_3$)

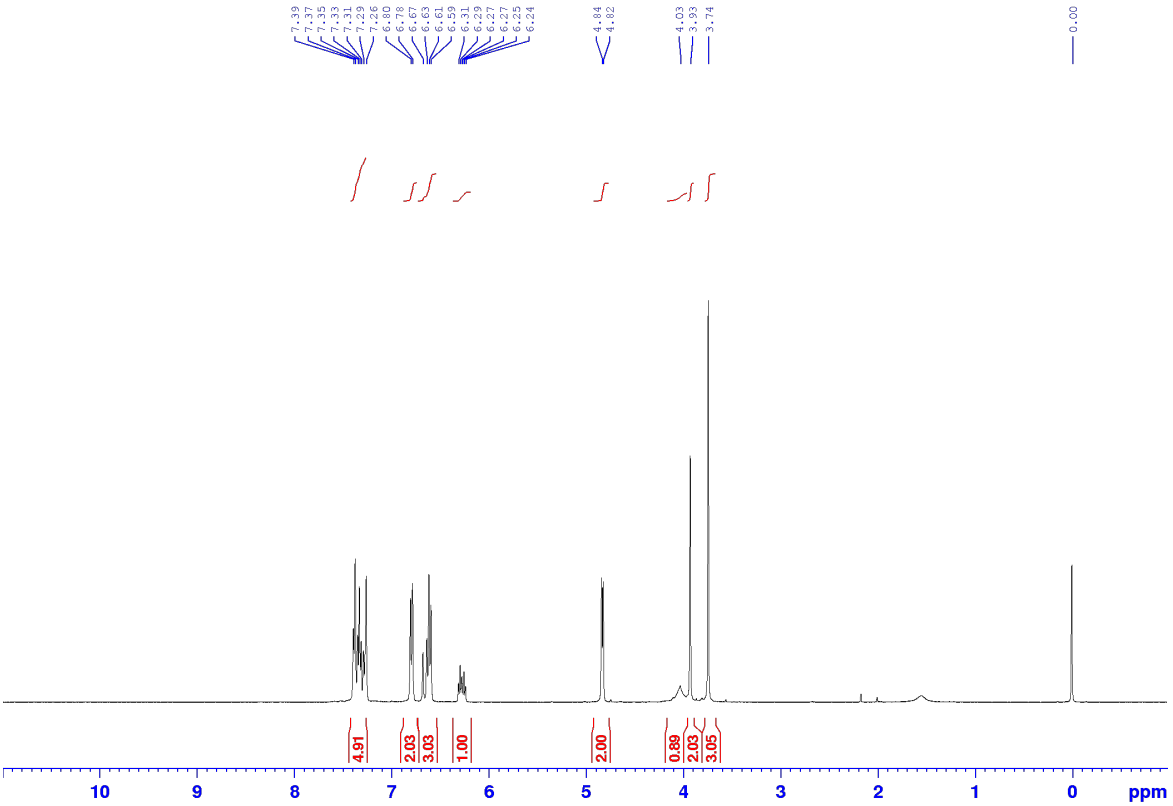

^{13}C NMR (100.6 MHz, DMSO-d_6)

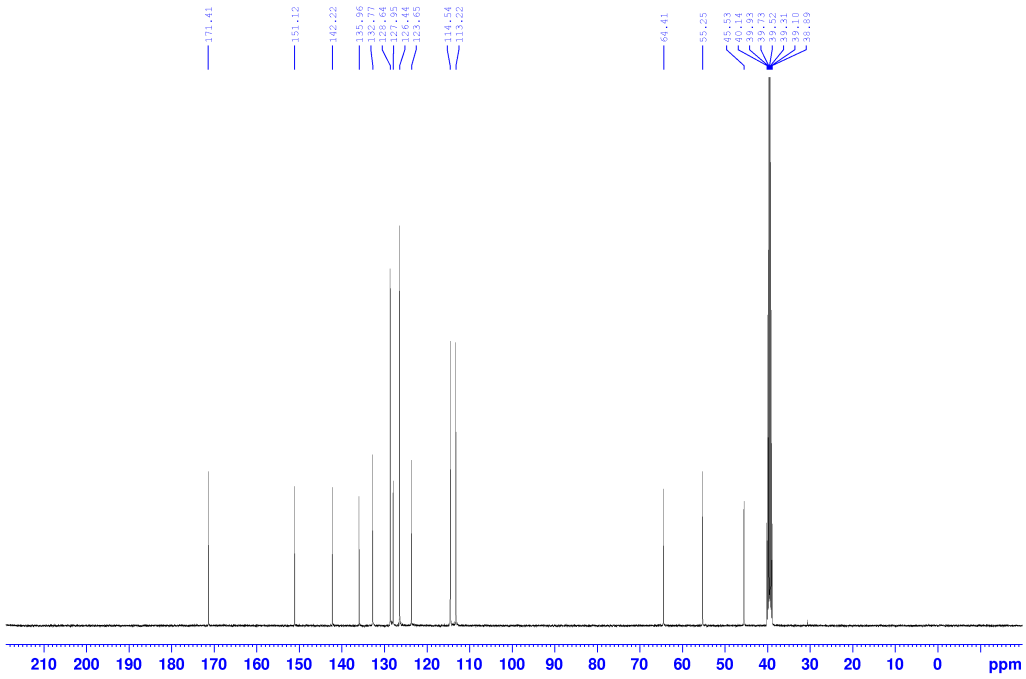

Cinnamyl (2-methoxyphenyl)glycinate 1c

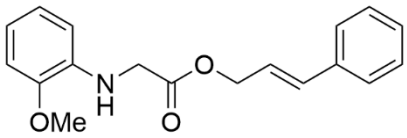

^{1}H NMR (400 MHz, $CDCl_3$)

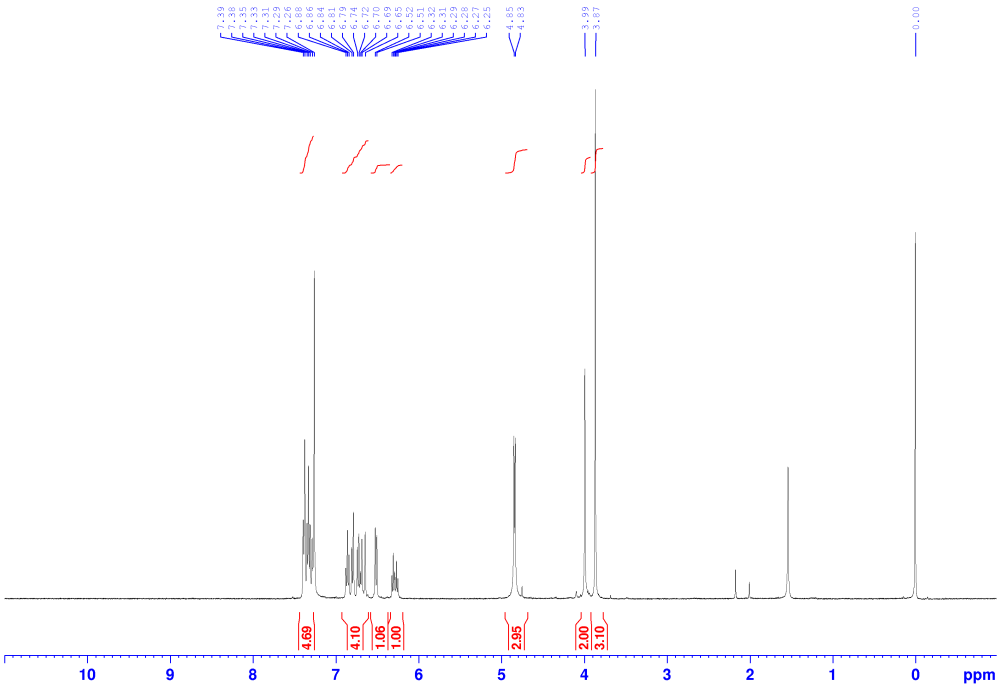

^{13}C NMR (100.6 MHz, $CDCl_3$)

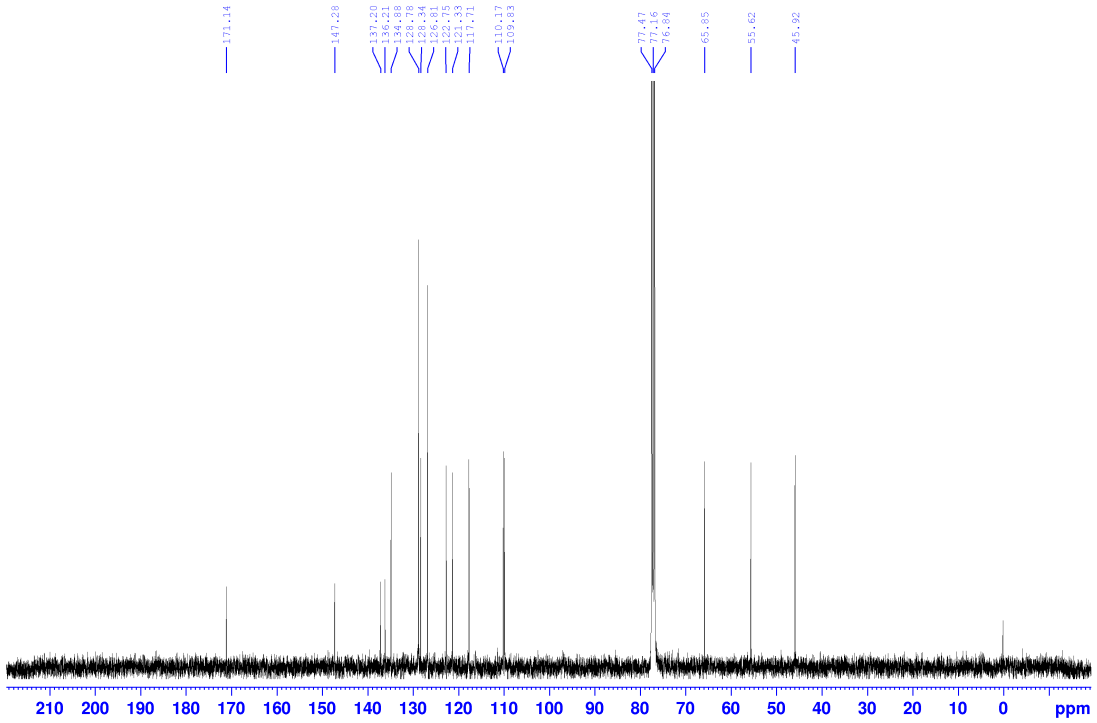
171.14
147.28
137.20
136.21
134.88
128.78
128.34
126.51
125.55
123.33
117.71
110.17
109.83
77.47
77.16
76.84
65.85
55.62
45.92
210 200 190 180 170 160 150 140 130 120 110 100 90 80 70 60 50 40 30 20 10 0 ppm

Cinnamyl (4-fluorophenyl)glycinate 1d

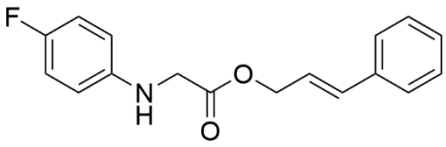

^{1}H NMR (400 MHz, $CDCl_3$)

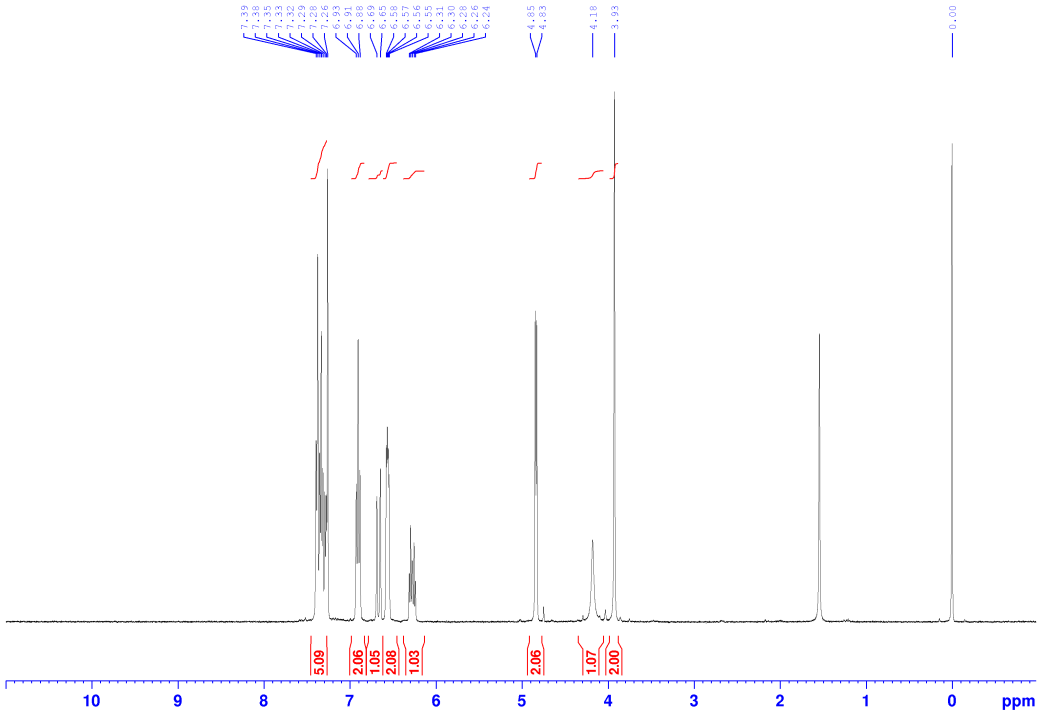

^{13}C NMR (100.6 MHz, $CDCl_3$)

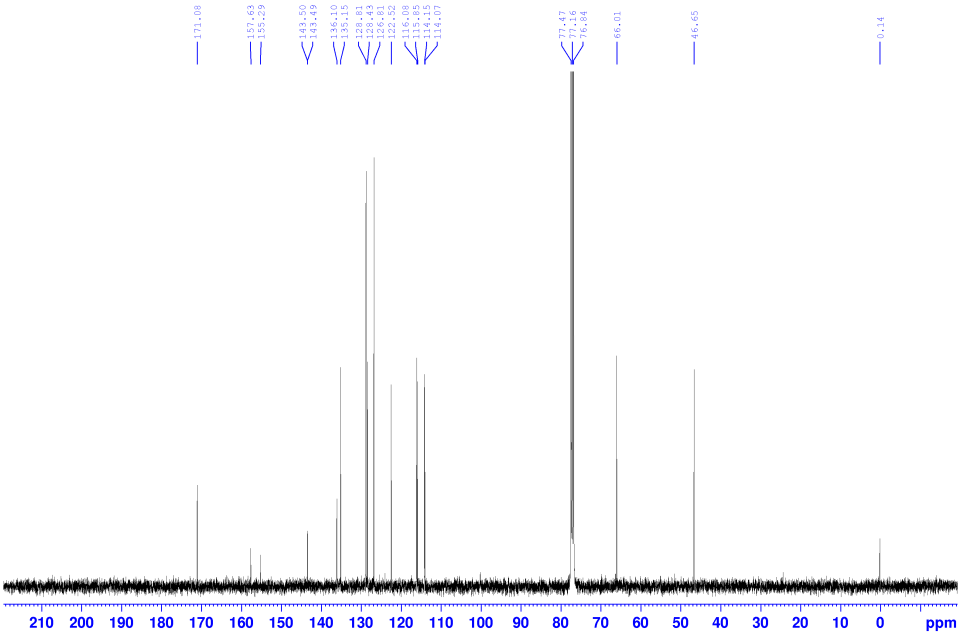
171.08
157.63
155.29
143.50
143.49
136.10
135.15
128.81
128.43
125.31
122.52
116.08
115.85
114.15
114.07
77.47
77.16
76.84
66.01
46.65
0.14
210 200 190 180 170 160 150 140 130 120 110 100 90 80 70 60 50 40 30 20 10 0 ppm

Cinnamyl (3-(trifluoromethyl)phenyl)glycinate 1e

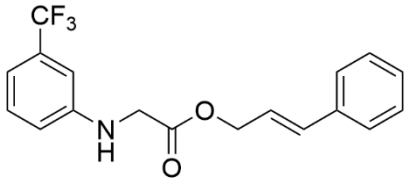

^{1}H NMR (400 MHz, $CDCl_3$)

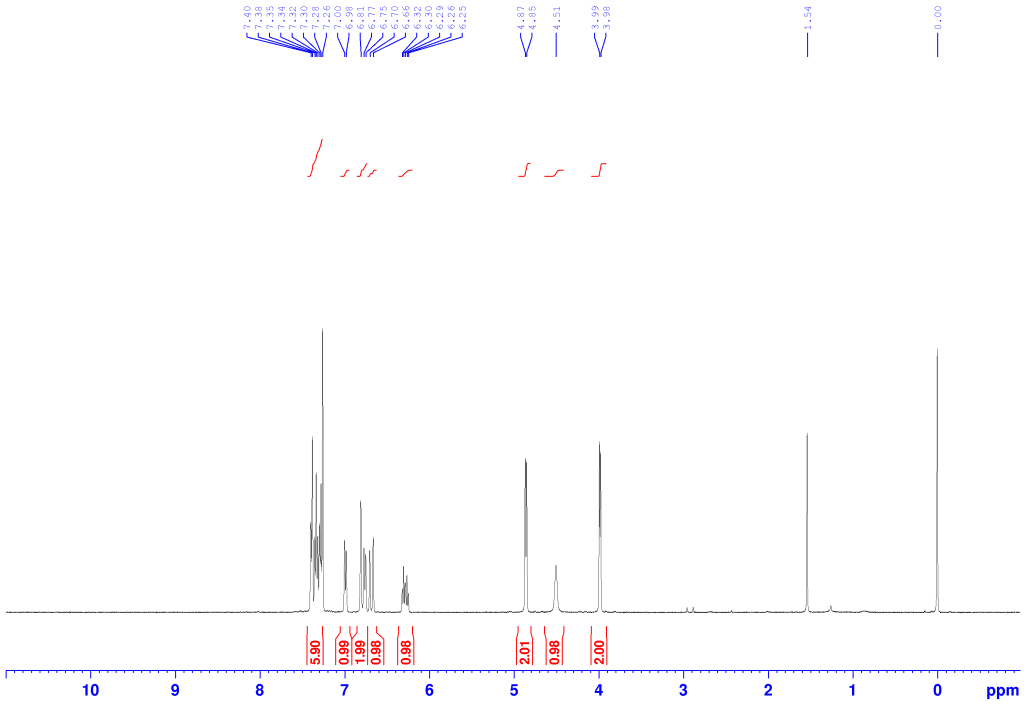

^{13}C NMR (100.6 MHz, $CDCl_3$)

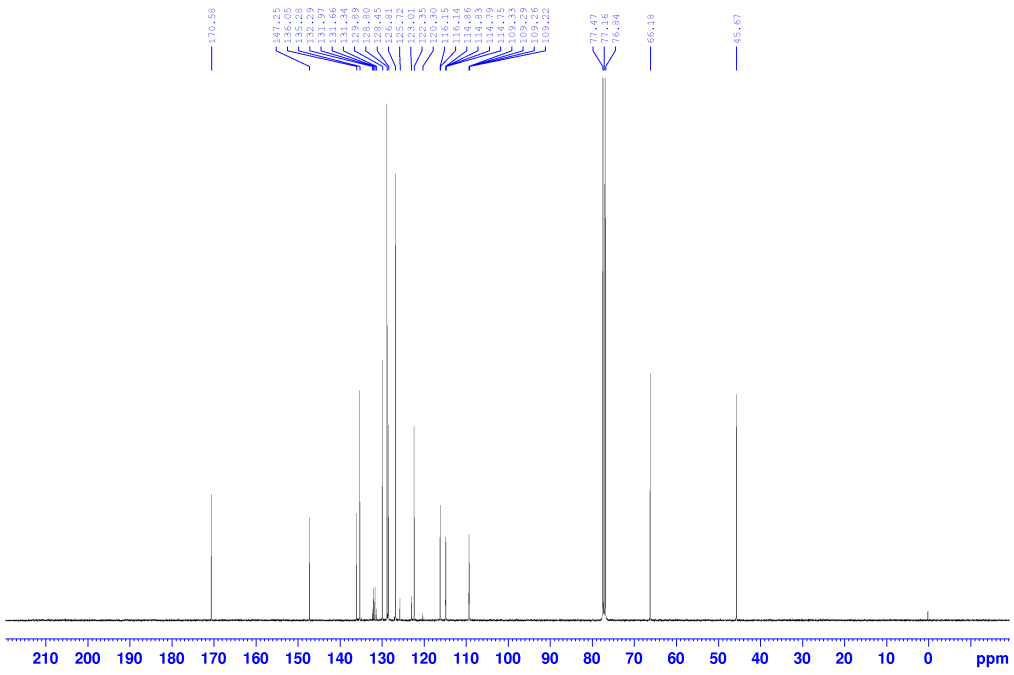

Cinnamyl (4-iodophenyl)glycinate 1f

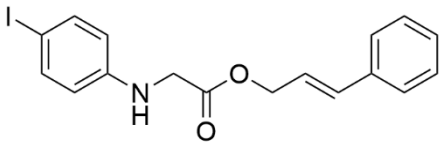

^{1}H NMR (400 MHz, $CDCl_3$)

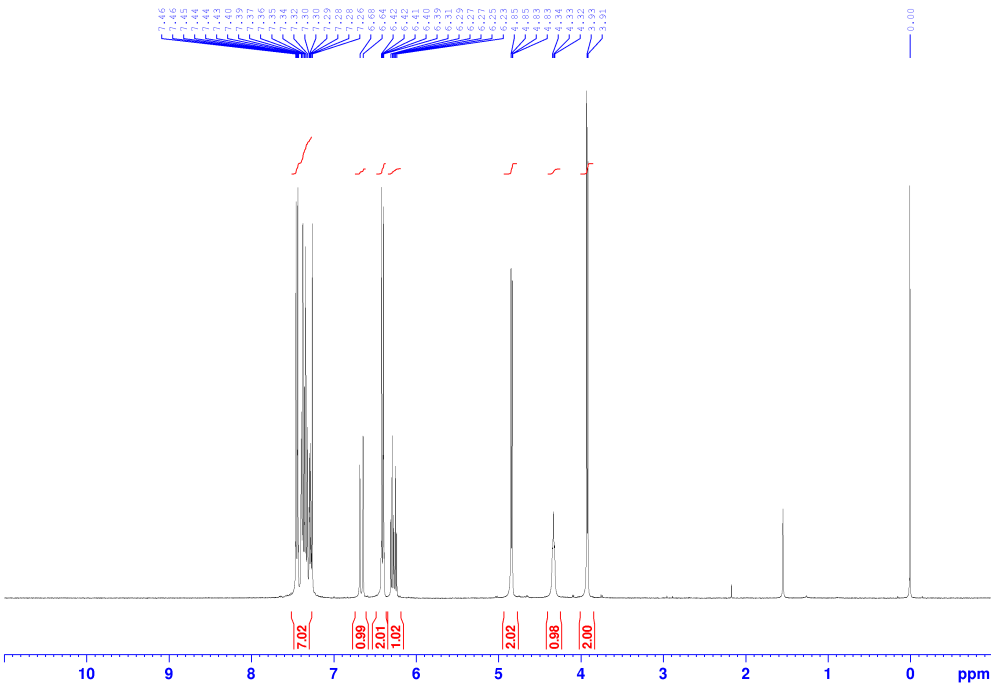

^{13}C NMR (100.6 MHz, $CDCl_3$)

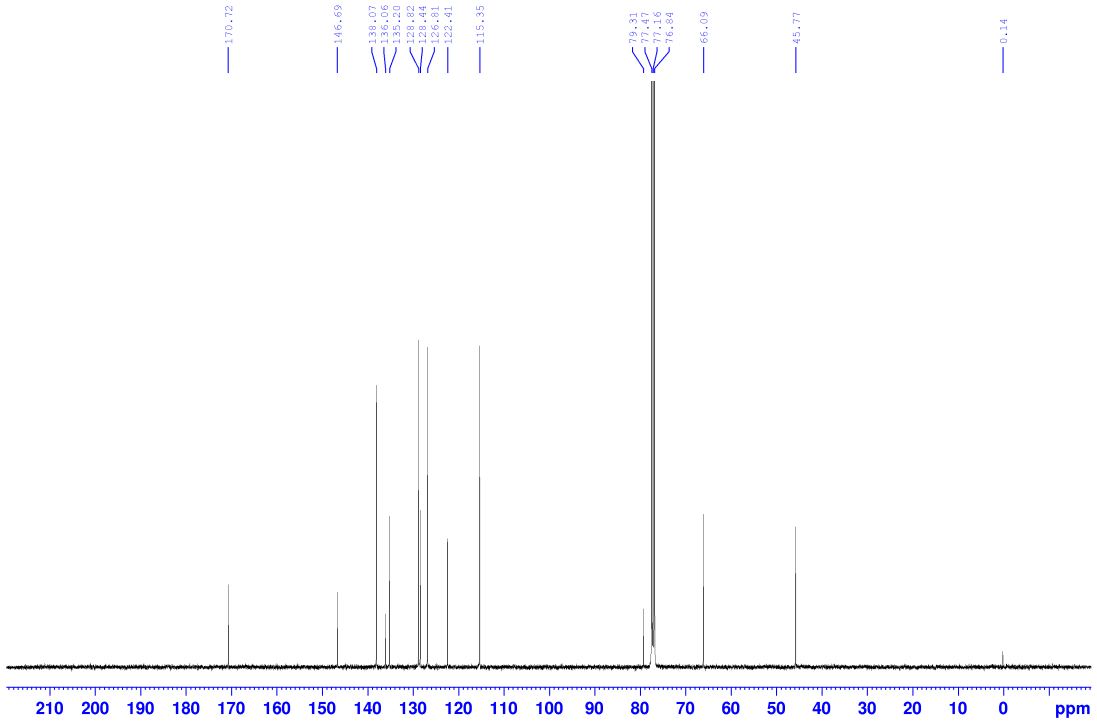

Cinnamyl (2-bromophenyl)glycinate 1g

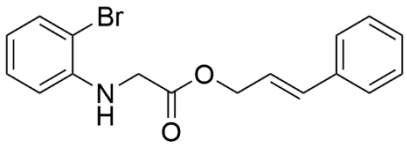

^{1}H NMR (400 MHz, $CDCl_3$)

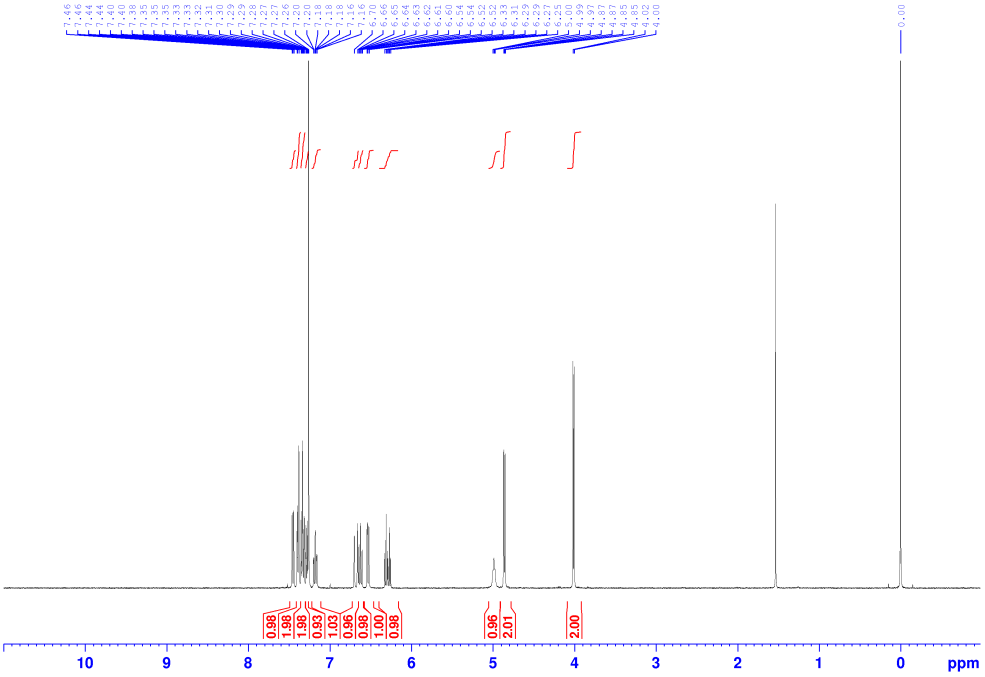

^{13}C NMR (100.6 MHz, $CDCl_3$)

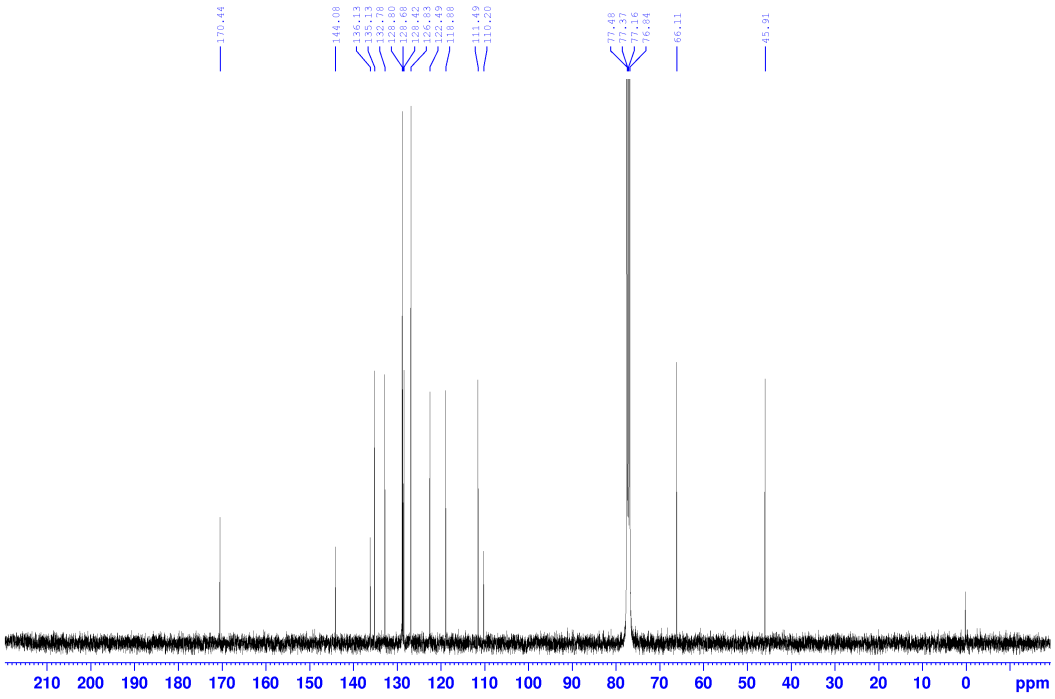
170.44
144.08
136.13
135.13
132.78
128.80
128.68
128.42
126.83
124.49
118.98
111.49
110.20
77.48
77.37
77.16
76.84
66.11
45.91
210 200 190 180 170 160 150 140 130 120 110 100 90 80 70 60 50 40 30 20 10 0 ppm

Cinnamyl m-tolylglycinate 1h

^{1}H NMR (400 MHz, $CDCl_3$)

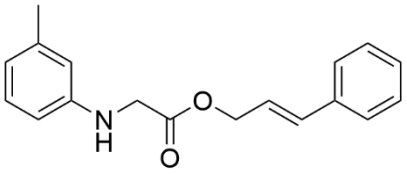

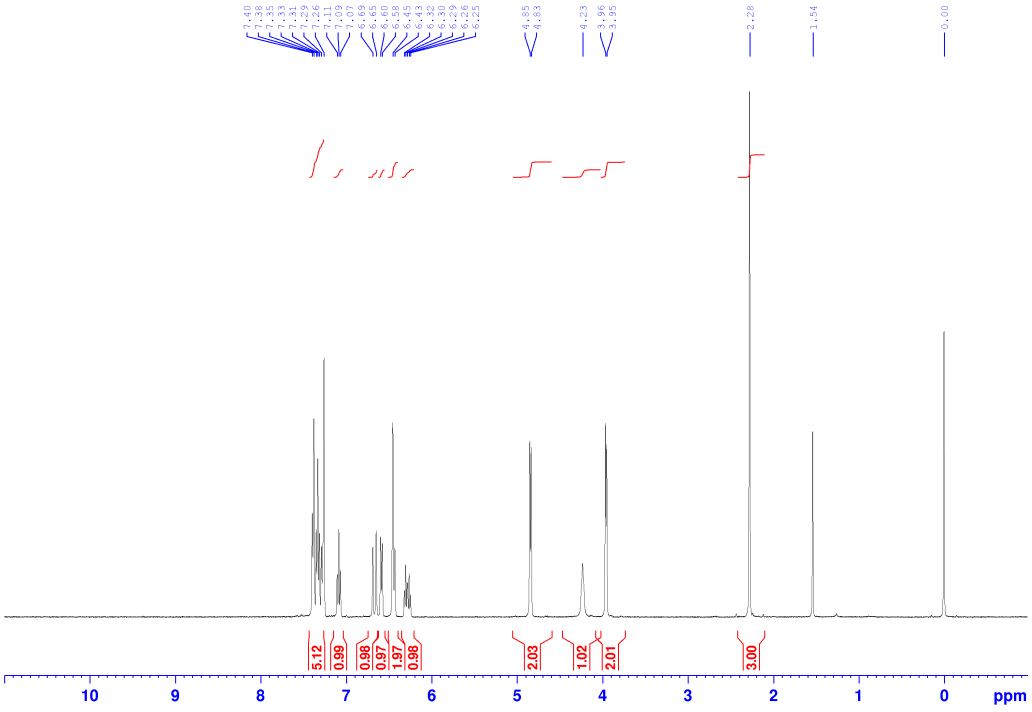

^{13}C NMR (100.6 MHz, $CDCl_3$)

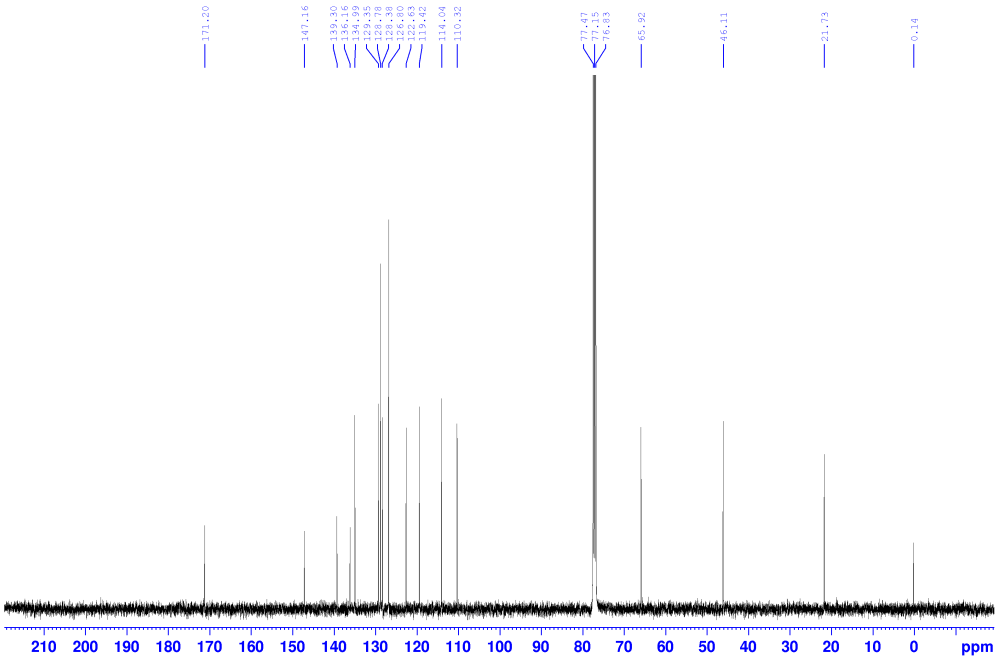

Cinnamyl o-tolylglycinate 1i

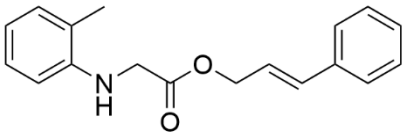

^{1}H NMR (400 MHz, $CDCl_3$)

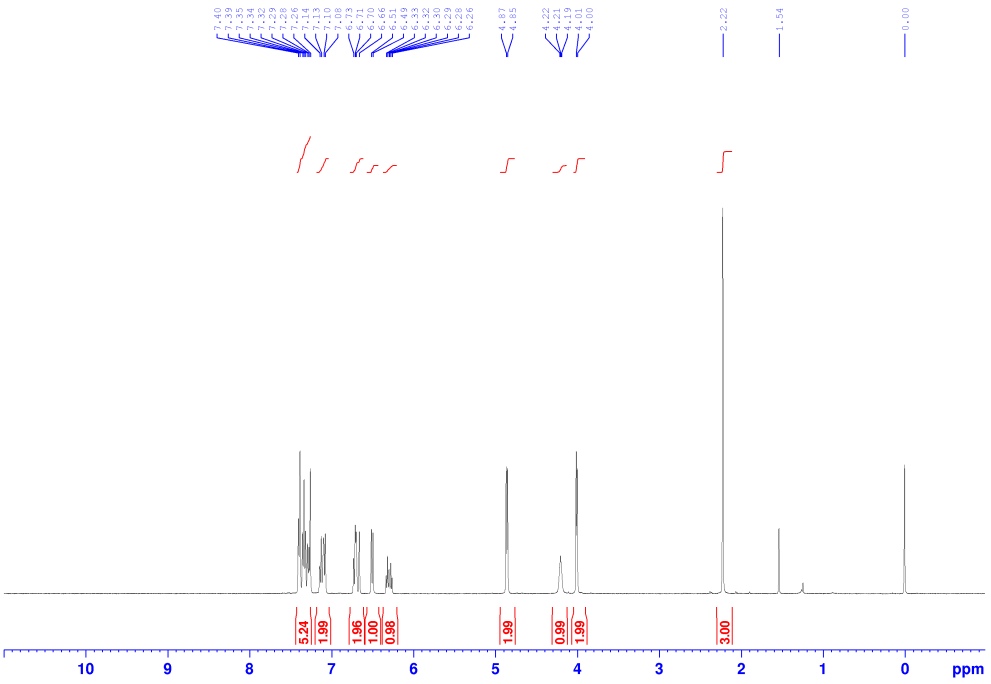

^{13}C NMR (100.6 MHz, $CDCl_3$)

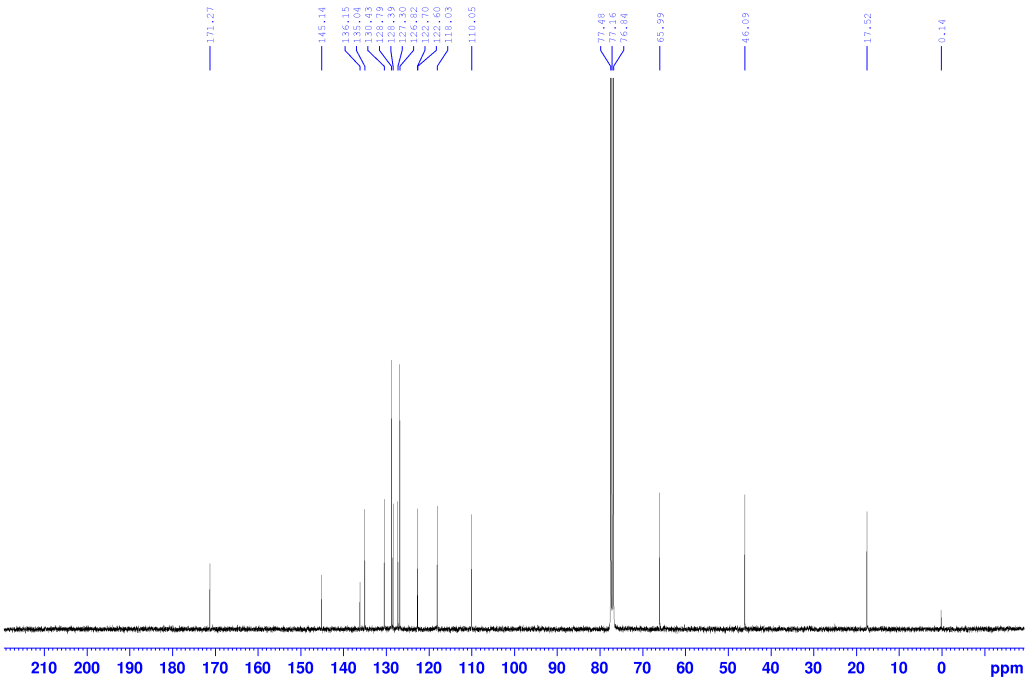
171.27
145.14
136.15
135.04
130.43
128.79
128.38
127.30
126.82
122.70
122.60
118.03
110.05
77.48
77.16
76.84
65.99
46.09
17.52
0.14
210 200 190 180 170 160 150 140 130 120 110 100 90 80 70 60 50 40 30 20 10 0 ppm

(*E*)-3-(Naphthalen-2-yl)allyl p-tolylglycinate 1j

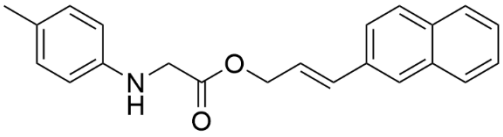

^{1}H NMR (400 MHz, $CDCl_3$)

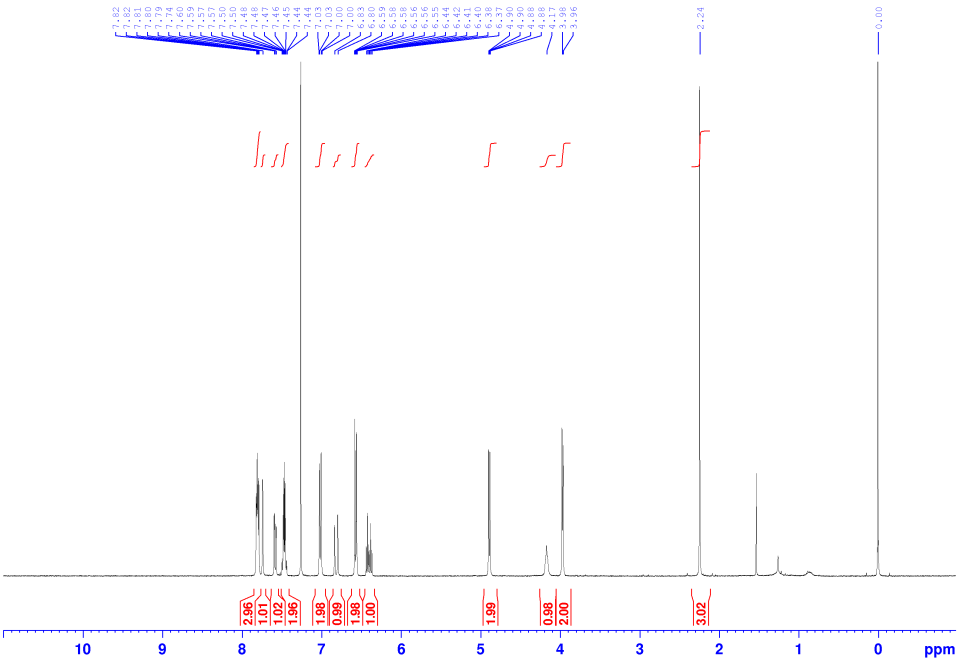

^{13}C NMR (100.6 MHz, $CDCl_3$)

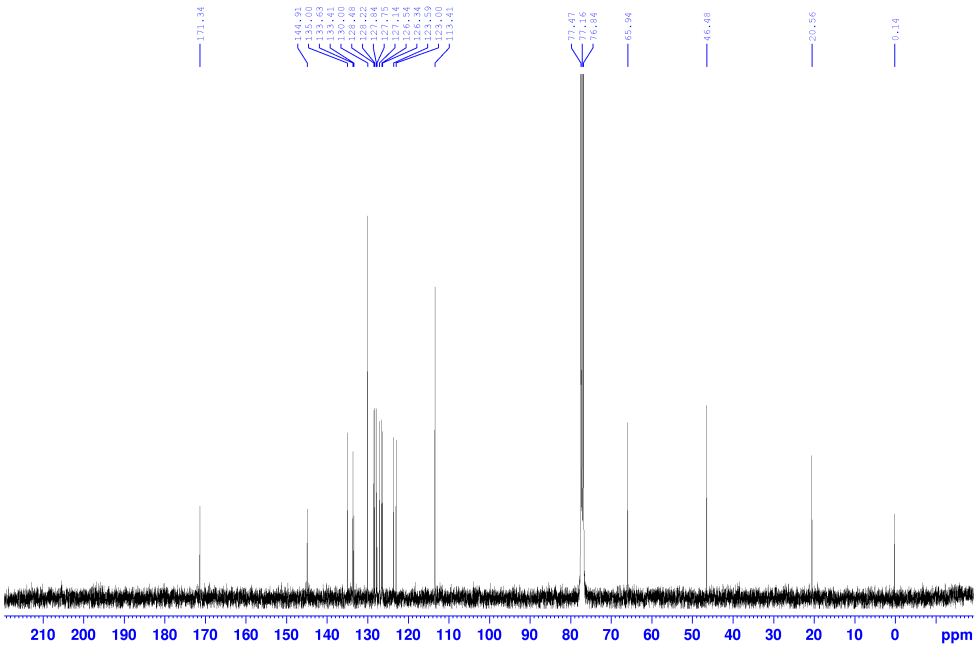
171.34
144.81
135.00
133.63
133.41
130.60
129.68
128.22
127.84
127.75
127.74
126.54
126.34
123.59
123.00
113.41
77.47
77.16
76.84
65.94
46.48
20.56
0.14
210 200 190 180 170 160 150 140 130 120 110 100 90 80 70 60 50 40 30 20 10 0 ppm

(*E*)-penta-2,4-dien-1-yl p-tolylglycinate 1k

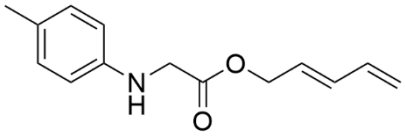

^{1}H NMR (400 MHz, $CDCl_3$)

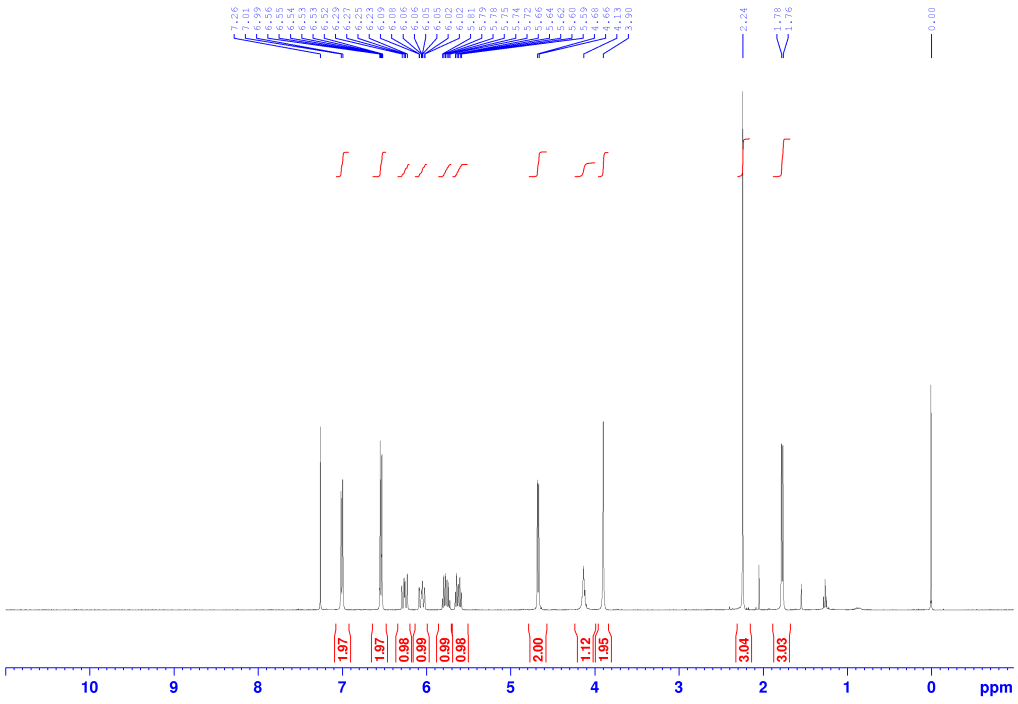

^{13}C NMR (100.6 MHz, $CDCl_3$)

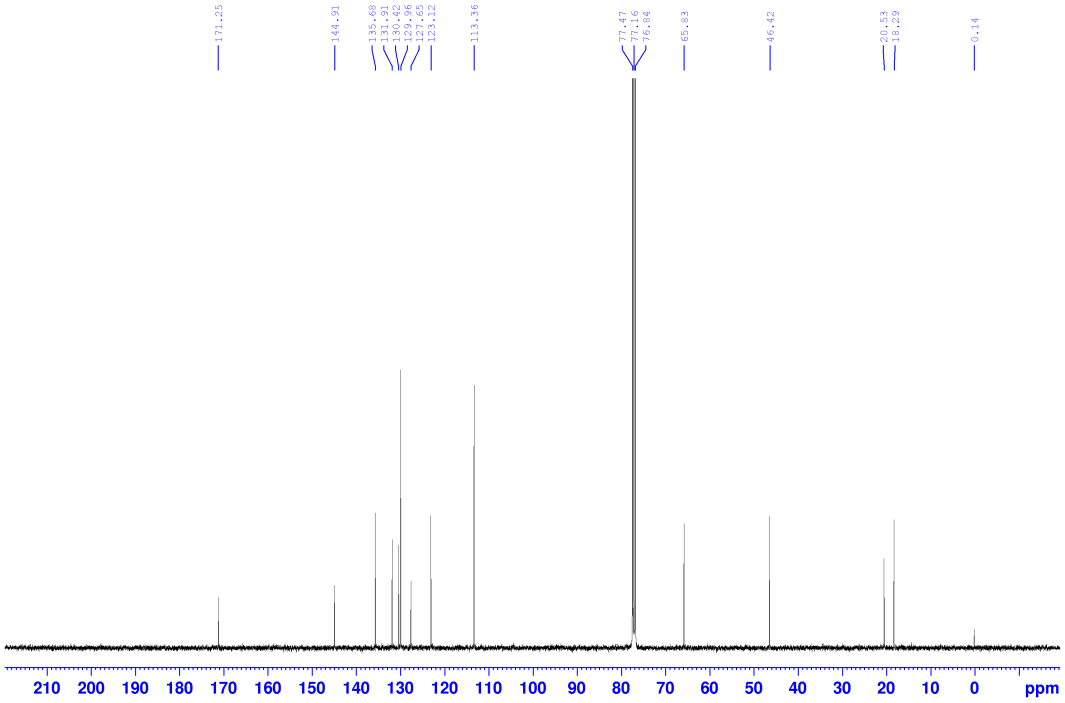

***N*-cinnamylaniline 30a**

^{1}H NMR (400 MHz, $CDCl_3$)

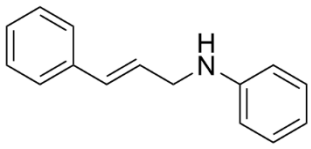

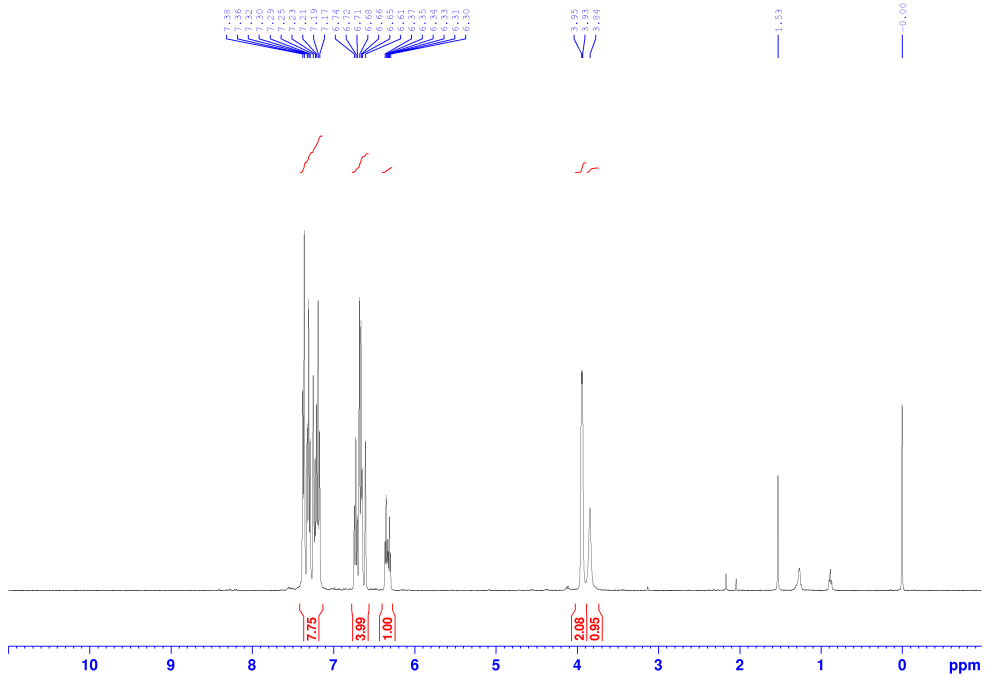

^{13}C NMR (100.6 MHz, $CDCl_3$)

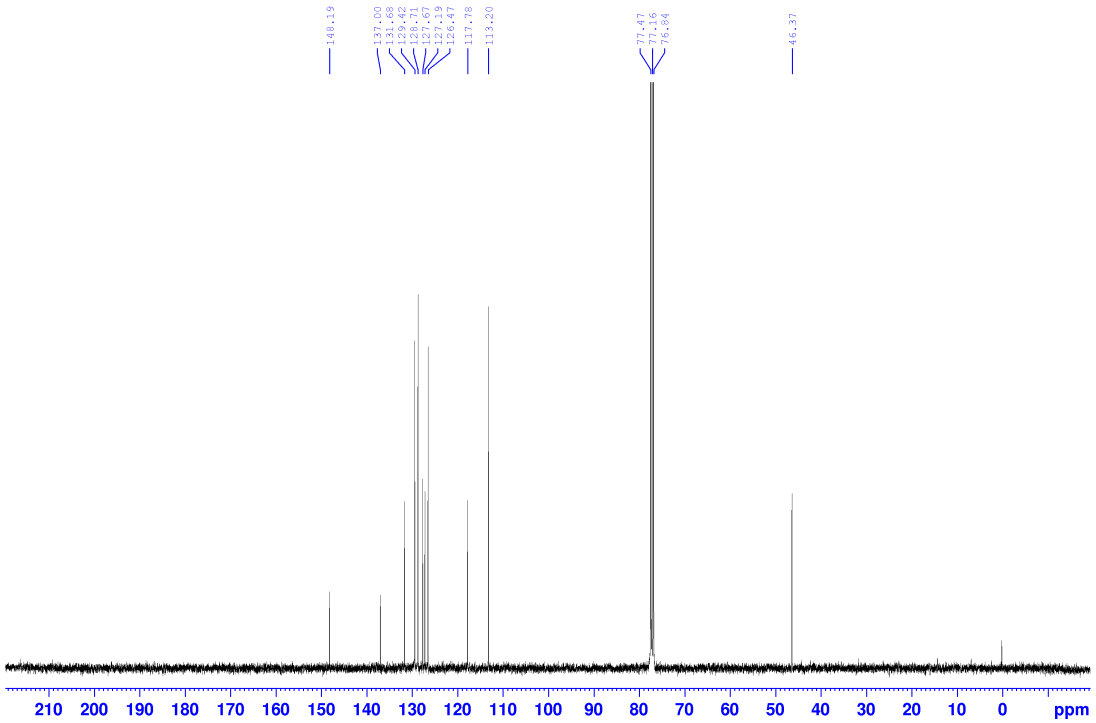

(*E*)-*N*-(4-methoxybenzyl)-3-phenylprop-2-en-1-amine 30b

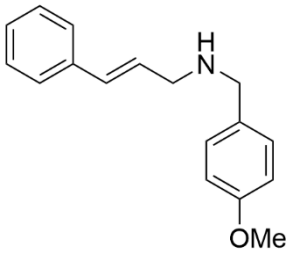

^{1}H NMR (400 MHz, $CDCl_3$)

^{13}C NMR (100.6 MHz, $CDCl_3$)

2-bromo-*N*-cinnamyl-*N*-phenylacetamide 31a

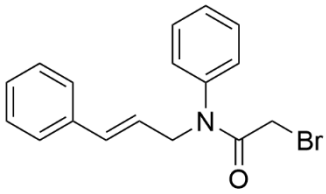

^{1}H NMR (400 MHz, $CDCl_3$)

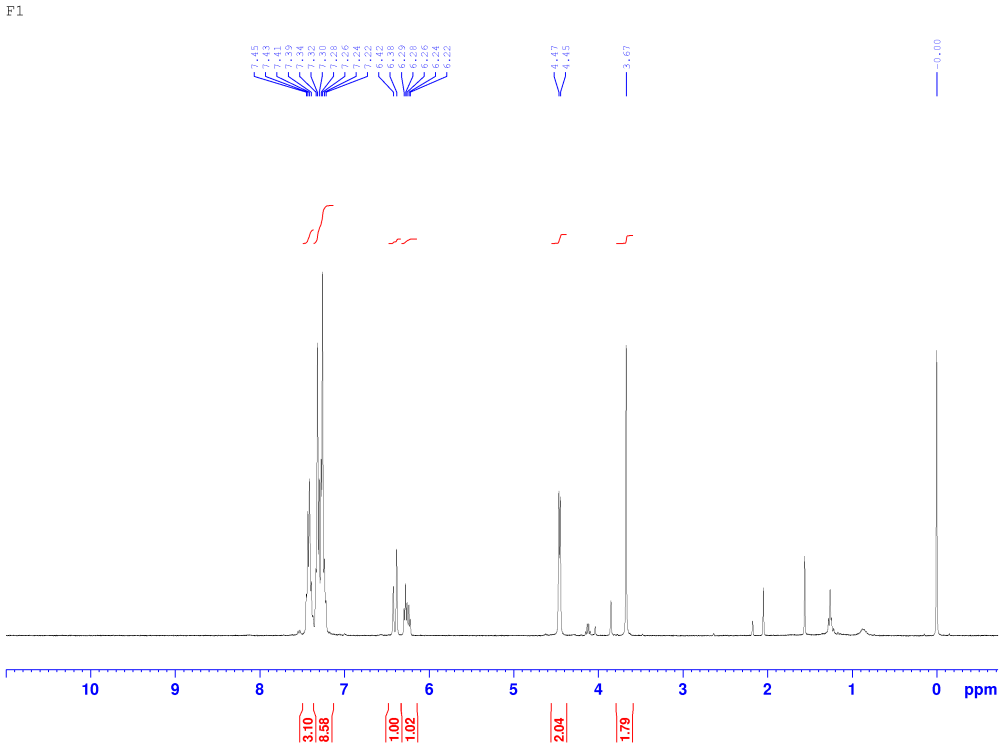

^{13}C NMR (100.6 MHz, $CDCl_3$)

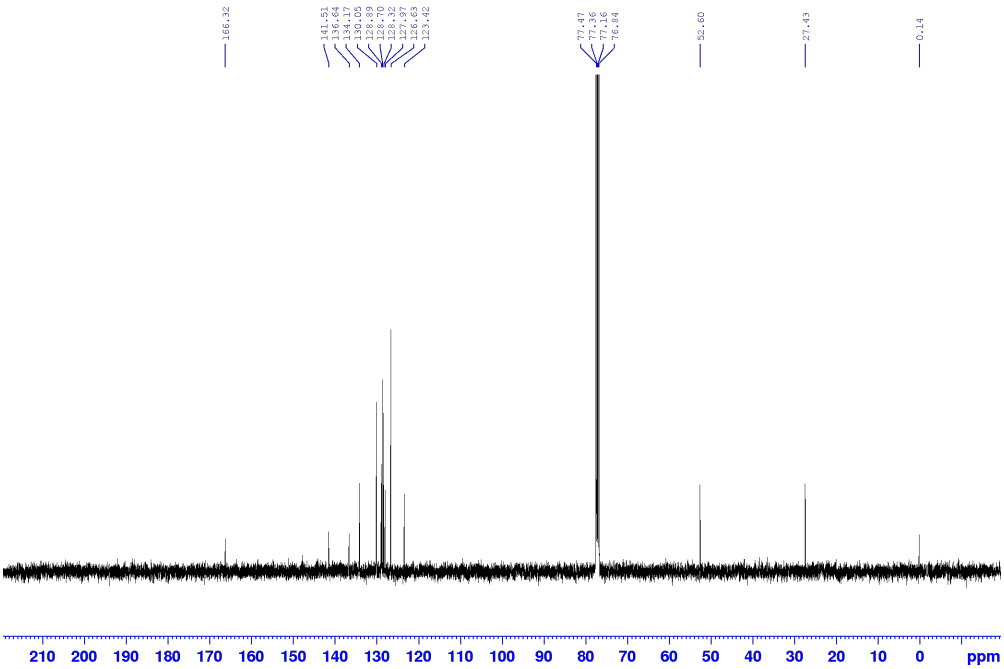

2-bromo-*N*-cinnamyl-*N*-(4-methoxybenzyl)acetamide 31b

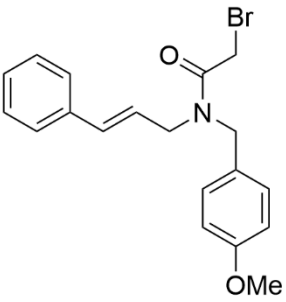

^{1}H NMR (400 MHz, $CDCl_3$)

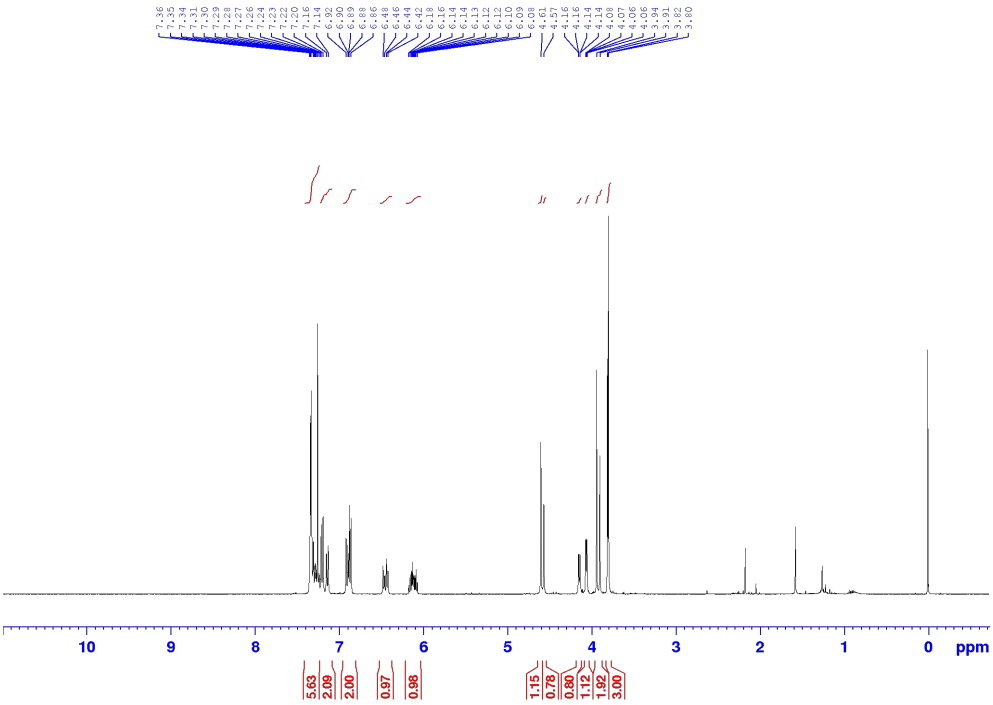

^{13}C NMR (100.6 MHz, $CDCl_3$)

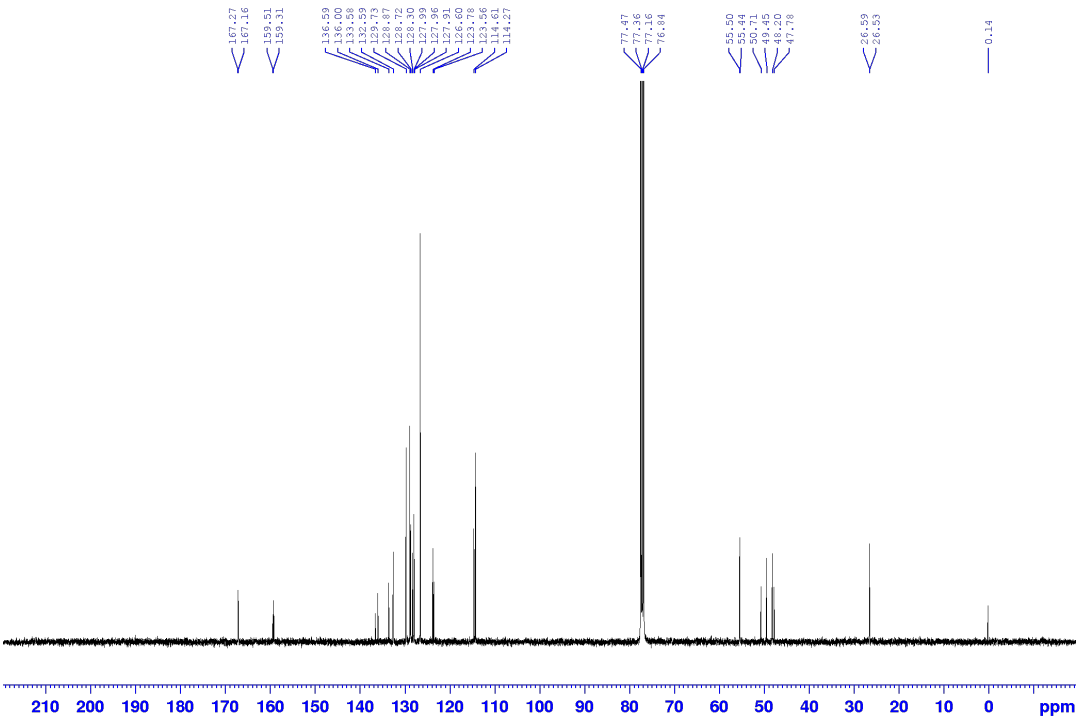
167.27
167.16
159.51
159.31
136.59
136.00
133.58
132.59
129.73
128.87
128.72
128.30
127.99
127.96
127.91
126.60
123.78
123.56
114.61
114.27
77.47
77.36
77.16
76.84
55.50
55.44
50.71
49.45
48.20
47.78
26.59
26.53
0.14
210 200 190 180 170 160 150 140 130 120 110 100 90 80 70 60 50 40 30 20 10 0 ppm

***N*-Cinnamyl-*N*-phenyl-2-(*p*-tolylamino)acetamide 1l**

^{1}H NMR (400 MHz, $CDCl_3$)

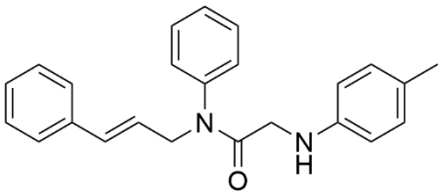

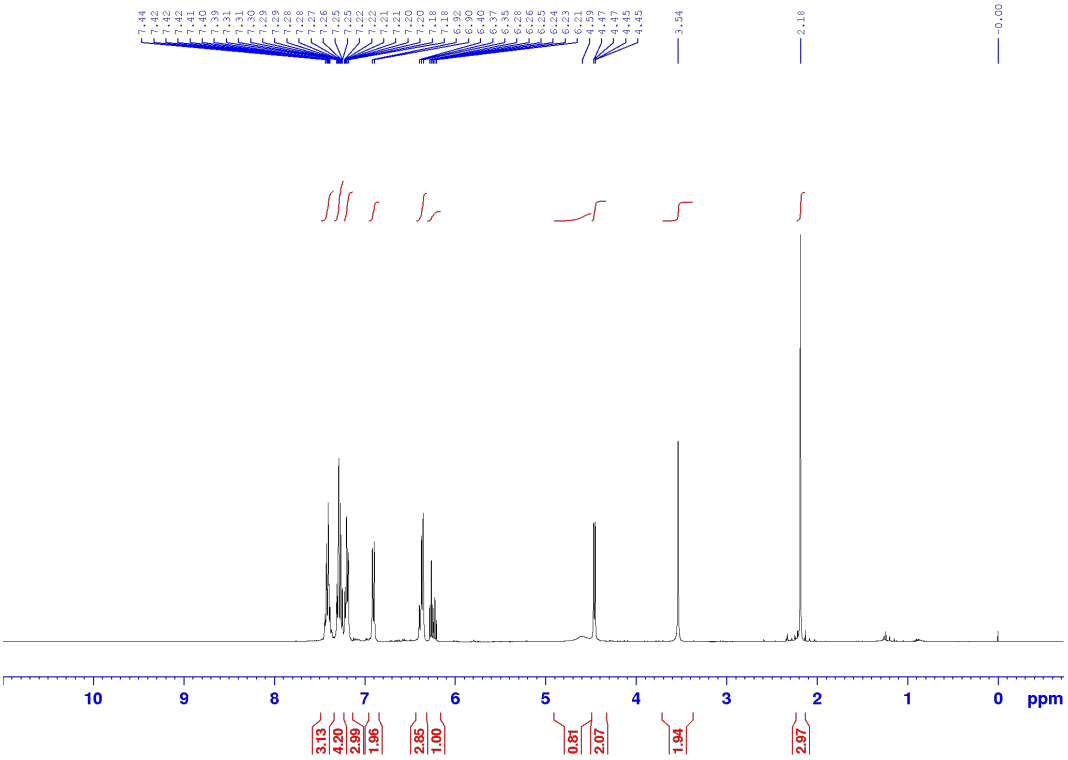

^{13}C NMR (100.6 MHz, $CDCl_3$)

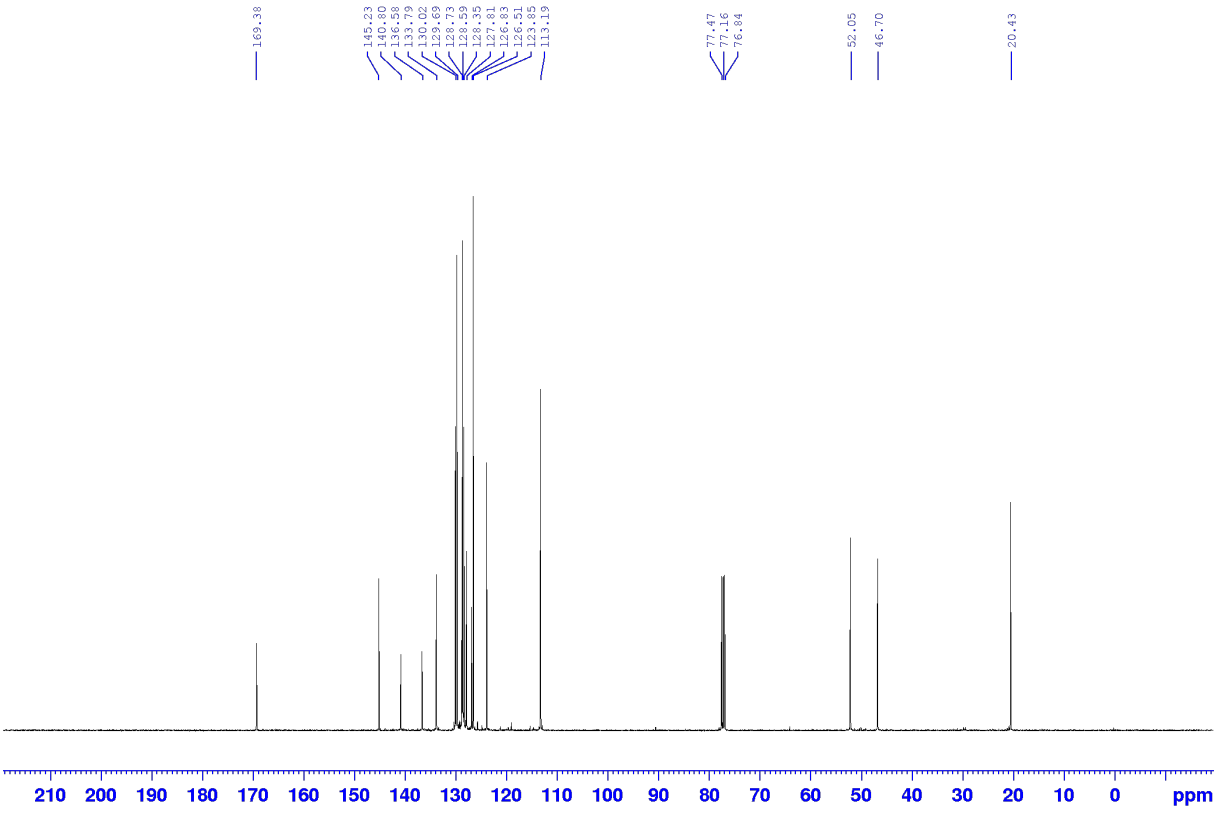
169.38
145.23
140.80
136.58
133.79
130.02
129.69
128.73
128.59
128.35
127.81
126.83
126.51
123.85
113.19
77.47
77.16
76.84
52.05
46.70
20.43
210 200 190 180 170 160 150 140 130 120 110 100 90 80 70 60 50 40 30 20 10 0 ppm

_N_-cinnamyl-_N_-(4-methoxybenzyl)-2-(_p_-tolylamino)acetamide 1m

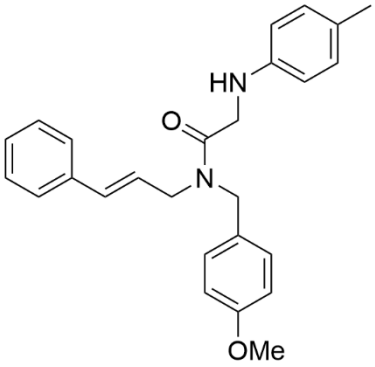

^{1}H NMR (400 MHz, $CDCl_3$)

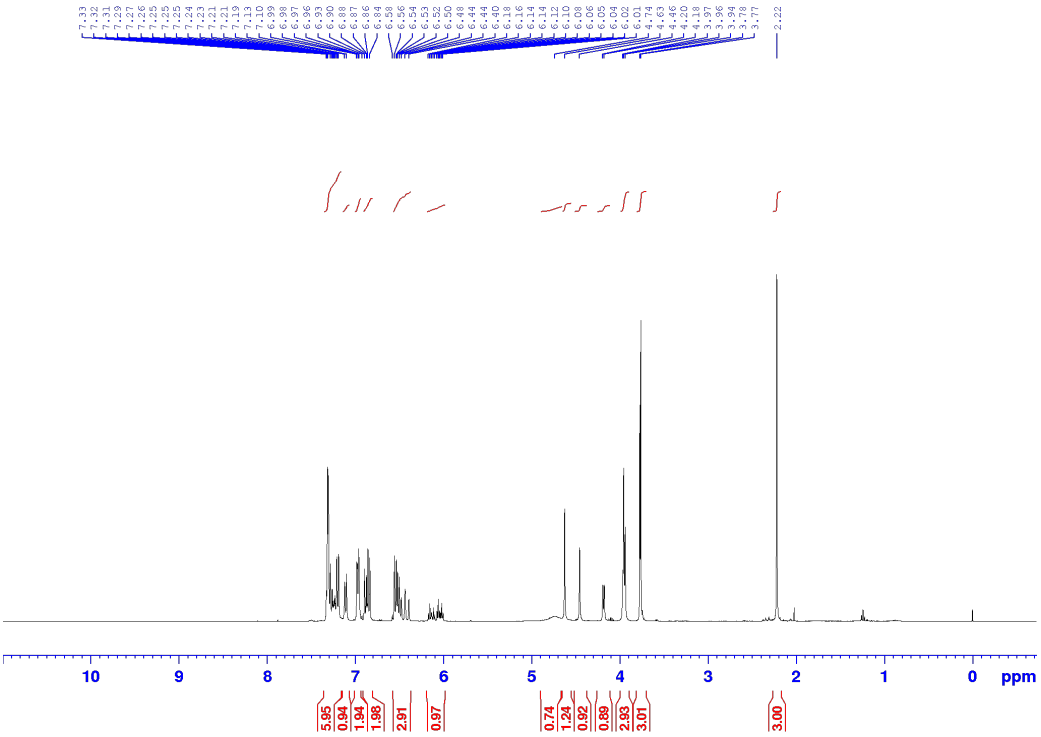

^{13}C NMR (100.6 MHz, $CDCl_3$)

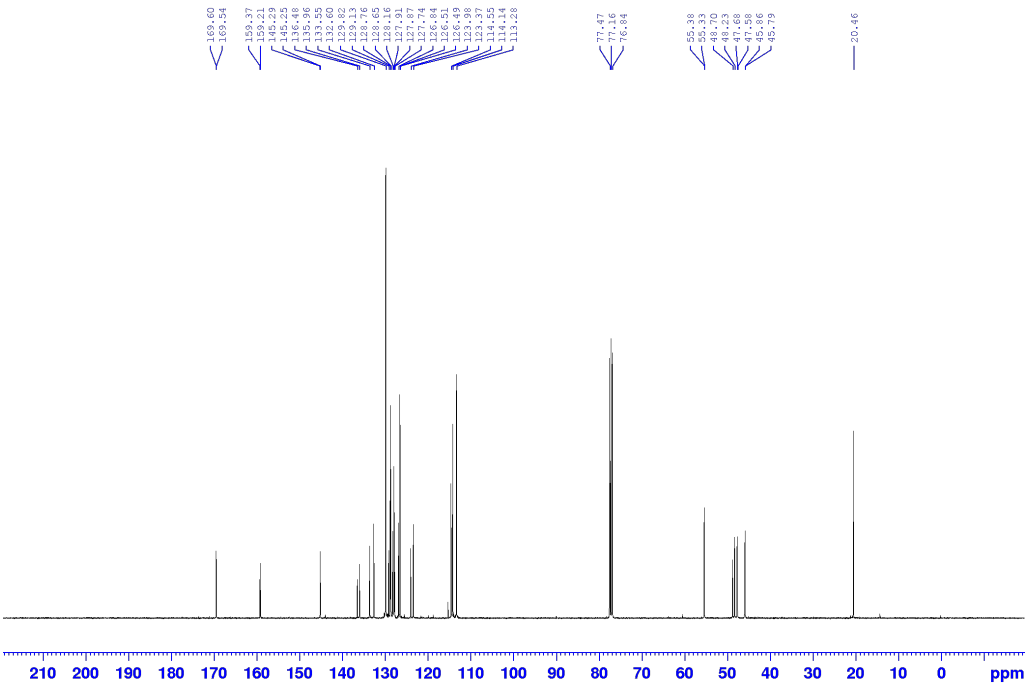
169.60
169.54
159.37
159.21
145.29
145.25
136.48
135.96
133.55
132.60
129.82
129.13
128.76
128.65
128.16
127.91
127.87
127.74
126.84
126.51
126.49
123.98
123.37
114.55
114.14
113.28
77.47
77.16
76.84
55.38
55.33
48.70
48.23
47.68
47.58
45.86
45.79
20.46
210 200 190 180 170 160 150 140 130 120 110 100 90 80 70 60 50 40 30 20 10 0 ppm

ethyl *p*-tolylglycinate 6i

^{1}H NMR (400 MHz, $CDCl_3$)

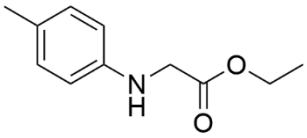

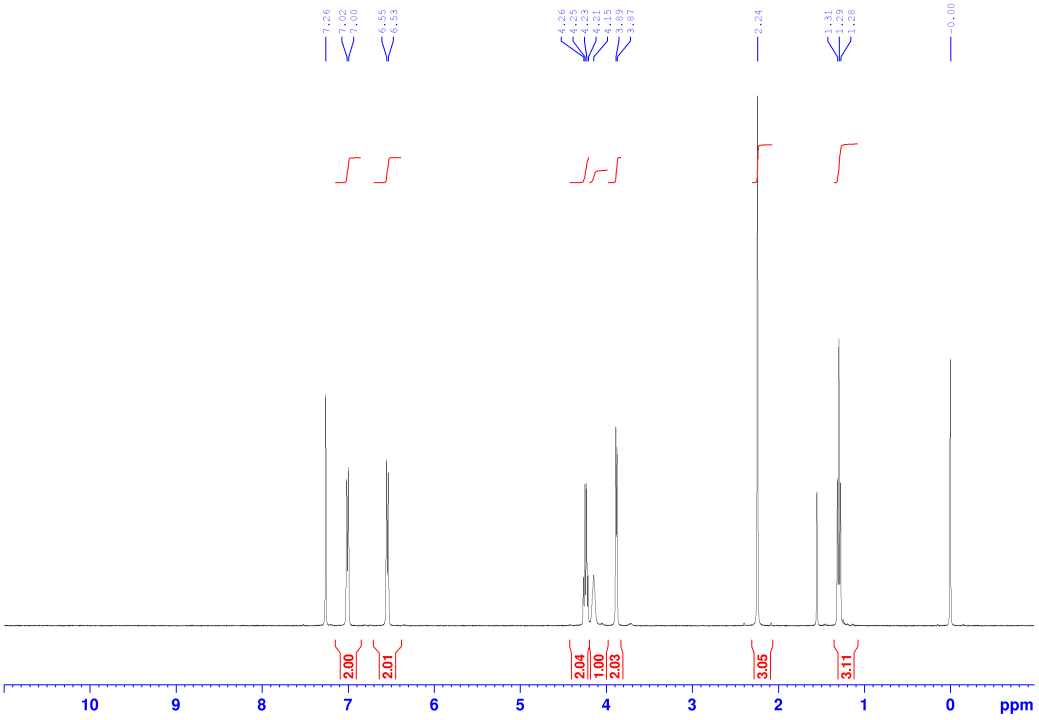

^{13}C NMR (100.6 MHz, $CDCl_3$)

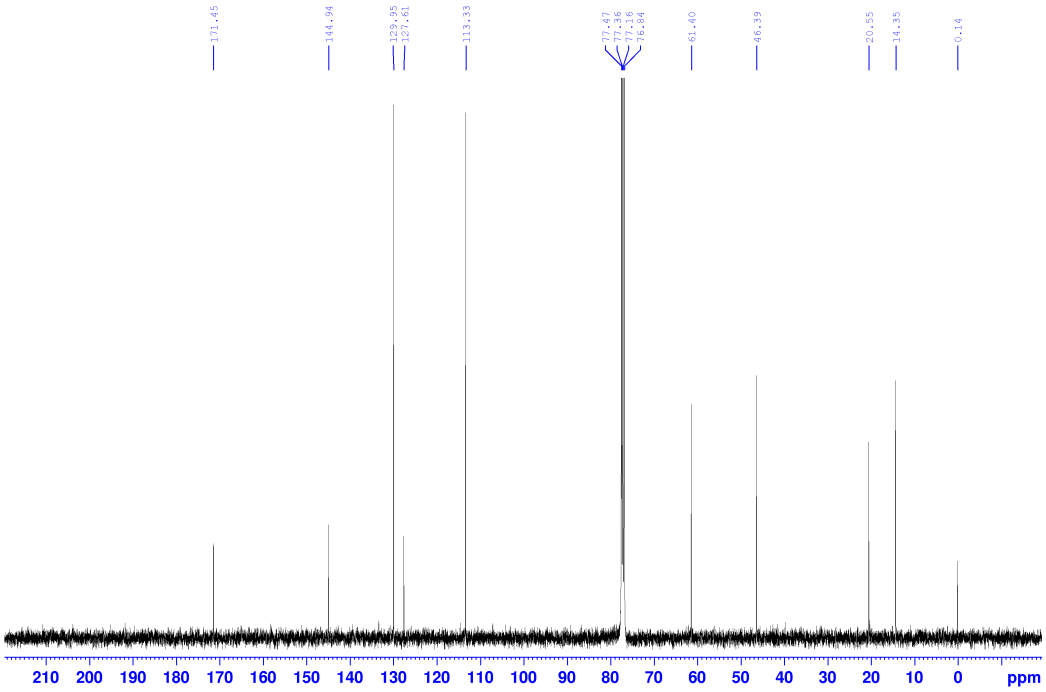
171.45
144.94
129.95
127.61
113.33
77.47
77.36
77.16
76.84
61.40
46.39
20.55
14.35
0.14
210 200 190 180 170 160 150 140 130 120 110 100 90 80 70 60 50 40 30 20 10 0 ppm

1-(*p*-tolylamino)propan-2-one 6n

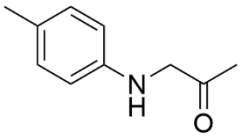

^{1}H NMR (400 MHz, $CDCl_3$)

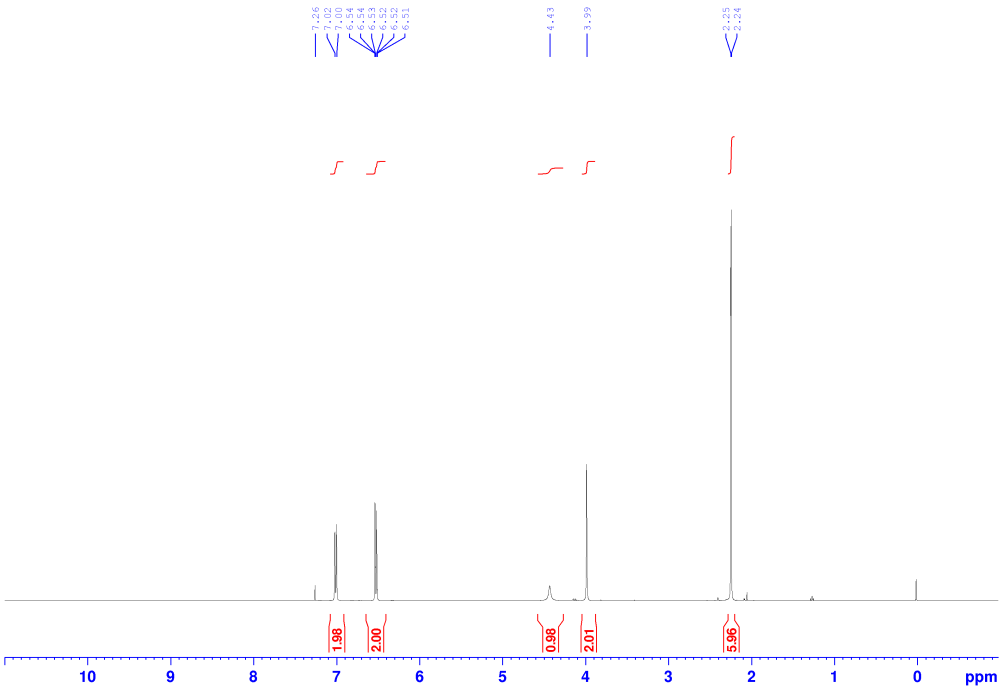

^{13}C NMR (100.6 MHz, $CDCl_3$)

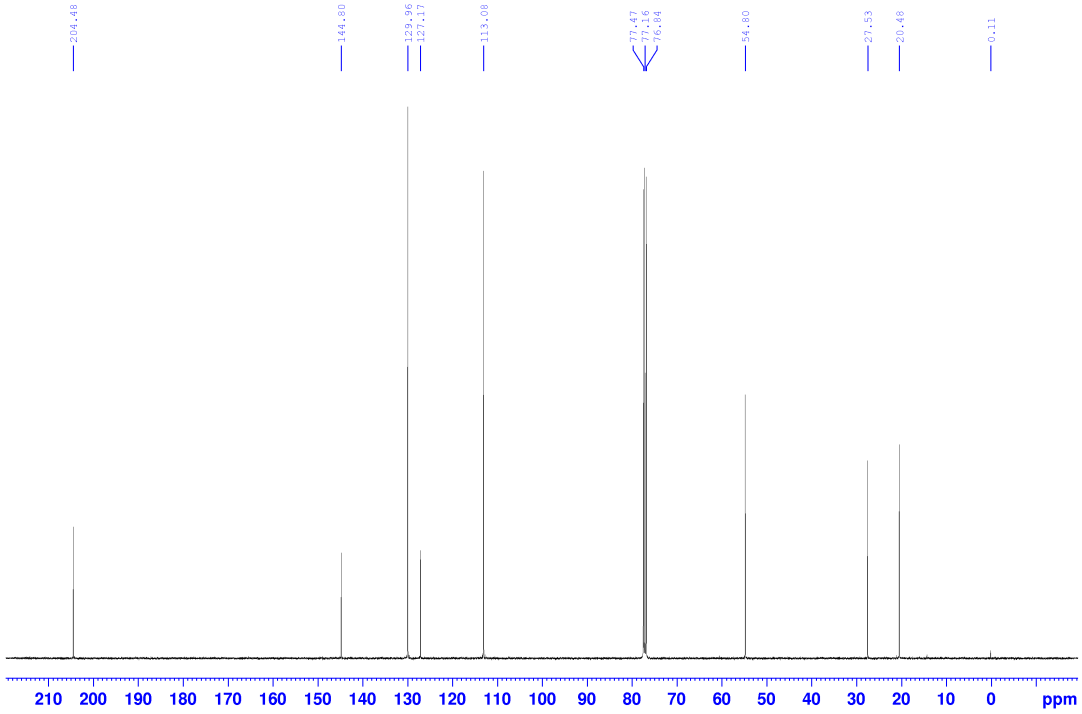
204.48
144.80
129.96
127.17
113.08
77.47
77.16
76.84
54.80
27.53
20.48
0.11
210 200 190 180 170 160 150 140 130 120 110 100 90 80 70 60 50 40 30 20 10 0 ppm

2-((4-methylphenyl)amino)acetic acid 33

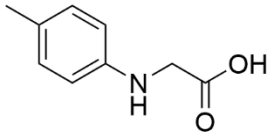

^{1}H NMR (400 MHz, $CDCl_3$)

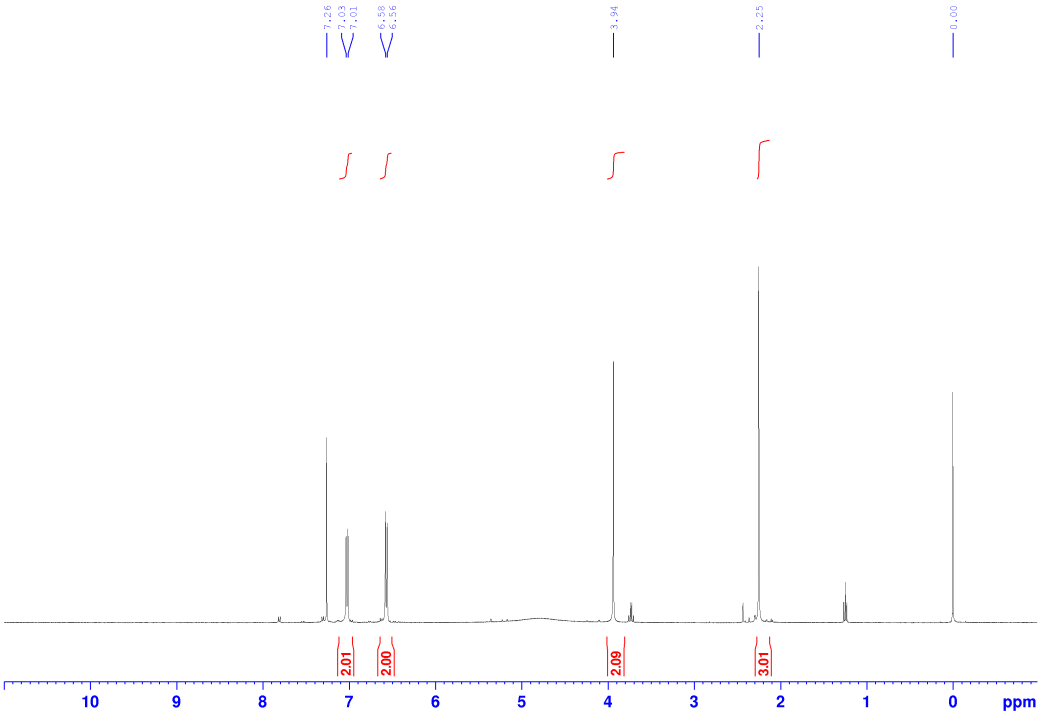

^{13}C NMR (100.6 MHz, $CDCl_3$)

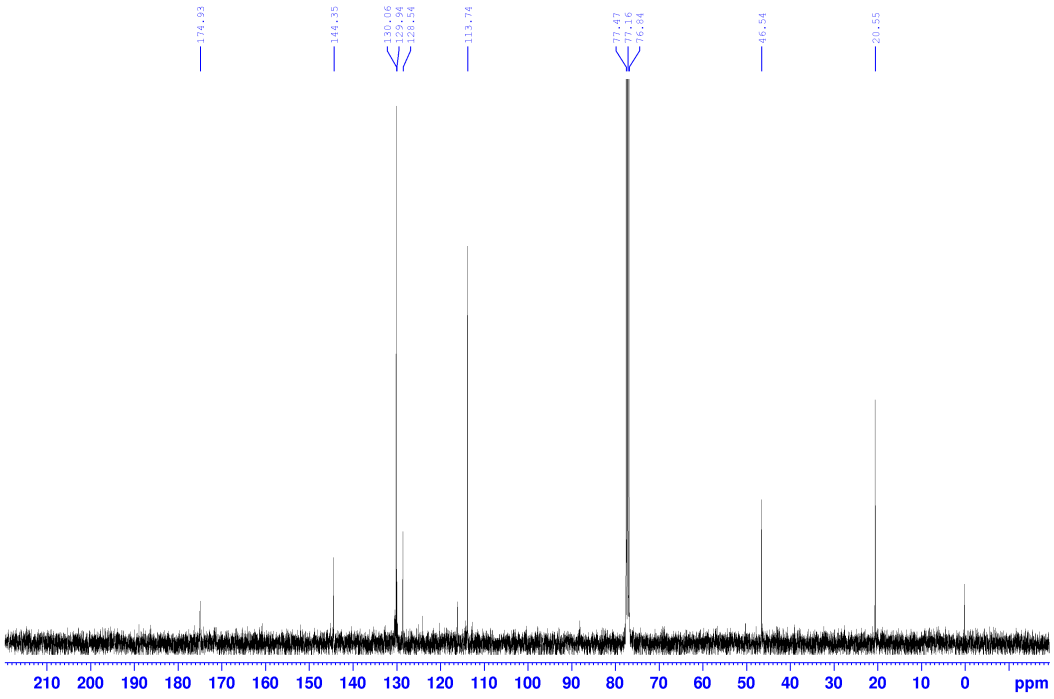
174.93
144.35
130.06
129.94
128.54
113.74
77.47
77.16
76.84
46.54
20.55
210 200 190 180 170 160 150 140 130 120 110 100 90 80 70 60 50 40 30 20 10 0 ppm

***N*-(*tert*-butoxycarbonyl)-*N*-(*p*-tolyl)glycine 34**

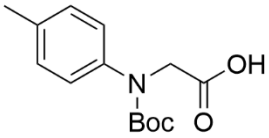

^{1}H NMR (400 MHz, $CDCl_3$)

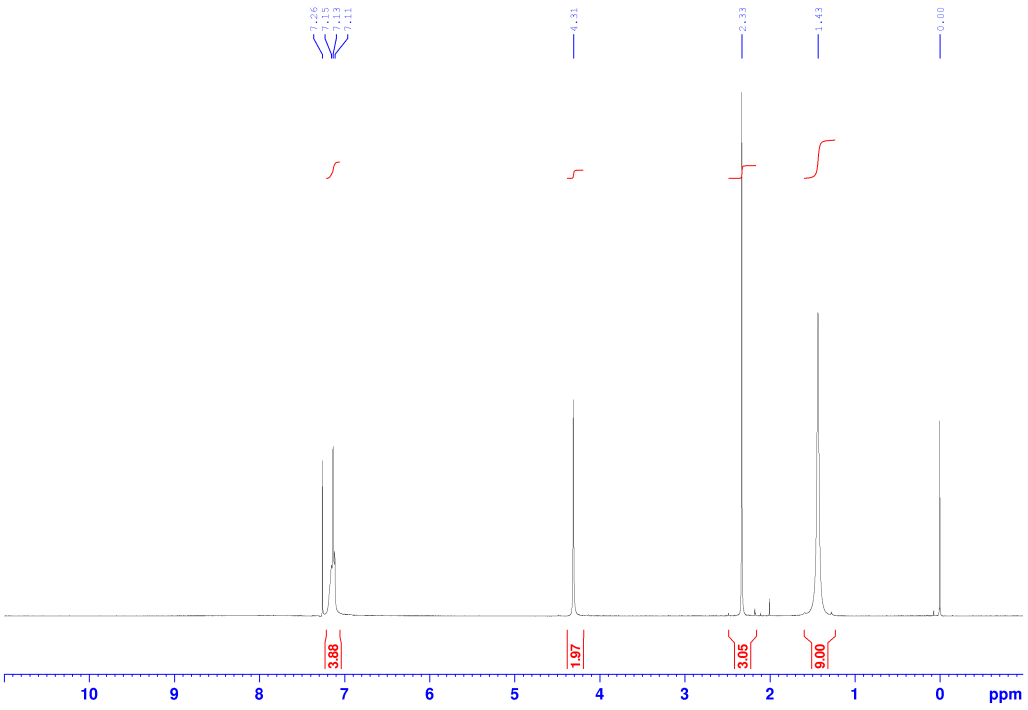

^{13}C NMR (100.6 MHz, $CDCl_3$)

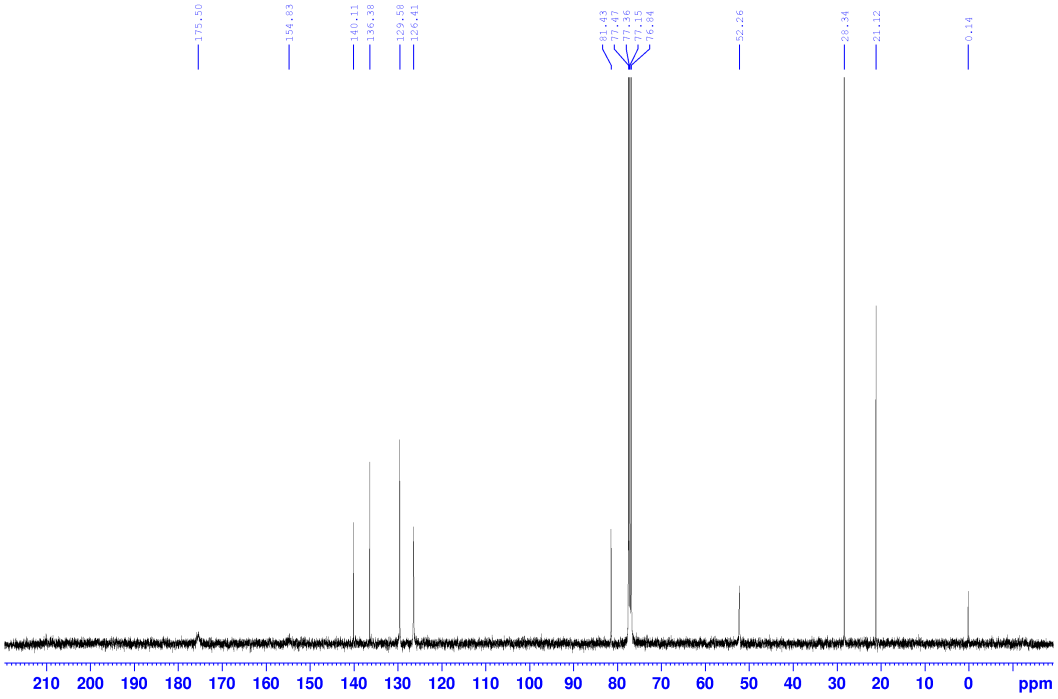
175.50
154.83
140.11
136.38
129.58
126.41
81.43
77.47
77.36
77.15
76.84
52.26
28.34
21.12
0.14
210 200 190 180 170 160 150 140 130 120 110 100 90 80 70 60 50 40 30 20 10 0 ppm

***tert*-butyl (2-(isopropylamino)-2-oxoethyl)(*p*-tolyl)carbamate 35a**

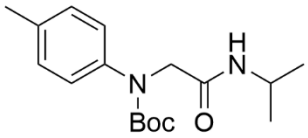

^{1}H NMR (400 MHz, $CDCl_3$)

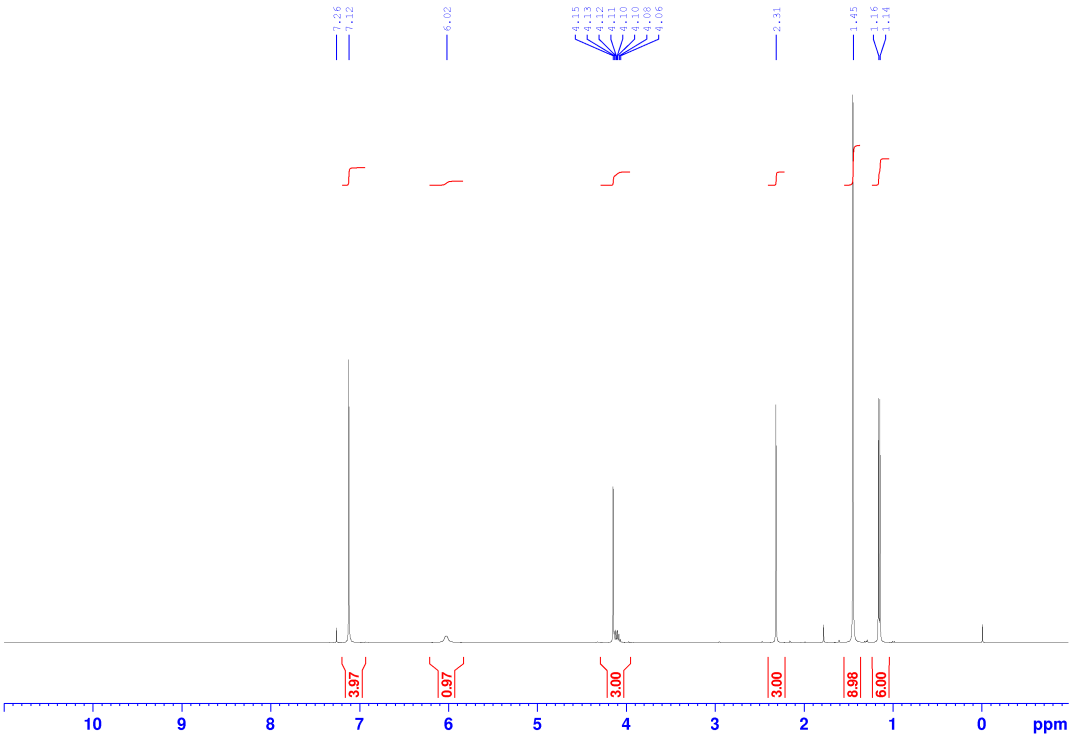

^{13}C NMR (100.6 MHz, $CDCl_3$)

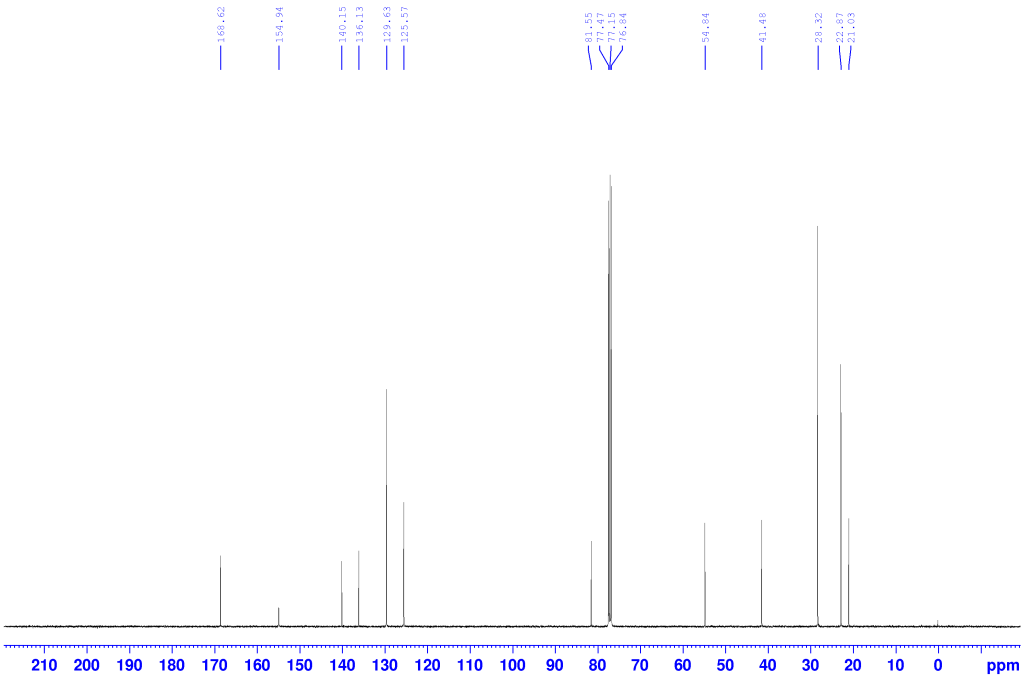
168.62
154.94
140.15
136.13
129.63
125.57
81.55
77.47
77.15
76.84
54.84
41.48
28.32
22.87
21.03
210 200 190 180 170 160 150 140 130 120 110 100 90 80 70 60 50 40 30 20 10 0 ppm

***tert*-butyl (2-oxo-2-(phenylamino)ethyl)(*p*-tolyl)carbamate 35b**

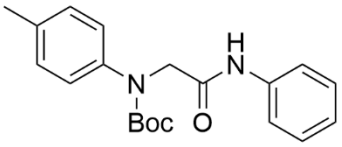

^{1}H NMR (400 MHz, $CDCl_3$)

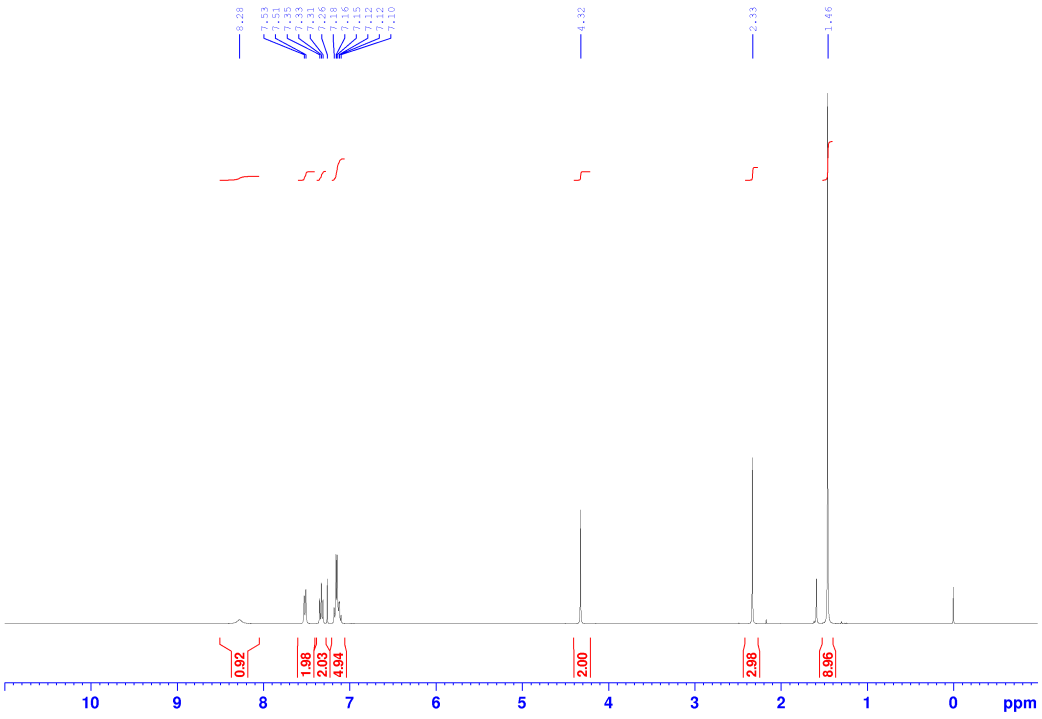

^{13}C NMR (100.6 MHz, $CDCl_3$)

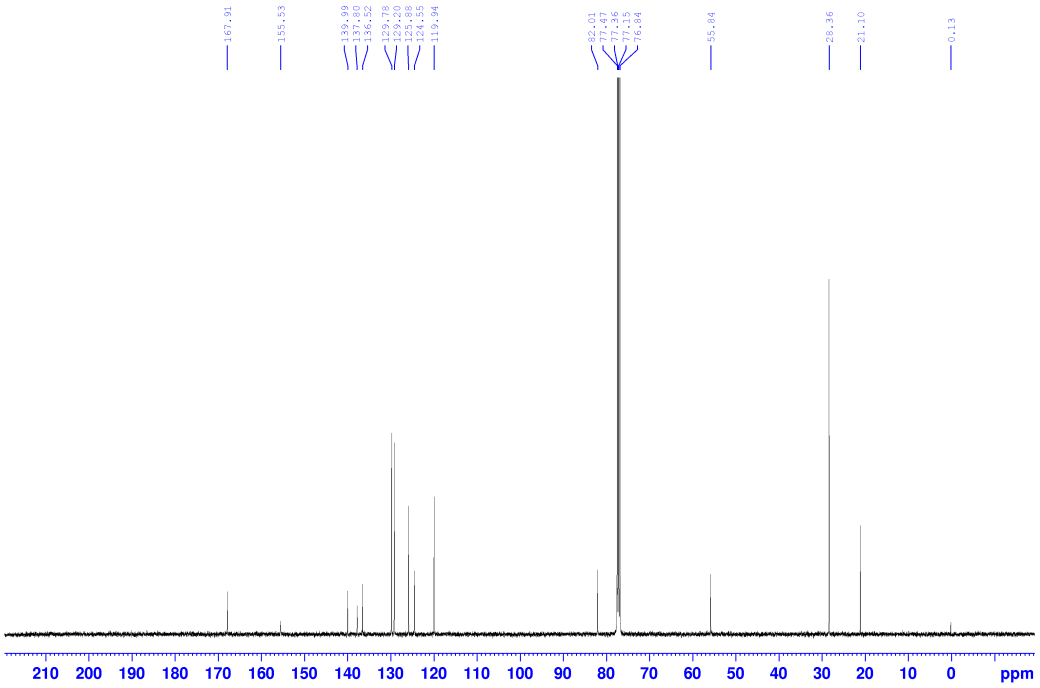

tert-butyl (2-oxo-2-((4-(trifluoromethoxy)phenyl)amino)ethyl)(p-tolyl)carbamate
35c

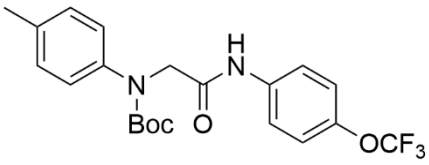

^{1}H NMR (400 MHz, $CDCl_3$)

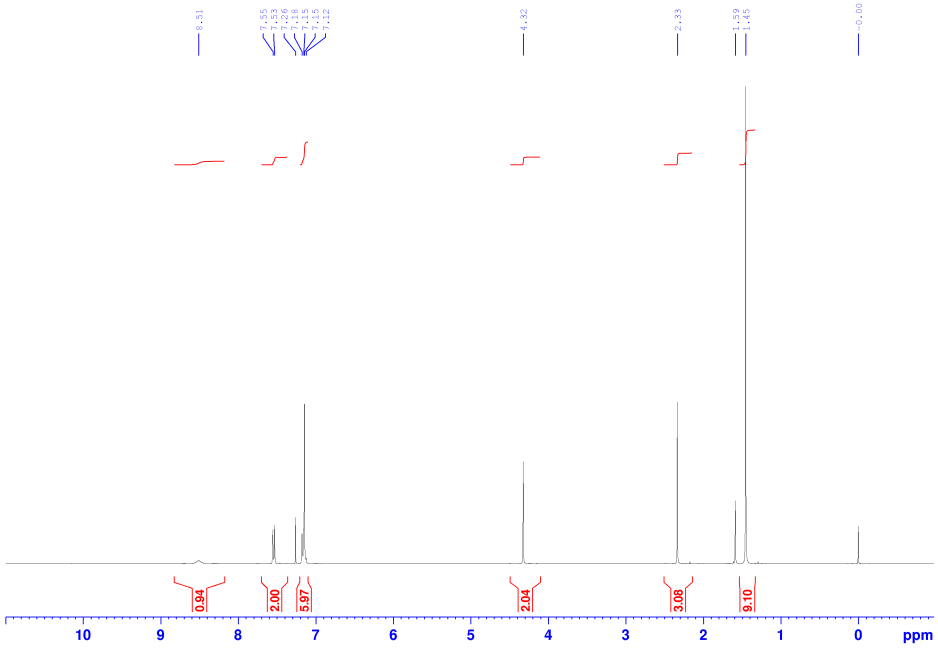

^{13}C NMR (100.6 MHz, $CDCl_3$)

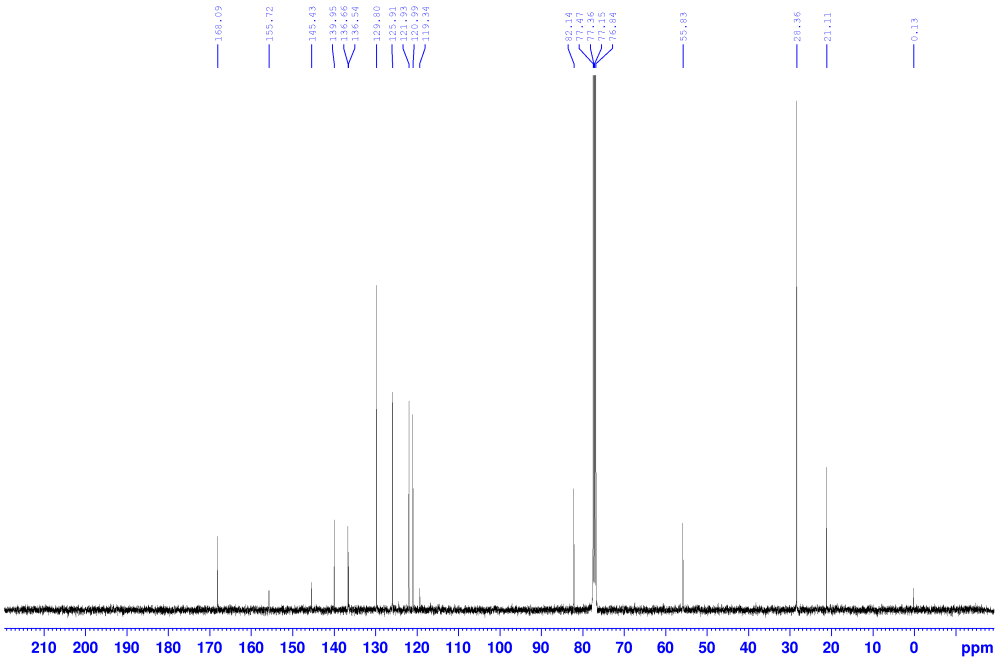

_S_-phenyl 2-((_tert_-butoxycarbonyl)(_p_-tolyl)amino)ethanethioate 35d

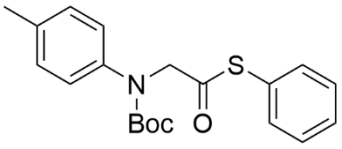

^{1}H NMR (400 MHz, $CDCl_3$)

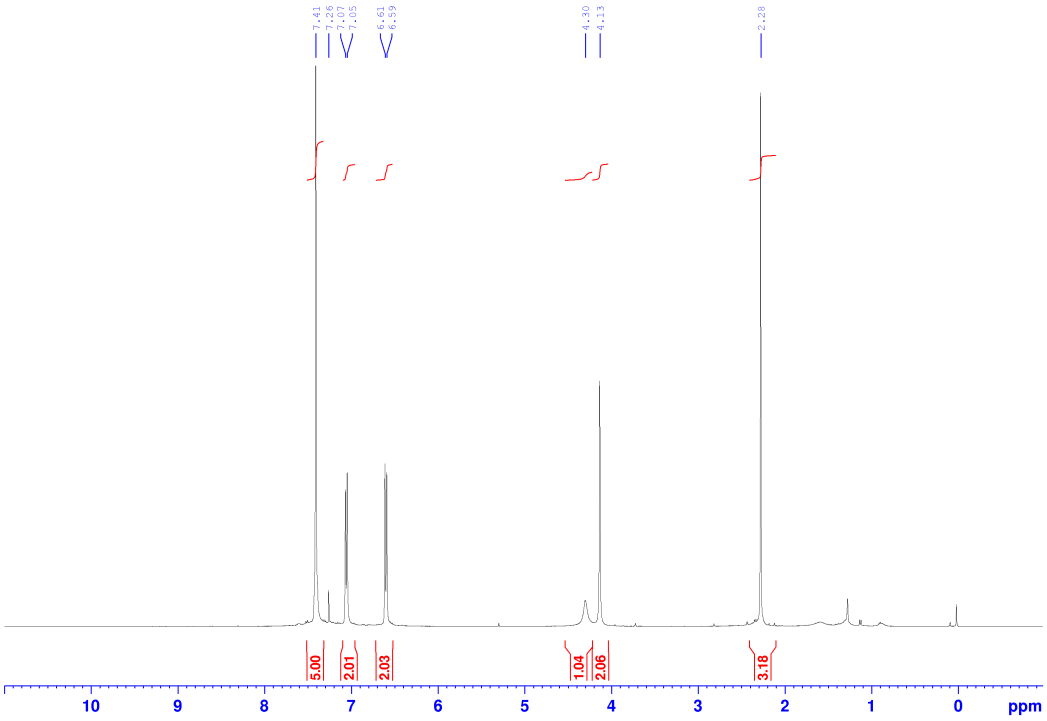

^{13}C NMR (100.6 MHz, $CDCl_3$)

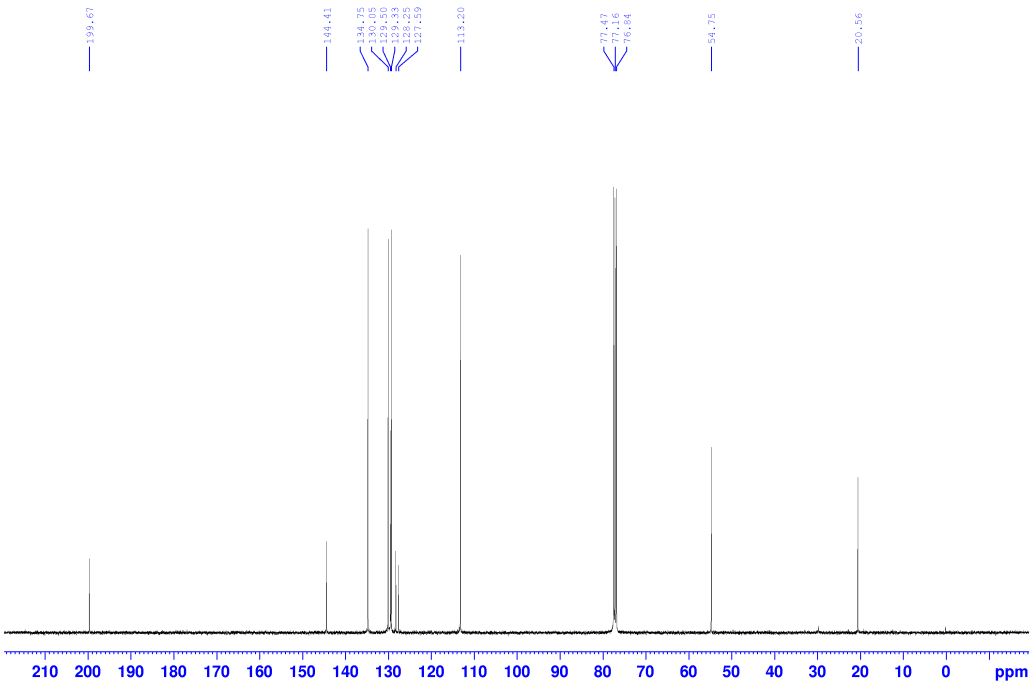
199.67
144.41
134.75
130.05
129.50
129.33
128.25
127.59
113.20
77.47
77.16
76.84
54.75
20.56
210 200 190 180 170 160 150 140 130 120 110 100 90 80 70 60 50 40 30 20 10 0 ppm

***N*-isopropyl-2-(*p*-tolylamino)acetamide6j**

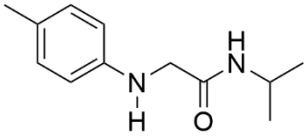

^{1}H NMR (400 MHz, $CDCl_3$)

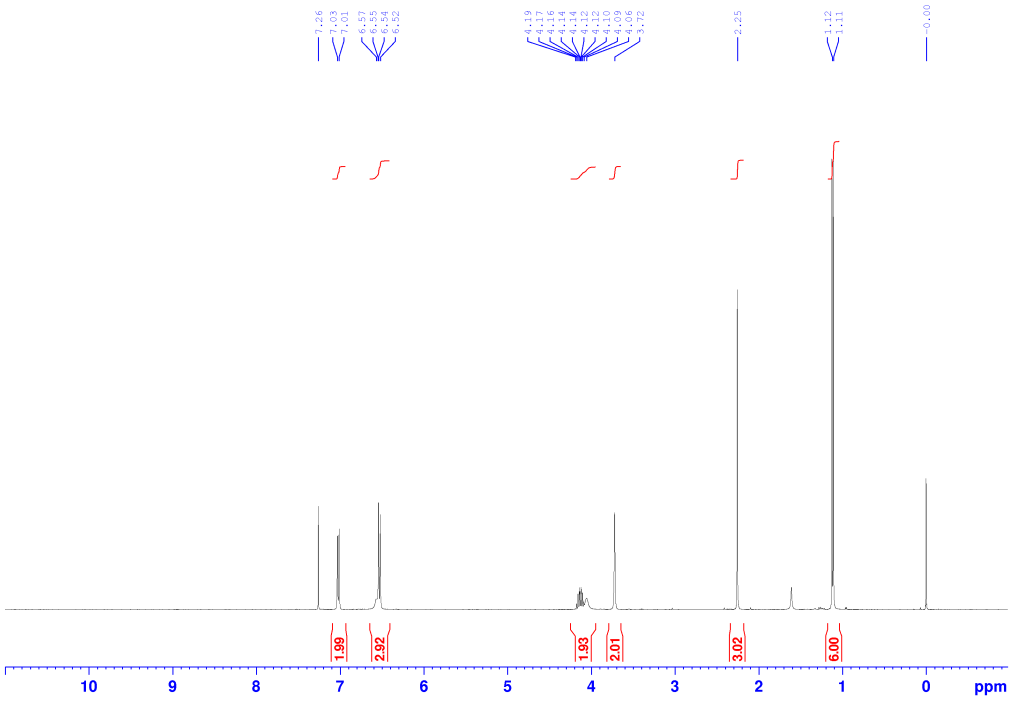

^{13}C NMR (100.6 MHz, $CDCl_3$)

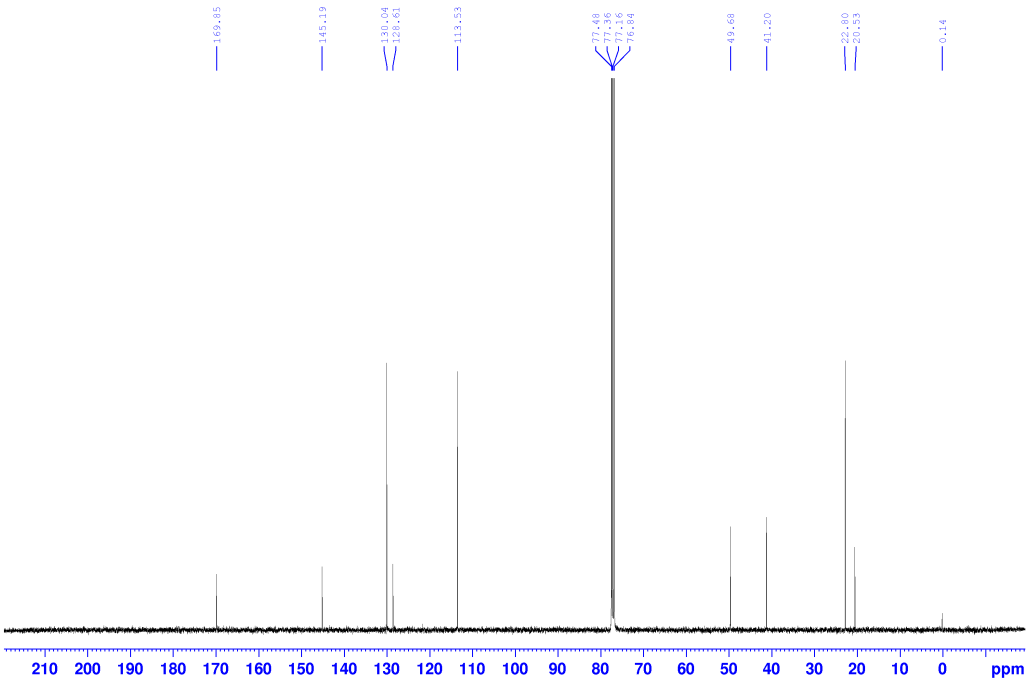
169.85
145.19
130.04
128.61
113.53
77.48
77.36
77.16
76.84
49.68
41.20
22.80
20.53
0.14
210 200 190 180 170 160 150 140 130 120 110 100 90 80 70 60 50 40 30 20 10 0 ppm

_N_-phenyl-2-(_p_-tolylamino)acetamide 6k

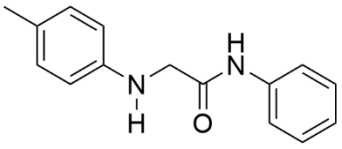

^{1}H NMR (400 MHz, $CDCl_3$)

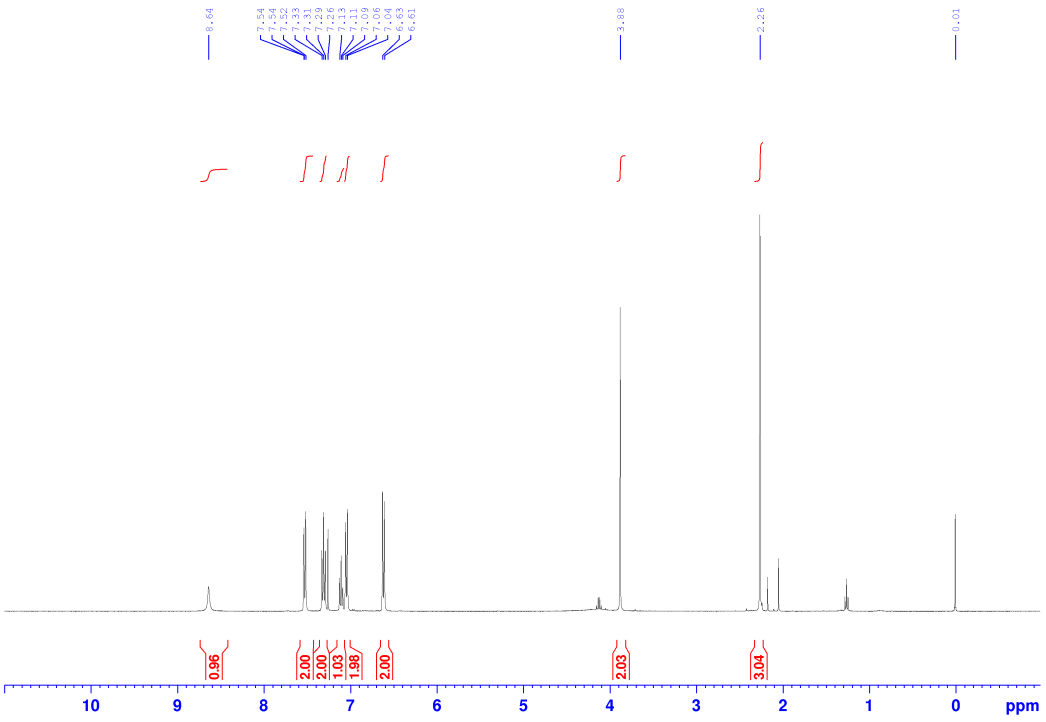

^{13}C NMR (100.6 MHz, $CDCl_3$)

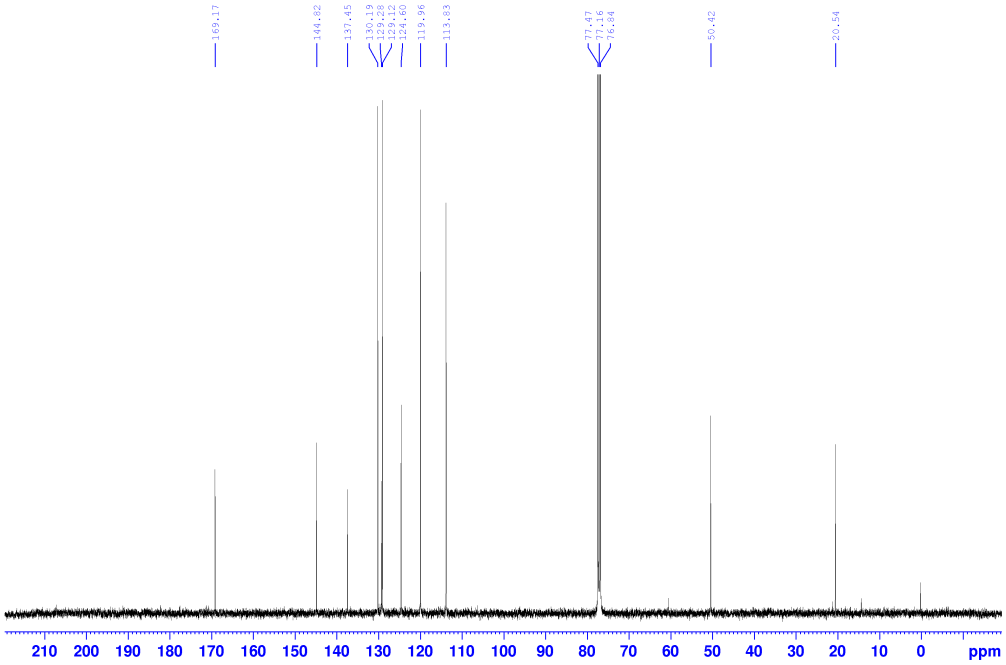
169.17
144.82
137.45
130.19
130.08
129.12
124.60
119.96
113.83
77.47
77.16
76.84
50.42
20.54
210 200 190 180 170 160 150 140 130 120 110 100 90 80 70 60 50 40 30 20 10 0 ppm

2-(*p*-tolylamino)-*N*-(4-(trifluoromethoxy)phenyl)acetamide 6i

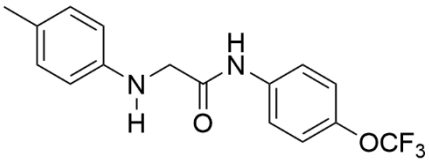

^{1}H NMR (400 MHz, $CDCl_3$)

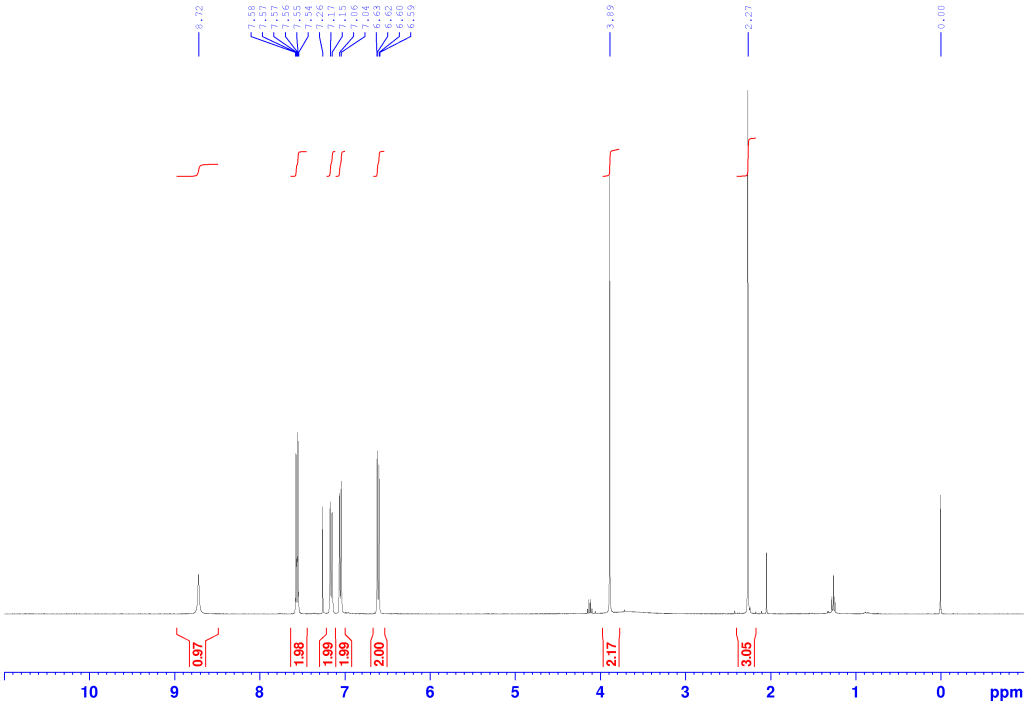

^{13}C NMR (100.6 MHz, $CDCl_3$)

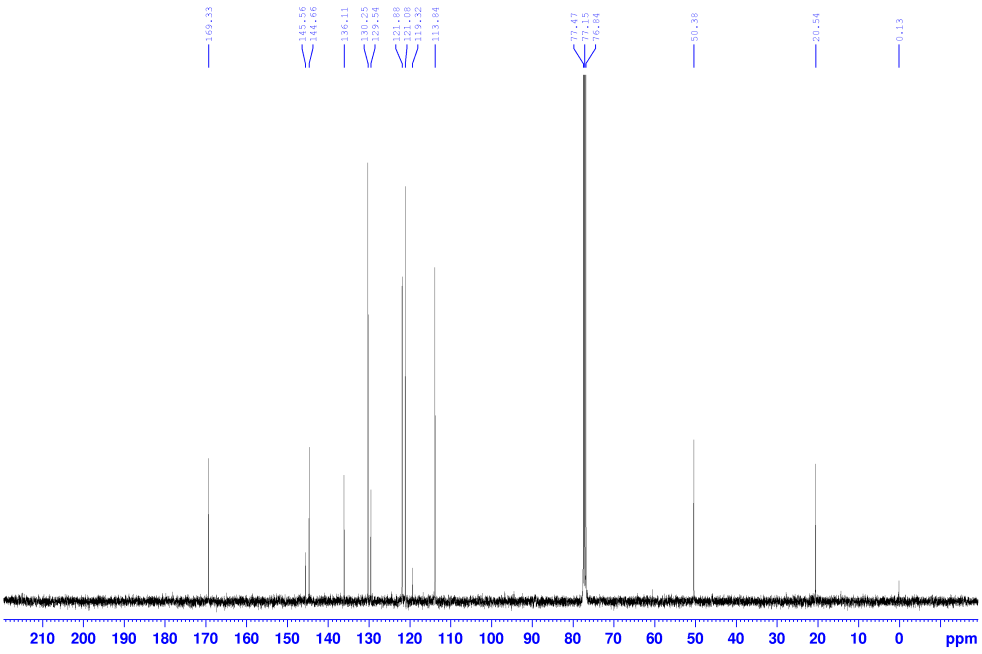
169.33
145.56
144.66
136.11
130.25
129.54
121.88
121.38
119.32
113.84
77.47
77.15
76.84
50.38
20.54
0.13
210 200 190 180 170 160 150 140 130 120 110 100 90 80 70 60 50 40 30 20 10 0 ppm

_S_-phenyl 2-(_p_-tolylamino)ethanethioate 6m

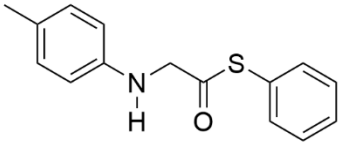

^{1}H NMR (400 MHz, $CDCl_3$)

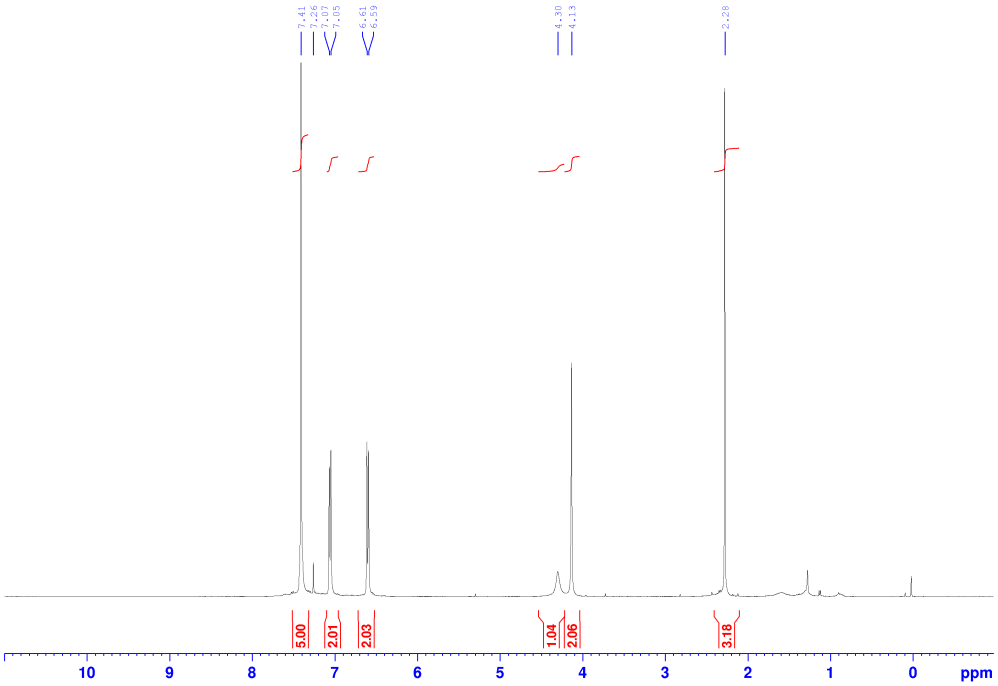

^{13}C NMR (100.6 MHz, $CDCl_3$)

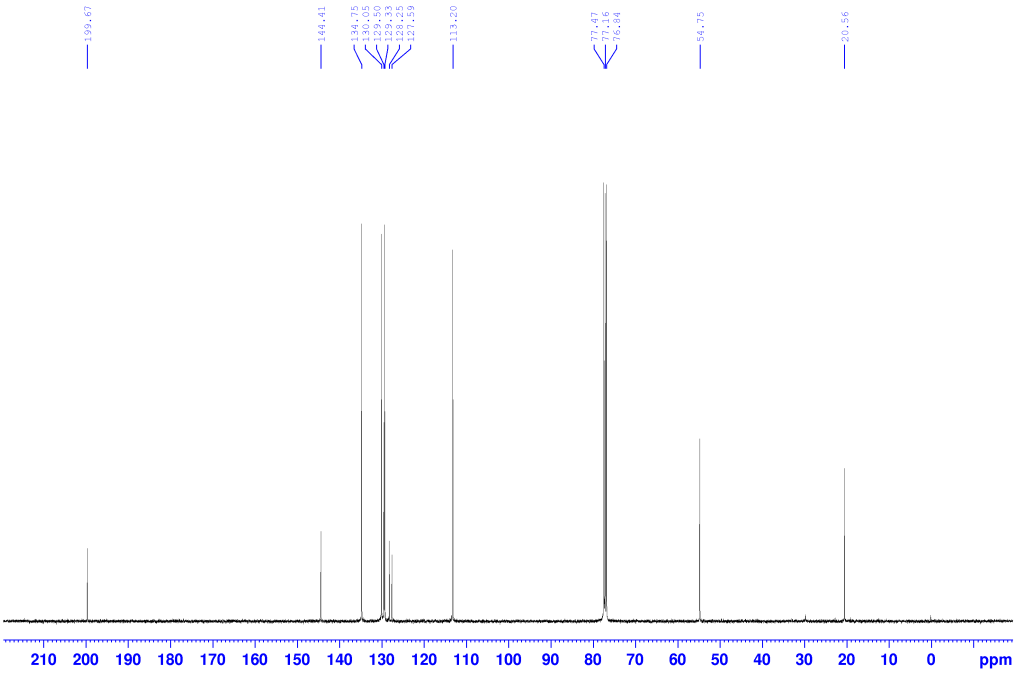
199.67
144.41
134.75
130.05
129.50
129.33
128.25
127.59
113.20
77.47
77.16
76.84
54.75
20.56
210 200 190 180 170 160 150 140 130 120 110 100 90 80 70 60 50 40 30 20 10 0 ppm

ethyl cyclohexylglycinate 6n

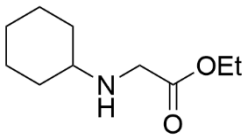

^{1}H NMR (400 MHz, $CDCl_3$)

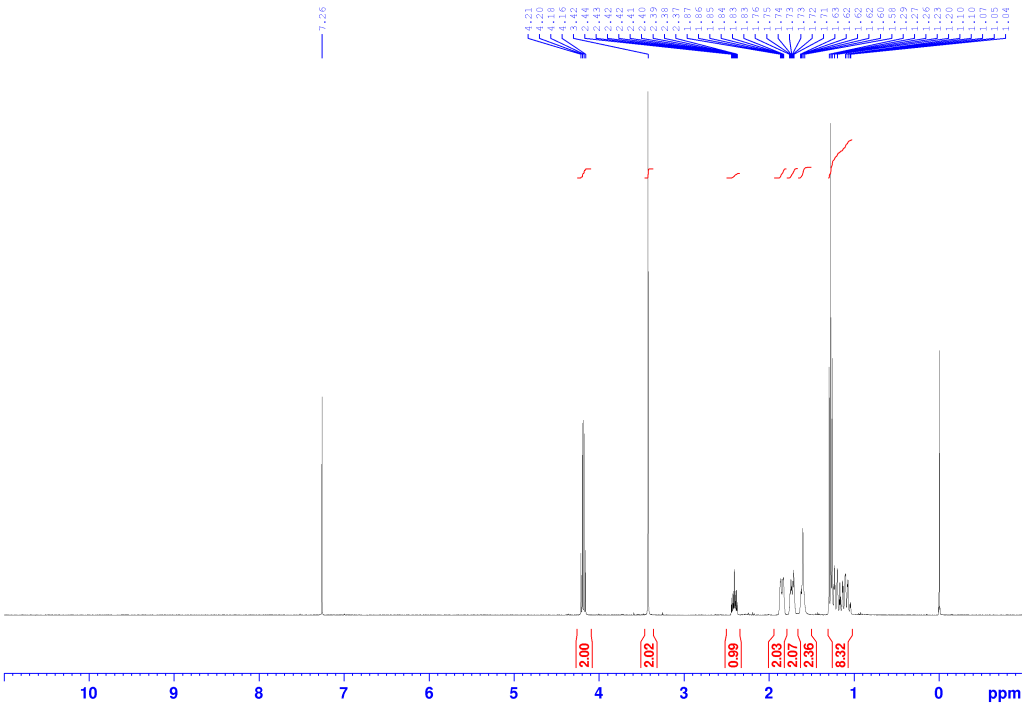

^{13}C NMR (100.6 MHz, $CDCl_3$)

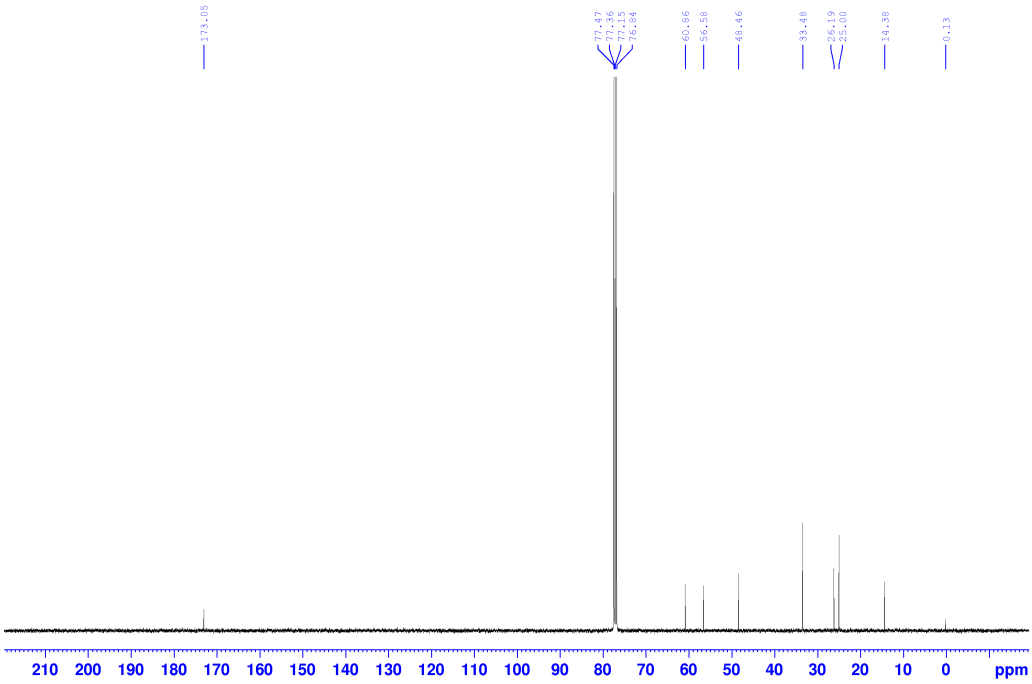
173.05
77.47
77.36
77.15
76.84
60.86
56.58
48.46
33.48
26.19
25.00
14.38
0.13
210 200 190 180 170 160 150 140 130 120 110 100 90 80 70 60 50 40 30 20 10 0 ppm

S6.3 Products

7-Methyl-9-phenylfuro[3,4-*b*]quinolin-3(1*H*)-one 4a

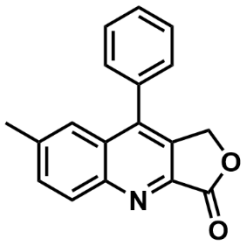

^{1}H NMR (400 MHz, $CDCl_3$)

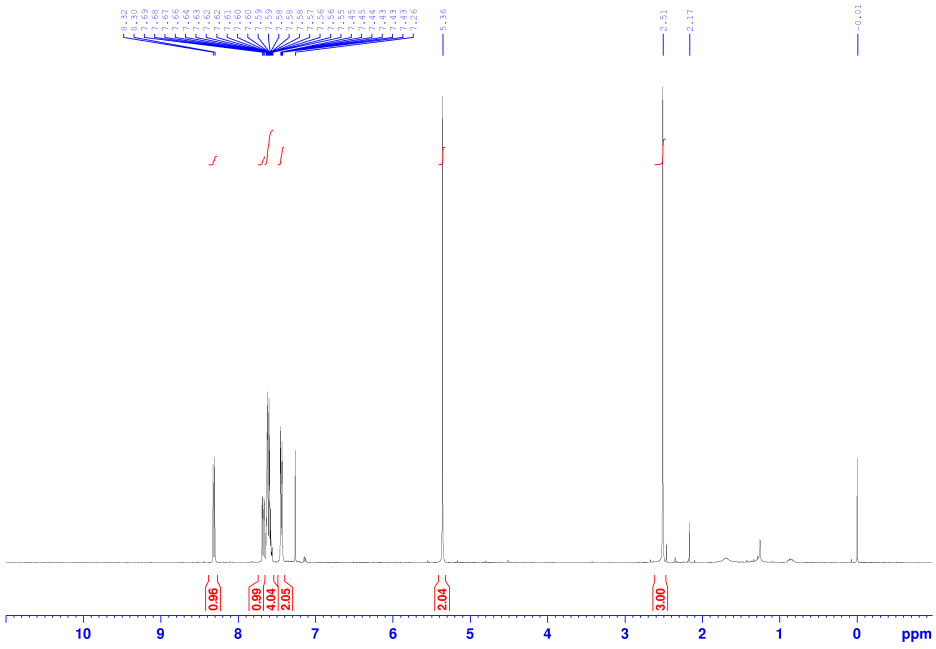

^{13}C NMR (100.6 MHz, $CDCl_3$)

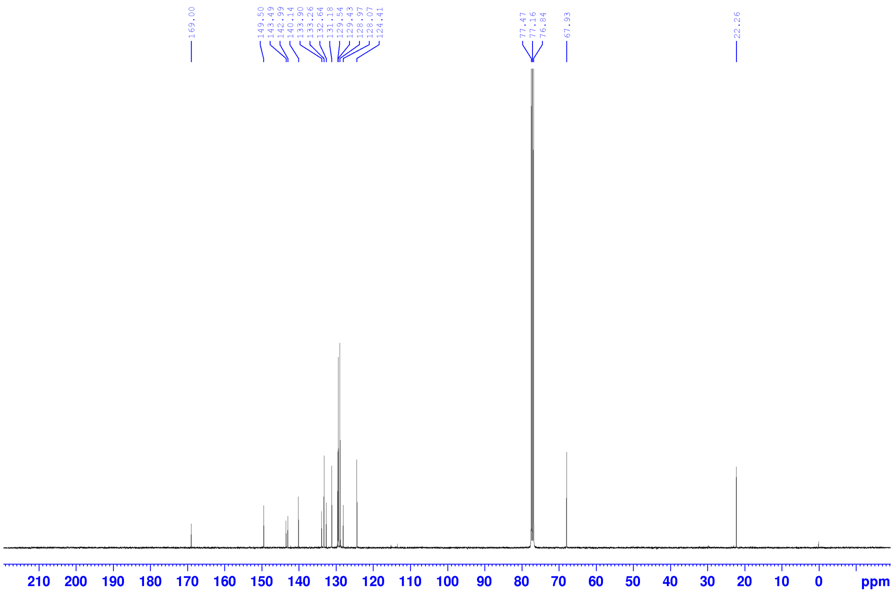
169.00
149.50
143.49
142.99
140.14
133.90
133.26
132.64
131.18
129.54
129.43
128.97
128.07
124.41
77.47
77.16
76.84
67.93
22.26
210 200 190 180 170 160 150 140 130 120 110 100 90 80 70 60 50 40 30 20 10 0 ppm

7-Methoxy-9-phenylfuro[3,4-*b*]quinolin-3(1*H*)-one 4b

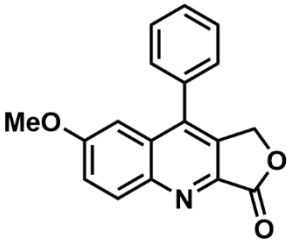

^{1}H NMR (400 MHz, $CDCl_3$)

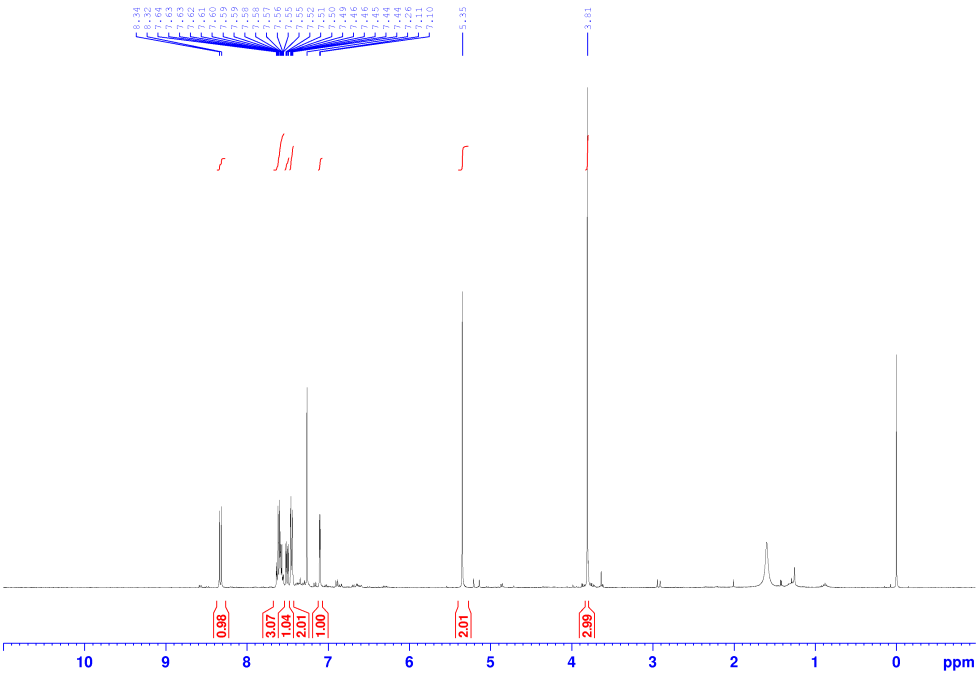

^{13}C NMR (100.6 MHz, $CDCl_3$)

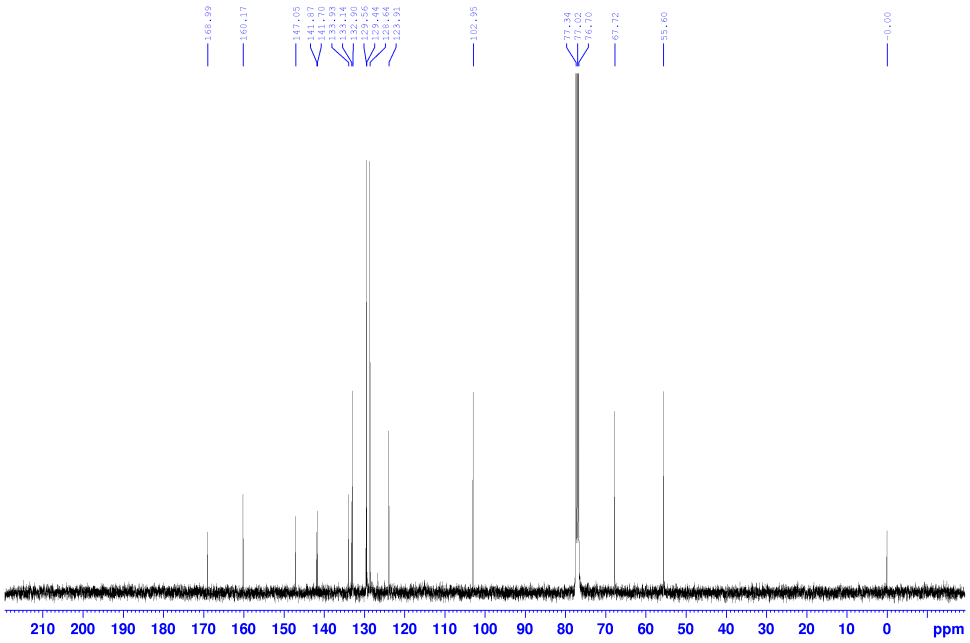
168.99
160.17
147.05
141.87
141.70
138.78
133.14
132.90
129.56
129.44
128.64
123.91
102.95
77.34
77.02
76.70
67.72
55.60
0.00
210 200 190 180 170 160 150 140 130 120 110 100 90 80 70 60 50 40 30 20 10 0 ppm

5-Methoxy-9-phenylfuro[3,4-*b*]quinolin-3(1*H*)-one 4c

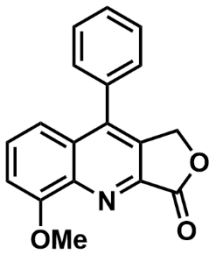

^{1}H NMR (400 MHz, $CDCl_3$)

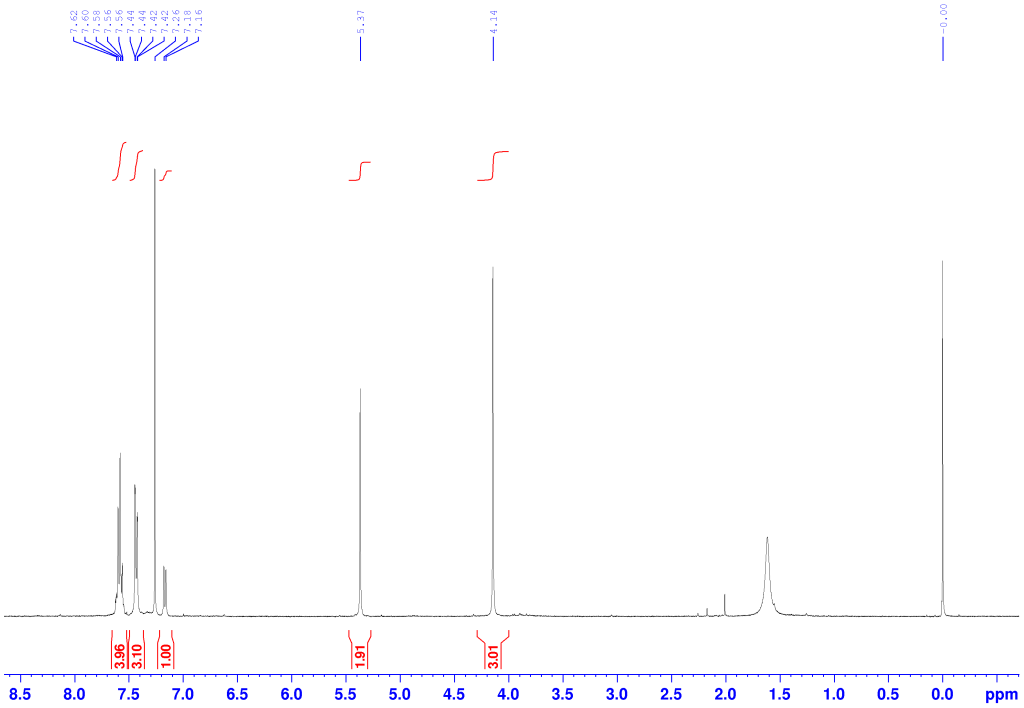

^{13}C NMR (100.6 MHz, $CDCl_3$)

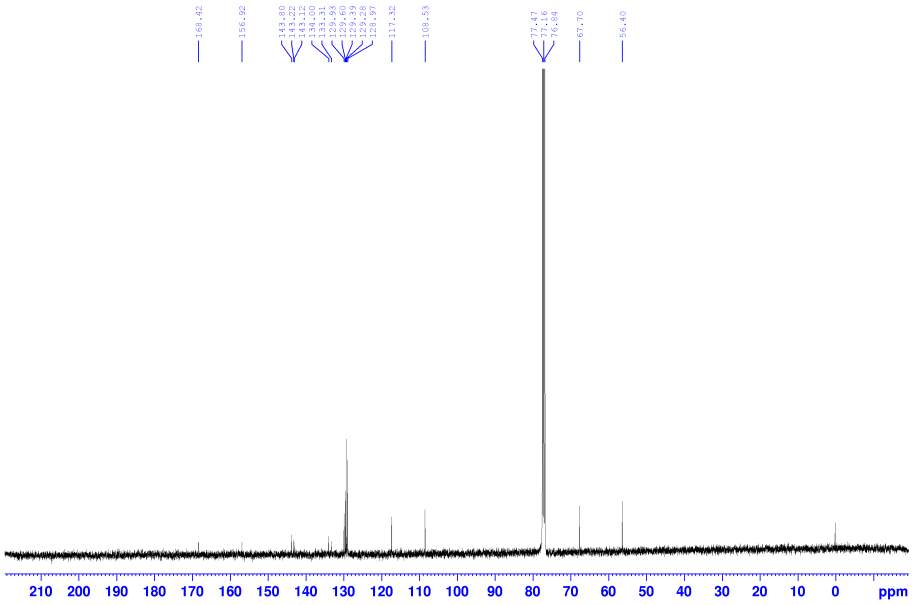
169.42
156.92
143.80
143.22
143.12
134.00
133.31
129.98
129.60
129.39
129.28
128.97
117.32
108.53
77.47
77.16
76.84
67.70
56.40
210 200 190 180 170 160 150 140 130 120 110 100 90 80 70 60 50 40 30 20 10 0 ppm

7-fluoro-9-phenylfuro[3,4-*b*]quinolin-3(1*H*)-one 4d

^{1}H NMR (400 MHz, $CDCl_3$)

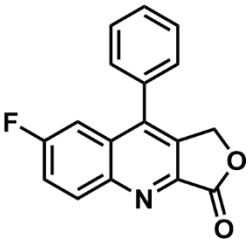

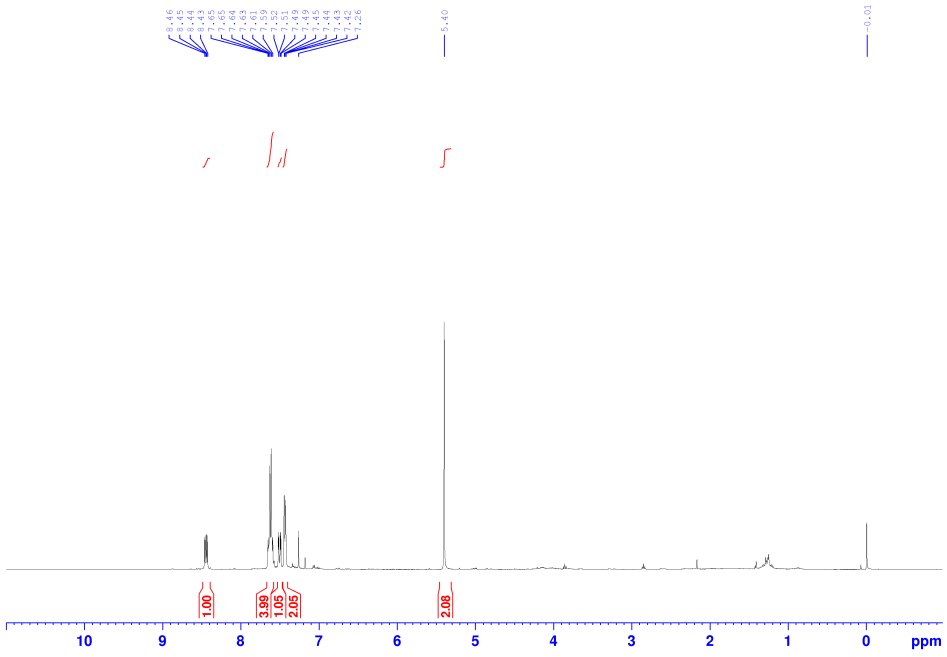

^{13}C NMR (100.6 MHz, $CDCl_3$)

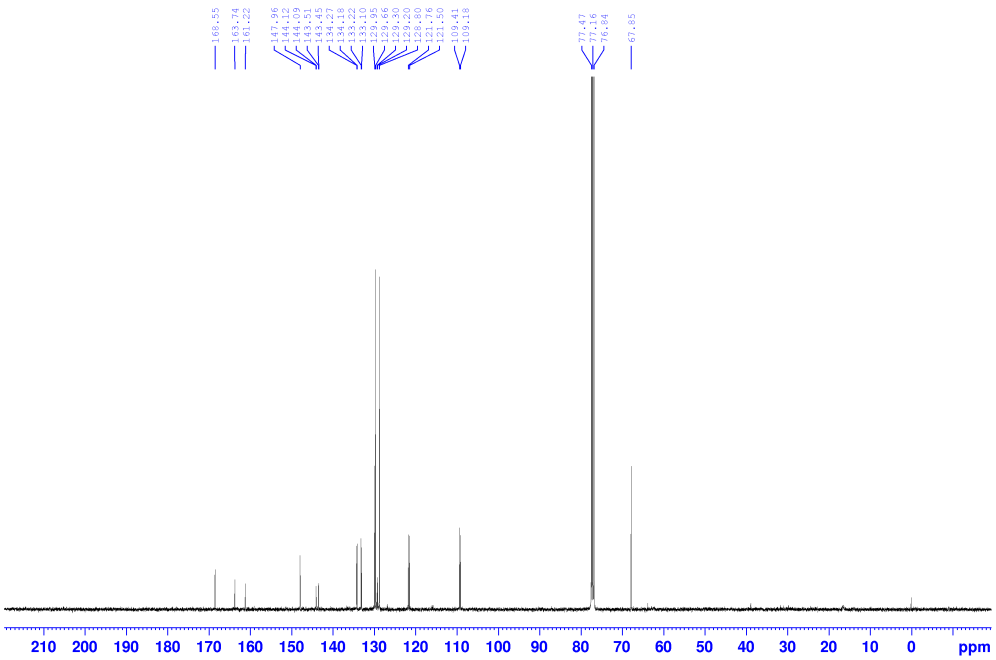
168.55
163.74
161.22
147.96
144.12
144.09
143.51
143.45
134.27
134.18
133.22
133.10
129.95
129.66
129.20
127.20
126.80
121.76
121.50
109.41
109.18
77.47
77.16
76.84
67.85
210 200 190 180 170 160 150 140 130 120 110 100 90 80 70 60 50 40 30 20 10 0 ppm

9-Phenyl-6-(trifluoromethyl)furo[3,4-*b*]quinolin-3(1*H*)-one 4e

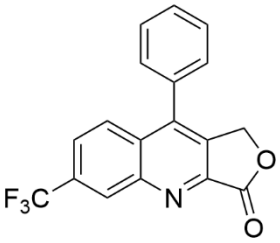

^{1}H NMR (400 MHz, $CDCl_3$)

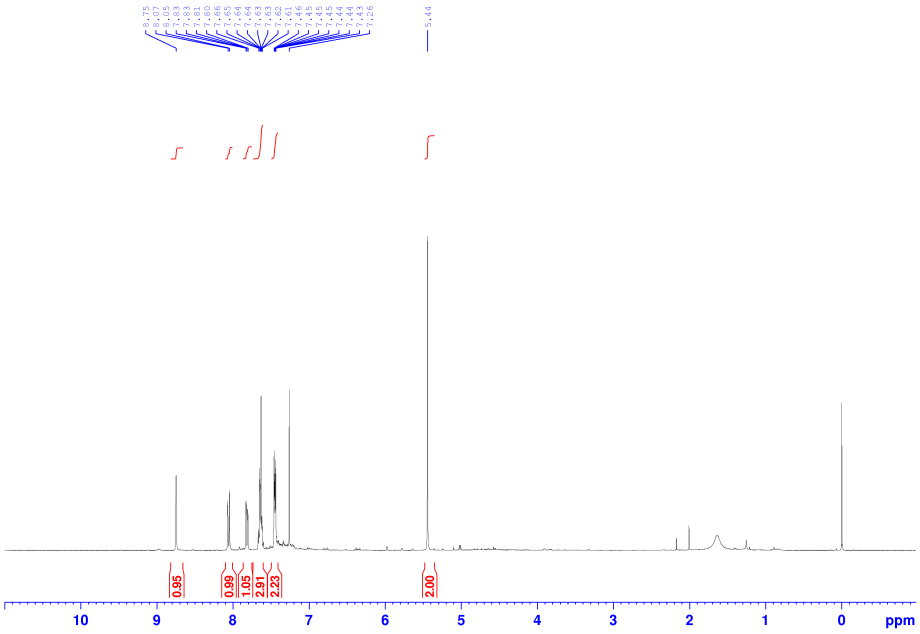

^{13}C NMR (100.6 MHz, $CDCl_3$)

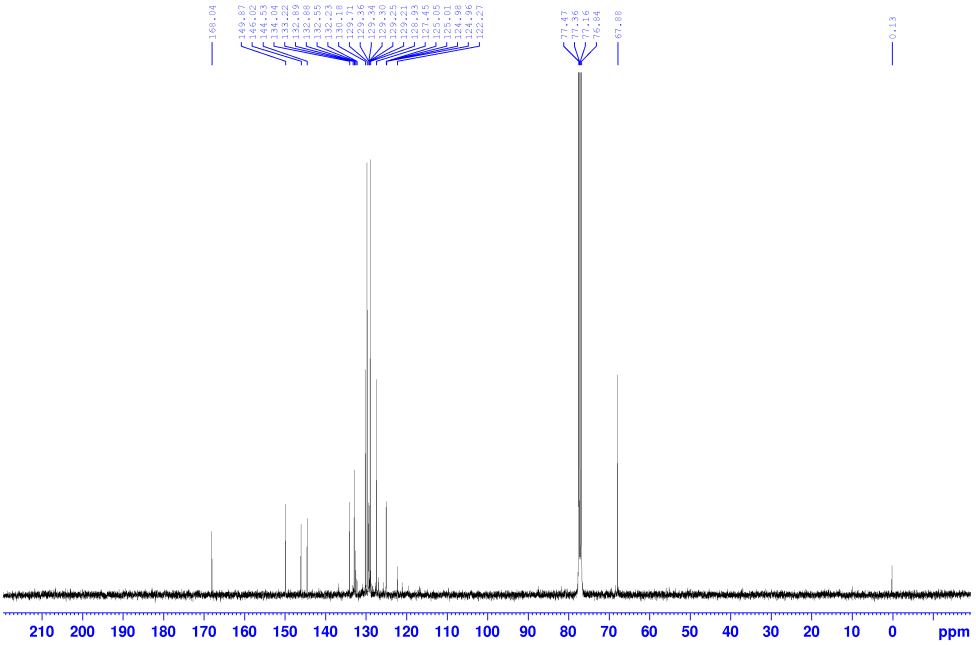
168.04
149.87
146.02
144.53
144.04
133.22
132.89
132.88
132.55
132.23
130.18
129.71
129.36
129.34
129.30
129.25
129.21
129.18
129.05
125.05
125.01
124.98
124.96
122.27
77.47
77.36
77.16
76.84
67.88
0.13
210 200 190 180 170 160 150 140 130 120 110 100 90 80 70 60 50 40 30 20 10 0 ppm

7-Iodo-9-phenylfuro[3,4-*b*]quinolin-3(1*H*)-one 4f

^{1}H NMR (400 MHz, $CDCl_3$)

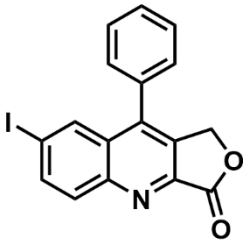

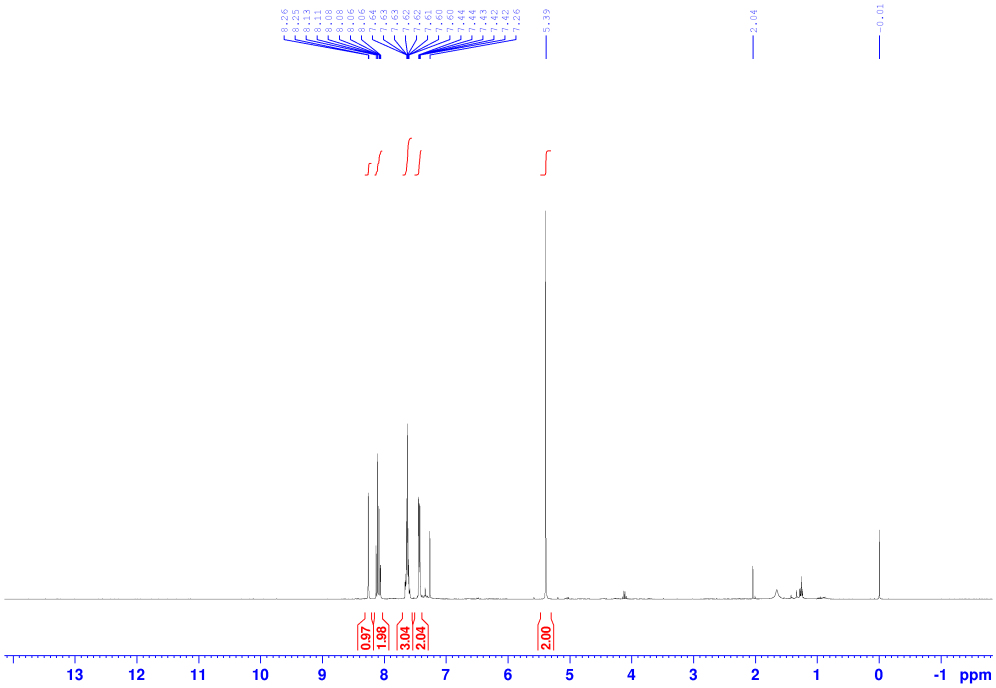

^{13}C NMR (100.6 MHz, $CDCl_3$)

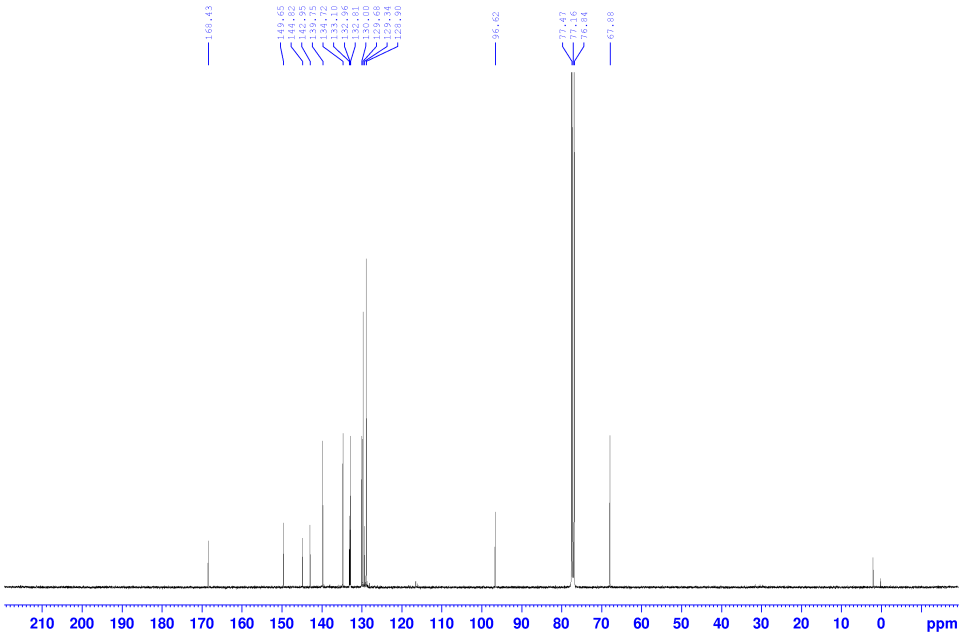
168.43
149.65
144.62
142.95
139.75
134.72
133.10
132.86
132.81
130.00
129.88
129.34
128.90
96.62
77.47
77.16
76.84
67.88
210 200 190 180 170 160 150 140 130 120 110 100 90 80 70 60 50 40 30 20 10 0 ppm

5-Bromo-9-phenylfuro[3,4-*b*]quinolin-3(1*H*)-one 4g

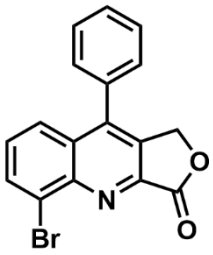

^{1}H NMR (400 MHz, $CDCl_3$)

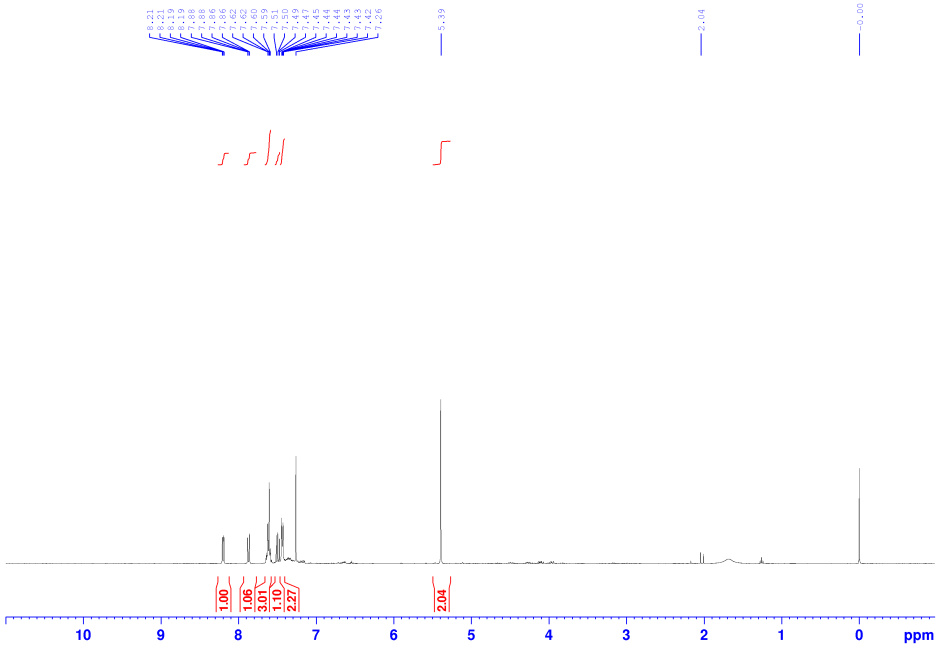

^{13}C NMR (100.6 MHz, $CDCl_3$)

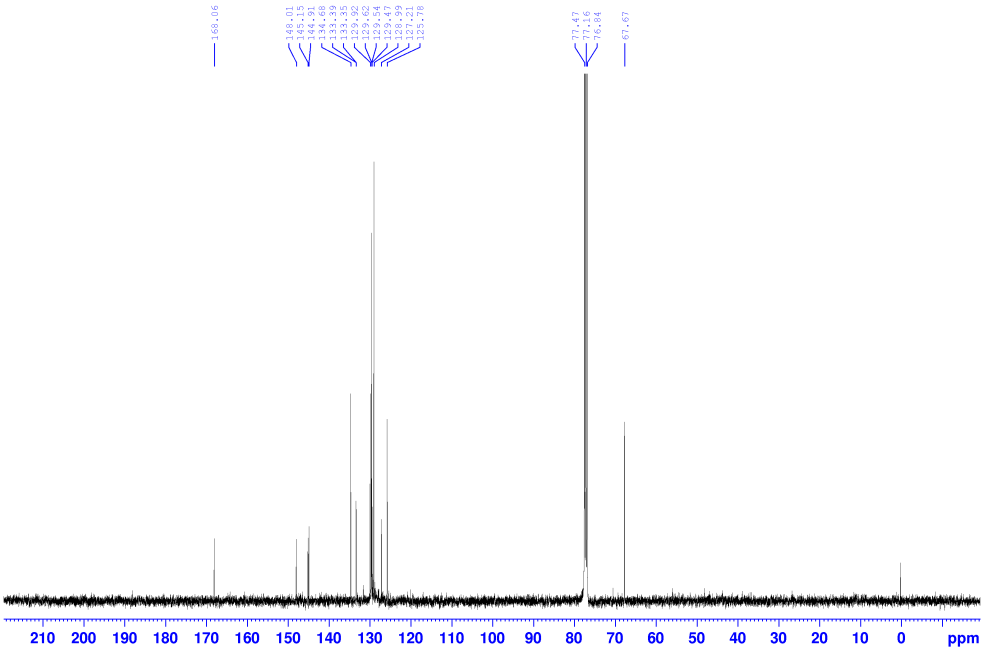
168.06
148.01
145.15
144.91
134.68
133.39
132.55
129.92
129.62
129.54
129.47
128.99
127.21
125.78
77.47
77.16
76.84
67.67
210 200 190 180 170 160 150 140 130 120 110 100 90 80 70 60 50 40 30 20 10 0 ppm

8- and 6-Methyl-9-phenylfuro[3,4-*b*]quinolin-3(1*H*)-one 4h

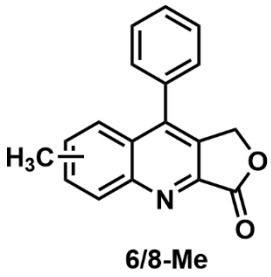

6/8-Me

^{1}H NMR (400 MHz, $CDCl_3$)

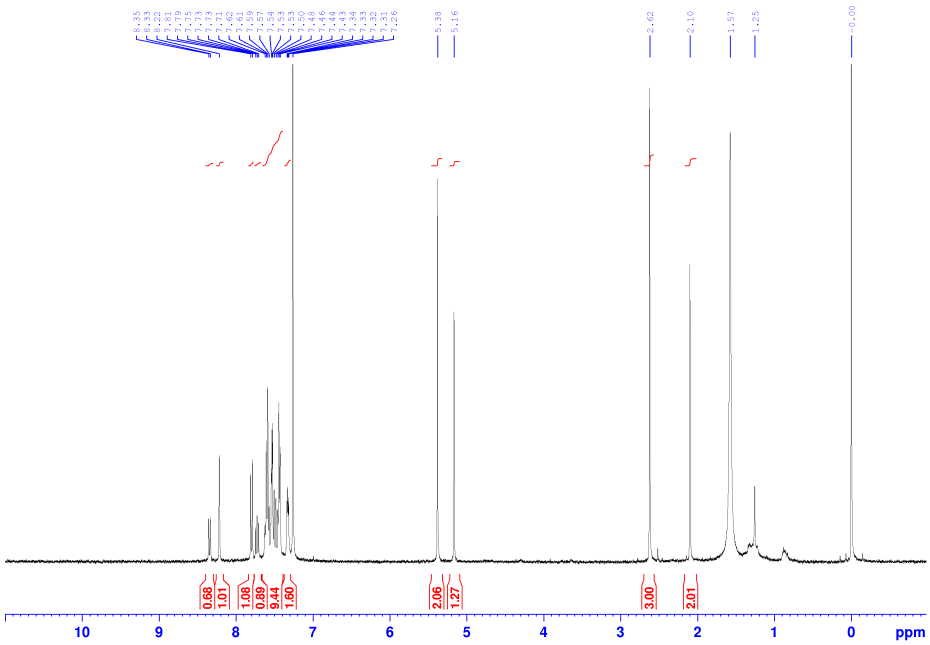

^{13}C NMR (100.6 MHz, $CDCl_3$)

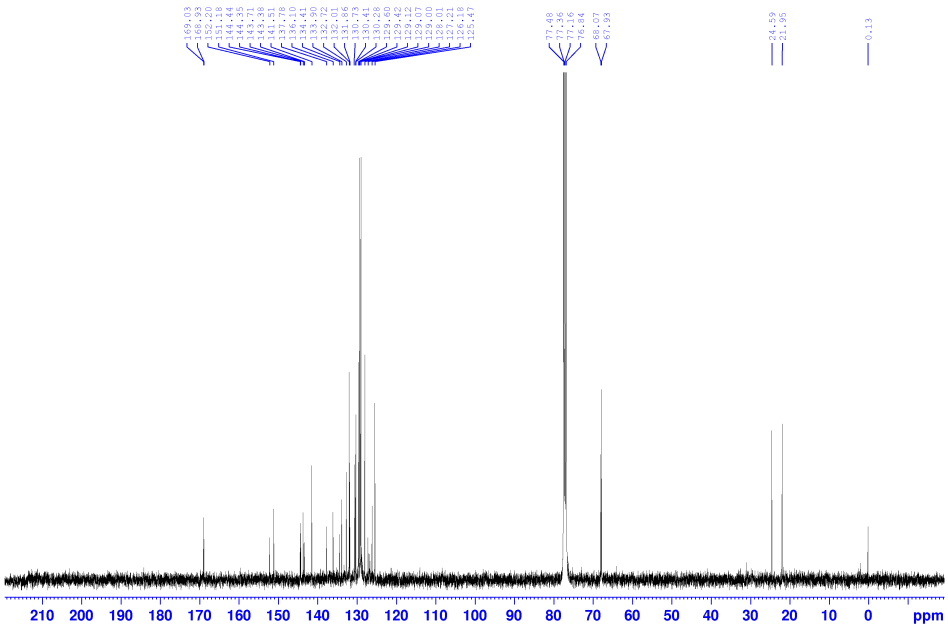

5-Methyl-9-phenylfuro[3,4-*b*]quinolin-3(1*H*)-one 4i

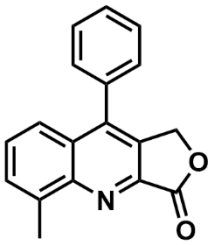

^{1}H NMR (400 MHz, $CDCl_3$)

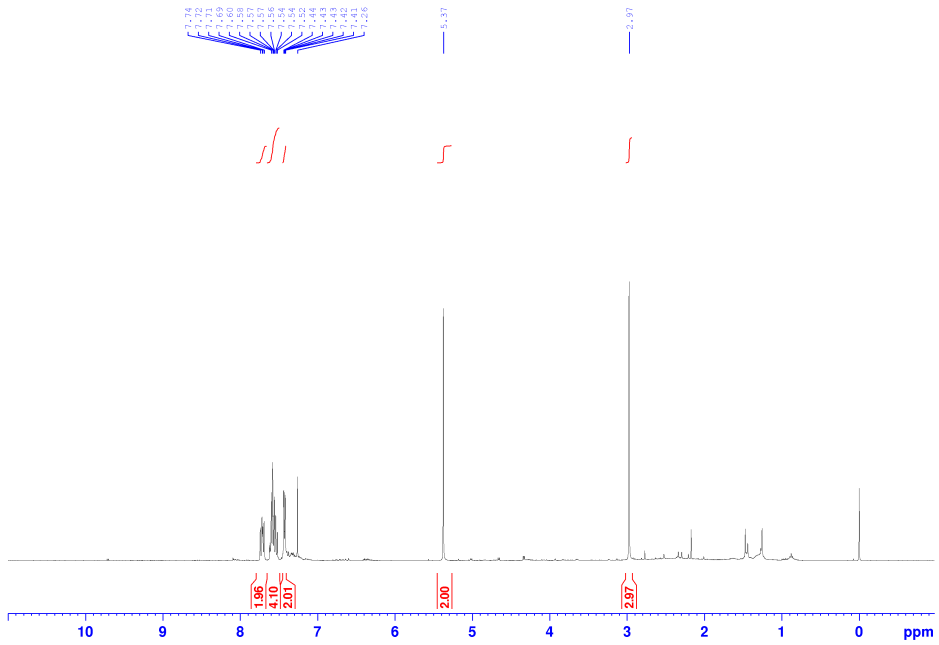

^{13}C NMR (100.6 MHz, $CDCl_3$)

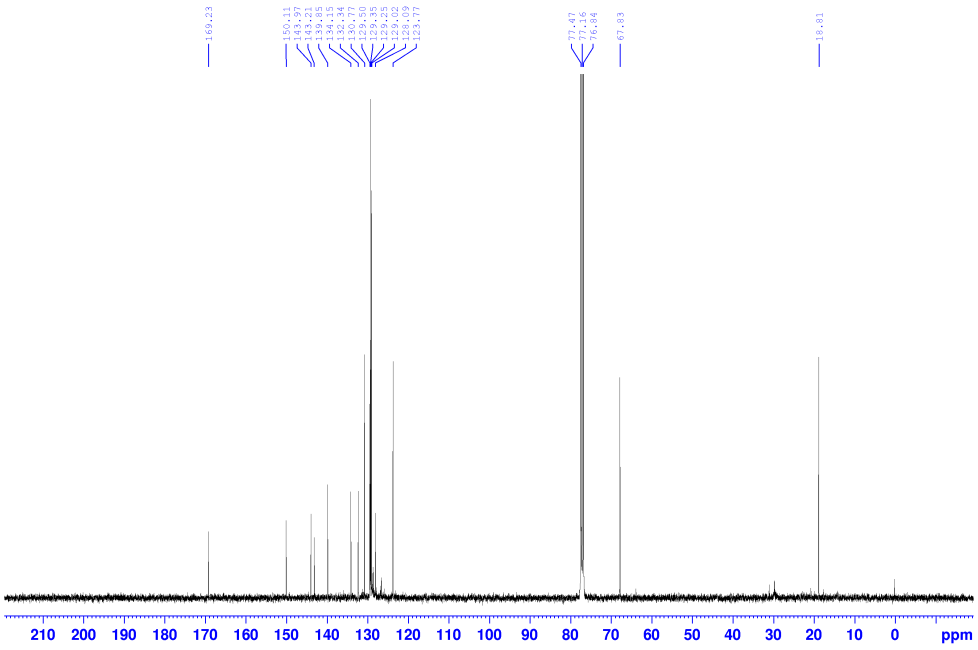

7-methyl-9-(naphthalen-2-yl)furo[3,4-*b*]quinolin-3(1*H*)-one 4j

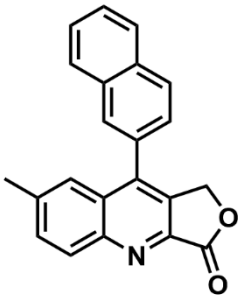

^{1}H NMR (400 MHz, $CDCl_3$)

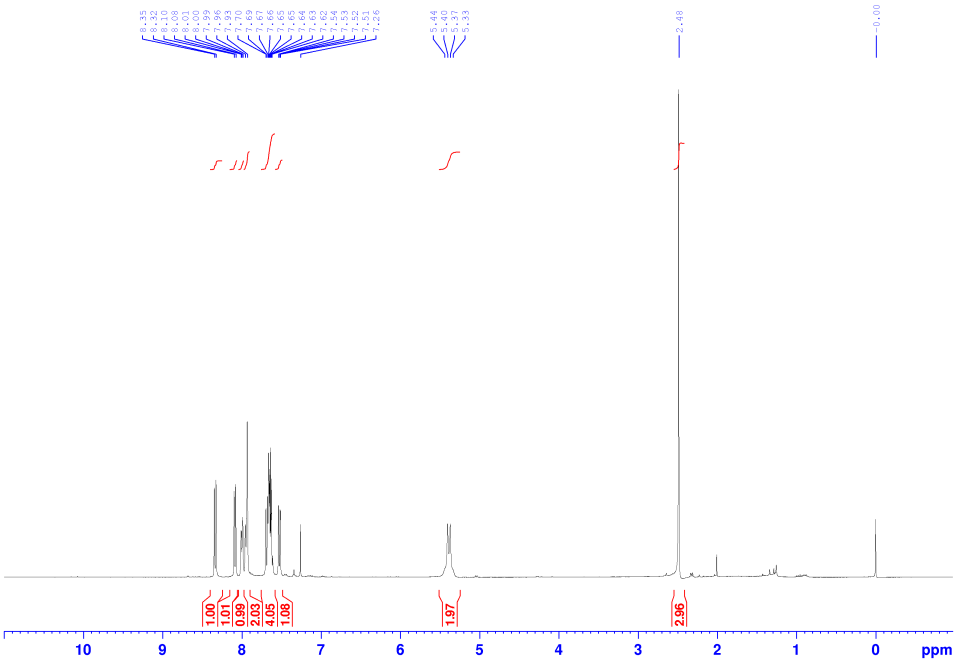

^{13}C NMR (100.6 MHz, $CDCl_3$)

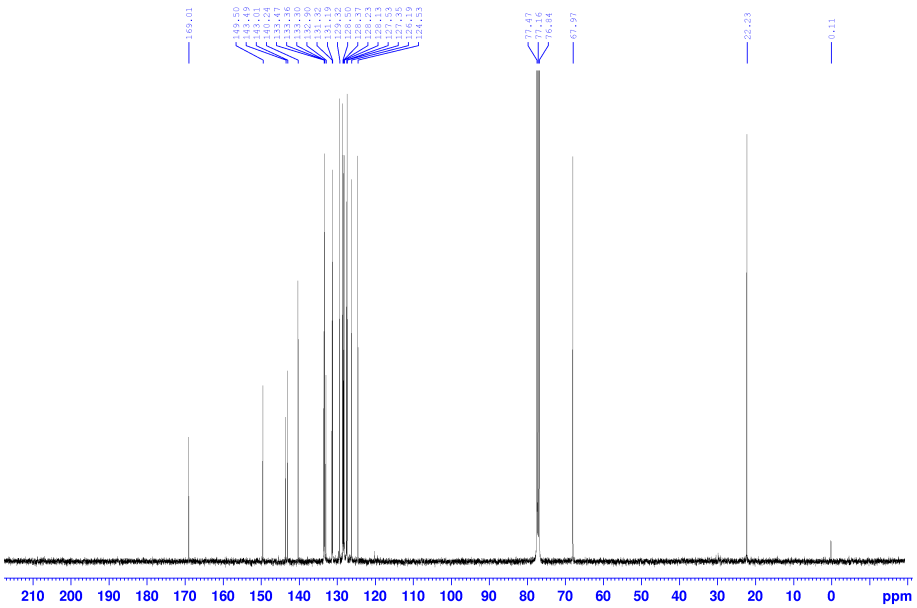
169.01
149.50
143.49
141.71
140.24
133.47
133.36
133.30
132.90
131.52
131.19
130.52
128.50
128.37
128.23
128.13
127.53
127.45
126.99
124.53
77.47
77.16
76.84
67.97
22.23
0.11
210 200 190 180 170 160 150 140 130 120 110 100 90 80 70 60 50 40 30 20 10 0 ppm

(*E*)-7-methyl-9-(prop-1-en-1-yl)furo[3,4-*b*]quinolin-3(1*H*)-one 4k

^{1}H NMR (400 MHz, $CDCl_3$)

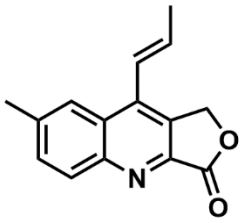

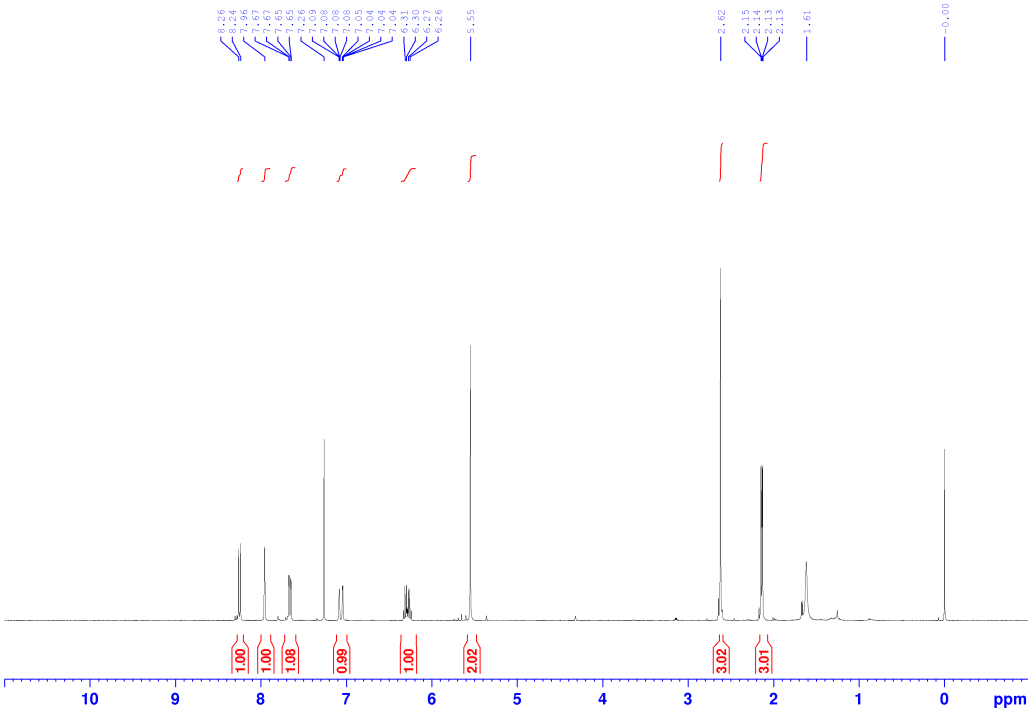

^{13}C NMR (100.6 MHz, $CDCl_3$)

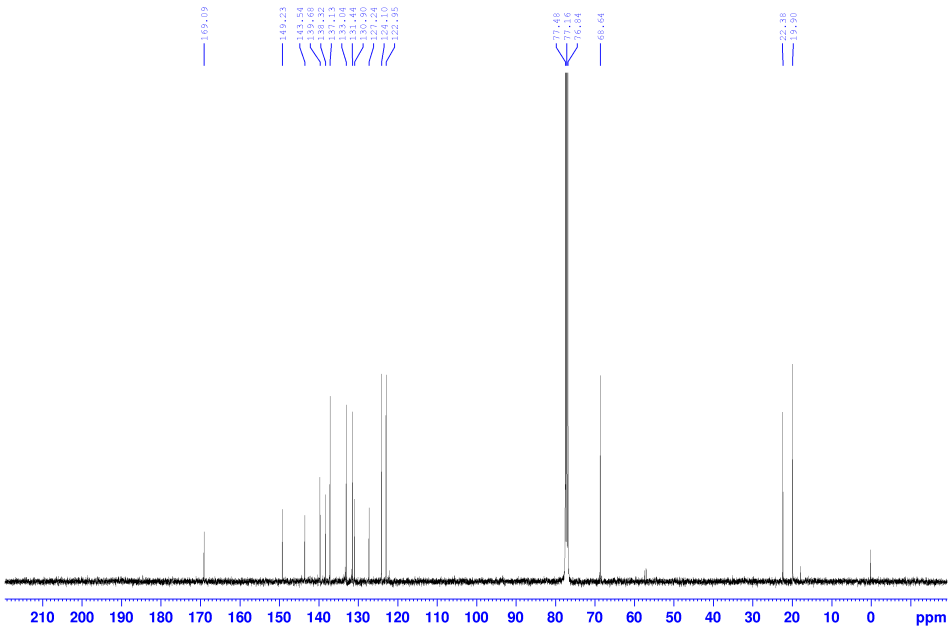
169.09
149.23
143.54
143.08
138.32
137.13
133.04
131.44
130.90
127.24
124.10
122.95
77.48
77.16
76.84
68.64
22.38
19.90
210 200 190 180 170 160 150 140 130 120 110 100 90 80 70 60 50 40 30 20 10 0 ppm

7-methyl-2,9-diphenyl-1,2-dihydro-3*H*-pyrrolo[3,4-*b*]quinolin-3-one
4l

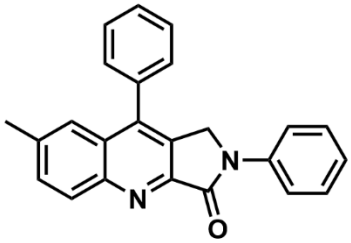

^{1}H NMR (400 MHz, $CDCl_3$)

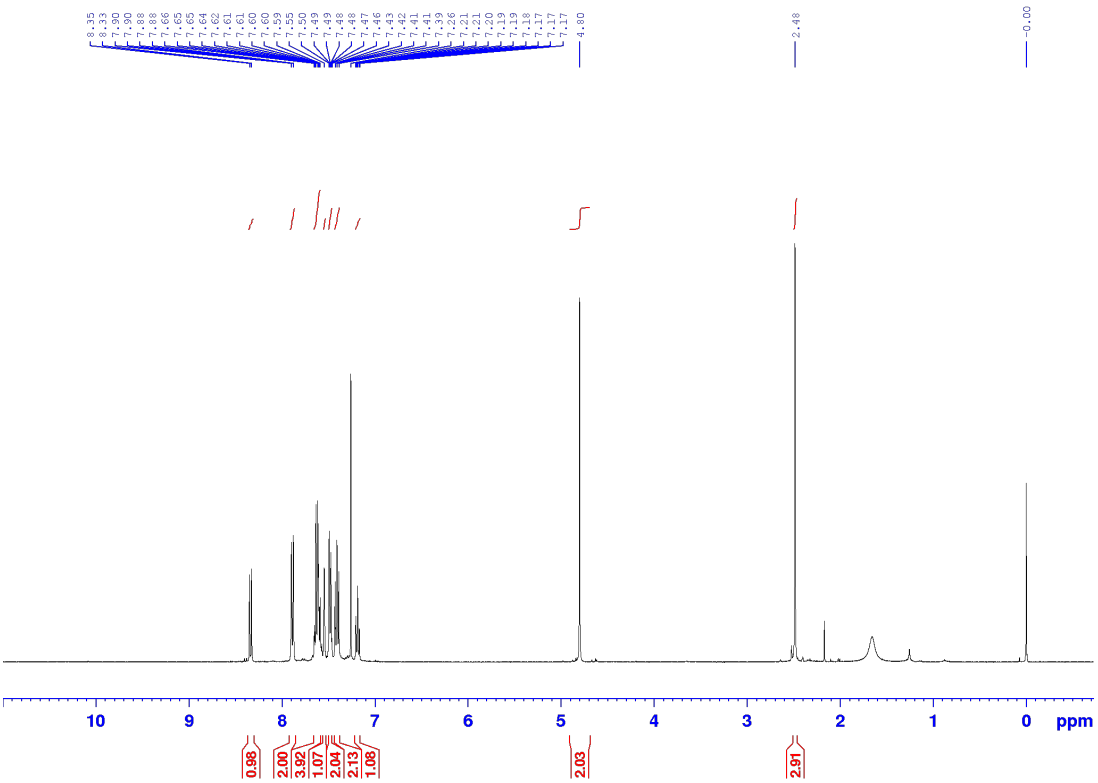

^{13}C NMR (100.6 MHz, $CDCl_3$)

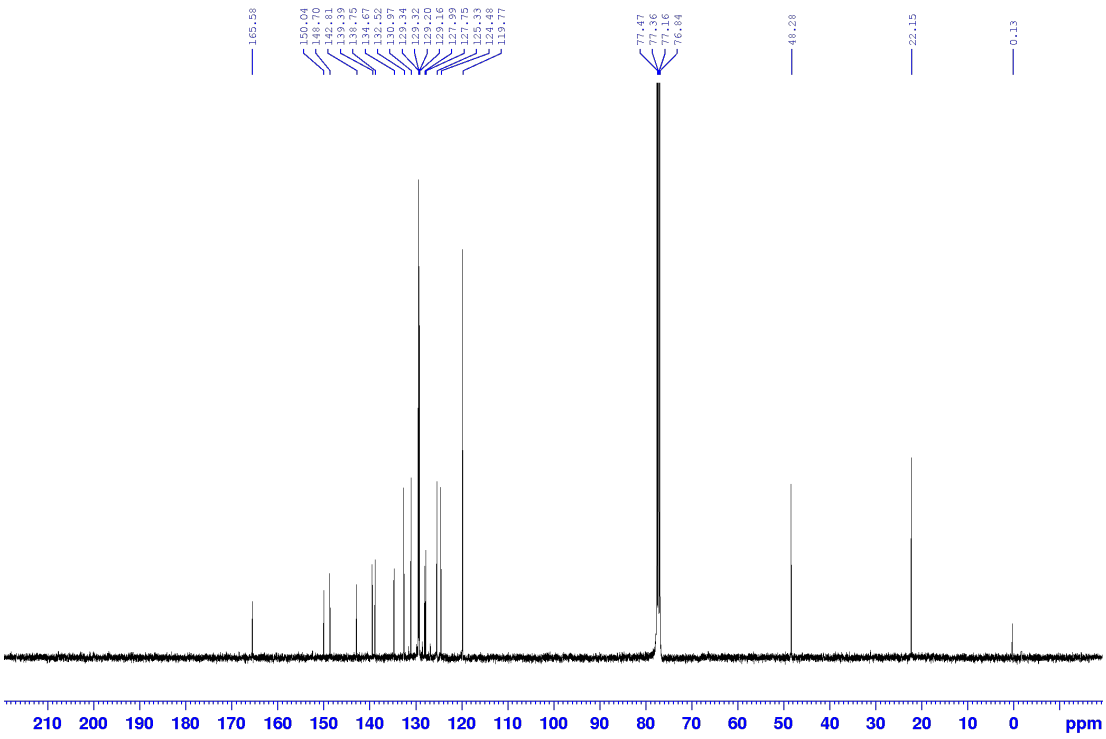
165.58
150.04
148.70
142.81
139.39
138.75
134.67
132.52
130.37
130.34
129.32
129.20
129.16
127.99
127.75
125.33
124.48
119.77
77.47
77.36
77.16
76.84
48.28
22.15
0.13
210 200 190 180 170 160 150 140 130 120 110 100 90 80 70 60 50 40 30 20 10 0 ppm

2-(4-methoxybenzyl)-7-methyl-9-phenyl-1,2-dihydro-3*H*-pyrrolo[3,4-*b*]quinolin-3-one 4m

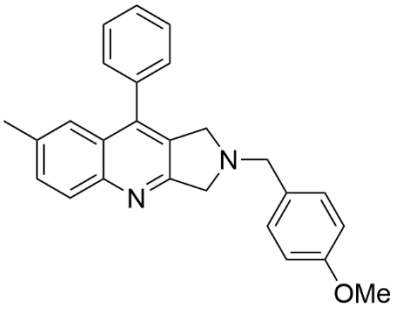

^{1}H NMR (400 MHz, $CDCl_3$)

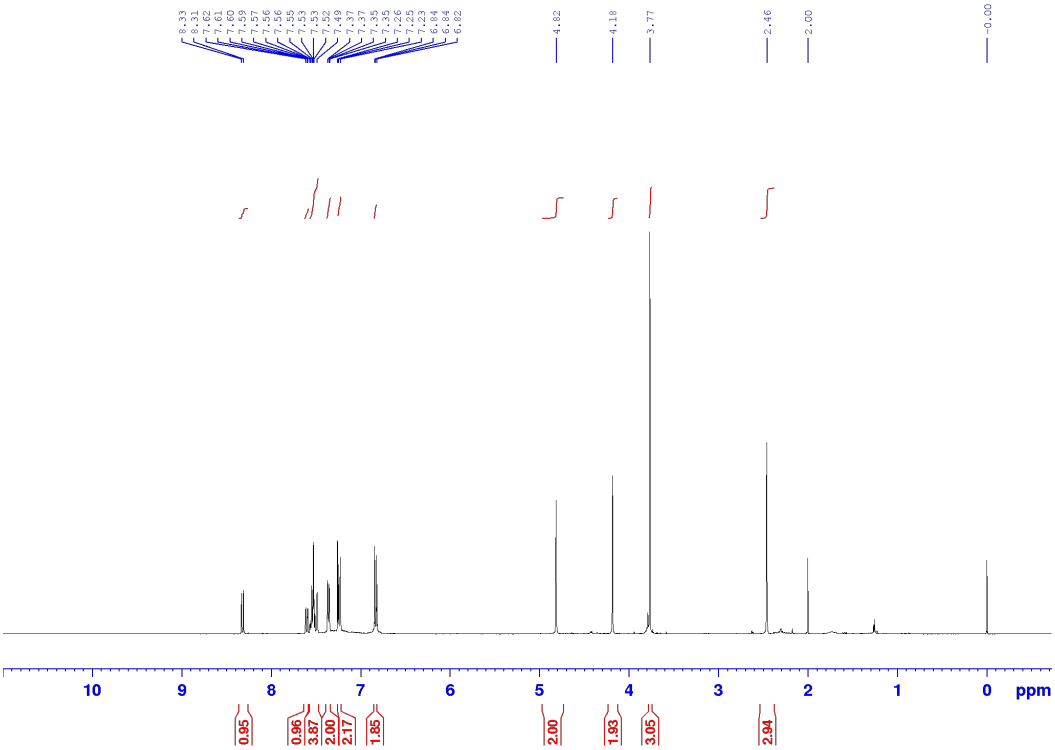

^{13}C NMR (100.6 MHz, $CDCl_3$)

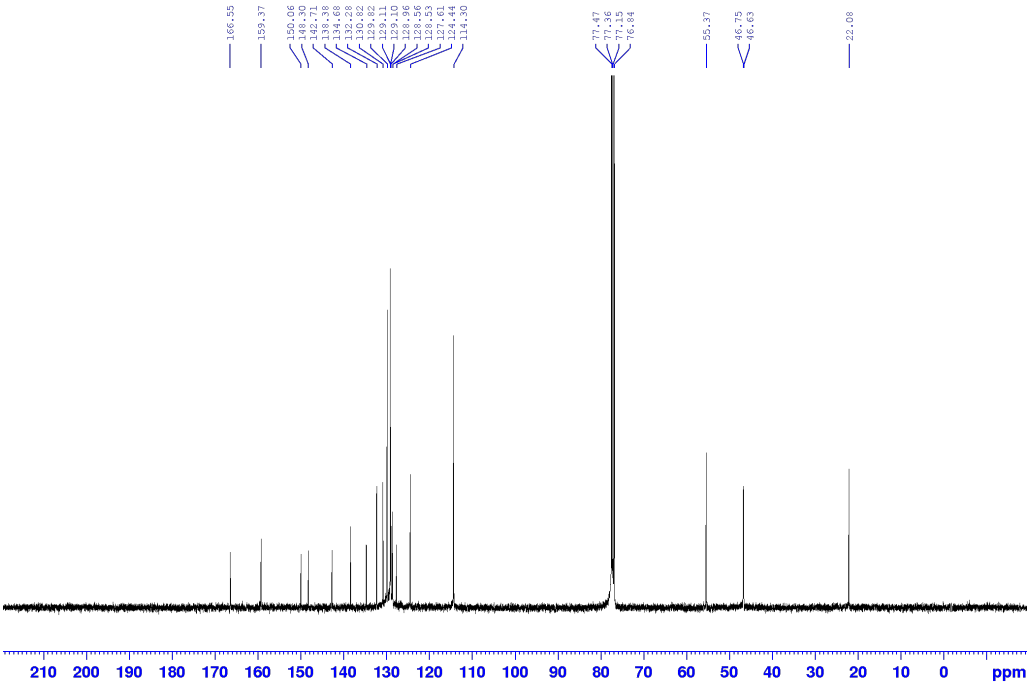
166.55
159.37
150.06
148.30
142.71
138.38
134.68
132.28
130.82
129.82
129.11
129.10
128.96
128.56
128.35
127.61
124.44
114.30
77.47
77.36
77.15
76.84
55.37
46.75
46.63
22.08
210 200 190 180 170 160 150 140 130 120 110 100 90 80 70 60 50 40 30 20 10 0 ppm

Cinnamyl 2-oxo-2-(*p*-tolylamino)acetate 7a

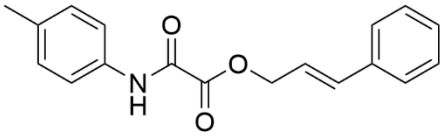

^{1}H NMR (400 MHz, $CDCl_3$)

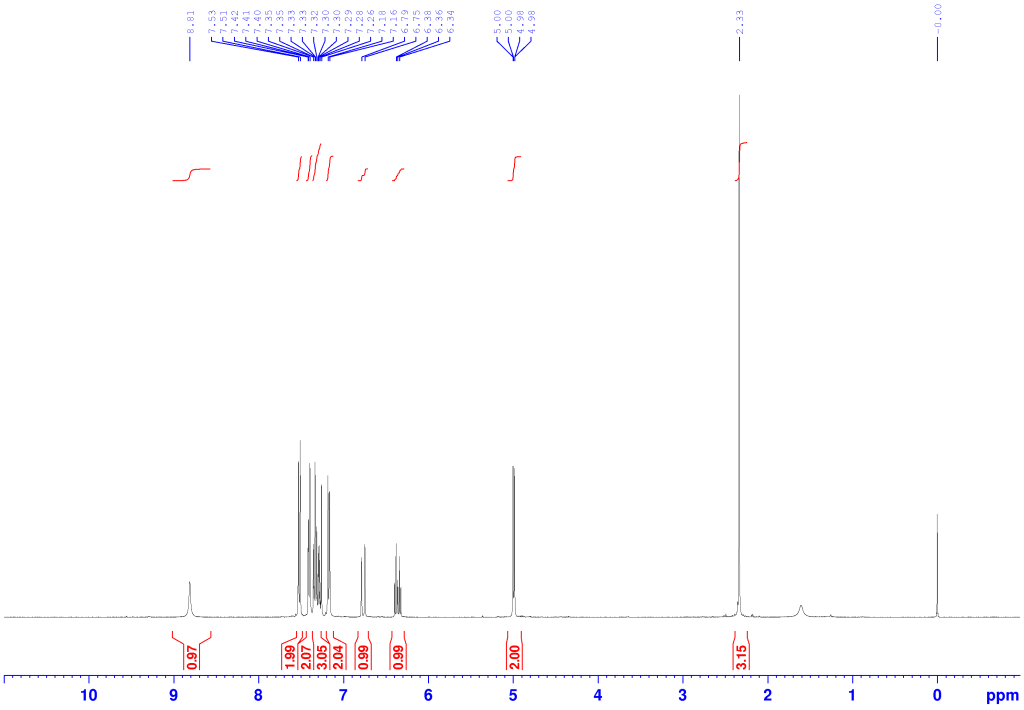

^{13}C NMR (100.6 MHz, $CDCl_3$)

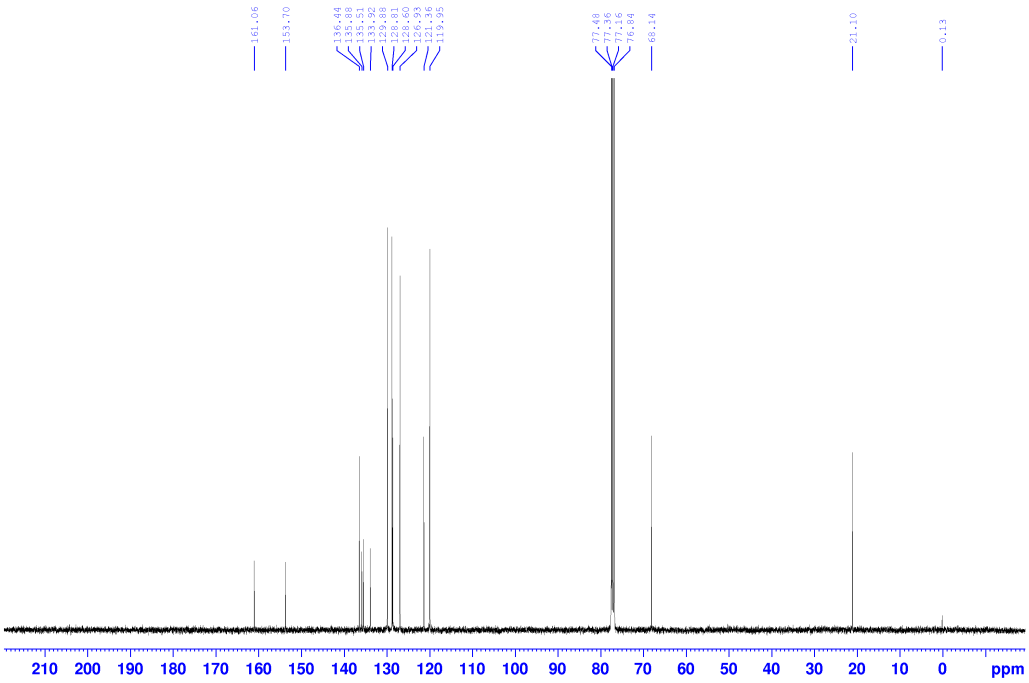
161.06
153.70
136.44
135.88
135.51
133.92
129.88
128.81
128.60
126.93
121.36
119.95
77.48
77.36
77.16
76.84
68.14
21.10
0.13
210 200 190 180 170 160 150 140 130 120 110 100 90 80 70 60 50 40 30 20 10 0 ppm

Cinnamyl 2-((4-methoxyphenyl)amino)-2-oxoacetate 7b

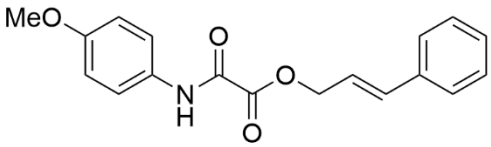

^{1}H NMR (400 MHz, $CDCl_3$)

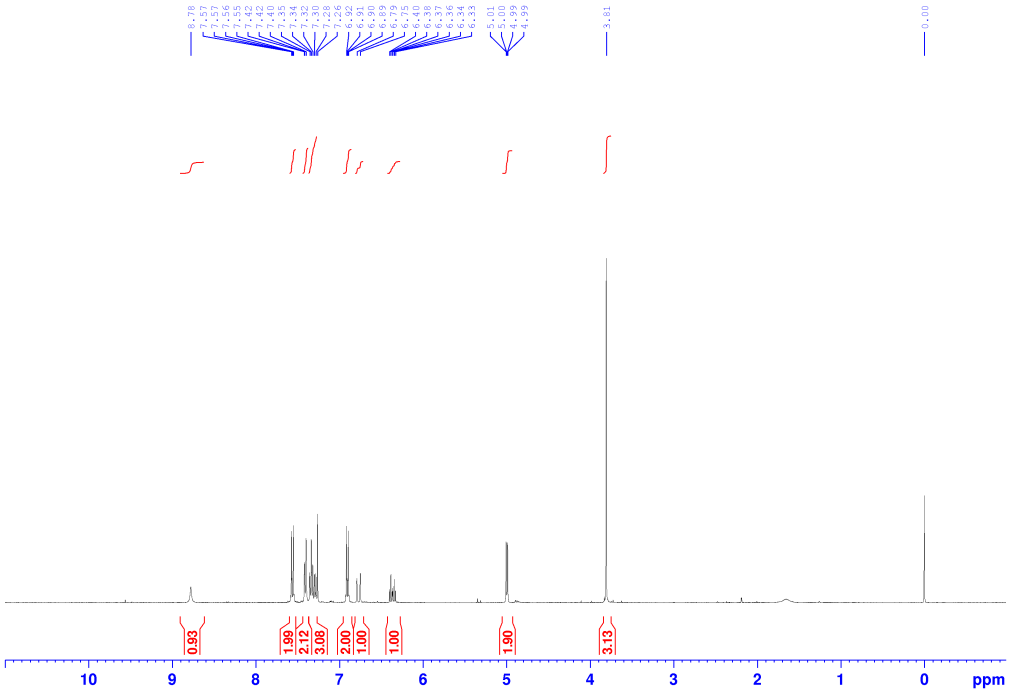

^{13}C NMR (100.6 MHz, $CDCl_3$)

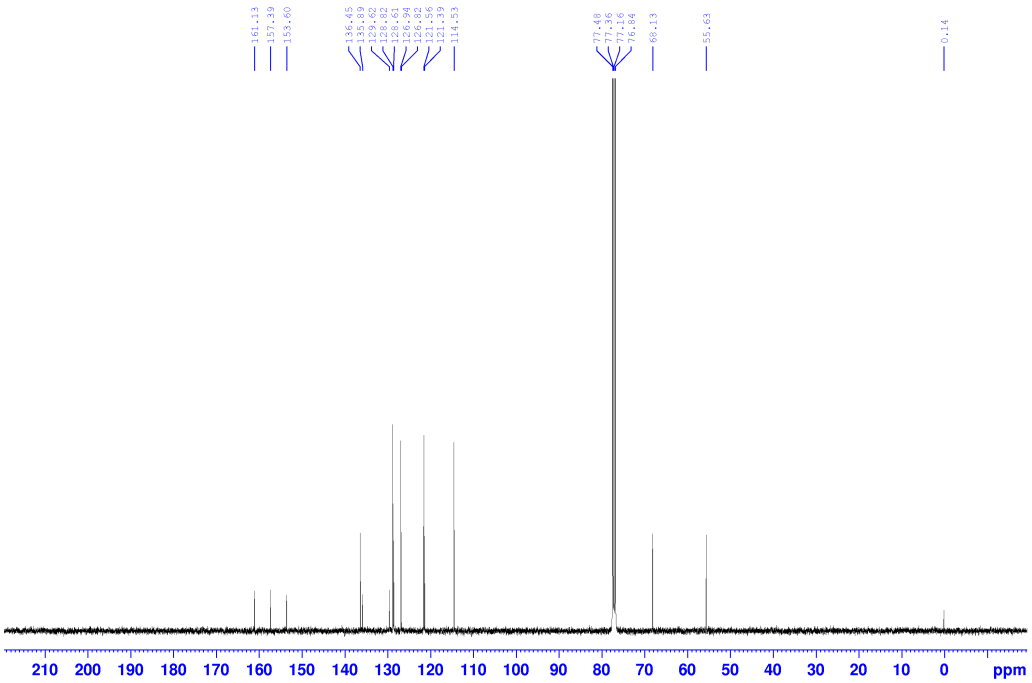
161.13
157.39
153.60
136.45
135.89
129.62
128.82
128.61
126.84
126.82
121.56
121.39
114.53
77.48
77.36
77.16
76.84
68.13
55.63
0.14
210 200 190 180 170 160 150 140 130 120 110 100 90 80 70 60 50 40 30 20 10 0 ppm

Cinnamyl 2-((2-methoxyphenyl)amino)-2-oxoacetate 7c

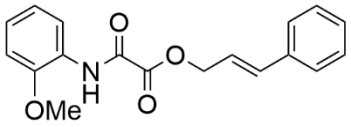

^{1}H NMR (400 MHz, $CDCl_3$)

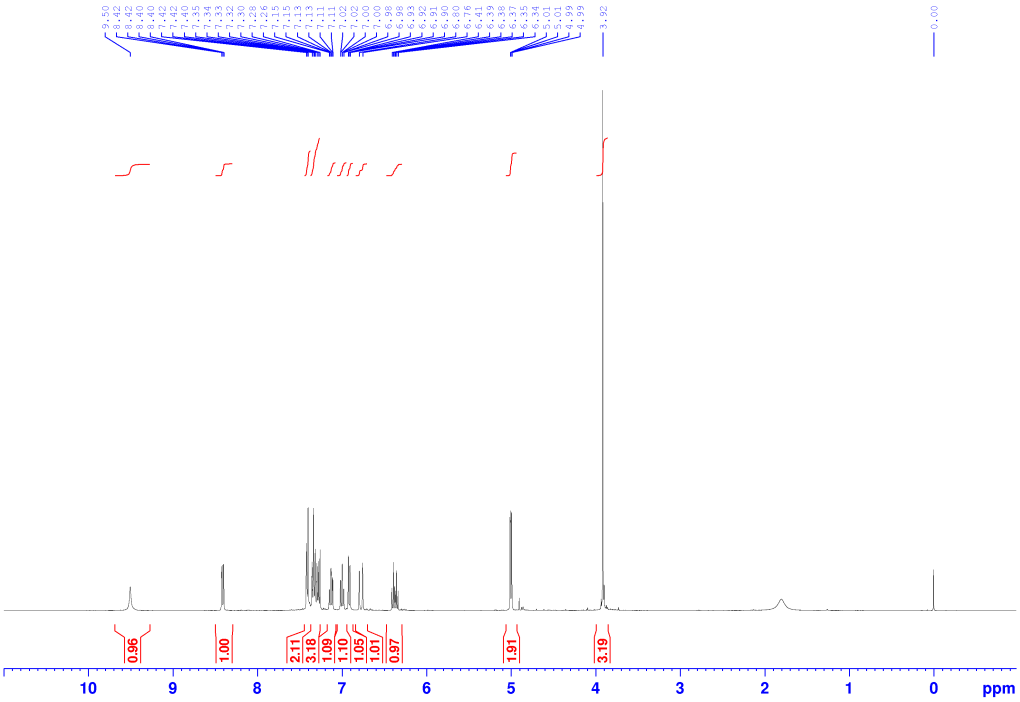

^{13}C NMR (100.6 MHz, $CDCl_3$)

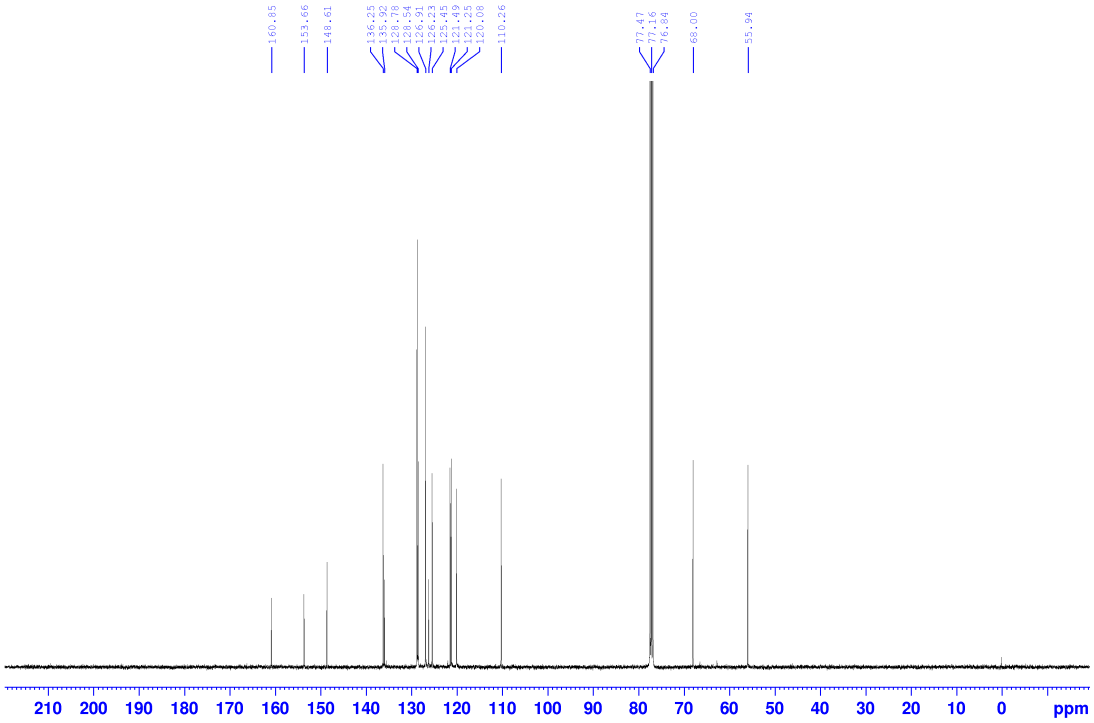
160.85
153.66
148.61
136.25
135.92
128.78
128.54
126.91
126.23
125.45
123.49
121.11
121.25
120.08
110.26
77.47
77.16
76.84
68.00
55.94
210 200 190 180 170 160 150 140 130 120 110 100 90 80 70 60 50 40 30 20 10 0 ppm

Cinnamyl 2-oxo-2-(*m*-tolylamino)acetate 7d

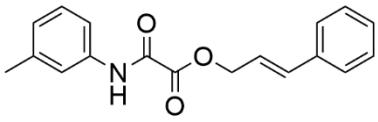

^{1}H NMR (400 MHz, $CDCl_3$)

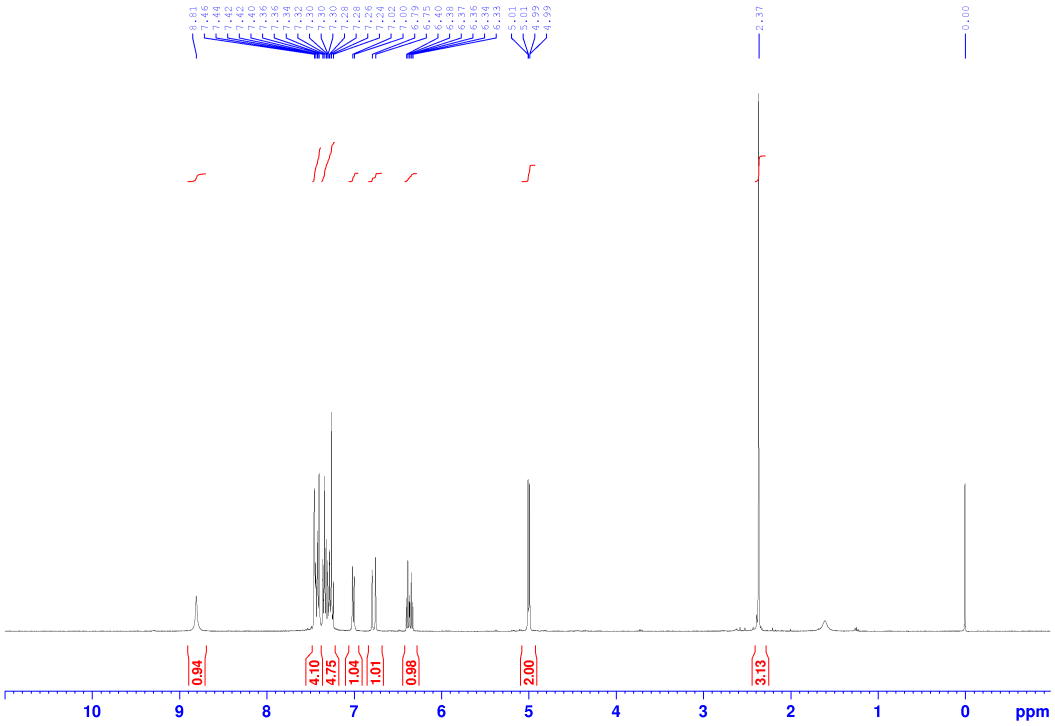

^{13}C NMR (100.6 MHz, $CDCl_3$)

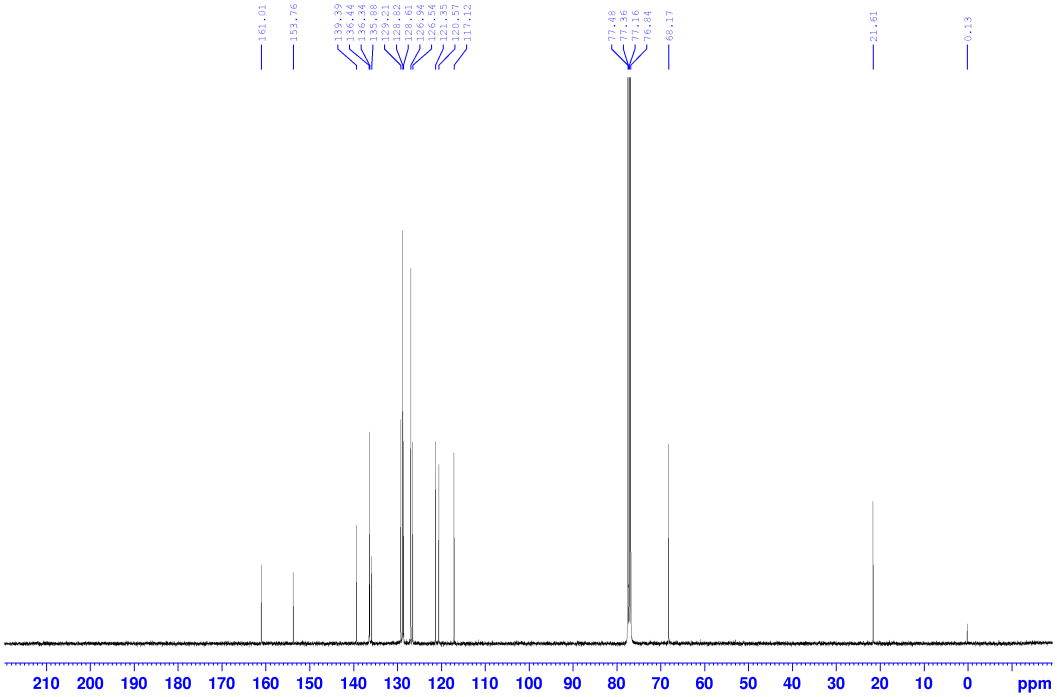
161.01
153.76
139.39
136.44
136.34
135.88
129.21
128.82
128.61
126.94
126.58
121.35
120.57
117.12
77.48
77.36
77.16
76.84
68.17
21.61
0.13
210 200 190 180 170 160 150 140 130 120 110 100 90 80 70 60 50 40 30 20 10 0 ppm

Cinnamyl 2-((4-iodophenyl)amino)-2-oxoacetate 7e

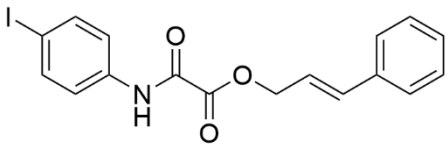

^{1}H NMR (400 MHz, $CDCl_3$)

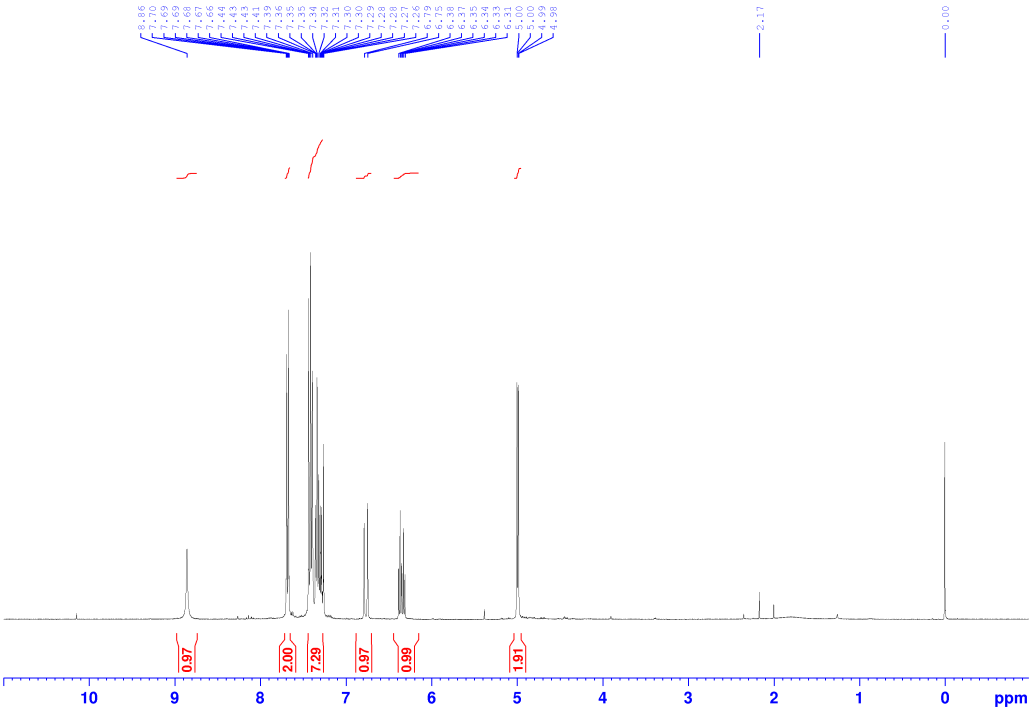

^{13}C NMR (100.6 MHz, $CDCl_3$)

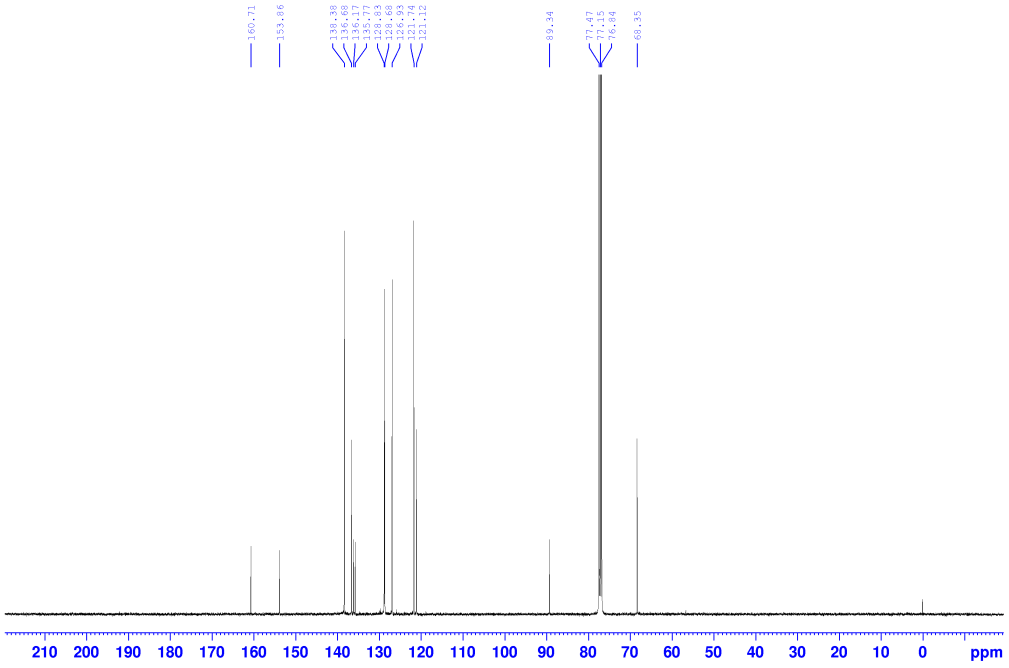
160.71
153.86
138.38
136.68
136.17
135.73
133.83
128.68
126.93
121.74
121.12
89.94
77.47
77.15
76.84
69.35
210 200 190 180 170 160 150 140 130 120 110 100 90 80 70 60 50 40 30 20 10 0 ppm

(*E*)-3-(naphthalen-2-yl)allyl 2-oxo-2-(*p*-tolylamino)acetate 7f

^{1}H NMR (400 MHz, $CDCl_3$)

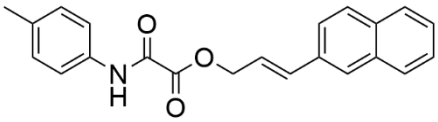

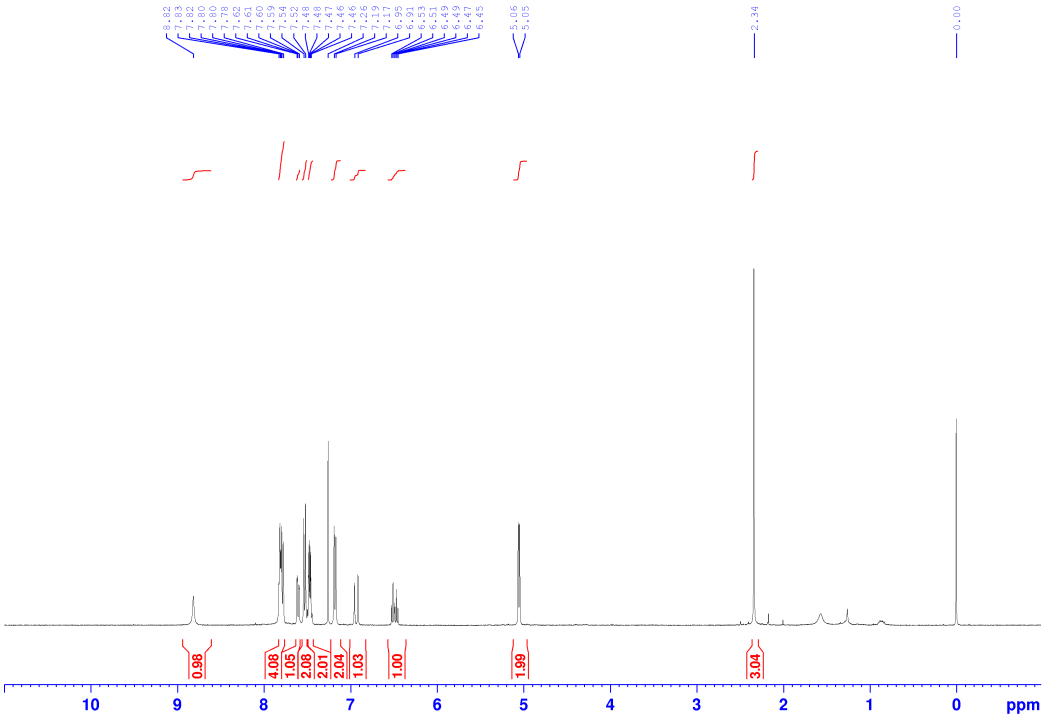

^{13}C NMR (100.6 MHz, $CDCl_3$)

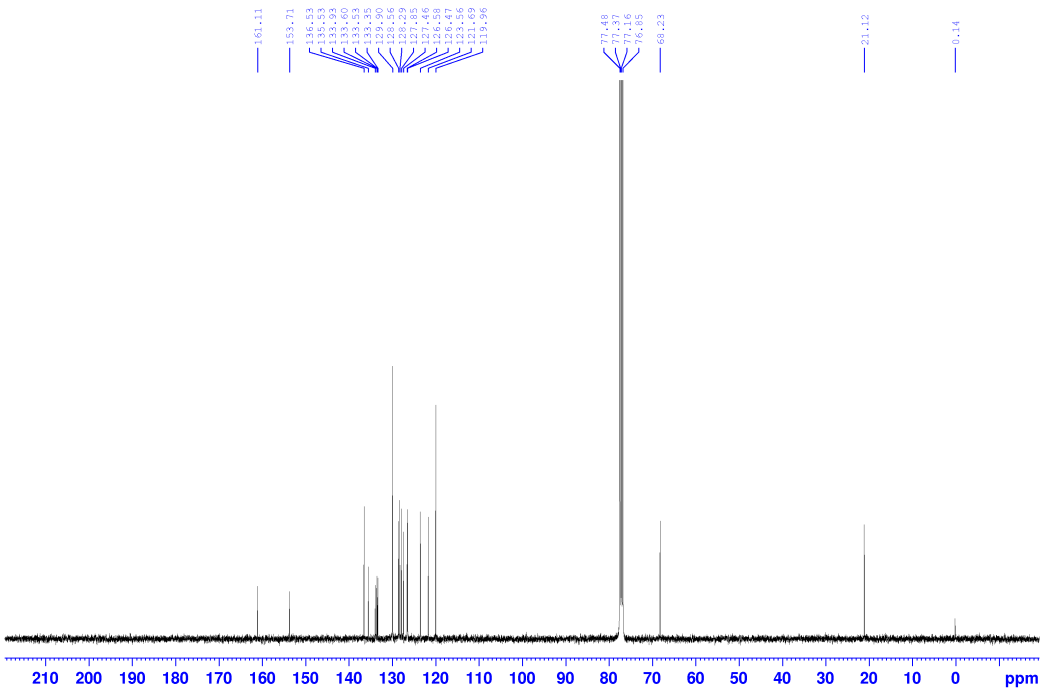

Cinnamyl 2-((4-fluorophenyl)amino)-2-oxoacetate 7g

^{1}H NMR (400 MHz, $CDCl_3$)

^{13}C NMR (100.6 MHz, $CDCl_3$)

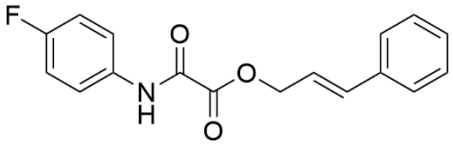

(2*E*,4*E*)-hexa-2,4-dien-1-yl 2-oxo-2-(*p*-tolylamino)acetate 7h

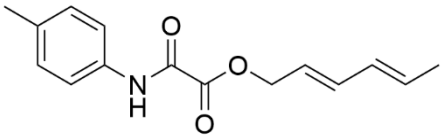

^{1}H NMR (400 MHz, $CDCl_3$)

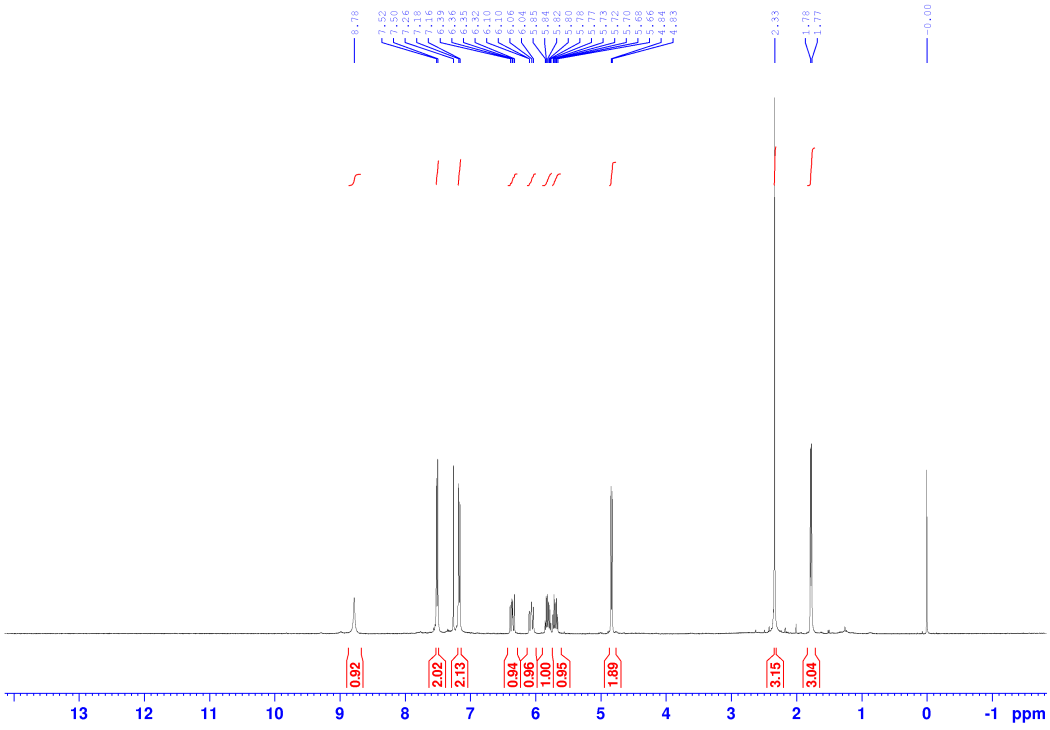

^{13}C NMR (100.6 MHz, $CDCl_3$)

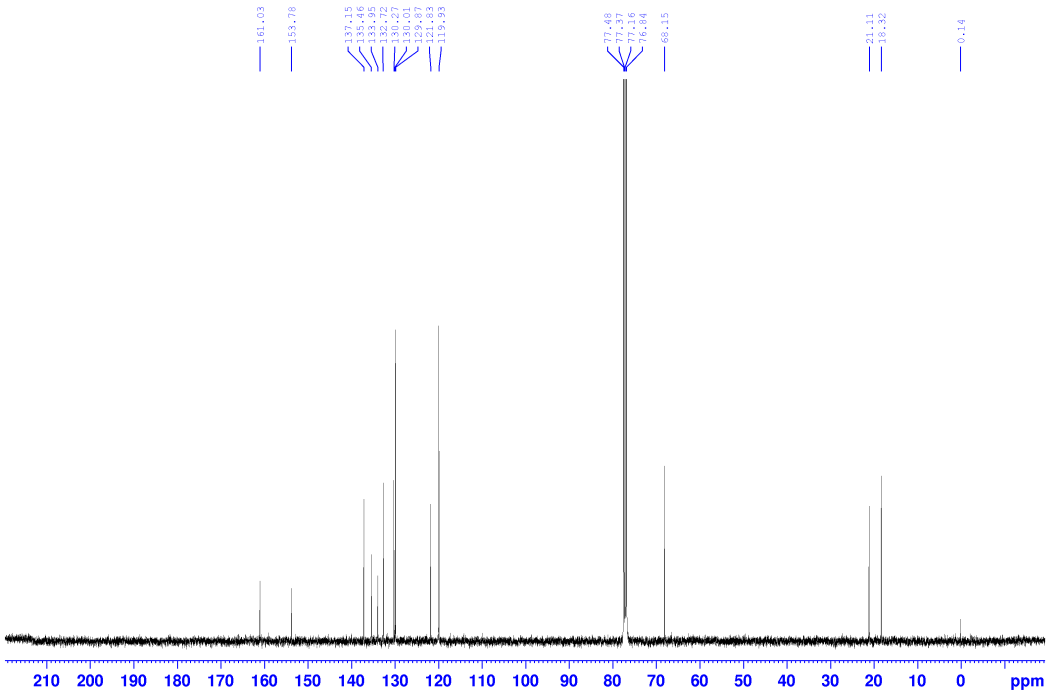
161.03
153.78
137.15
135.46
133.95
132.72
130.27
129.01
128.82
121.83
119.93
77.48
77.37
77.16
76.84
68.15
21.11
18.52
0.14
210 200 190 180 170 160 150 140 130 120 110 100 90 80 70 60 50 40 30 20 10 0 ppm

Ethyl 2-oxo-2-(*p*-tolylamino)acetate 7i

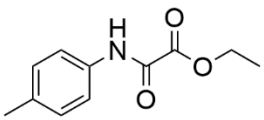

^{1}H NMR (400 MHz, $CDCl_3$)

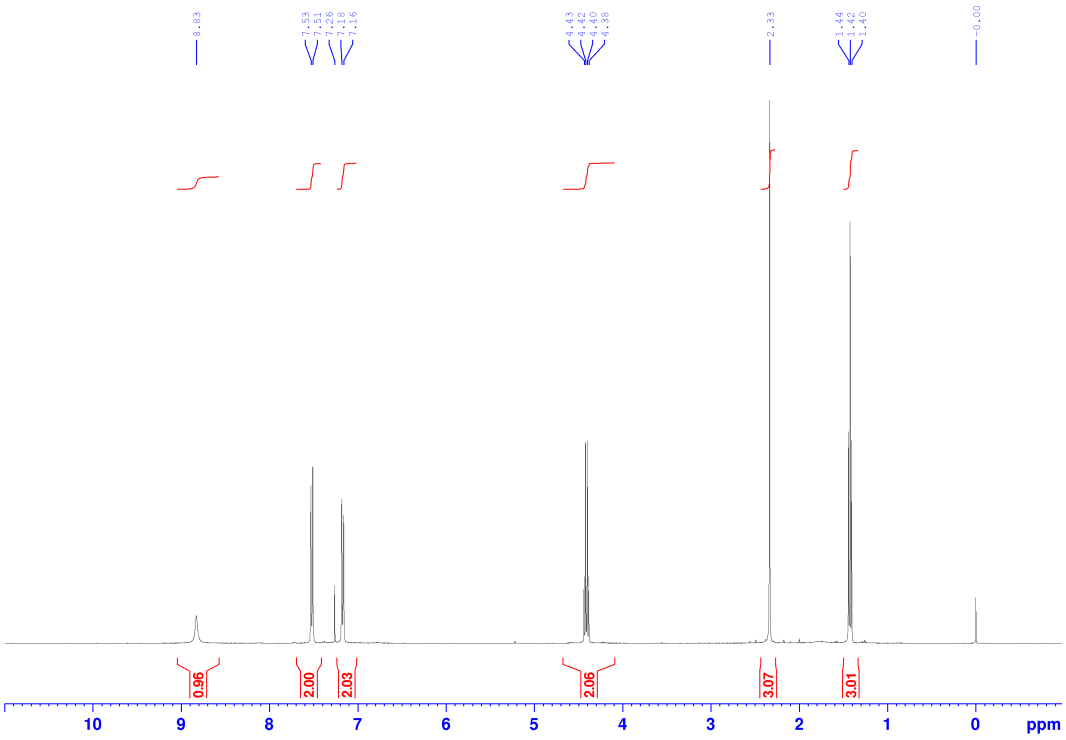

^{13}C NMR (100.6 MHz, $CDCl_3$)

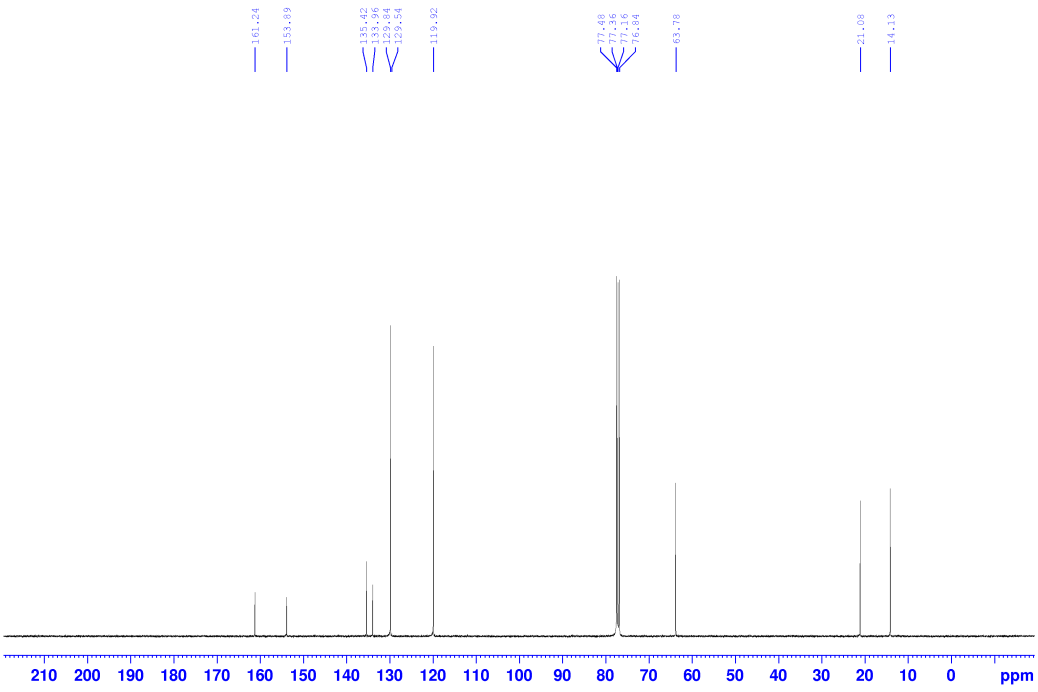
161.24
153.89
135.42
133.96
129.84
129.54
119.92
77.48
77.36
77.16
76.84
63.78
21.08
14.13
210 200 190 180 170 160 150 140 130 120 110 100 90 80 70 60 50 40 30 20 10 0 ppm

N^1-isopropyl-N^2-(*p*-tolyl)oxalamide 7j

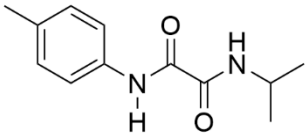

^{1}H NMR (400 MHz, $CDCl_3$)

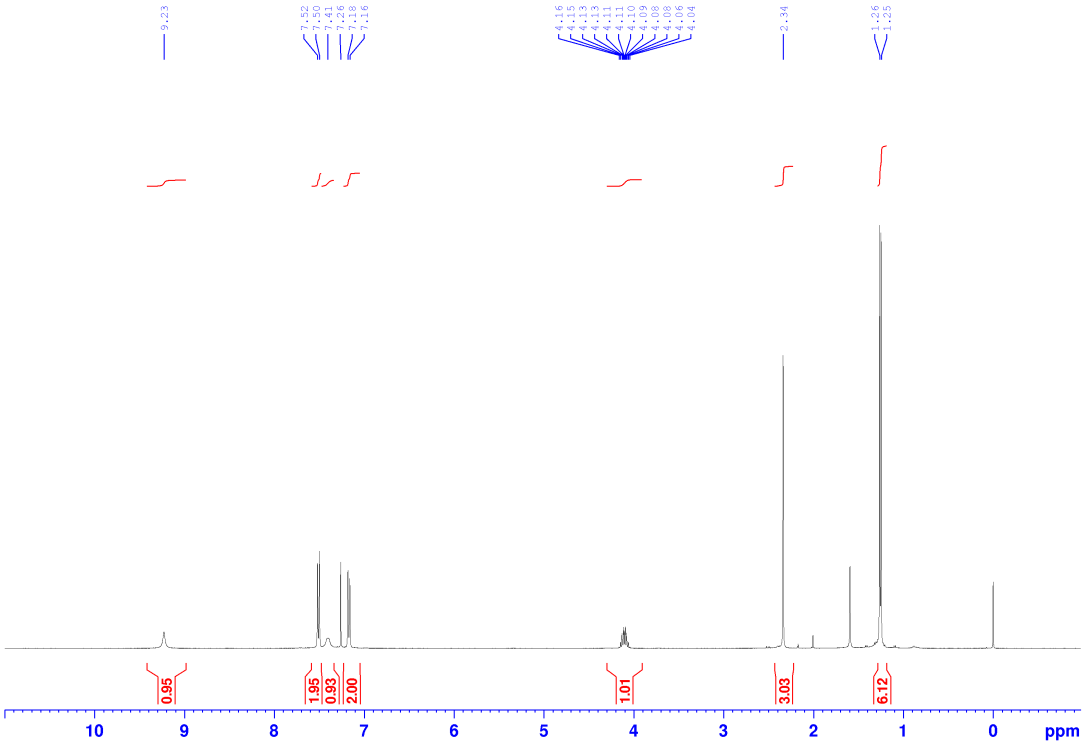

^{13}C NMR (100.6 MHz, $CDCl_3$)

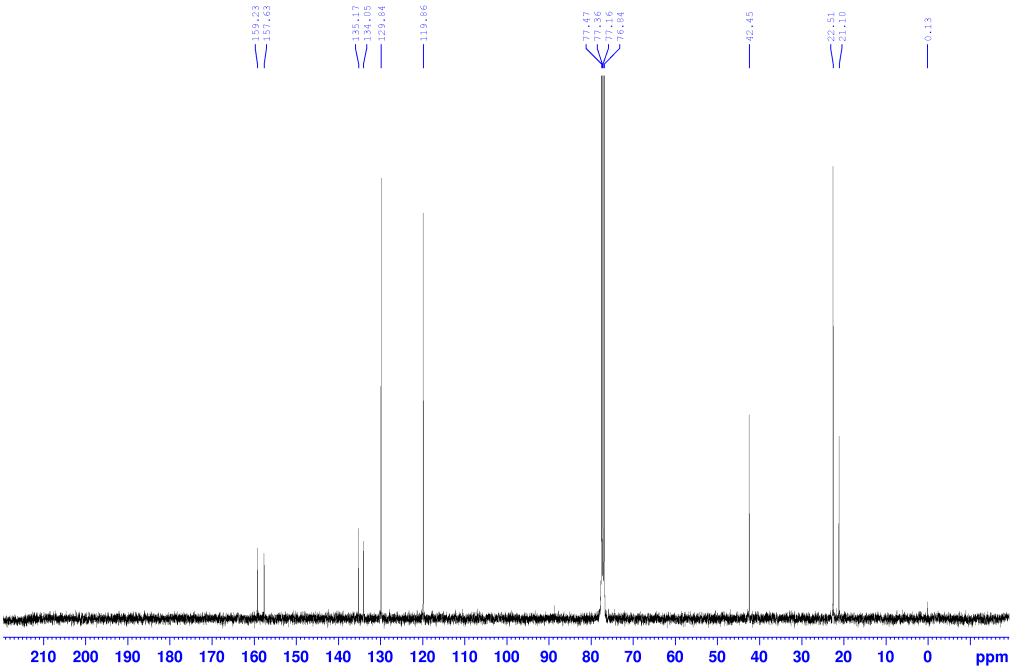
159.23
137.63
135.17
134.05
129.84
119.86
77.47
77.36
77.16
76.84
42.45
22.51
21.10
0.13
210 200 190 180 170 160 150 140 130 120 110 100 90 80 70 60 50 40 30 20 10 0 ppm

N^1-phenyl-N^2-(*p*-tolyl)oxalamide 7k

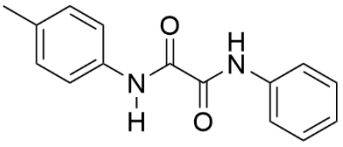

^{1}H NMR (400 MHz, $CDCl_3$)

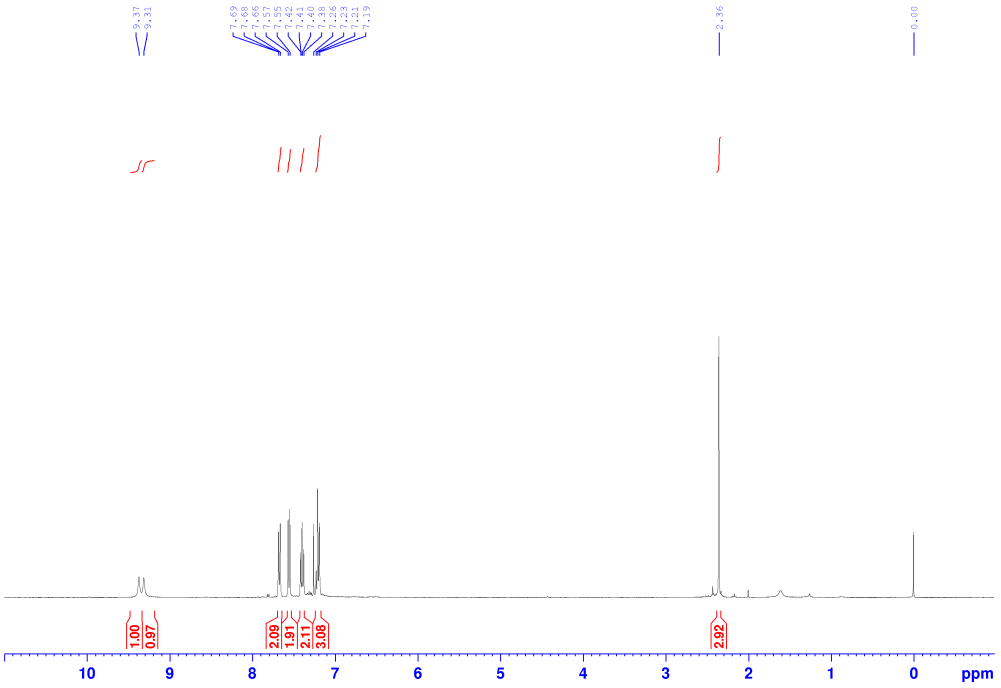

^{13}C NMR (100.6 MHz, $CDCl_3$)

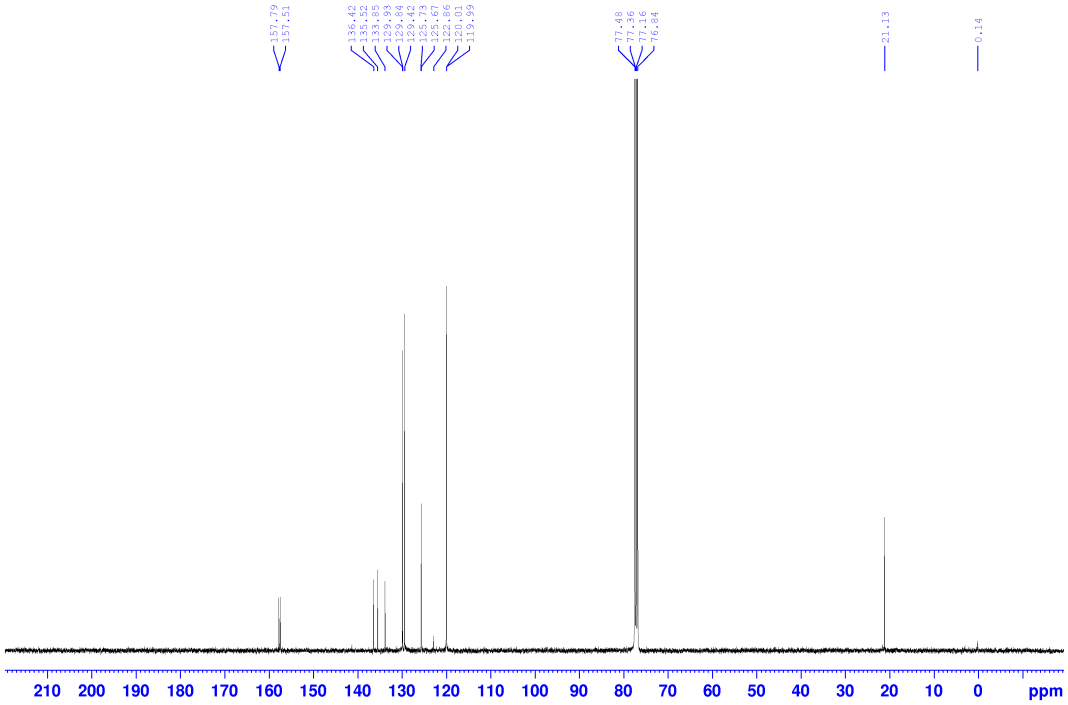
157.79
157.51
136.42
135.22
133.85
129.93
129.84
129.42
125.73
125.67
122.65
120.01
119.99
77.48
77.36
77.15
76.84
21.13
0.14
210 200 190 180 170 160 150 140 130 120 110 100 90 80 70 60 50 40 30 20 10 0 ppm

_S_-phenyl 2-oxo-2-(_p_-tolylamino)ethanethioate (impure)

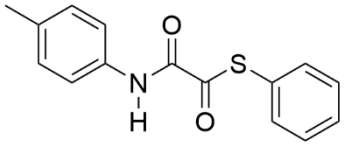

^{1}H NMR (400 MHz, $CDCl_3$)

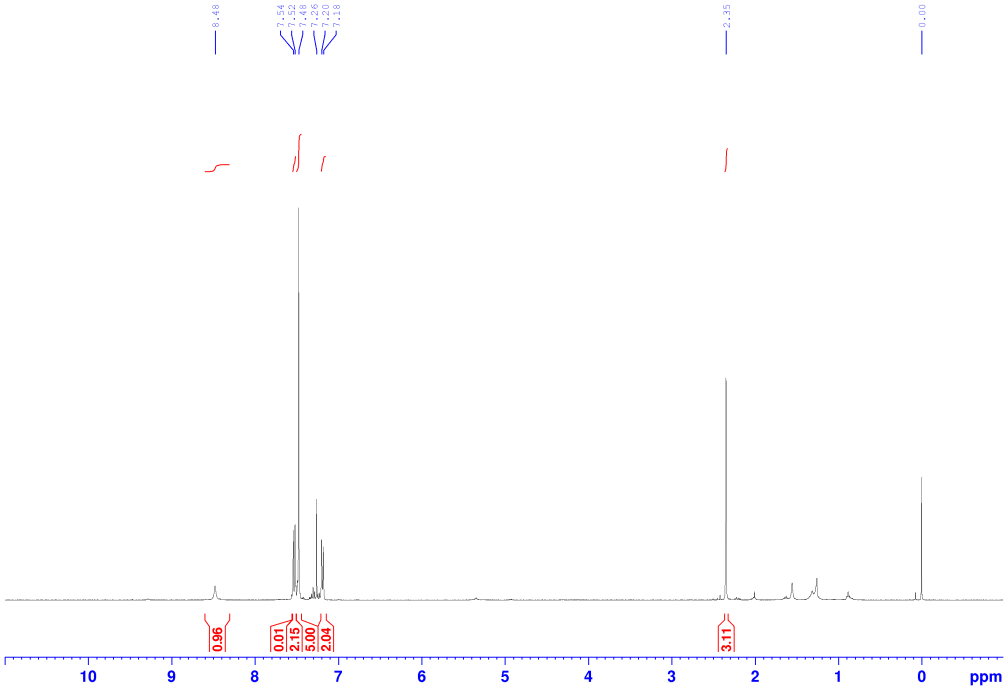

^{13}C NMR (100.6 MHz, $CDCl_3$)

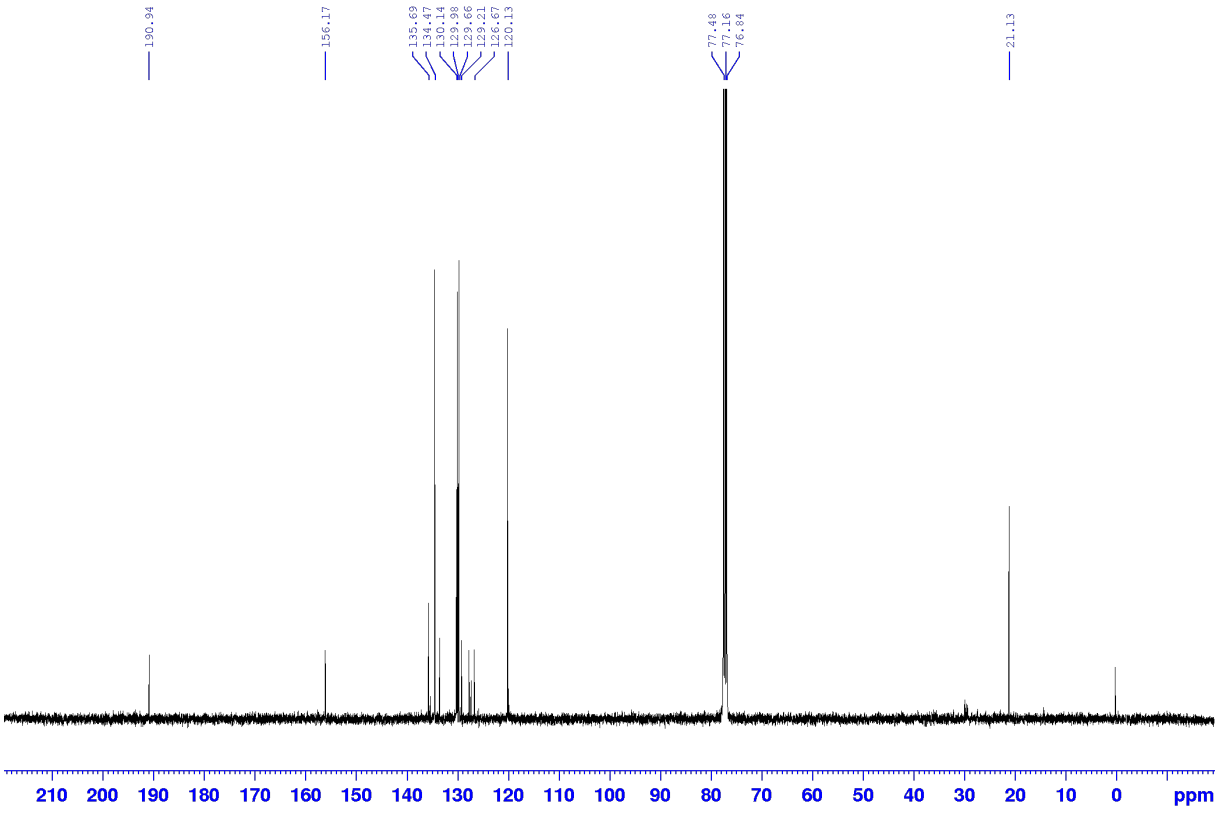
190.94
156.17
135.69
134.47
130.14
129.98
129.66
129.21
126.67
120.13
77.48
77.16
76.84
21.13
210 200 190 180 170 160 150 140 130 120 110 100 90 80 70 60 50 40 30 20 10 0 ppm

2-oxo-*N*-(p-tolyl)propenamide

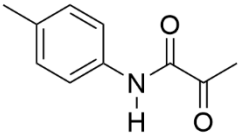

^{1}H NMR (400 MHz, $CDCl_3$)

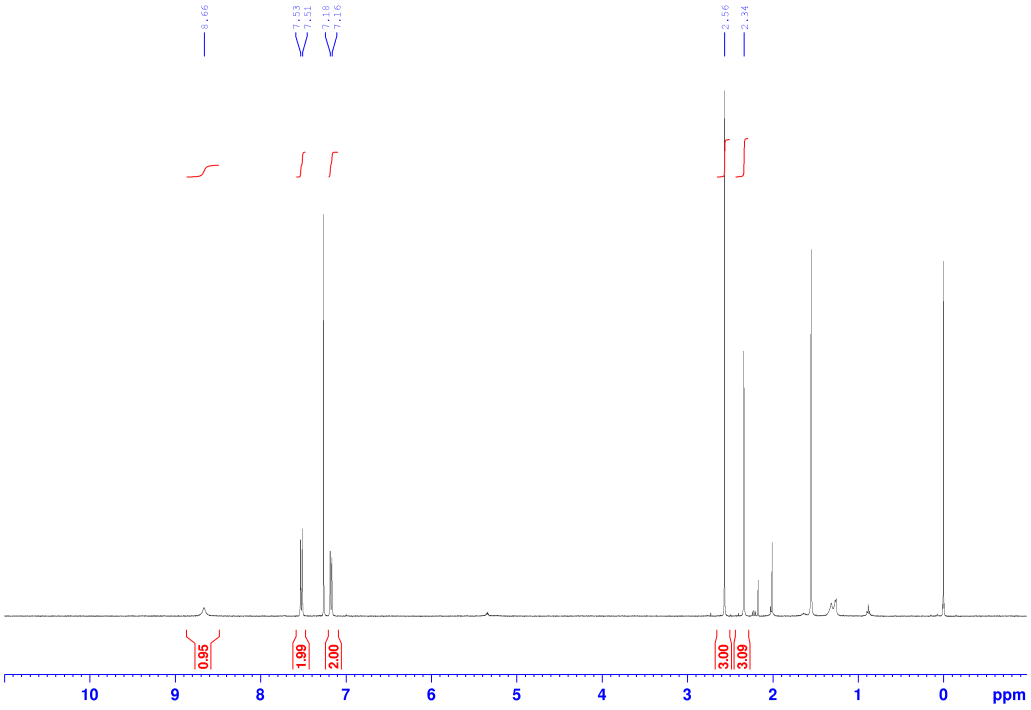

^{13}C NMR (100.6 MHz, $CDCl_3$)

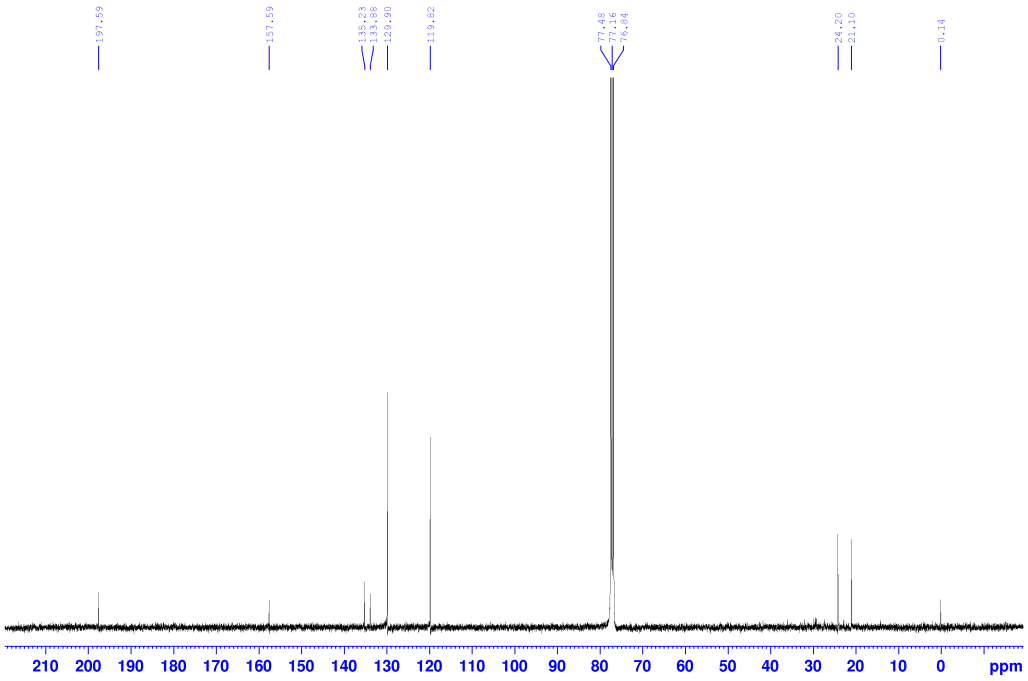

S7 References

(1) Li, H.; Homan, E. A.; Lampkins, A. J.; Ghiviriga, I.; Castellano, R. K. Synthesis and Self-Assembly of Functionalized Donor − σ − Acceptor Molecules. *Org. Lett.* **2005**, *7* (3), 443–446.

(2) Nielsen, B. E.; Gotfredsen, H.; Rasmussen, B.; Tortzen, C. G.; Pittelkow, M. Simple procedures for the preparation of 1,3,5-substituted 2,4,6-trimethoxybenzenes. *Synlett* **2013**, *24* (18), 2437–2442.

(3) Halder, A.; Karak, S.; Addicoat, M.; Bera, S.; Chakraborty, A.; Kunjattu, S. H.; Pachfule, P.; Heine, T.; Banerjee, R. Ultrastable Imine-Based Covalent Organic Frameworks for Sulfuric Acid Recovery: An Effect of Interlayer Hydrogen Bonding. *Angew. Chem. Int. Ed.* **2018**, *57* (20), 5797–5802.

(4) Foster, J. S.; Prentice, A. W.; Forgan, R. S.; Paterson, M. J.; Lloyd, G. O. Targetable Mechanical Properties by Switching between Self-Sorting and Co-assembly with In Situ Formed Tripodal Ketoenamine Supramolecular Hydrogels. *ChemNanoMat* **2018**, *4* (8), 853–859.

(5) Gupta, G.; Iqbal, P.; Yin, F.; Liu, J.; Palmer, R. E.; Sharma, S.; Leung, K. C. F.; Mendes, P. M. Pt Diffusion Dynamics for the Formation Cr-Pt Core-Shell Nanoparticles. *Langmuir* **2015**, *31* (24), 6917–6923.

(6) Albrecht, M.; Janser, I.; Lützen, A.; Hapke, M. 5,5 ’ -Diamino-2,2 ’ -bipyridine: A Versatile Building Block for the Synthesis of Bipyridine/Catechol Ligands That Form Homo- and Heteronuclear Helicates. *Chemistry - A European Journal* **2005**, *11*, 5742–5748.

(7) Lützen, A.; Hapke, M.; Staats, H.; Bunzen, J. Synthesis of Differently Disubstituted 2,2’-Bipyridines by a Modified Negishi Cross-Coupling Reaction. *Eur. J. Org. Chem.* **2003**, No. 20, 3948–3957.

(8) Sun, Q.; Aguila, B.; Perman, J.; Nguyen, N.; Ma, S. Flexibility Matters: Cooperative Active Sites in Covalent Organic Framework and Threaded Ionic Polymer. *J. Am. Chem. Soc.* **2016**, *138* (48), 15790–15796.

(9) Gofman, I. v.; Goikhman, M. Y.; Podeshvo, I. v.; Eliseeva, E. E.; Bol'Bat, E. E.; Abalov, I. v.; Yakimanskii, A. v. Films of polyamides with phenylpyridine units in the backbone. *Russ. J. Appl. Chem.* **2010**, *83* (10), 1862–1867.

(10) Krishnaraj, C.; Sekhar Jena, H.; Bourda, L.; Laemont, A.; Pachfule, P.; Roeser, J.; Chandran, C. V.; Borgmans, S.; Rogge, S. M. J.; Leus, K.; Stevens, C. v.; Martens, J. A.; van Speybroeck, V.; Breynaert, E.; Thomas, A.; van der Voort, P. Strongly Reducing (Diarylamino)benzene-Based Covalent Organic Framework for Metal-Free Visible Light Photocatalytic H2O2 Generation. *J. Am. Chem. Soc.* **2020**, *142* (47), 20107–20116.

(11) Tafipolsky, M.; Amirjalayer, S.; Schmid, R. Ab initio parametrized MM3 force field for the metal-organic framework MOF-5. *J. Comput. Chem.* **2007**, *28* (7), 1169–1176.

(12) Schmid, R.; Tafipolsky, M. An Accurate Force Field Model for the Strain Energy Analysis of the Covalent Organic Framework COF-102. *J. Am. Chem. Soc.* **2008**, *130* (38), 12600–12601.

(13) Tafipolsky, M.; Schmid, R. Systematic First Principles Parameterization of Force Fields for Metal-Organic Frameworks using a Genetic Algorithm Approach. *J. Phys. Chem. B* **2009**, *113* (5), 1341–1352.

(14) Vanduyfhuys, L.; Verstraelen, T.; Vandichel, M.; Waroquier, M.; van Speybroeck, V. Ab Initio Parametrized Force Field for the Flexible Metal-Organic Framework MIL-53(Al). *J. Chem. Theory Comput.* **2012**, *8* (9), 3217–3231.

(15) Bureekaew, S.; Amirjalayer, S.; Tafipolsky, M.; Spickermann, C.; Roy, T. K.; Schmid, R. MOF-FF - A flexible first-principles derived force field for metal-organic frameworks. *Phys. Status Solidi B* **2013**, *250* (6), 1128–1141.

(16) Tafipolsky, M.; Amirjalayer, S.; Schmid, R. First-principles-derived force field for copper paddle-wheel-based metal-organic frameworks. *J. Phys. Chem. C* **2010**, *114* (34), 14402–14409.

(17) Amirjalayer, S.; Snurr, R. Q.; Schmid, R. Prediction of structure and properties of boron-based covalent organic frameworks by a first-principles derived force field. *J. Phys. Chem. C* **2012**, *116* (7), 4921–4929.

(18) Wieme, J.; Vanduyfhuys, L.; Rogge, S. M. J.; Waroquier, M.; van Speybroeck, V. Exploring the flexibility of MIL-47(V)-type materials using force field molecular dynamics simulations. *J. Phys. Chem. C* **2016**, *120* (27), 14934–14947.

(19) Rogge, S. M. J.; Wieme, J.; Vanduyfhuys, L.; Vandenbrande, S.; Maurin, G.; Verstraelen, T.; Waroquier, M.; van Speybroeck, V. Thermodynamic Insight in the High-Pressure Behavior of UiO-66: Effect of Linker Defects and Linker Expansion. *Chem. Mater.* **2016**, *28* (16), 5721–5732.

(20) Frisch, M. J.; Trucks, G. W.; Schlegel, H. B.; Scuseria, G. E.; Robb, M. A.; Cheeseman, J. R.; Scalmani, G.; Barone, V.; Petersson, G. A.; Nakatsuji, H.; Li, X.; Caricato, M.; Marenich, A. v; Bloino, J.; Janesko, B. G.; Gomperts, R.; Mennucci, B.; Hratchian, H. P.; Ortiz, J. v; Izmaylov, A. F.; Sonnenberg, J. L.; Williams-Young, D.; Ding, F.; Lipparini, F.; Egidi, F.; Goings, J.; Peng, B.; Petrone, A.; Henderson, T.; Ranasinghe, D.; Zakrzewski, V. G.; Gao, J.; Rega, N.; Zheng, G.; Liang, W.; Hada, M.; Ehara, M.; Toyota, K.; Fukuda, R.; Hasegawa, J.; Ishida, M.; Nakajima, T.; Honda, Y.; Kitao, O.; Nakai, H.; Vreven, T.; Throssell, K.; Montgomery Jr., J. A.; Peralta, J. E.; Ogliaro, F.; Bearpark, M. J.; Heyd, J. J.; Brothers, E. N.; Kudin, K. N.; Staroverov, V. N.; Keith, T. A.; Kobayashi, R.; Normand, J.; Raghavachari, K.; Rendell, A. P.; Burant, J. C.; Iyengar, S. S.; Tomasi, J.; Cossi, M.; Millam, J. M.; Klene, M.; Adamo, C.; Cammi, R.; Ochterski, J. W.; Martin, R. L.; Morokuma, K.; Farkas, O.; Foresman, J. B.; Fox, D. J. Gaussian~16 Revision C.01. **2016**.

(21) Lee, C.; Yang, W.; Parr, R. G. Development of the Colle-Salvetti correlation-energy formula into a functional of the electron density. *Phys Rev B* **1988**, *37* (2), 785.

(22) Becke, A. D. Becke's three parameter hybrid method using the LYP correlation functional. *J. Chem. Phys* **1993**, *98* (492), 5648–5652.

(23) Stephens, P. J.; Devlin, F. J.; Chabalowski, C. F.; Frisch, M. J. Ab Initio Calculation of Vibrational Absorption and Circular Dichroism Spectra Using Density Functional Force Fields. *J. Phys. Chem.* **1994**, *98* (45).

(24) Grimme, S.; Antony, J.; Ehrlich, S.; Krieg, H. A consistent and accurate ab initio parametrization of density functional dispersion correction (DFT-D) for the 94 elements H-Pu. *J. Chem. Phys.* **2010**, *132* (15), 154104.

(25) Frisch, M. J.; Pople, J. A.; Binkley, J. S. Self-consistent molecular orbital methods 25. Supplementary functions for Gaussian basis sets. *J. Chem. Phys.* **1984**, *80* (7), 3265–3269.

(26) Verstraelen, T.; Vandenbrande, S.; Heidar-Zadeh, F.; Vanduyfhuys, L.; van Speybroeck, V.; Waroquier, M.; Ayers, P. W. Minimal Basis Iterative Stockholder: Atoms in Molecules for Force-Field Development. *J. Chem. Theory Comput.* **2016**, *12* (8), 3894–3912.

(27) Verstraelen, T.; Tecmer, P.; Heidar-Zadeh, F.; González-Espinoza, C. E.; Chan, M.; Kim, T. D.; Boguslawski, K.; Fias, S.; Vandenbrande, S.; Berrocal, D.; Ayers, P. W. HORTON 2.1.1. **2017**.

(28) Vanduyfhuys, L.; Vandenbrande, S.; Verstraelen, T.; Schmid, R.; Waroquier, M.; van Speybroeck, V. QuickFF: A program for a quick and easy derivation of force fields for metal-organic frameworks from ab initio input. *J. Comput. Chem.* **2015**, *36* (13), 1015–1027.

(29) Vanduyfhuys, L.; Vandenbrande, S.; Wieme, J.; Waroquier, M.; Verstraelen, T.; van Speybroeck, V. Extension of the QuickFF force field protocol for an improved accuracy of structural, vibrational, mechanical and thermal properties of metal–organic frameworks. *J. Comput. Chem.* **2018**, *39* (16), 999–1011.

(30) Chen, J.; Martínez, T. J. QTPIE: Charge transfer with polarization current equalization. A fluctuating charge model with correct asymptotics. *Chem. Phys. Lett.* **2007**, *438* (4–6), 315–320.

(31) Bush, B. L.; Bayly, C. I.; Halgren, T. A. Consensus bond-charge increments fitted to electrostatic potential or field of many compounds: Application to MMFF94 training set. *J. Comput. Chem.* **1999**, *20* (14), 1495–1516.

(32) Allinger, N. L.; Yuh, Y. H.; Lii, J. H. Molecular mechanics. The MM3 force field for hydrocarbons. 1. *J. Am. Chem. Soc.* **1989**, *111* (23), 8551–8566.

(33) Verstraelen, T.; Vanduyfhuys, L.; Vandenbrande, S.; Rogge, S. M. J. Yaff, yet another force field.

(34) Cui, Q.; Bahar, I. Normal mode analysis: theory and applications to biological and chemical systems; CRC press, **2005**.

(35) Ghysels, A.; Verstraelen, T.; Hemelsoet, K.; Waroquier, M.; van Speybroeck, V. TAMkin: a versatile package for vibrational analysis and chemical kinetics. ACS Publications **2010**.

(36) Colón, Y. J.; Snurr, R. Q. High-throughput computational screening of metal–organic frameworks. *Chem. Soc. Rev.* **2014**, *43* (16), 5735–5749.

(37) Borgmans, S.; Rogge, S. M. J.; de Vos, J. S.; Stevens, C. v.; van der Voort, P.; van Speybroeck, V. Quantifying the Likelihood of Structural Models through a Dynamically Enhanced Powder X-Ray Diffraction Protocol. *Angew. Chem. Int. Ed.* **2021**, *60* (16), 8913–8922.

(38) Favre-Nicolin, V.; Černý, R. FOX, free objects for crystallography: a modular approach to ab initio structure determination from powder diffraction. *J. Appl. Crystallogr.* **2002**, *35* (6), 734–743.

(39) Plimpton, S. Fast Parallel Algorithms for Short-Range Molecular Dynamics. *J. Comput. Phys.* **1995**, *117* (1), 1–19.

(40) Rogge, S. M. J.; Vanduyfhuys, L.; Ghysels, A.; Waroquier, M.; Verstraelen, T.; Maurin, G.; van Speybroeck, V. A Comparison of Barostats for the Mechanical Characterization of Metal-Organic Frameworks. *J. Chem. Theory Comput.* **2015**, *11* (12), 5583–5597.

(41) Nosé, S. A Molecular Dynamics Method for Simulations in the Canonical Ensemble. *Mol. Phys.* **1984**, *52* (2), 255–268.

(42) Hoover, W. G. Canonical Dynamics: Equilibrium Phase-Space Distributions. *Phys. Rev. A* **1985**, *31* (3), 1695–1697.

(43) Martyna, G. J.; Klein, M. L.; Tuckerman, M. Nosé–Hoover Chains: The Canonical Ensemble via Continuous Dynamics. *J. Chem. Phys.* **1992**, *97* (4), 2635–2643.

(44) Martyna, G. J.; Tobias, D. J.; Klein, M. L. Constant Pressure Molecular Dynamics Algorithms. *J. Chem. Phys.* **1994**, *101* (5), 4177–4189.

(45) Martyna, G. J.; Tuckerman, M. E.; Tobias, D. J.; Klein, M. L. Explicit Reversible Integrators for Extended Systems Dynamics. *Mol. Phys.* **1996**, *87* (5), 1117–1157.

(46) Blöchl, P. E. Projector augmented-wave method. *Phys. Rev. B* **1994**, *50* (24), 17953–17979.

(47) Kresse, G.; Hafner, J. Ab. initio molecular dynamics for liquid metals. *Phys. Rev. B* **1993**, *47* (1), 558–561.

(48) Kresse, G.; Furthmiiller B ', J. Efficiency of ab-initio total energy calculations for metals and semiconductors using a plane-wave basis set. *Comput. Mater. Sci.* **1996**, *6*, 15–50.

(49) Kresse, G.; Furthmü, J. Efficient iterative schemes for ab initio total-energy calculations using a plane-wave basis set. *Phys. Rev. B* **1996**, *54* (16), 11169–11186.

(50) Perdew, J. P.; Burke, K.; Ernzerhof, M. Generalized Gradient Approximation Made Simple. *Phys. Rev. Lett.* **1996**, *77* (18), 3865–3868.

(51) Grimme, S.; Antony, J.; Ehrlich, S.; Krieg, H. A consistent and accurate ab initio parametrization of density functional dispersion correction (DFT-D) for the 94 elements H-Pu. *J. Chem. Phys.* **2010**, *132* (15), 154104.

(52) Grimme, S.; Ehrlich, S.; Goerigk, L. Effect of the damping function in dispersion corrected density functional theory. *J. Comput. Chem.* **2011**, *32* (7), 1456–1465.

(53) Heyd, J.; Scuseria, G. E.; Ernzerhof, M. Hybrid functionals based on a screened Coulomb potential. *J. Chem. Phys.* **2003**, *118* (18), 8207–8215.

(54) Pickard, C. J.; Mauri, F. All-electron magnetic response with pseudopotentials: NMR chemical shifts. *Phys. Rev. B Condens. Matter Mater. Phys.* **2001**, *63* (24), 2451011–2451013.

(55) Pinheiro, M.; Martin, R. L.; Rycroft, C. H.; Jones, A.; Iglesia, E.; Haranczyk, M. Characterization and comparison of pore landscapes in crystalline porous materials. *J. Mol. Graph. Model.* **2013**, *44*, 208–219.

(56) Willems, T. F.; Rycroft, C. H.; Kazi, M.; Meza, J. C.; Haranczyk, M. Algorithms and tools for high-throughput geometry-based analysis of crystalline porous materials. *Microporous Mesoporous Mater* **2012**, *149* (1), 134–141.

(57) Wu, F.; Wang, L.; Ji, Y.; Zou, G.; Shen, H.; Nicewicz, D. A.; Chen, J.; Huang, Y. Direct Synthesis of Bicyclic Acetals via Visible Light Catalysis. *iScience* **2020**, *23* (8), 101395.

(58) Bouziane, A.; Hélou, M.; Carboni, B.; Carreaux, F.; Demerseman, B.; Bruneau, C.; Renaud, J. L. Ruthenium-catalyzed synthesis of allylic alcohols: Boronic acid as a hydroxide source. *Chem. Eur. J.* **2008**, *14* (18), 5630–5637.

(59) Jia, X.; Peng, F.; Qing, C.; Huo, C.; Wang, X. Catalytic radical cation salt induced Csp 3-H functionalization of glycine derivatives: Synthesis of substituted quinolines. *Org. Lett.* **2012**, *14* (15), 4030–4033.

(60) More, D. A.; Shinde, G. H.; Shaikh, A. C.; Muthukrishnan, M. Oxone promoted dehydrogenative Povarov cyclization of: N -aryl glycine derivatives: An approach towards quinoline fused lactones and lactams. *RSC Adv.* **2019**, *9* (52), 30277–30291.

(61) Dong, W.; Hu, B.; Gao, X.; Li, Y.; Xie, X.; Zhang, Z. Visible-Light-Induced Photocatalytic Aerobic Oxidation/Povarov Cyclization Reaction: Synthesis of Substituted Quinoline-Fused Lactones. *J. Org. Chem.* **2016**, *81* (19), 8770–8776.

(62) Wang, Y.; Peng, F.; Liu, J.; Huo, C.; Wang, X.; Jia, X. Radical cation salt-promoted catalytic aerobic sp3 C-H oxidation: Construction of quinoline-fused lactones and lactams. *J. Org. Chem.* **2015**, *80* (1), 609–614.

(63) Ohshima, T.; Miyamoto, Y.; Ipposhi, J.; Nakahara, Y.; Utsunomiya, M.; Mashima, K. Platinum-catalyzed direct amination of allylic alcohols under mild conditions: Ligand and microwave effects, substrate scope, and mechanistic study. *J. Am. Chem. Soc.* **2009**, *131* (40), 14317–14328.

(64) Peilleron, L.; Retailleau, P.; Cariou, K. Synthesis of Cyclic N-Hydroxylated Ureas and Oxazolidinone Oximes Enabled by Chemoselective Iodine(III)-Mediated Radical or Cationic Cyclizations of Unsaturated N-Alkoxyureas. *Adv. Synth. Catal.* **2019**, *361* (22), 5160–5169.

(65) Li, X. M.; Tang, L.; Qian, Z. M.; He, Y. H.; Guan, Z. Copper catalysis: One-pot simultaneous synthesis of quinolines and gem-diamine derivatives. *Tetrahedron Lett* **2020**, *61* (47), 152346.

(66) Li, X. M.; Tang, L.; Qian, Z. M.; He, Y. H.; Guan, Z. Copper catalysis: One-pot simultaneous synthesis of quinolines and gem-diamine derivatives. *Tetrahedron Lett.* **2020**, *61* (47).

(67) Jerezano, A. V.; Labarrios, E. M.; Jiménez, F. E.; Del Cruz, M. C.; Pazos, D. C.; Gutiérrez, R. U.; Delgado, F.; Tamariz, J. Iodine-mediated one-pot synthesis of indoles and 3-dimethylaminoindoles via annulation of enaminones. *Arkivoc* **2013**, *2014* (3), 18–53.

(68) Specklin, S.; Decuypere, E.; Plougastel, L.; Aliani, S.; Taran, F. One-pot synthesis of 1,4-disubstituted pyrazoles from arylglycines via copper-catalyzed sydnone-alkyne cycloaddition reaction. *J. Org. Chem.* **2014**, *79* (16), 7772–7777.

(69) Arcelli, A.; Bongini, A.; Porzi, G.; Rinaldi, S. Ammonolysis of morpholine-2,5-diones: Participation of the primary amide group. Part 2. *J. Phys. Org. Chem.* **2012**, *25* (2), 132–141.

(70) Desrat, S.; van de Weghe, P. Intramolecular imino Diels - Alder reaction: Progress toward the synthesis of uncialamycin. *J. Org. Chem.* **2009**, *74* (17), 6728–6734.

(71) Huo, C.; Yuan, Y.; Wu, M.; Jia, X.; Wang, X.; Chen, F.; Tang, J. Auto-oxidative coupling of glycine derivatives. *Angew. Chem. Int. Ed.* **2014**, *53* (49), 13544–13547.

(72) Zhan, Z.; Cheng, X.; Ma, X.; Li, J.; Hai, L.; Wu, Y. Hydrogen peroxide-promoted metal free oxidative amidation of 2-oxoaldehydes: A facile access to unsymmetrical oxamides. *Tetrahedron* **2015**, *71* (38), 6928–6934.

(73) Wang, D.; Li, L.; Feng, H.; Sun, H.; Almeida-Veloso, F.; Charavin, M.; Yu, P.; Désaubry, L. Catalyst-free three-component synthesis of highly functionalized 2,3-dihydropyrroles. *Green Chem.* **2018**, *20* (12), 2775–2780.